

# Open Research Online

---

The Open University's repository of research publications and other research outputs

## Molecular pathways of degradation of wool-related peptides

### Thesis

#### How to cite:

Ghadimi, Moharam (1991). Molecular pathways of degradation of wool-related peptides. PhD thesis The Open University.

For guidance on citations see [FAQs](#).

© 1990 The Author



<https://creativecommons.org/licenses/by-nc-nd/4.0/>

Version: Version of Record

Link(s) to article on publisher's website:

<http://dx.doi.org/doi:10.21954/ou.ro.0001013b>

---

Copyright and Moral Rights for the articles on this site are retained by the individual authors and/or other copyright owners. For more information on Open Research Online's data [policy](#) on reuse of materials please consult the policies page.

---

[oro.open.ac.uk](http://oro.open.ac.uk)

DX 94672.

UNRESTRICTED

# **MOLECULAR PATHWAYS OF DEGRADATION OF WOOL-RELATED PEPTIDES**

**A thesis submitted to the Open University**

**for the degree of**

**DOCTOR OF PHILOSOPHY**

**BY**

**M. GHADIMI (B.Sc., M.Sc.)**

*Date of submission: 29<sup>th</sup> October 1990*

*Date of award: 8<sup>th</sup> March 1991*

1990

ProQuest Number: 27758390

All rights reserved

INFORMATION TO ALL USERS

The quality of this reproduction is dependent on the quality of the copy submitted.

In the unlikely event that the author did not send a complete manuscript and there are missing pages, these will be noted. Also, if material had to be removed, a note will indicate the deletion.



ProQuest 27758390

Published by ProQuest LLC (2019). Copyright of the Dissertation is held by the Author.

All Rights Reserved.

This work is protected against unauthorized copying under Title 17, United States Code  
Microform Edition © ProQuest LLC.

ProQuest LLC  
789 East Eisenhower Parkway  
P.O. Box 1346  
Ann Arbor, MI 48106 - 1346

**IN  
MEMORY  
OF  
MY PARENTS**



## Acknowledgements

I would like to express my sincere gratitude to my supervisor, Dr R. R. Hill, for his unfailing support, encouragement and advice throughout this project. I appreciate the opportunity to be able to work under his guidance.

Special thanks are due to both Open University and British Textile Technology Group (formerly WIRA) for providing financial support throughout this work. I am also grateful to Mr A. Walters for arranging a visit to the textile processor in Leeds.

I would like to thank the SERC for the use of the high field NMR facility at the University of Warwick.

Thanks are due to Mr G. Jeffs for his cooperation throughout the project, particularly at the preliminary stages. I would also like to thank Mr P. Patel for his help in the laboratory.

I would like to thank my dearest girl friend Miss Laura Whitemore, for her continuous help, moral support and friendship throughout the preparation of this thesis. Finally, thanks are due to Mrs Shirley Foster for kindly typing this thesis.

## Abstract

The thermal and alkali-promoted reactions of *N*-acetyl-*N*-methylamides of alanine, cystine, glycine, histidine, methionine, phenylalanine, proline, serine, threonine, tryptophan and tyrosine have been studied as models for the reaction of heat and alkali on wool protein. The cystine model, *N,N*-diacetyl-L-cystine-*N,N*-dimethylamide (DCDMA), has been the principal substrate. The amino acid derivatives were usually heated either as wet solids at 125 °C or in aqueous solution buffered at pH 10-11 at 55° and 100 °C. A brief photochemical study was conducted with DCDMA. Reactions were monitored by uv spectroscopy and HPLC. Products were isolated by preparative HPLC, characterised by spectroscopy and quantified by analytical HPLC.

All the reactions with DCDMA give bright yellow product mixtures. The major components, however, are colourless, and include *N,N*-diacetyl-thiocystine-*N,N*-dimethylamide (DTCDMA), diastereoisomers of *N,N*- diacetyl lanthionine-*N,N*-dimethylamide (DLDMA) and *N*-acetyl-*N*-methylamides of cysteine (NACMA) and dehydroalanine (NADMA). Their formation is best explained by a  $\beta$ -elimination mechanism involving thiocysteiny and dehydroalanyl derivative intermediates. The product distribution and yields from wet solid samples, however, differ significantly from those obtained with aqueous alkali. DTCDMA is the major product (65%) in wet solid-state conditions, and is formed so readily that it is usually present as a contaminant of the substrate. *N*-Acetylthiocysteine-*N*-methylamide (NATCMA) is also present amongst thermolysis products, but we could not determine its yield due to intrinsic instability. NADMA is the principal product formed in aqueous alkali (~58%) followed by DLDMA, DTCDMA and NACMA. NADMA is shown to be unstable under acid conditions and decomposes to methylpyruvamide (MPA) and acetamide. Elemental sulphur was isolated from the decomposition of DCDMA under both conditions.

Yellow reaction mixtures of DCDMA show three regions of increased absorptions at 300, 385 and 455 nm. Results implicate methylthiopiruvamide as one of the pigments contributing to the yellowing and that polysulphides may also be involved.

Of the mono peptides examined, *N*-acetyl-*N*-methylamides of histidine, serine, threonine, tryptophan, tyrosine and DCDMA both degrade and yellow in wet solid-state conditions. The derivative of cystine is by far the most reactive mono peptide on treatment with alkali. *N*-Acetylserine-*N*-methylamide is the only amino acid derivative which both degrades and yellows in dry solid-state conditions. The protection of the hydroxyl group by benzyl reduces thermal or alkaline yellowing but it remains ineffective against decomposition.

Irradiation of DCDMA leads to a drop in pH, decomposition, and the formation of bright yellow solution with *N*-acetylcysteine-*N*-methylamide as the principal product. The derivatives of glycine, alanine, serine, and DTCDMA are also observed but in small amounts. Although the occurrence of the minor products is invoked as evidence for the cleavage of C-S bond, the cleavage of S-S bond appears to be predominant.

The implications of the results from these model compounds for wool degradation are briefly discussed. The principal conclusion is that the ready formation of the thiocystinyl derivative in the thermal degradation of DCDMA suggests analogous structures within wool proteins play a far more significant role in their chemistry than has been considered hitherto.

# CONTENTS

	Page
Abstract	iv
1 Introduction	2
2 Experimental	55
3 Results	84
4 Discussion	119
Conclusion	165
References	170

## Abbreviations

- (DCDMA) *N,N*-Diacetyl-L-cystine-*N,N*-dimethylamide  
(DLDMA) *N,N*-Diacetyl-RS-lanthionine-*N,N*-dimethylamide  
(DTCDMA) *N,N*-Diacetylthiocystine-*N,N*-dimethylamide  
(MPA) *N*-Methylpyruvamide  
(NAAMA) *N*-Acetylalanine-*N*-methylamide  
(NABSMA) *N*-Acetylbenzylserine-*N*-methylamide  
(NACMA) *N*-Acetylcysteine-*N*-methylamide  
(NADMA) *N*-Acetyldehydroalanine-*N*-methylamide  
(NAFMA) *N*-Acetylphenylalanine-*N*-methylamide  
(NAGMA) *N*-Acetylglycine-*N*-methylamide  
(NAHMA) *N*-Acetylhistidine-*N*-methylamide  
(NAMMA) *N*-Acetylmethionine-*N*-methylamide  
(NAPMA) *N*-Acetylproline-*N*-methylamide  
(NASMA) *N*-Acetylserine-*N*-methylamide  
(NATCMA) *N*-Acetylthiocystine-*N*-methylamide  
(NATMA) *N*-Acetylthreonine-*N*-methylamide  
(NAWMA) *N*-Acetyltryptophan-*N*-methylamide  
(NAYMA) *N*-Acetyltyrosine-*N*-methylamide

# **1 Introduction**

## **1.1 Preview**

## **1.2 Biochemistry of wool**

## **1.3 Morphological structure of wool**

### **1.3.1 The structure of peptides and proteins**

### **1.3.2 Keratins**

## **1.4 The chemistry of disulphides**

### **1.4.1 The structure of disulphides**

### **1.4.2 The reaction of disulphide groups**

## **1.5 Thermal degradation of wool and yellowing**

### **1.5.1 The effect of alkali**

### **1.5.2 The effect of heat**

## **1.6 Photochemistry**

### **1.6.1 Photoyellowing of wool**

### **1.6.2 Ultraviolet and visible spectra**

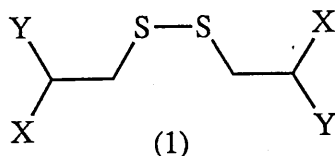
### **1.6.3 Photochemistry of cystine**

## **1.7 The objectives of the project**

# 1 Introduction

## 1.1 Preview

During processing, wool is treated repeatedly with alkali and/or heat. Unless fully controlled, this action can result in both yellowing and weakening of the fibre. The yellowing of wool is undesirable and reduces market value and, in practice its occurrence is a costly problem. Although it is important to find out the relevant chemistry at the molecular level, wool is a complex protein structure and results from direct studies of the thermally and/or alkali promoted degradation of wool are variable and difficult to evaluate. It is clear, however that the amino acid cystine is heavily implicated, especially in the alkali treatment, and we have selected *N,N*-diacetyl-L-cystine *N,N*-dimethyl amide (DCDMA...1) as a model of the amino acid in a protein.



$X = \text{CO}_2\text{H}$	$Y = \text{NH}_2$	cystine
$X = \text{COR}'$	$Y = \text{NHR}'$	protein
$X = \text{CONHCH}_3,$	$Y = \text{NHCOCH}_3$	DCDMA

It has been heated under conditions relevant to those occurring in wool processing, the objective being to determine by product analysis the chemistry of its degradation including the formation of yellow products if any. The photochemistry of the model has also been investigated briefly as has the thermal chemistry of analogous models of other amino acids.

Therefore this introduction reviews briefly the biochemistry and morphological structure of wool, followed by the chemistry of disulphides, particularly their interactions with heat and alkali. The thermal and alkaline degradation including

yellowing of wool is reviewed and, finally, current theories concerning the photodegradation of wool and of cystine are outlined.

## 1.2 Biochemistry of wool

Each hair originates from a single follicle in the skin (Fig. 1.1). The hair follicle derives from the epidermis and the general biochemical activity of both tissues resemble one another. However, during the differentiating process that the basal cells of both tissues undergo, several intermediate filament-associated proteins (IFAPs) are produced in the hair follicle which are chemically distinct from those functionally equivalent proteins in the epidermal cells. These IFAPs include the high glycine/tyrosine (HGT), the ultra-high sulphur (UHS) and trichohyalin proteins [Rogers et al., 1989].

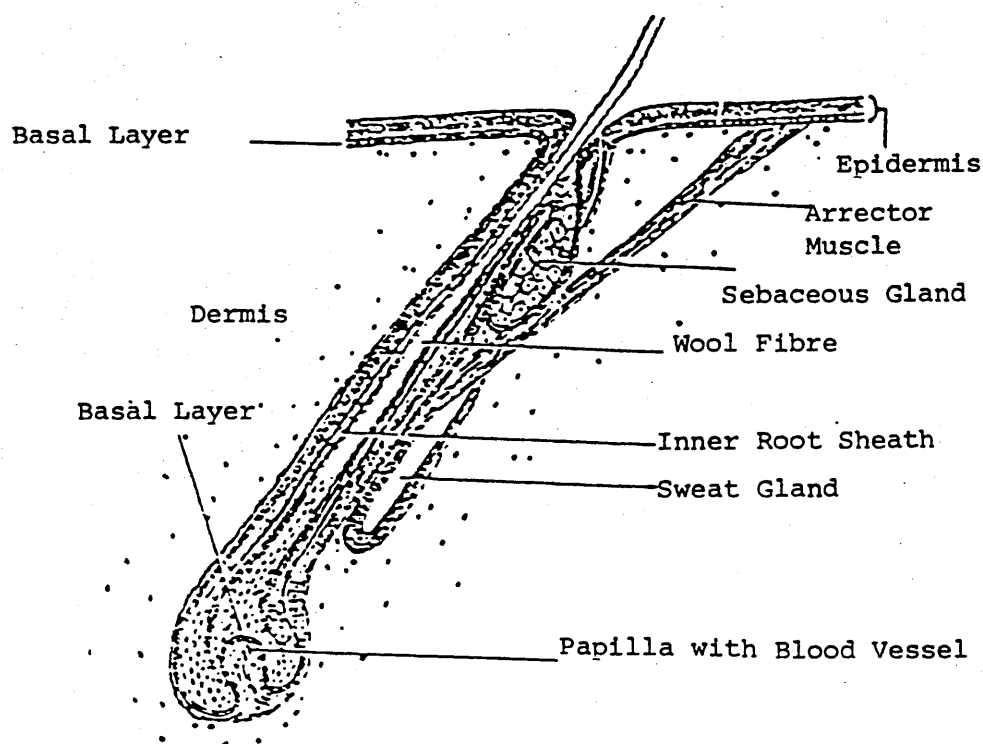


Figure 1.1 Cross-section through hair follicle showing development of wool fibre



The HGT and UHS proteins provide a structural matrix for the filaments in the hair and are located primarily in the cortex of the fibre. The HGT proteins are divided into two groups [Gillespie and Darkus, 1971], Type I (cystine poor) and type II (cystine rich). So there are two proteins with a high proportion of cystine. They can vary with species and the amounts of these proteins even in a single species such as sheep can also vary markedly as is illustrated in the one dimensional polyacryl amide gel electrophoresis (PAGE) analyses of HGT proteins in the wool of different strains of sheep and between species (Fig. 1.2). Here it is seen that the HGT proteins are undetectable in the wool of a mutant merino strain, present in merino wool and low in the lincoln breed, but prominent in mouse hair.

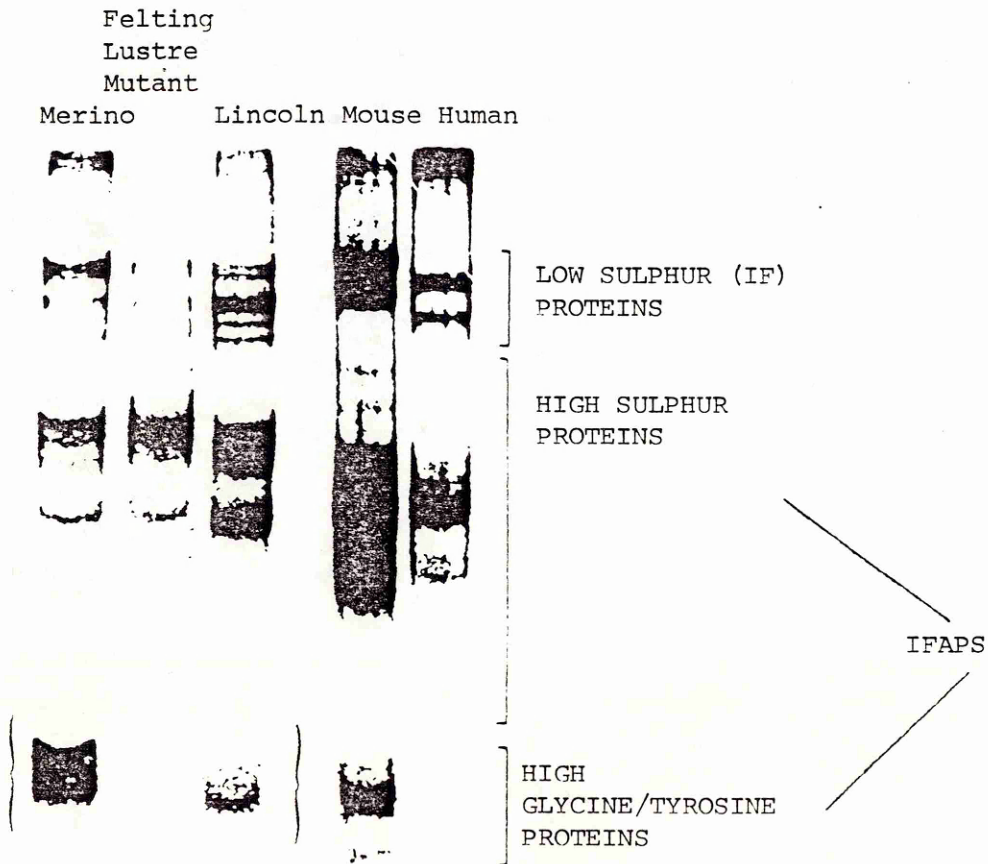


Figure 1.2 One-dimensional display of wool and hair proteins from different species separated by polyacrylamide gel electrophoresis (PAGE) in the presence of sodium dodecylsulphate (SDS). [Gillespie, 1983]

The UHS proteins belong to the HS protein family [Powell et al., 1983] and contain up to 36 mole % of half cystine (Fig. 1.3). The level of expansion of these proteins in wool is known to increase with an increase in available cysteine. The sulphur content of wool varies with the breed and nutritional status of the sheep [Gillespie and Reis, 1966]. Their presence in wool or hair is routinely detected by extracting the keratin proteins as S-carboxymethylated derivatives and then separating the components by two dimensional PAGE [Gillespie, 1983]. Although UHS proteins have been known over 20 years they remain largely uncharacterised. The UHS gene of human hair has recently been isolated and sequenced (Fig. 1.3) and shows an extraordinarily high content of cysteinyl residues (~36 mole %).

Tricholyalin exists as granules which make up the inner root sheath of the hair and is present in the cells of the medulla when they are present in hair. It has been partially characterised as a large protein (200 Kd) and is believed to play a matrix-type role. A considerable amount of information is available concerning the biochemistry of hair growth, but falls outside the scope of this thesis. Thus it appears that there are two groups of fibrous proteins which have high proportions of cystine, the UHS and HGT proteins.

```

GGAGGAAGGGCTCATACTTGGATCCAGAAATATCAACATAGCCAAAGAAAAACAATCAA
10      20      30      40      50      60
GACATACCTCCAGGAGCTGTGTAACAGAACCGGAAAGAGAAACAATGGTGTGTTCTATG
70      80      90      100     110     120
TGGGATATAAAGAGCCGGGGCTCAGGGGGCTCCACACCTGCACCTCCTTCTCACCTGCTC
130     140     150     160     170     180
CTCTACCTGCTCCACCCTCAATCCACCAGAACCATGGGCTGCTGTGGCTGCTCCGGAGGC
190     200     210     220     230     240
      C G S S C G G C D C S S C G S C G S R C
TGTGGCTCCAGCTGTGGAGGCTGTGACTGCAGCTCGTGTGGGAGCTGTGGCTCTCGCTGC
250     260     270     280     290     300
      R G C R P S C C A P V Y C C K P V C C C
AGGGGCTGTGGCCAGCTGCTGTGCACCCGTCTACTGTGCAAGCCGTGTGCTGTGT
310     320     330     340     350     360
      V P A C T S C S C G K R G G S C G G S
GTTCCAGCCTTCTCTAGCTGTGGCAAGCGGGGCTGTGGCTCCTGTGGGGGCTCC
370     380     390     400     410     420
      K G G C G G S C G C S Q C S C C K P C C C
AAGGGAGGCTGTGGTCTTGTGGCTGCCAGTGCAGTTGCTGCAAGCCCTGCTGTTGC
430     440     450     460     470     480
      S S G C G S S C C Q C S C C K P Y C S Q
TCTTCAGGCTGTGGGTCATCCTGCTGCCAGTGCAGCTGCTGCAAGCCCTACTGCTCCAG
490     500     510     520     530     540
      C S C C K P C C S S S G R G S S C C Q S
TGCAGCTGCTGTAAGCCCTGTTGCTCCTCCTCGGGTCGTGGGTCATCCTGCTGCCAATCC
550     560     570     580     590     600
      S C C C K P C C S S S G G C G S S C C Q S S
AGCTGCTGCAAGCCCTGCTGCTCATCCTCAGGCTGTGGGTCATCCTGCTGCCAGTCCAGC
610     620     630     640     650     660
      C C K P C C S Q S R C C V P V C Y Q C K
TGCTGCAAGCCCTGCTGCTCCAGTCCAGATGCTGTGTCCTGTGTGTACCAAGTGAAG
670     680     690     700     710     720
      I
ATCTGAGGCTCTAGTGGGAAACCTCAGGTAGCTCCCGAAGATCTGTGCTTTCCAACAAGT
730     740     750     760     770     780
TACCCTTGAAGCACATCCCCTTCTGAATCTGAAAAGAGCCTTGGCTCAGGGCGTCTTTTT
790     800     810     820     830     840
CCAGCCCCTGAGGAAATGGAATGAACCACTCCCTGCCATTCCCTATAAGAATATCCCAA
850     860     870     880     890     900
GACCCAGGCAATTTTGCCCTCTTTCCACATGCCCCCATATGTCTGAGCCAAACTGCAC
910     920     930     940     950     960
TGGGGGCTGCC
970

```

Figure 1.3 The DNA sequence (preliminary data) for the human gene coding for one of the UHS proteins. The protein has 160 amino acids including an extraordinarily high content of cysteinyl residues (36 moles %) and is also rich in serine (24 moles %) and glycine (16 moles %) residues. Repeating regions can be identified in the conceptual amino acid sequence and two of these, each 19 amino acid residues long, are underlined.

### 1.3 Morphological structure of wool

Wool belongs to the same family of proteins, the keratins, which form the major constituents of epithelial cells such as in horn, skin and quills of feathers. There are special features which distinguishes wool from other hairs which also render it supremely valuable as a textile fibre. But the differences are of a physical nature,

and the basic tissues and chemical structure of all animal hair including wool, are similar. Despite the complex nature of the morphological structure of wool fibre, it comprises essentially two distinct regions, the cuticle and the cortex as shown in Fig. 1.4.

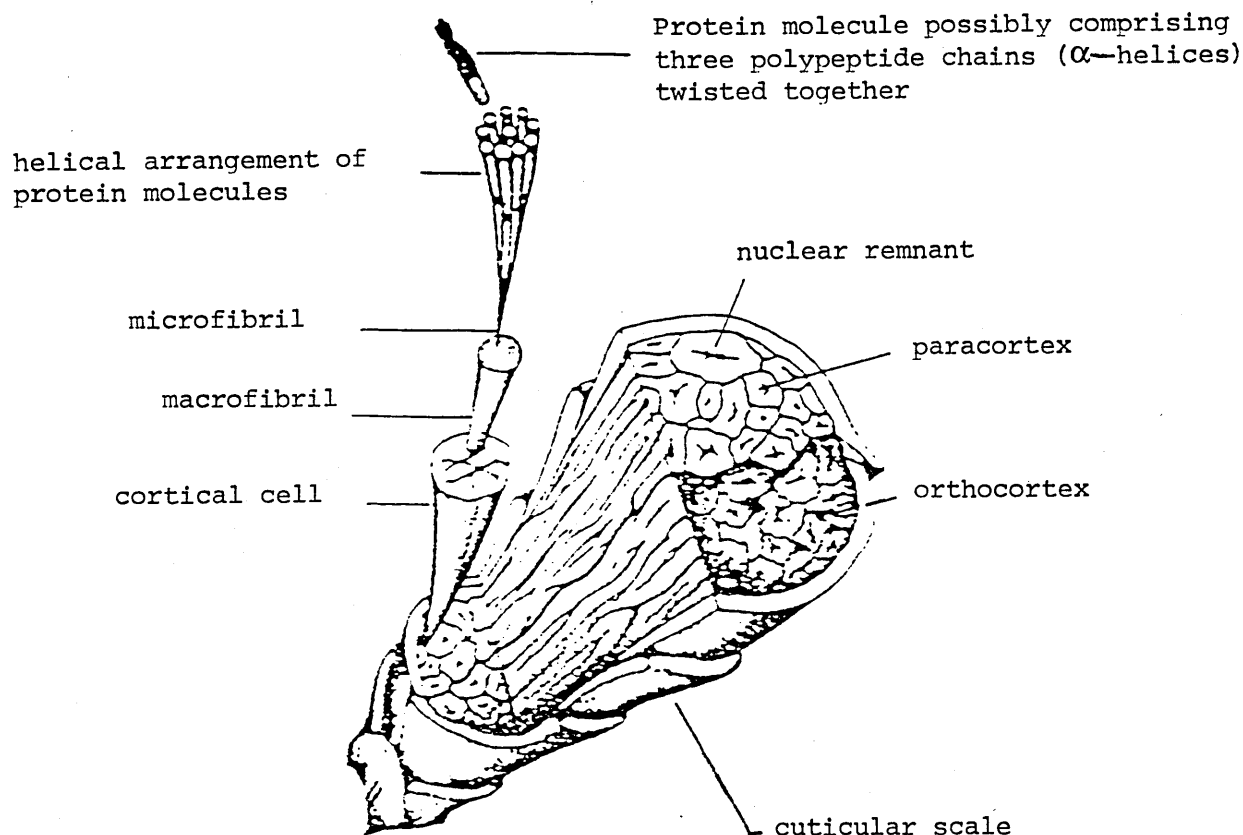


Figure 1.4 Sketch of a broken section of a fine wool fibre showing the major cellular components and the detailed structure within them.

The cortex is the main body of the fibre and consists of spindle shaped cells that are of the order of 100  $\mu\text{m}$  long and 4  $\mu\text{m}$  wide [Brown and Onions, 1961]. These cells are cemented together by an intercellular membrane located mainly at the cell tips [Dobb, 1963]. The cortical cells comprise more than 90% of the total fibre mass of most wool fibres. Mercer [1953] showed that in naturally-crimped wool fibres there are two types of cortical cells, the orthocortical and paracortical (Fig. 1.4), the less stable and the more chemically labile, respectively.

He [1953] found that the paracortex has a higher content of cystine than the orthocortex; a more reactive fraction of the cystine of keratin occurs predominantly in the orthocortex. The disulphide bridge of the amino acid cystine is thought to stabilise the keratin by cross-linking the peptide chains, and an uneven cystine distribution could be a cause of the difference in stability. Horio and Kondo [1953] showed that the distribution of the ortho- and the para-cortical cell is bilateral by using a method of differential scanning, and each forms an approximate semi-cylinder (Fig. 1.5).

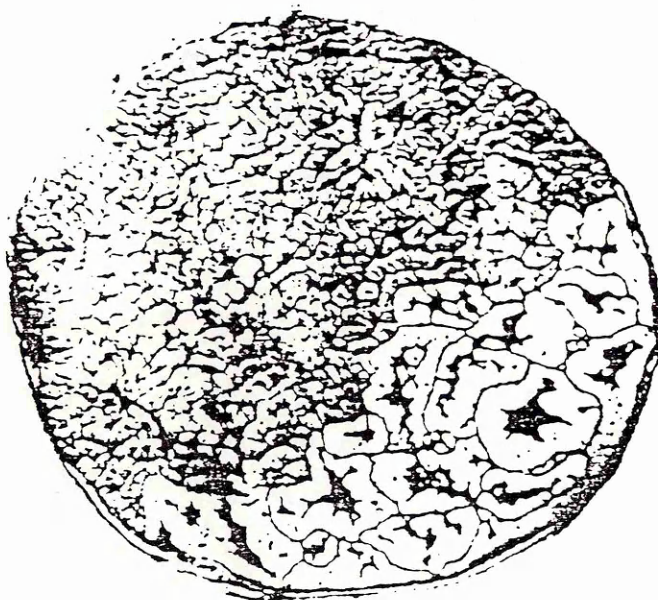


Figure 1.5 Electron micrograph of a cross-section of a Merino wool fibre showing the darkly stained orthocortex and the lightly stained paracortex.

[Fraser, R.D.B. et al., 1972]

Microscopic examination of cross-sections of wool fibres show that cortical cells are composed of filamentous material, called macrofibrils which span the length of the cell and contain small nuclear fragments. Electron and light microscopy of wool fibres that have been reduced with thiols, and stained with heavy metals, have shown that nine protofibrils are bundled in a circle around two more to form an eleven stranded cable, the microfibril. Microfibrils are themselves further

divided into even smaller fibres, protofibrils. The protofibrils appear to be made up of three alpha helices which are the fundamental structure of the keratin molecule. All the above mentioned features of the ultrastructure of wool fibre is represented schematically in Figure 1.4. Protofibrils, however, are not composed entirely of alpha helices arranged in an orderly manner parallel with the longitudinal axis of the fibre, but something like two-thirds is amorphous, with the keratin molecules oriented in a random manner, constituting a zone known as the matrix as illustrated in Figure 1.6. The molecules are bound together with disulphide linkages in both regions, but they are more numerous in the matrix [Hearle and Miles, 1971].

The exterior surface of a wool fibre comprises of flattened overlapping cuticle cells or scales, cemented to one another and to underlying cortex cells by a cell membrane complex which is also susceptible to enzymic or acidic attack. In fine wool fibres, it is normally only one cell thick, whereas the cuticle of human hair and other coarse fibres are several cells thick. The shape and size of the scale may be used to identify some hair fibre types. Microscopic examinations of fibre cross-section shows that each cuticle cell consists of an enzyme-resistant exocuticle region, and enzyme-digestible endocuticle region, surrounded by a thin hydrophobic membrane, the epicuticle [Alexander and Hudson, 1963; Ismail G.M., 1987; Peckett N, 1977]. Some wool fibres contain an axial cavity of cellular construction called the medulla. This is not very significant in most wool fibres and its proportion depends on the type of wool. The coarser type of wool (eg kemp wool) contains ~15% of medulla cells. Generally, the absence of a medulla distinguishes fine wool from all other hairs.

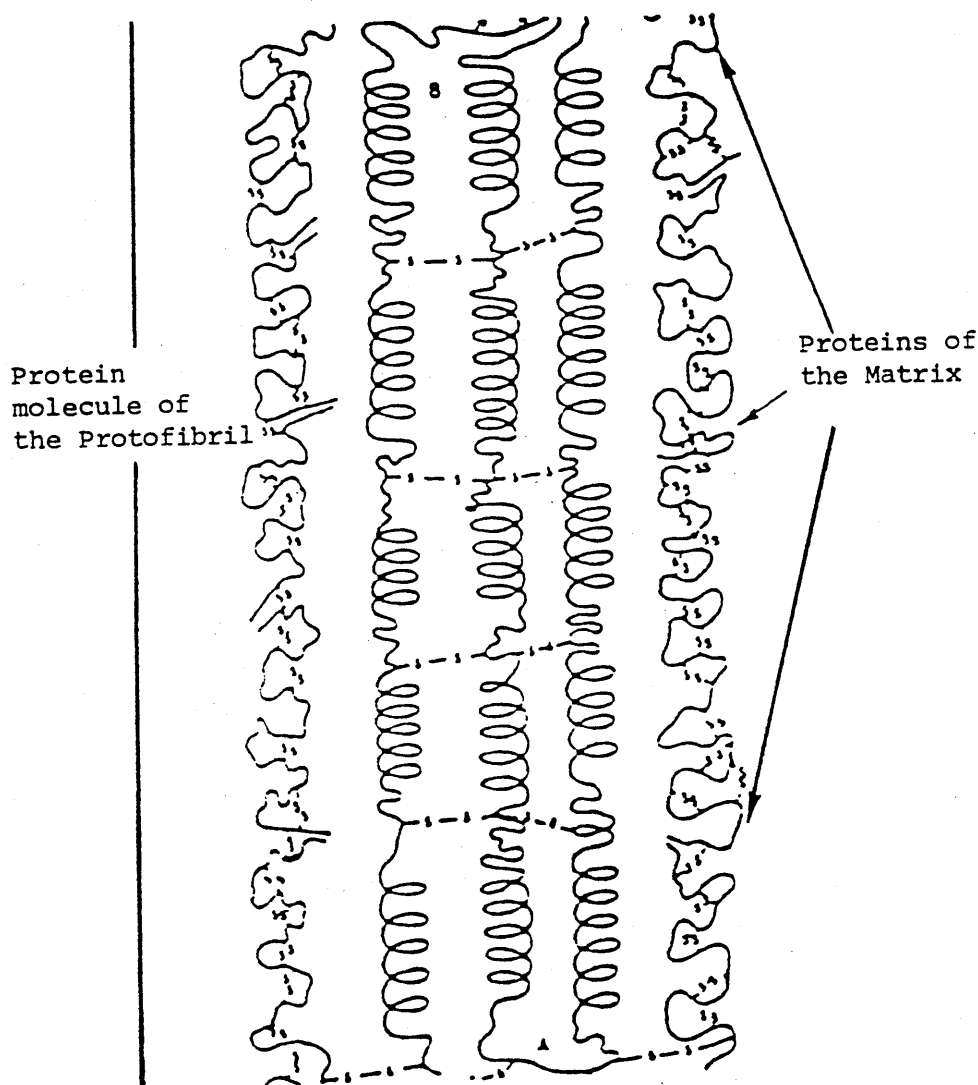


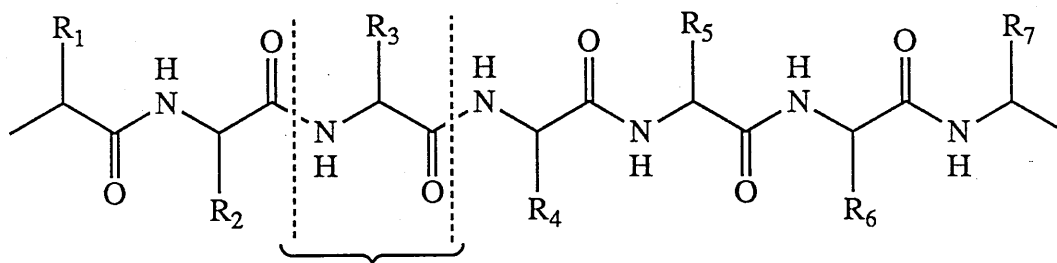
Figure 1.6 Protofibril matrix model for wool. [Hearle and Miles, 1971]

In summary, the cortical region is the main constituent of wool fibres and that the protofibrils which make up the fine structure of wool have a high proportion of cystenyl residues which may undergo chemical reactions. It is now desirable to consider briefly the general structures of proteins in order to understand more fully the properties of wool fibres.

### 1.3.1 The structure of peptides and proteins

Proteins are complex macromolecular compounds composed of long chains of amino acids bonded to each other by amide linkages between the carboxylic groups of one amino acid and the amino group of another. The sequence is known

as a peptide chain, and in proteins contains typically 100-500 amino acid residues (2).



One of the twenty amino acid residues

(2)

The substituent R is one of twenty different side chains of various chemical types. All of the protein amino acids but glycine are chiral and only enantiomers with L-configuration are found. The order of amino acids in the back bone of a peptide chain is known as the primary structure of the molecule. The conformation of the peptide chain gives it a secondary structure through the formation of non-bonding interactions of various types such as hydrogen bonds between  $\text{-NH-}$  and  $\text{-CO-}$  groups. Further bending and folding of the peptide chain creates a tertiary structure of minimum free energy in which the pairing of half-cystine residues to form disulphide bonds such as that found in the fibrous proteins of  $\alpha$ -keratin or in globular proteins of lysozyme occurs. Finally, several peptide units may be associated with each other and with other simple molecules (eg sugars, inorganic residues) to give a quaternary structure as in the haemoglobins and to some extent in the  $\alpha$ -keratins [Open University, 1977; Fletcher and Buchanan, 1977].

Almost all the cysteine residues in normal hair are oxidised in pairs to form disulphide linkages. Some of these linkages are essential for maintaining the structure and function of the proteins, whilst others can be broken without radically changing the protein's behaviour. Therefore, disulphides play an



important role in maintaining the polypeptide chain and disruption can affect the properties of proteins, and hence is worthy of investigation.

The conformation of a peptide chain is determined by the successive rotational angles around the  $C_{\alpha}$ -N( $\phi$ ) and  $C_{\alpha}$ -C( $\psi$ ) bonds as shown in Fig. 1.7 [Phillips and North, 1973]. Only certain values of  $\psi$  and  $\phi$  are energetically favourable, largely because of the repulsive Van der Waals forces between the atoms of the amide units.

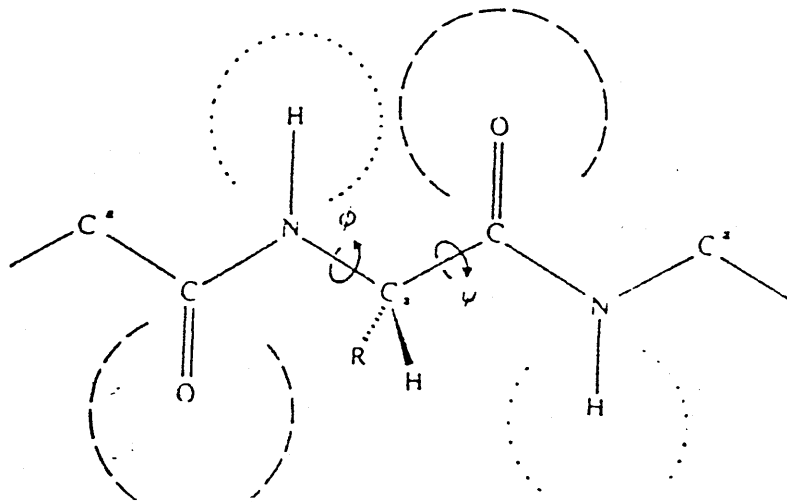
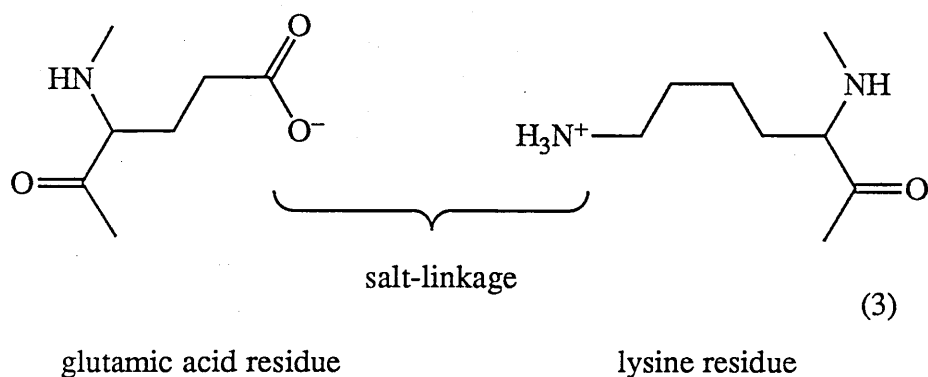


Figure 1.7 Segment of a peptide chain. The only geometrical flexibility lies in rotation about the  $C_{\alpha}$ -N and  $C_{\alpha}$ -C bonds, indicated by the angles  $\phi$  and  $\psi$ .

Apart from hydrogen bonding, there may be other cross-links formed by the interactions of the various sidechains of the amino acid residues, which project out from the main chain to an extent depending on the nature of the group. Such cross-links include: (i) Salt-linkages where carboxyl and amino groups are situated opposite each other (3).



(ii) Covalent linkages which is a very important feature of keratin in which the two cysteine half-residues are joined together to form a covalently bind disulphide bonds (Fig. 1.8, also illustrated in Fig. 1.6). Covalent bonds are much stronger than hydrogen bonds [Wool Sc. Review, 1962]

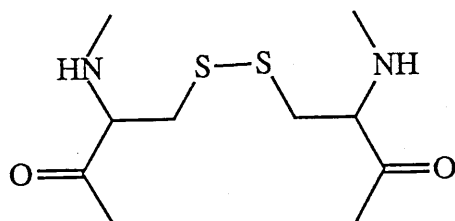


Figure 1.8 Formation of disulphide bond by oxidation of two cysteinyl residues.

### 1.3.2 Keratins

One of the most widely occurring classes of fibrous proteins are the keratins which are insoluble intracellular proteins. Keratins are classified into two groups: (i) the  $\alpha$ -keratins which have high sulphur content (cystine rich, see also Section 1.2) and include the hard proteins of horns, nails as well as the softer, more flexible ones of skin, hair and wool and (ii) the  $\beta$ -keratins that contain no sulphur and are rich in glycine and alanine.

Astbury [1930's] noted that proteins in  $\alpha$ -keratin give X-ray diffraction patterns with a major unit of 0.5 nm along their axes, where as the  $\beta$ -keratin X-ray diffraction pattern had a repeat unit of 0.7 nm. When wool is stretched after

steaming, it produces an X-ray pattern similar to that of  $\beta$ -keratin. Astbury and Bell [1941] explained the elasticity of wool, together with the differences in the X-ray patterns, by the presence of a fold in the peptide chain in the unstretched state. A cable of three helical strands conforms very well with the X-ray diffraction patterns as illustrated in Fig. 1.9. In the helical structure, H-bonds are formed between carbonyl and secondary amide groups in adjacent turns of the coil, as shown by the dotted lines in Fig. 1.9. In  $\alpha$ -keratin the H-bonds are intramolecular and become intermolecular forming the  $\beta$ -structure when the fibre is stretched (Fig. 1.10).

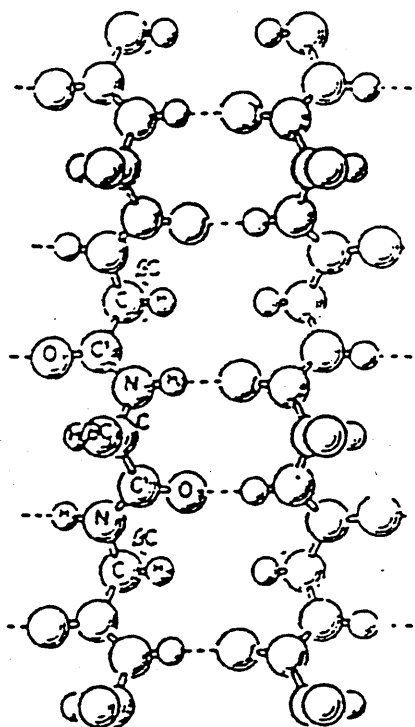


Figure 1.10  $\beta$ -Keratin. The hydrogen bond donors and acceptors are positioned linearly allowing good H-bonding

When all the impurities have been removed (Section 1.5), keratin can be converted into its constituent amino acids by careful hydrolysis and their relative abundance estimated by chromatographic methods. The amino acid content of three typical fibrous proteins and *E. coli* proteins are shown in Table 1.1. It is apparent the high sulfur content in wool is due to the amino acid cystine.

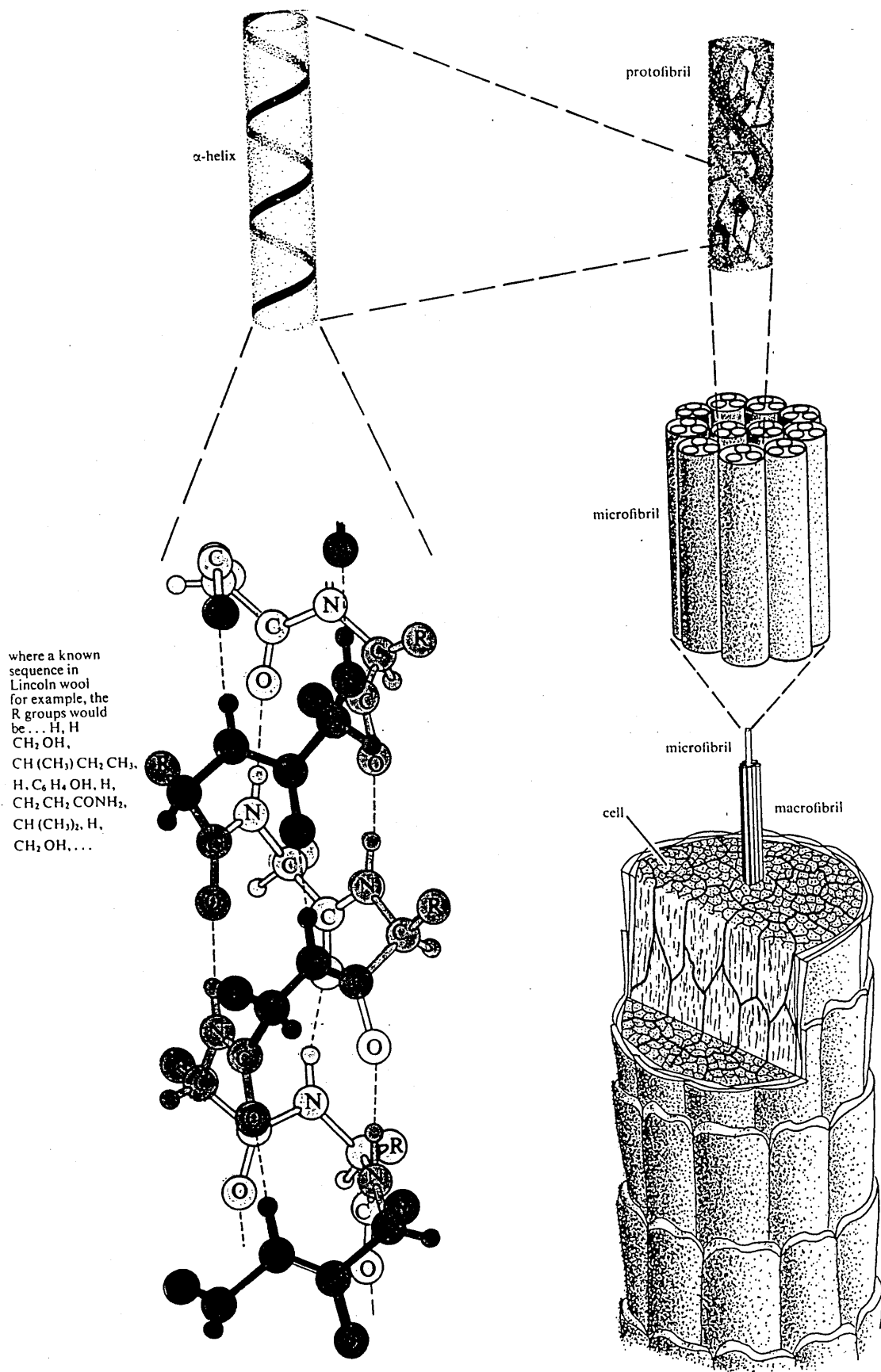


Figure 1.9 Probable organization of  $\alpha$ -keratin within a single hair.

Table 1.1      Amino-acid content of three typical fibrous proteins and *E. coli* proteins, expressed in mole percent of amino acids.

	GLY	ALA	SER	GLU + GLN	CYS	PRO	ARG	LEU	THR	ASP + ASN	VAL	HYP RO	TYR	ILU	PHE	LYS	TRP	HIS	MET
<i>E.coli</i> proteins	7.8	13.0	6.0	10.8	1.8	4.6	5.3	7.8	4.6	9.9	6.0	-	2.2	4.4	3.3	7.0	1.0	0.7	3.8
SILK	44.6	29.4	12.2	1.0	-	0.3	0.5	0.54	0.9	1.3	2.2	-	5.2	0.7	0.5	0.3	0.2	0.2	-
WOOL	8.1	5.0	10.2	12.1	11.2	7.5	7.5	6.9	6.5	6.0	5.1	-	4.2	2.8	2.5	2.3	1.2	0.7	0.5
COLL- AGEN	33.0	10.7	4.3	7.1	-	12.2	5.0	2.4	2.0	4.5	2.3	9.4	0.4	0.9	1.2	2.7	-	0.4	0.8

We have seen that a major constituent of wool is the protein  $\alpha$ -keratin a long chain macromolecule containing many types of amino acids largely in the form of an  $\alpha$ -helix. The helices are linked to each other and to other protein chains by non-covalent forces and also covalently through the sulphur-sulphur bonds of cystine (Fig. 1.6). Chemical changes affecting properties of wool will reflect to some extent the chemistry of the individual residues. Clearly that of cystine deserves particular attention but, as will be seen later, that of other amino acids is also significant.

## 1.4 The chemistry of disulphides

### 1.4.1 Structure of disulphides

It has been shown so far that the proteins of keratin are characterised chemically by a high sulphur content which is present mainly in the amino acid cystine. It is now appropriate to consider the bond forming characteristics of sulphur before discussing the reactions of disulphide groups.

Sulphur-sulphur bonds are found in numerous inorganic, organic and biologically active compounds. One of the causes of this may be the high bond energy of disulphide bonds which, at  $265 \text{ kJ mol}^{-1}$  takes third place among all homonuclear single bonds and is exceeded only by hydrogen ( $435 \text{ kJ mol}^{-1}$ ) and the carbon-carbon single bond ( $330 \text{ kJ mol}^{-1}$ ). The bond energies vary up to  $430 \text{ kJ mol}^{-1}$ , the bond lengths vary between  $1.8$  and  $3.0 \text{ \AA}$ , and bond angles between  $90$  to  $180^\circ$  and the dihedral angles between  $0^\circ$  and  $180^\circ$ . Pauling suggested the  $\sigma$ -bond joining the two sulphur atoms is nearly pure p- in character, which is consistent with a bond angle for two atoms attached to sulphur of  $105^\circ$ . An alternative to the p-bond is  $sp^3$  hybridization since the bond angles are close to that of the tetrahedral value of  $109^\circ$  and since the repulsion of non-bonding  $sp^3$  orbital might explain the dihedral angle [Pryor, 1962]). The optimum strain-free dihedral angle,  $\phi$ , between two substituents attached to the sulphur-sulphur bond in open chain

disulphides is  $\sim 90^\circ$  [Hordvick, A; 1966; H. Yanube et al., 1971]. This conformation is illustrated in Fig. 1.11 which shows repulsion between the non-bonding lone-pairs (shaded) of the sulphur atom is minimized and maximum overlap of these orbitals with the d-orbitals of adjacent sulphur atoms is permitted, leading to a sulphur-sulphur bond with double bond character and restricted rotation [G. Silents, 1960].

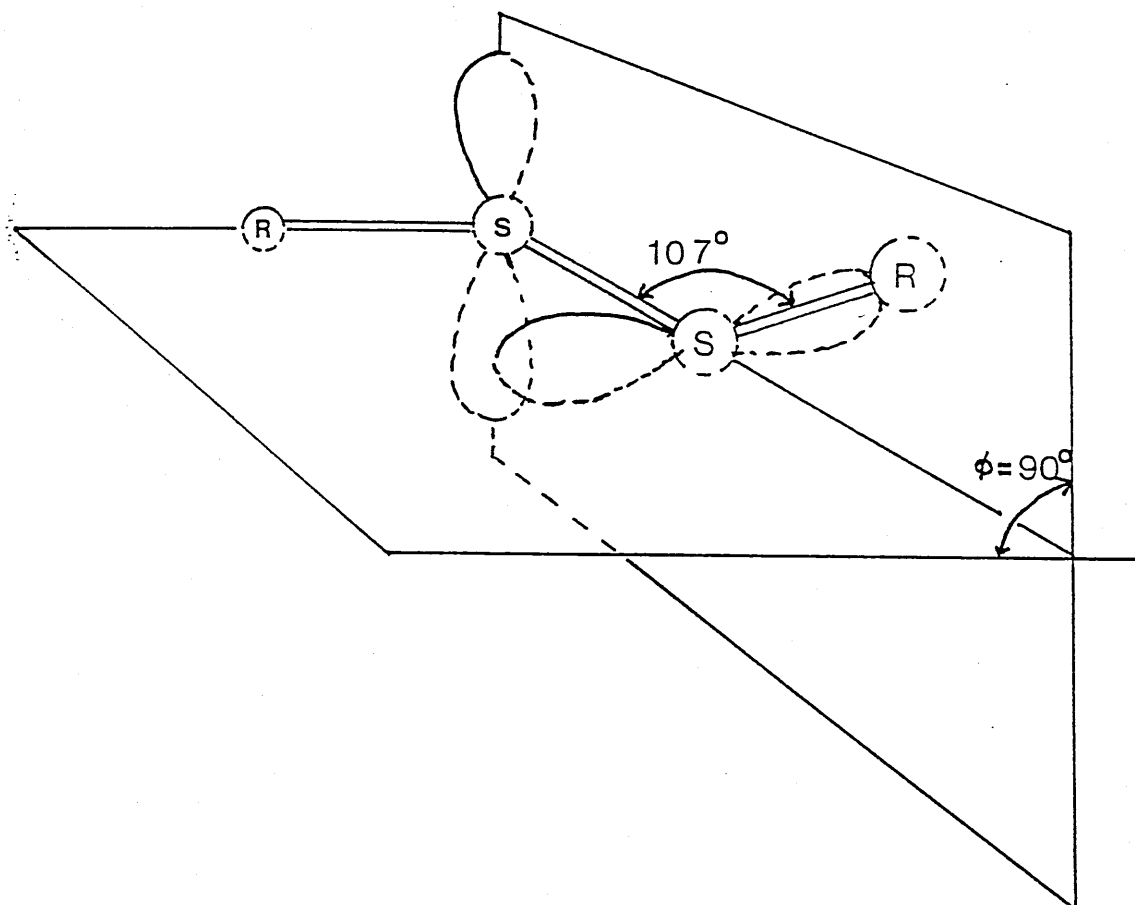


Figure 1.11 Disulphide structure showing orthogonal p-orbitals

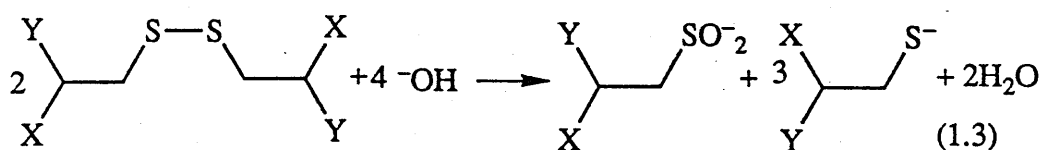
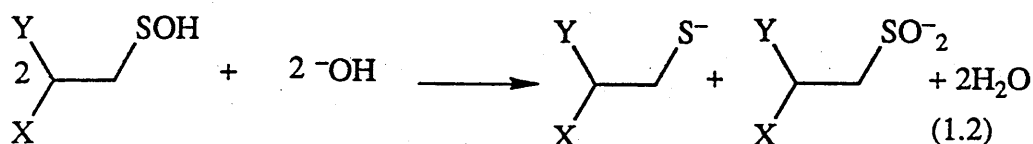
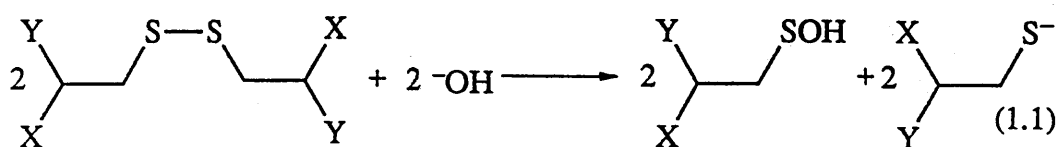
#### 1.4.2 Reactions of disulphide groups

The reactions of disulphide groups are widely investigated because of the importance of disulphides in proteins. Accordingly, much of the discussion derives from amino acid residues in proteins. The chemical reactivity of proteins containing disulphide bonds, is frequently attributed to the reactivity of the cystine sulphur-sulphur bonds. Disulphide bonds are readily oxidized, reduced or cleaved

by hydrolytic mechanisms. This suggests that they may be involved whenever proteins are subjected to chemical stress. The identity of the products formed and mechanisms of such decomposition are important both theoretically and practically in the technology of wool, hair, leather and fuel, and in biochemistry and enzyme chemistry in particular. This section summarises the important thermal and alkaline reactions of disulphide groups in sulphur-containing proteins.

Three mechanisms have been proposed to explain the various products obtained when disulphide compounds are treated with aqueous alkali:

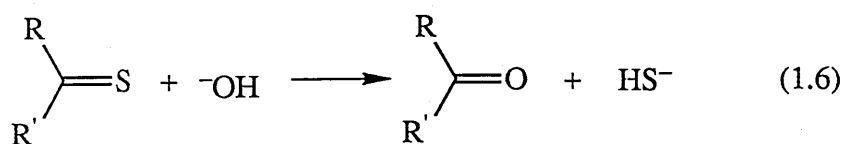
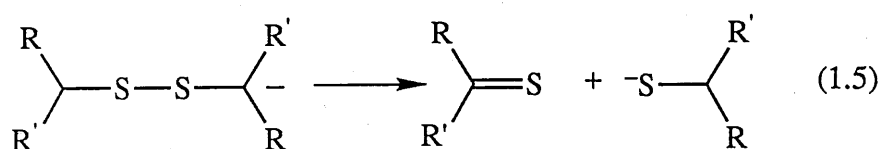
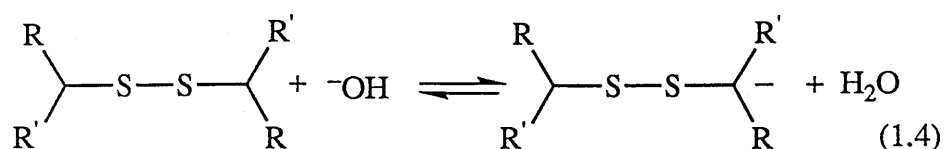
(i) hydrolysis which involves direct nucleophilic attack of hydroxide ion on one of the sulphur atoms of disulphide bonds to form a thiol and a sulphenic acid derivatives (eqns. 1.1-1.3).



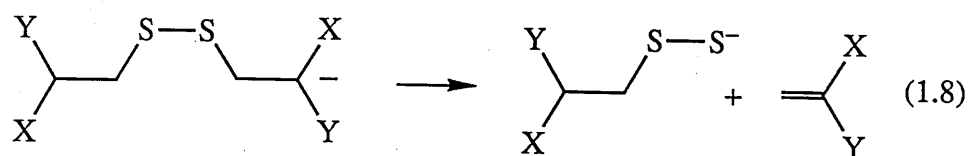
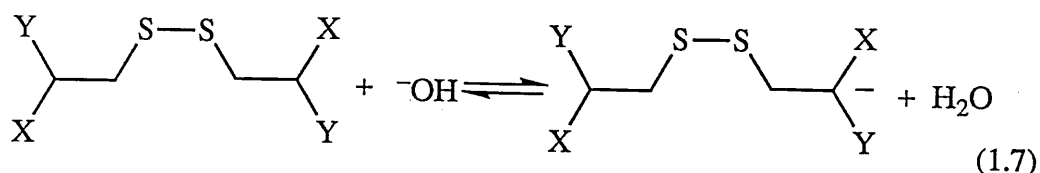
The sulphenic acid formed is unstable or highly nucleophilic [Kice and Cleveland, 1970] and probably undergoes further reaction with disulphide [Rivett et al., 1965] or by dismutation to form RS<sup>-</sup> and sulphinic acid, RSO<sub>2</sub><sup>-</sup> (eqn. 1.2). The overall reaction would be represented as in equation 1.3 assuming decomposition into sulphinic acid. This reaction mechanism is also supported by Schöberl [1937]; Shöberl et al. [1934].



(ii) The  $\alpha$ -elimination mechanism, first proposed by Rosenthal and Oster [1954] involves the initial abstraction of a proton from a carbon  $\alpha$  to a sulphur followed by heterolytic cleavage of the sulphur-sulphur bond giving a mercaptide anion and thioaldehyde or thioketone which would decompose further into an aldehyde or ketone and hydrogen sulphide (eqns. 1.4, 1.5 and 1.6).

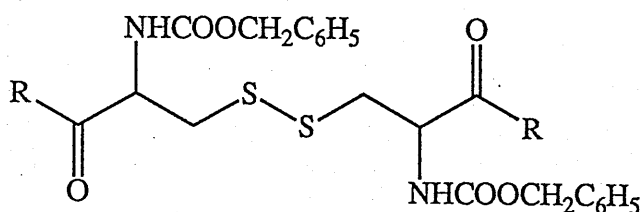


(iii) The most favoured mechanism for the disulphide cleavage has been proposed to be by  $\beta$ -elimination in which hydroxide ion abstracts a proton  $\beta$  to the disulphide bond to form a carbanion, which then fragments to a dehydroalanine derivative and an unstable persulphide (eqns. 1.7 and 1.8).



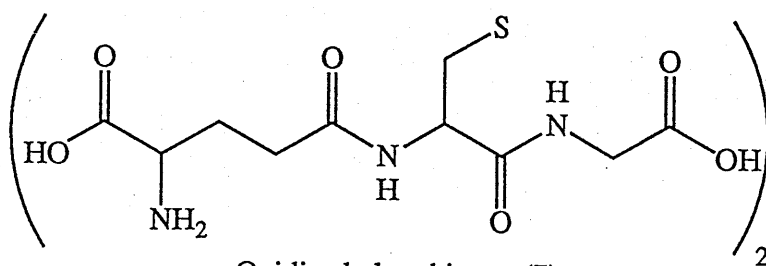
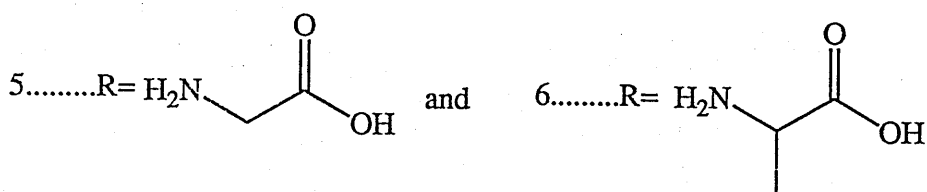
Numerous authors who have studied the alkaline degradation of disulphides in proteins have supported the  $\beta$ -elimination mechanism. Some of the most important and recent studies are summarised below.

Gawron et al. [1967] studied the rate of alkaline decomposition of  $N,N'$ -dicarbobenzyloxy-L-cystinyl diamide, DCCDA (4), diglycine, DCCG (5), dialanine, DCCA(6) and of oxidised glutathione(7) by following the formation of pyruvic acid (acid hydrolysis of dehydroalanyl residue, the intermediate product, eqn. 1.9) and the persulphide [Cavallini, et al., 1960].

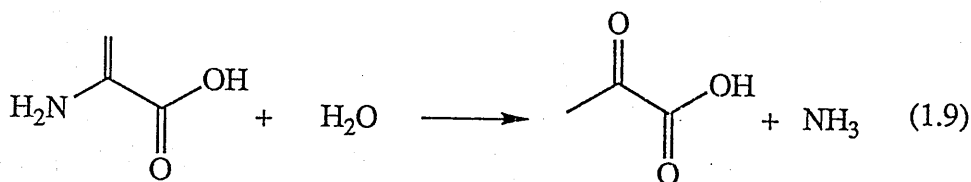


$N,N'$ -Dicarbobenzyloxy-L-cystinyl.....

4.....  $R = NH_2$



Oxidized glutathione (7)



They showed the rate determining step for the base catalysed  $\beta$ -elimination may be either proton abstraction by the  $\text{OH}^-$  group (eqn. 1.7) or the fragmentation of the carbanion formed (eqn. 1.8). In both cases they expected the reaction to be first order in disulphide concentration and the interpretation of their results supported the  $\beta$ -elimination mechanism. These authors also studied the rate of formation of pyruvic acid and persulphide by the decomposition of DCCG at 100 °C at several pH values (Fig. 1.12). Comparison of the kinetic curves for persulphide

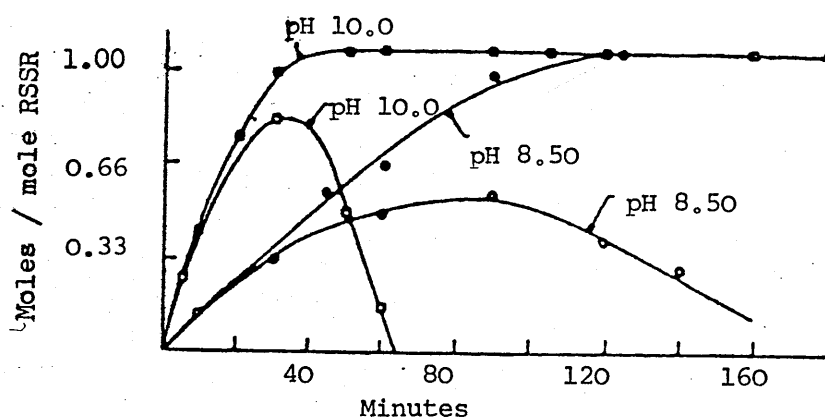
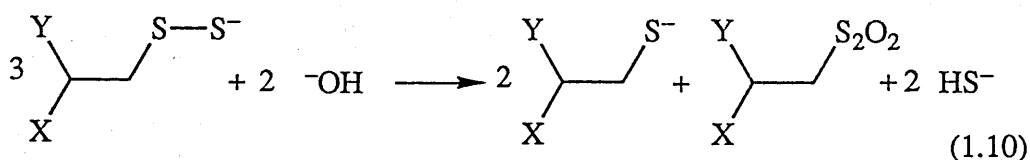


Figure 1.12 Rate curves for formation of pyruvic acid and persulphide by the decomposition of dicarbobenzyloxy-L-cystinyldiglycine at 100 °C at several pH values in 0.2 M borate buffers: ●, pyruvate, ○, persulphide.

and pyruvic acid indicated a similar pH dependence for initial rates of appearances of the two products and alkyl persulphide instability under the reaction conditions. Investigation of persulphide decomposition showed the presence of alkyl mercaptan and sulphide ion but not sulphur (eqn. 1.10).



At 100 °C, pH = 10, the stoichiometric ratios of products per mole of DCCG are 0.67 mercaptan, 0.67 sulphide ion, and 1.0 pyruvate while at 30 °C in 0.1 M sodium

hydroxide the corresponding ratios are 0.73, 0.1 and 0.97. These data clearly indicate the labile nature of persulphides at high temperature and alkaline conditions.

Donovan and White [1971] studied the rate of reaction of hydroxide ion with disulphide bonds of ovomocoid from chicken egg white as a function of temperature by following the appearance of thiol spectro-photometrically at 240 nm. These authors proposed the  $\alpha$  and  $\beta$ -elimination mechanisms responsible for the degradation of disulphides with the latter more dominant on the basis of their observations.

Giorgio et al. [1977] studied the cleavage of oxidized glutathione (7) by alkali as representative of the cleavage of protein disulphides. The kinetics of the reaction were monitored at  $\lambda = 240$  nm and 335 nm. Oxidised glutathione behaved differently at different hydroxide ion concentration (Figures 1.13 A and B). In dilute alkaline medium little reaction was apparent as was seen from the

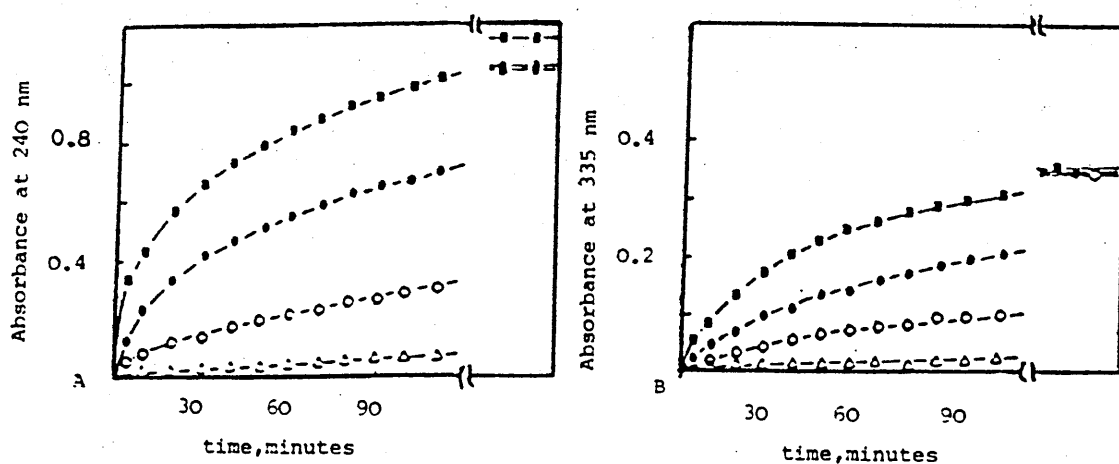


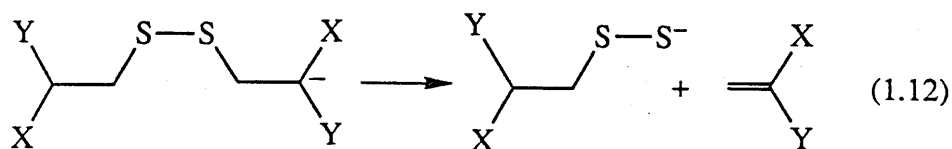
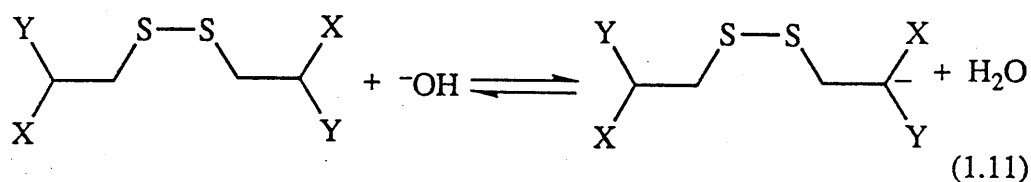
Figure 1.13 Time course of the degradation of oxidized glutathione (A, 0.033 mg/mL at 240 nm; B, 3.33 mg/mL at 335 nm respectively) in alkali [NaOH ( $\Delta$  0.02 N,  $\circ$  0.05 N,  $\bullet$  0.1 N,  $\blacksquare$  0.2)]

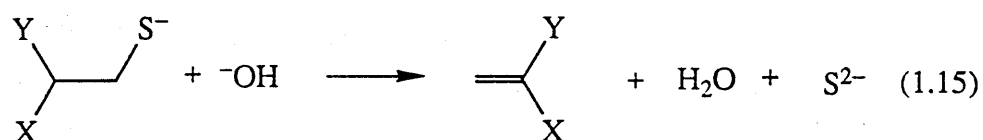
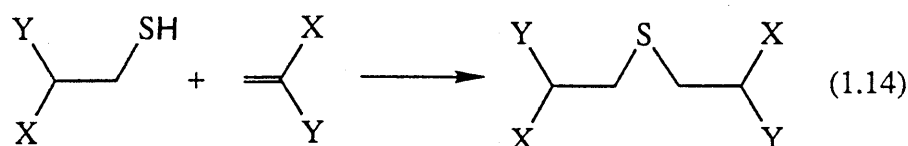
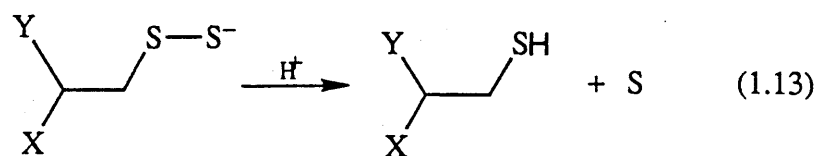
amino acid analysis (Table 1.2), and from the lack of thiocyanate formation (persulphides react with cyanide in alkaline medium producing thiocyanate, Cavallini et al. [1960]). From their results they confirmed that oxidised glutathione undergoes  $\beta$ -elimination at high pH values, and excluded the possibility of alkaline hydrolysis of disulphide bonds as was proposed by Donovan and White [1971] for ovomocoid. They also showed that persulphide groups absorb not only at 335 nm (as already known) but also at 240 nm where, under these conditions, the contribution of other absorbing species is not very high.

Table 1.2 Amino acid analysis of oxidized glutathione after 3h reaction at two different NaOH concentrations

	NaOH $10^{-1}$ N	NaOH $10^{-4}$ N
Gly	1.0	1.0
CySO <sub>3</sub> H	0.43	0.91
Glu	0.96	0.98

Nashef et al. [1977] interpreted the results of their studies on the alkali-treated proteins containing disulphides such as lysozyme as supporting  $\beta$ -elimination as the main mechanism for the cleavage of the disulphide bonds in proteins (eqns. 1.11-1.15).





Lanthionine [S.M. Swan, 1957; Crewther et al., 1965] (eqn. 1.14) is an amino acid formed after treating cystine containing proteins or related compounds with alkali. The base initiates  $\beta$ -elimination to produce a dehydroalanyl residue and an unstable hydropersulphide residue which decomposes to a thiol and elemental sulphur [Bergmann and Stather, 1926; Nicolet, 1931, Tarbell and Hornish, 1951; Nashef et al., 1977]. Thiol adds to the dehydroalanine residue to form combined lanthionine which is hydrolysed to form lanthionine itself.

The formation of meso and racemic-lanthionine [Nashef, et al., 1977] provides more evidence in support of the ready formation of  $\alpha$ -carbanion intermediate where hydrogen can add back from either side of the plane. The elution pattern of meso- and DL-lanthionine in amino acids analysis of a hydrolysate in alkali-treated lysozyme is shown in Fig. 1.14.

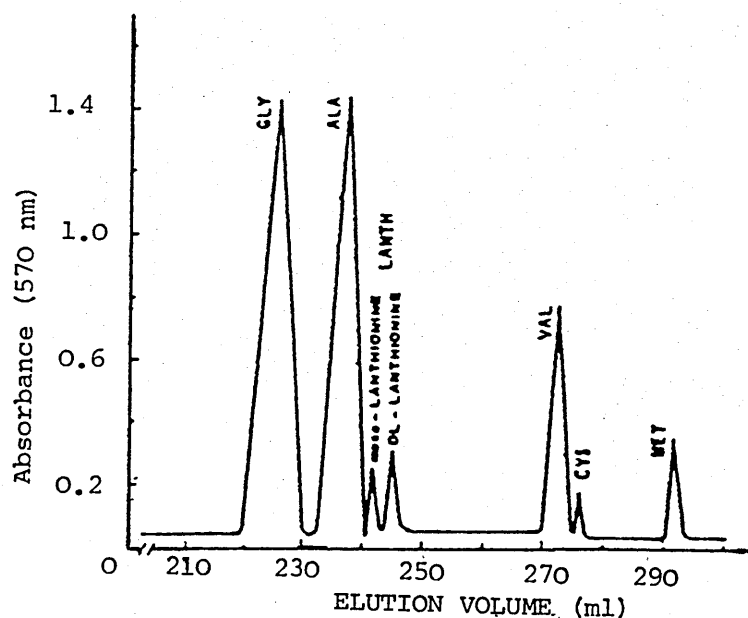
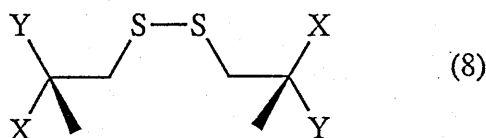


Figure 1.14 Absorbance at 570 nm as a function of elution volume (millilitres) of amino acids of a hydrolysate in alkali-treated lysozyme showing meso- and DL-Lanthionine as a twin peak.

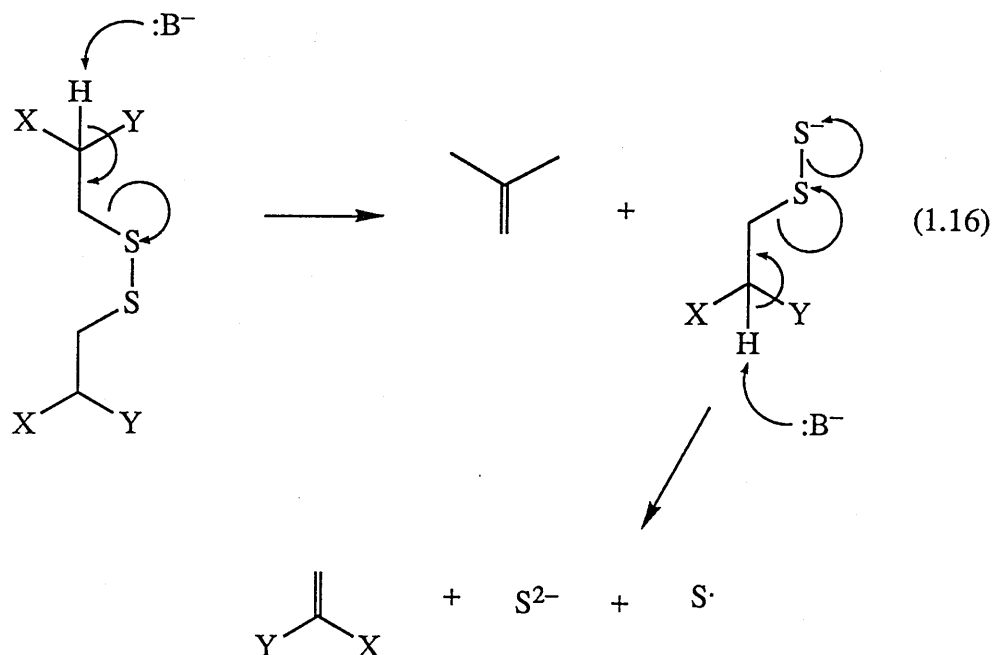
The best evidence supporting  $\beta$ -eliminations mechanism comes from  $\sigma, \sigma'$ -dimethyl cystine (8) which cannot undergo  $\beta$ -elimination because it has no hydrogen on the  $\beta$ -carbon atom, and is not degraded by alkali [J.M. Swan, 1957].



Further evidence for the  $\beta$ -elimination mechanism and the formation of dehydroalanine (DHA) residue is provided by NMR measurements on the formation of DHA from the lysis of the disulphide bonds of alkaline treated insulin and oxidised glutathione [Jones, 1983].

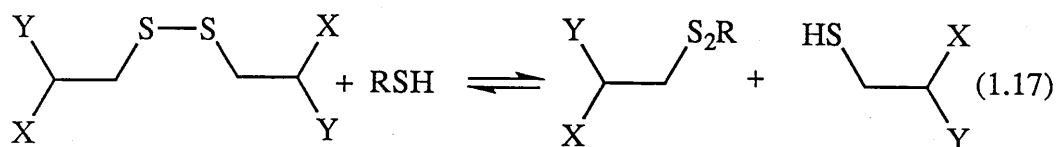
Zahn and Golch [1962] studied effects of pH on the decomposition of cystine and related compounds. The pH-rate profile showed  $\text{H}_2\text{S}$  is eliminated from cystine more readily than from cystine between pH 6 and 11.5. The opposite is true above pH 11.5. When cystine, cystine peptides and wool proteins are heated to  $140^\circ\text{C}$  in polar non-aqueous solvents such as dimethyl formamide (DMF), and in the presence of potassium acetate, blue solutions form. The enhanced

nucleophilic reactivity of potassium acetate appears to promote an elimination reaction and following mechanism is proposed (eqn. 1.16).

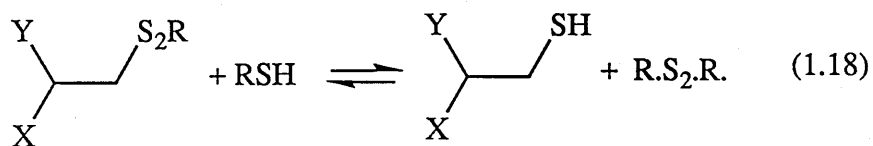


Disulphide cleavage by potassium acetate in hot aprotic solvents.

Thiols which are produced during the alkaline degradation of disulphides (eqn. 1.13) may proceed to react with the disulphide bonds in protein by an interchange mechanism involving two sequential nucleophilic attacks at sulphur by thiol anion, with mixed disulphides being formed as intermediates [Asquith & Leon, 1977], eqns. 1.17 and 1.18.







The equilibrium constants of the reactions are dependent on the redox potential of the reducing agent used and on pH.

Thus it appears that the formation of products from proteins treated with alkali follows a  $\beta$ -elimination mechanism involving the intermediacy of dehydroalanyl residues.

### 1.5 Thermal degradation of wool and yellowing

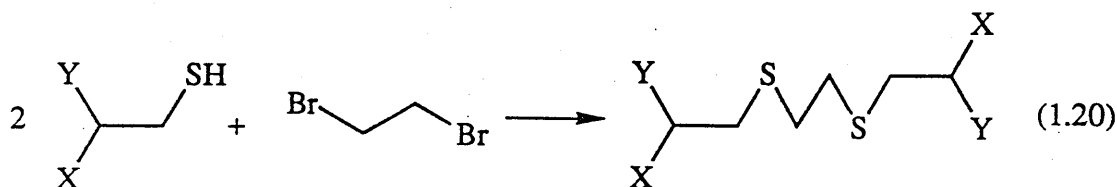
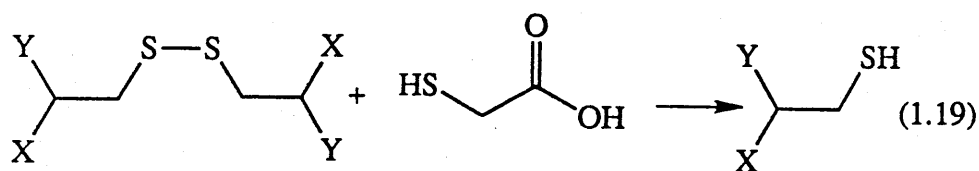
The term "yellow" as applied in the literature of wool, covers a variety of shades from a bright, canary yellow to a deep brown. Howitt [1963] classified wool yellowing as either endogenous, being produced from keratin itself such as pigments produced by irradiation, heat or chemical agents, or exogenous pigments produced by external factors, such as those excreted from the sheep's skin or produced by grass, bacterial or fungal infections, etc. Commercially, most of the exogenous pigments are removed by raw wool scouring (an industrial operation in which the wool is agitated with aqueous soap or detergent), but the most common chemical yellowing is from the effect of heat, alkali or the combination of both on the fibre. It remains a significant industrial problem. Raw wool often contains less than 50% of clean fibre due to contamination by wool wax, dirt, sand and vegetable matter. They are removed by wool scouring in a similar manner as

described above. When all the impurities have been removed what remains is largely keratin.

This section reviews briefly the thermal and alkaline degradation of wool, describing effects of heat, alkali, time and temperature on wool.

### 1.5.1 The effect of alkali

The earliest work on the topic was reported by Font [1915] and Raynes [1927], but investigations started on the alkaline degradation of wool in earnest with the work of Norton and Nicholls [1960]. They found that wool heated in alkaline buffered solutions (pH = 10.6) at 110-140 °C for 30 minutes, yellows only slightly faster than wool moistened at neutral pH. Above pH 10.6 however, yellowing occurs much more rapidly. The increase in yellowness is directly proportional to the loss of cystine (Fig. 1.15), and the authors [Norton and Nicholls, 1964] concluded that the breakdown of disulphide bridge in cystine contributed to the alkaline yellowing of wool. In support of this, they found that by stabilising the disulphide link in cystine by reduction with thioglycolic acid and blocking the resultant cystine residue with 1,2-dibromo ethane (eqns. 1.19 and 1.20) yellowing was much reduced.



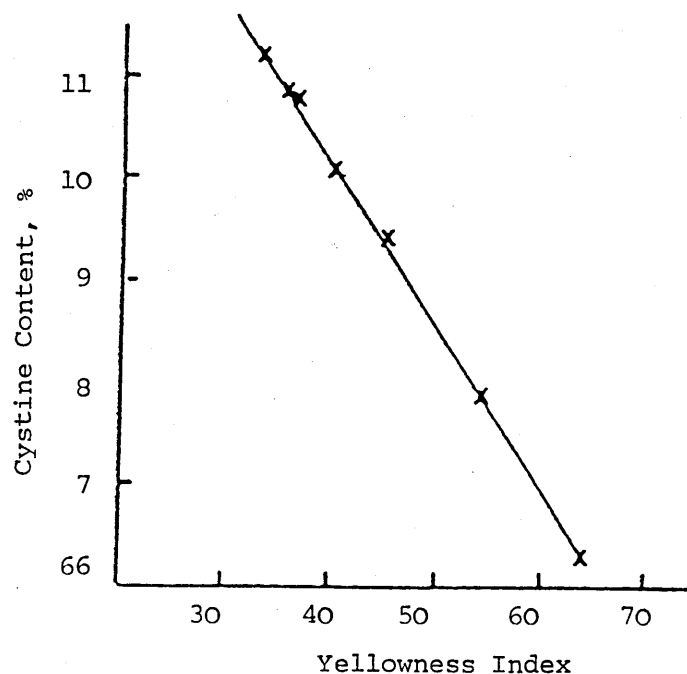
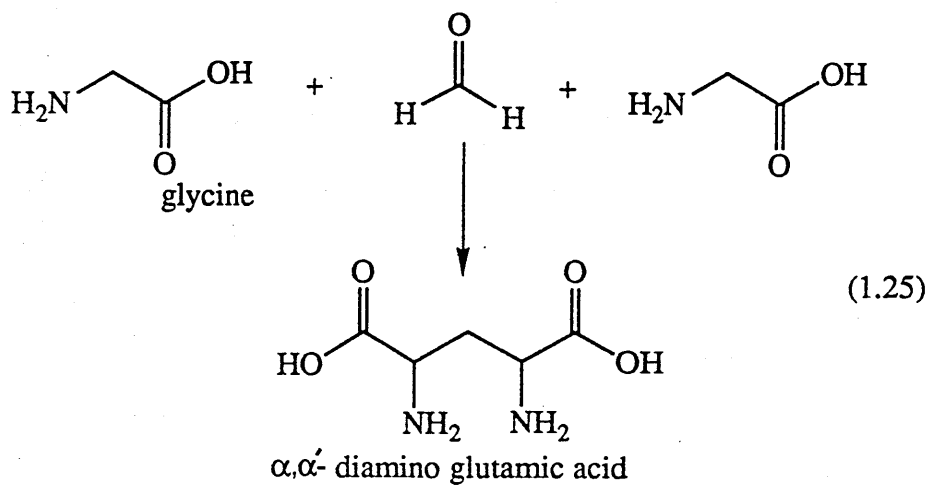
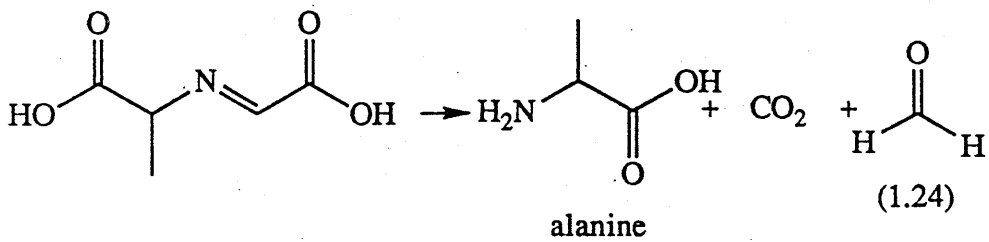
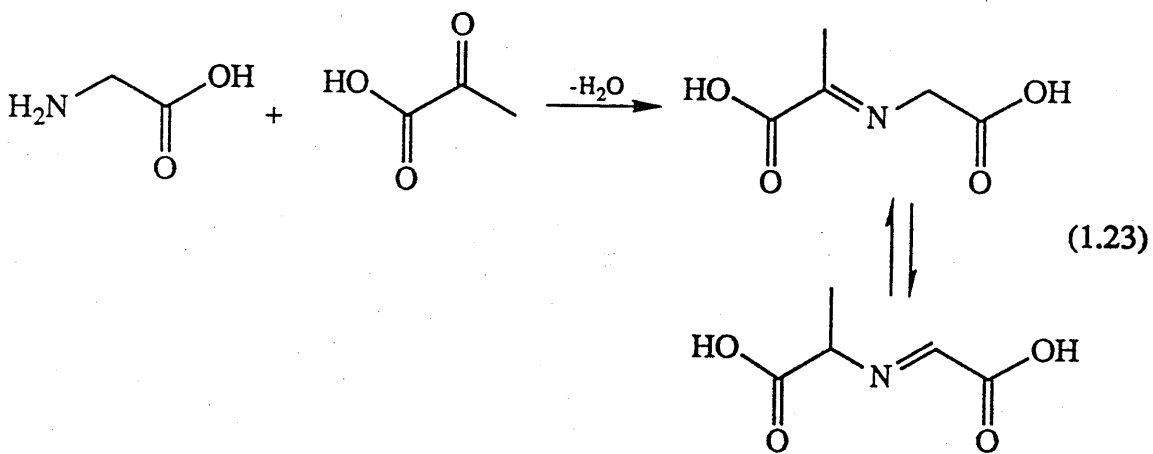
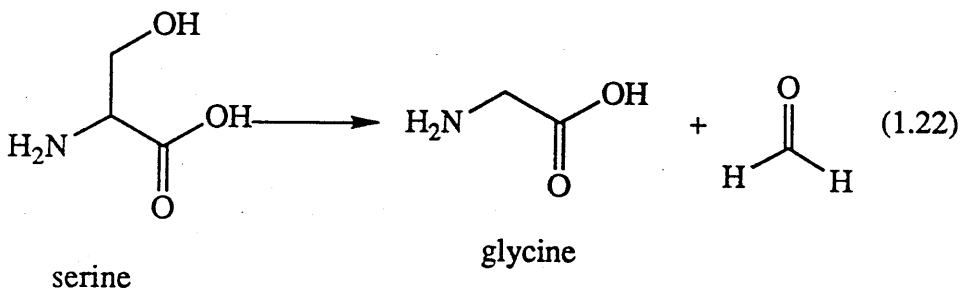
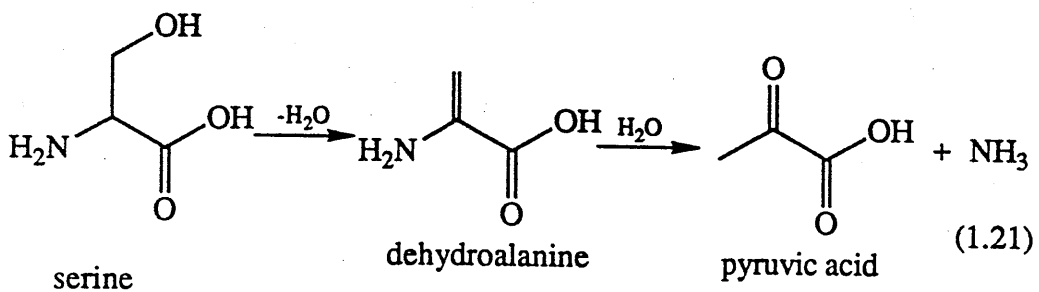
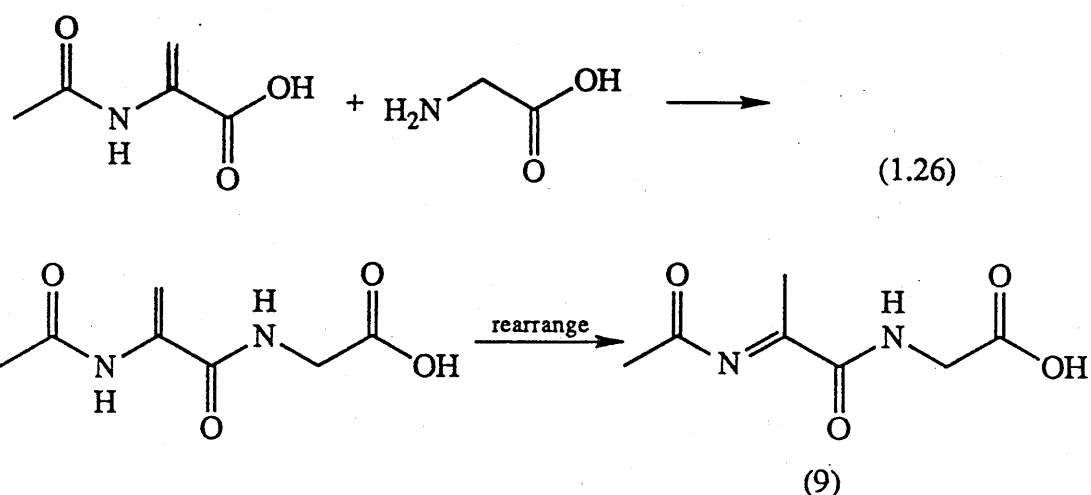


Figure 1.15 Yellowing vs cystine breakdown in alkaline solution. [Norton and Nicholls, 1964]

Norton and Nicholls [1967] continuing their search to establish a reaction mechanism for the heat/alkali degradation of wool, studied the effects on some of the most relevant amino acids in wool of 0.1 M sodium hydroxide for 30 minutes at 90 °C. Of the amino acids examined, cystine, cysteine, serine, threonine and tryptophan produced yellow solutions. Upon analysis of a solution that originally contained only cystine was found to contain cysteine, lanthionine, glycine, djenkolic acid, cysteine sulphinic acid, cysteic acid and some unknowns. Apart from the oxidation products, cysteine sulphinic and cysteic acids, the derivatives above may be formed following an initial  $\beta$ -elimination reaction as seen before. Serine broke down to give glycine, alanine, diamino glutamic and/or adipic acid (eqns. 1.21, 1.22, 1.23, 1.24, and 1.25).



A similar series of reactions has also been proposed to explain the formation of glycine,  $\alpha$ -amino-n-butyric acid and  $\alpha,\alpha'$ -diamino glutamic acid during the alkaline degradation of threonine. Tryptophan degraded to give alanine and an indole. Nicholls and Norton concluded from these studies and those using other model compounds that in the alkaline degradation of wool, chromophore production is started by  $\beta$ -elimination at cystine, serine and threonine to form dehydroalanyl residues and that this is linked in some way to chemical changes in carboxylic and amino side chains. For example, they found that when  $\alpha$ -acetamido acrylic acid is heated in the presence of glycine it yellows, and this suggested that the chemistry illustrated is analogous to that occurring in wool (eqn. 1.26).



Structure (9) is similar to unsaturated ene-diones which are known to be yellow. They did not identify (9), but suggested that if the reaction mechanism were correct then the chain segment  $(-\text{CHR}-\text{CO}-\text{N}=\text{C}(\text{CH}_3)-\text{CO}-\text{NH}-\text{CHR}-)$  would be present in a protein. Since such a segment has not been identified, the hypothesis is difficult to sustain.

Meisswinkel et al. [1982] studied the effects of heat, reaction time and alkali on a wool fibre. The results showed that wool yellowing increases with increases in bath temperature and reaction time (Fig. 1.16 A and B) and that minimum yellowing occurs at pH 6.5 (Fig. 1.17).

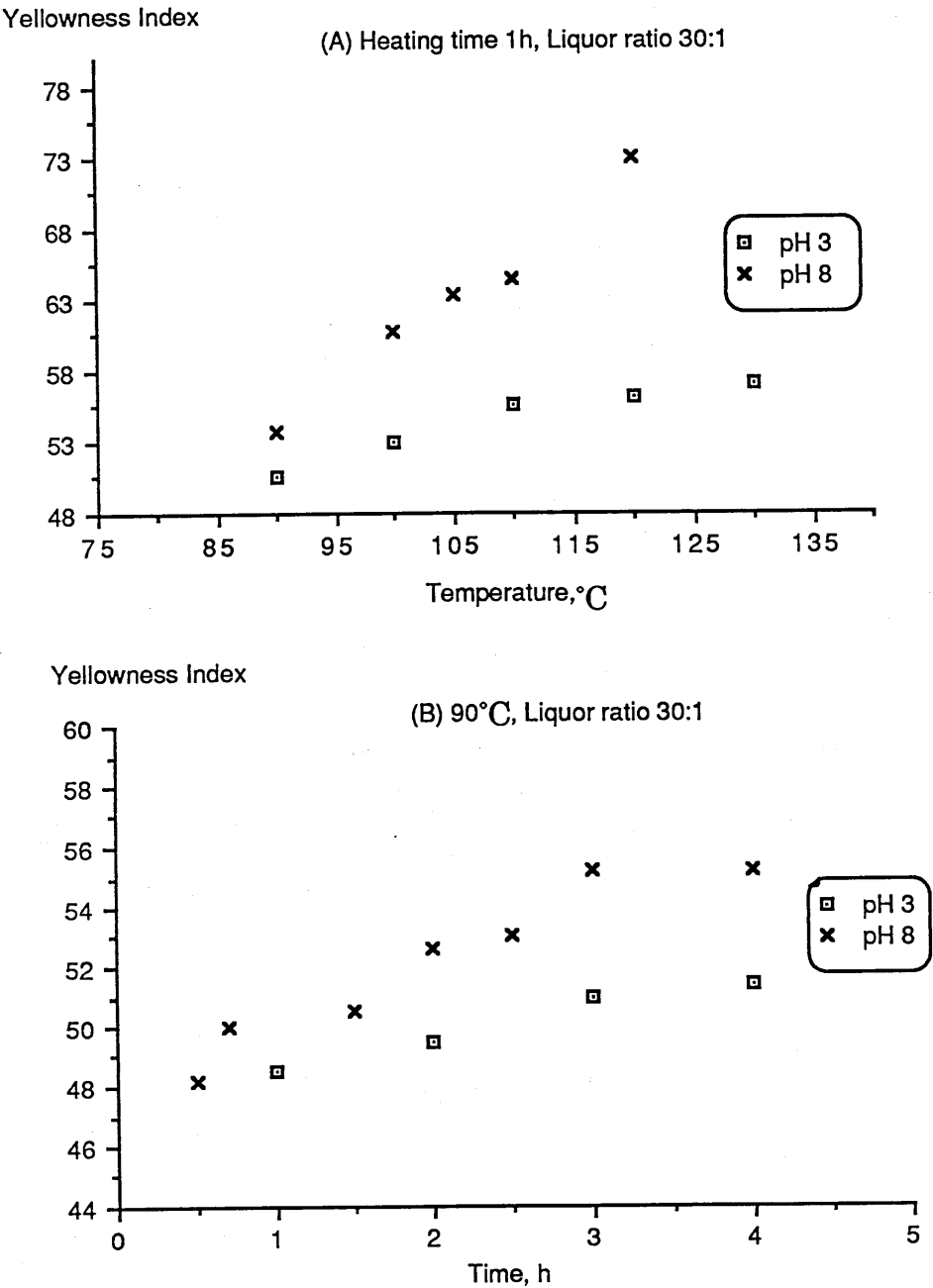


Figure 1.16 A and B show the effect of temperature and reaction times respectively on yellowing.

# Yellowness Index

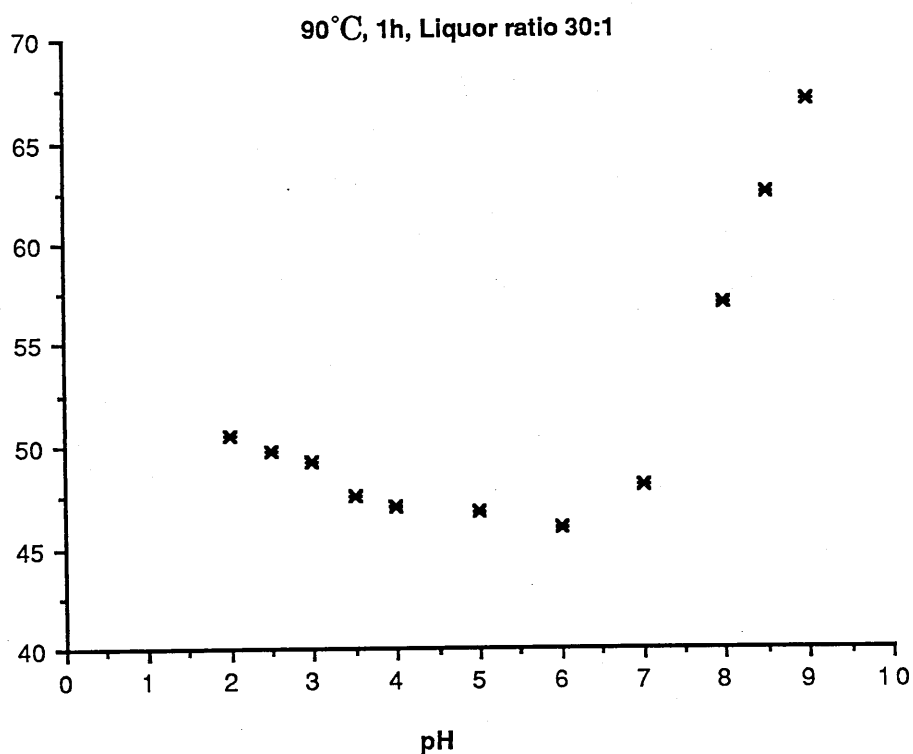


Figure 1.17 Effect of bath pH on wool yellowing

Asquith and Otterburn [1971] and others have shown that dehydroalanyl residues are formed in the alkaline treatment of wool largely on the basis of the addition reactions expected with thiols from cysteine, amines from lysine, and ammonia from other decomposition routes. These reactions are summarized in Fig. 1.18.

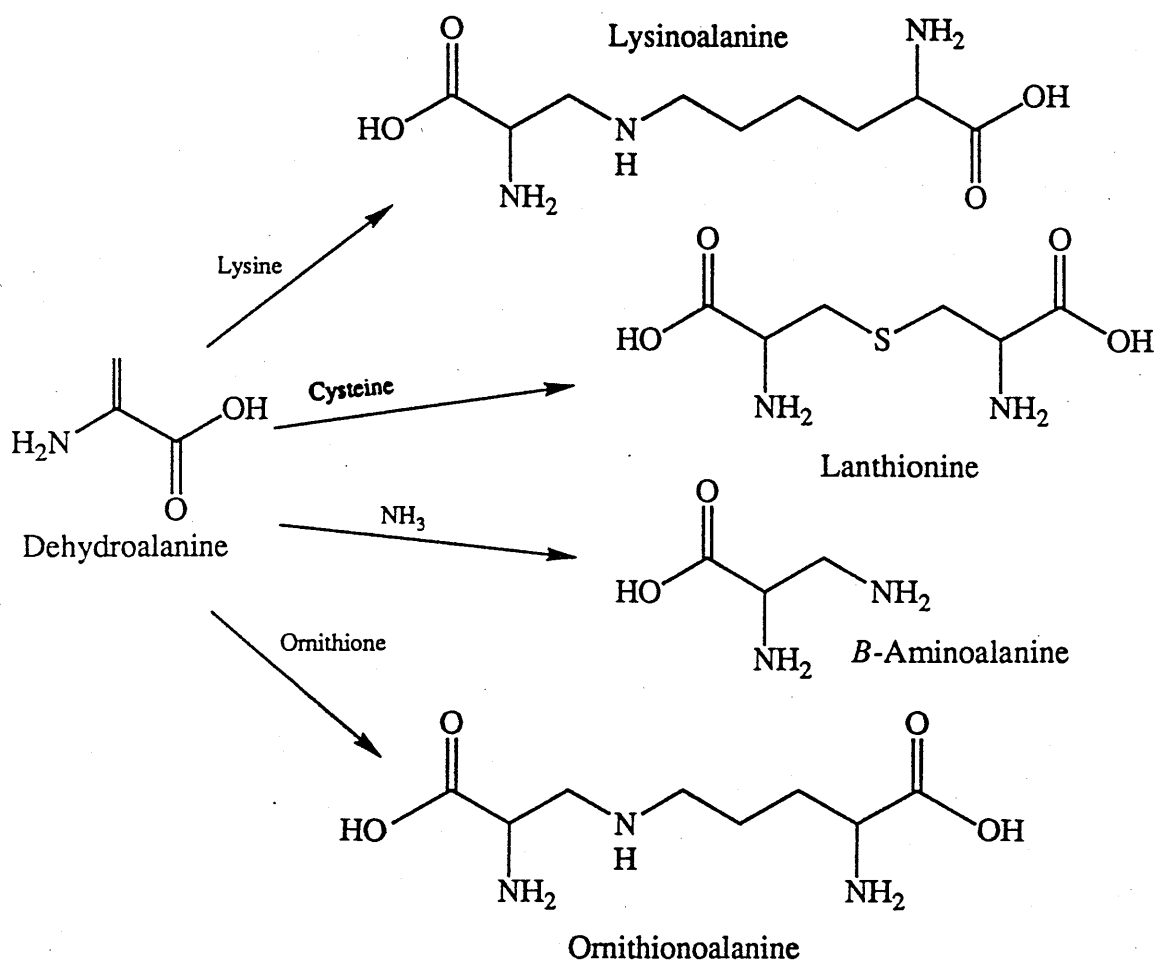


Figure 1.18 Possible products that may form through nucleophilic addition (Michael-type addition) to a dehydroalanine intermediate in alkali-treated proteins

The formation of dehydroalanyl residue was hypothetical for some time until Asquith and Carthew [1971a] synthesised  $\alpha$ -glutamyldehydroalanylglycine(dehydroglutathione) in pure form from reduced glutathione and then identified it in alkali-treated oxidized glutathione. They also suggested for every cysteine decomposition, two dehydroalanyl residues were formed. This observation is also supported by I. Steenken and H. Zahn [1986] who determined the concentration of dehydroalanyl residues and hydrogen sulphide of wool under certain alkaline conditions such as dyeing of wool/cotton blends. They postulated



two-reaction mechanisms closely similar to those of Donovan and White (Section 1.4.2) i.e. hydrolysis and  $\beta$ -elimination.

Steenken and Zahn compared the loss of cystine with the formation of hydrogen sulphide and related the results to alkali concentration and reaction time. Linear correlations were found (Fig. 1.19 and 1.20). From the very low values of hydrogen sulphide they concluded that cystine degradation follows a  $\beta$ -elimination pathway.

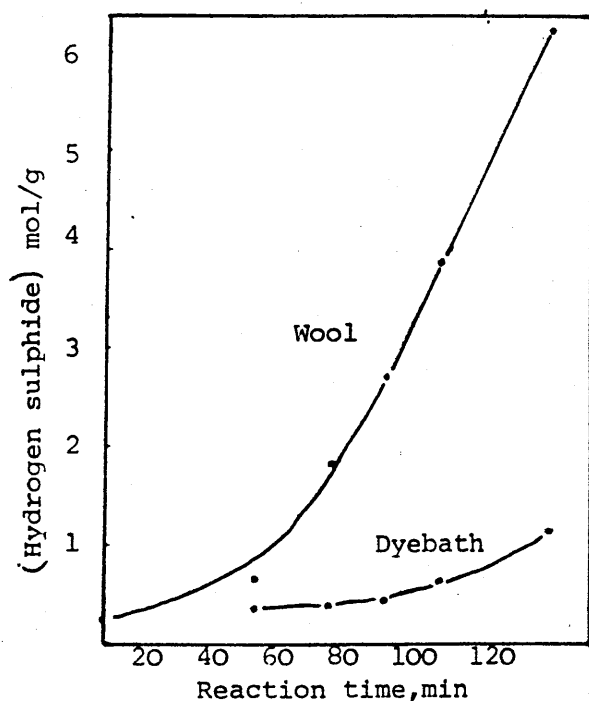


Figure 1.19 Hydrogen sulphide content of wool and dyebath as a function of reaction time

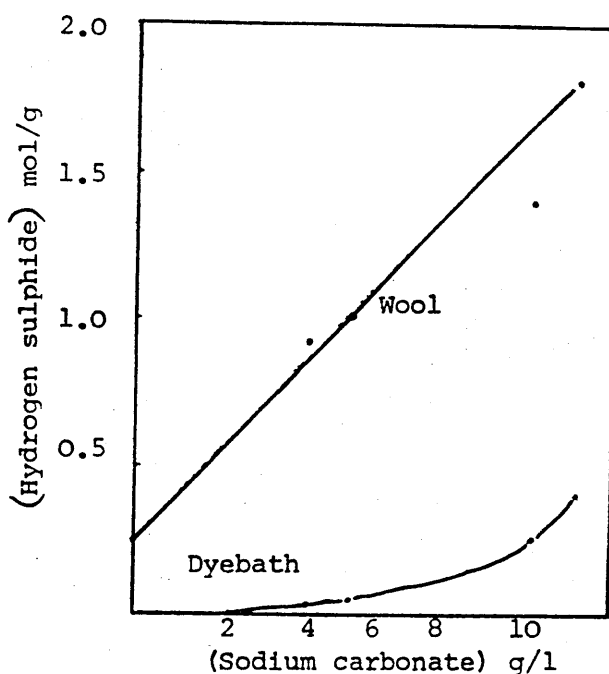


Figure 1.20 Hydrogen sulphide content of wool and dyebath as a function of sodium carbonate concentration (treatment with sodium sulphate, 40 g/l, for 60 min at 40 °C)

Asquith and Dominguez [1968] showed that the extent of addition of thiol or alkylamines to the dehydroalanyl residue is governed by their position, concentration, reactivities in the alkali-liquor, and by the structure of the amino acid or protein. They studied the reactions of wool keratin in sodium hydroxide

solution, noting the effect of various temperatures on the formation of dehydroalanyl addition products (Table 1.3). At low temperatures lanthionine and

Table 1.3 Effect of Temperature of Treatment of Wool Keratin (with 0.1 N Sodium Hydroxide for 30 mins) on the Formation of Dehydroalanine Addition Products

Temperature of Treatment (°C)	Lanthionine formed	Lysinoalanine formed	β-Amino Alanine formed
Control	Nil	Nil	Nil
0	0.15	0.21	-
10	0.29	0.31	trace
20	0.46	0.32	trace
30	1.05	0.49	0.10
40	2.39	1.14	0.14
50	3.40	1.69	0.17
55	3.96	1.88	-
60	4.25	2.01	0.23
70	5.25	2.34	0.26
80	-	-	0.17

lysinoalanine formation are comparable with trace amount of β-amino alanine. At higher temperatures the addition of thiol groups far exceeds the others. At low temperatures the protein structure is least disturbed and lysine groups are in close proximity to the dehydroalanine sites, when these are formed. The addition of ammonia reaches maximum at 70 °C and then declines at higher temperatures since the free ammonia can escape from the open reaction vessel (*cf* dry heat). At low temperatures, the hydrolysis of amide side chains to release ammonia is slower. Asquith and Carthew [1973] used wool keratin in assessing the competition for dehydroalanyl residues, resulting from alkaline treatment in the presence of ammonia and thioglycolic acid separately, and together in the reaction mixture. The results suggested that (a) in the presence of ammonia, ammonia competes partially successfully with the ε-amino group of lysine in addition to dehydroalanine (b) in the presence of a thiol, the decomposition of cystine is

catalysed (also shown by Elliot et al. [1960]) followed by enhanced formation of thioethers. Only at high concentrations of added thiol is lanthionine formation partially inhibited, and (c) thiol addition is more rapid under the conditions pH = 10, t = 60 °C and T = 24h than the amino addition. Lysinoalanine and  $\beta$ -aminoalanine formation is easily inhibited.

Dehydroalanyl residues have been shown to arise from amino acids other than cystine. Asquith and Dominguez [1968] on treatment of some proteins with sodium hydroxide at different temperatures showed that lysinoalanine formation in myoglobin which contains no cystine was comparable with those formed from cystine containing proteins such as insulin. This supports suggestions [Ziegler, 1967; Steenken, 1986 and many others] that dehydroalanyl residues can be formed in proteins by alkaline decomposition of serine.

### 1.5.2 The effect of heat

Although most studies on alkaline degradation have also involved heat, there is evidence that wool degrades at lower pH by a different mechanism. Many authors as early as 1900 [Font, 1916a and b; Woodmansey, 1918] have reported the effects of heat on wool. Above 100 °C, ammonia and hydrogen sulphide are formed and the fibre is both weakened and yellowed. Raynes [1927] claimed that while dry neutral wool was only slightly affected at 100 °C, most wool, especially if slightly alkaline, was both weakened and yellowed and its alkaline solubility was increased. Bell, Cleggy and Whewell [1960] showed that when wool was heated at 200 °C for 6h in air, it was weakened and its cystine and tyrosine content fell - it also became yellow, and both its alkaline and water solubilities were increased. They suggested that the chemical changes involved included the formation of internal peptide bonds.

Asquith and Otterburn [1971] observed that dry heating rendered wool more insoluble in standard solubility tests, and that lysinoalanine, lanthionine and  $\beta$ -

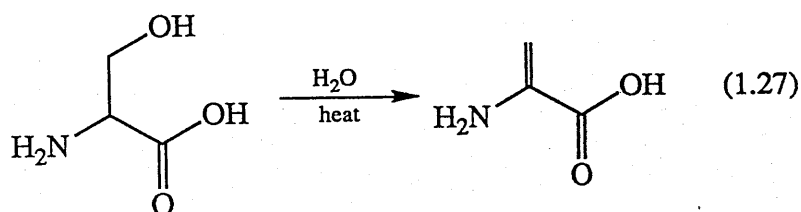
aminoalanine were all formed but not in sufficient amounts to explain the reduced solubility of the fibre. Asquith et al. [1969] postulated a reaction mechanism which involved the formation of dehydroalanyl residues from cystine and possibly serine which subsequently undergoes addition reactions with cysteine, lysine, ammonia to give products lanthionine, lysinoalanine and  $\beta$ -aminoalanine analogous to alkali degradation described in previous sections. It is interesting to note that the amount of  $\beta$ -aminoalanine formed under dry heat conditions (Table 1.4) is far greater than that formed in alkali-treated wool (Table 1.3). The amounts of lanthionine and lysinoalanine are comparable. Zahn [1950] showed lanthionine is formed in wools heated at  $>160^{\circ}\text{C}$  but Asquith [1969] observed some lanthionine is formed at temperatures as low as  $60^{\circ}\text{C}$ . Lanthionine formation is promoted from wool degradation in sealed tubes where there is accumulation of gaseous products especially water vapour which accelerates the degradation rate.

Table 1.4      Formation of Lysinoalanine and Lanthionine on Heating Dry Wool Keratin for 48 hrs.

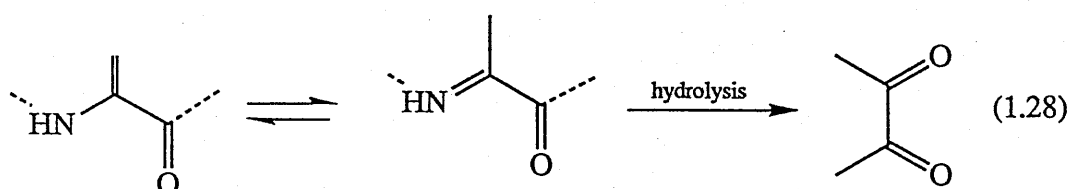
Temperature of Treatment $^{\circ}\text{C}$	$\beta$ -Aminoalanine Content ( $\mu$ moles $\text{g}^{-1}$ )	Lanthionine Content ( $\mu$ moles $\text{g}^{-1}$ )	Lysinoalanine Content ( $\mu$ moles $\text{g}^{-1}$ )
Control	nil	nil	nil
60	3.4	17.0	trace
100	6.7	32.0	1.2
140	8.6	43.0	4.4
160	18.0	44.2	4.8
180	11.0	11.1	6.9

Kirkpatrick and McClaren [1964] modified cystine by reduction and blocking with various reagents. They reported some protection against heat yellowing which was in disagreement with Speakman et al. [1965]. Meybeck [1967a] supported the reaction mechanism for cystine degradation from his experimental work on heated wool, but also suggested that dehydroalanyl residues may be formed from serine degradation (eqn. 1.27), and that Kirkpatrick and Speakman perhaps used

wools of different cystine and serine contents and therefore different susceptibilities of the wool to heat.

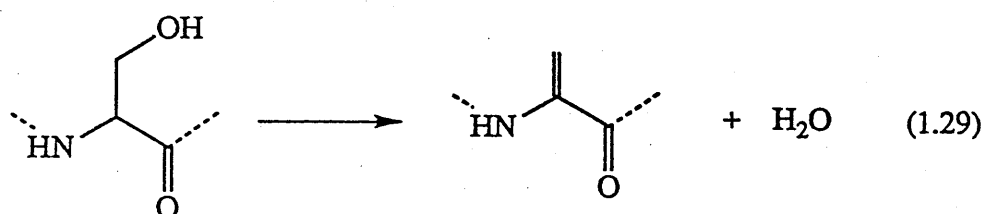


The dehydroalanyl residue is hydrolysed to produce  $\alpha$ -keto-acyl peptide (eqn. 1.28), although how this could cause yellowing is not clear.

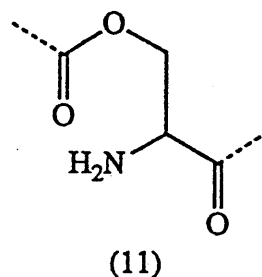
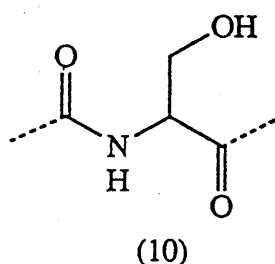


Horio et al. [1965] observed that both serine and threonine had degraded when wool had been heated at 130 °C for 6h. However, when acetylated wools, in which the –OH groups were protected, yellowing was not observed [Speakman and Janowski, 1965]. This led them to conclude that dehydroalanine residues were produced from serine and threonine degradation, but these authors could not see how acetylation techniques which can also acetylate –NH<sub>2</sub> and –CO<sub>2</sub> H groups in proteins could inhibit heat yellowing if dehydro-residues are involved since these are easily produced from cystine degradation. Norton and Nicholls [1964] showed that heat yellowing of wool was reduced when the amino and carboxyl groups in wool were acetylated and esterified, a view which agreed with that of Mazingue and Van Overbeke [1956], but it is difficult to believe that the simple conversion of salt linkages into –CO–NH– bonds is responsible for yellowing. Janowski and Speakman [1965] showed that methylated silk was not thermally yellowed when heated in air at 150 °C for 24h and they concluded that

the hydroxy-containing side chains of serine and threonine residues contributed to the thermal yellowing phenomenon. These authors excluded the hypothesis put forward by Norton and Nicholls and showed acetylation in presence of sulphuric acid gives noteworthy protection against heat yellowing, but the alkali-solubility of the wool is greatly increased. The damage seems to be due to the  $N \rightarrow O$  peptidyl shifts which may minimize heat discolouration by preventing the formation of unsaturated groups from hydroxylic side-chains. They suggested from the experiments with methylated silk a first step in the process of heat yellowing may well be loss of water from serine or threonine to form unsaturated side chains eqn. 1.29.

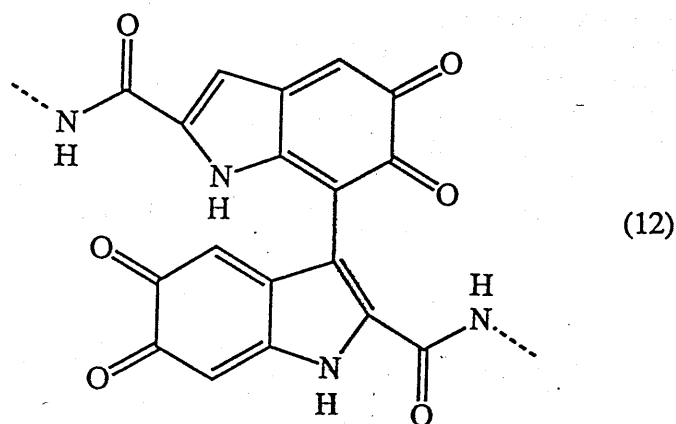


Were this the case, reactions promoting the  $N \rightarrow O$  peptidyl shift might be expected to minimize yellowing (10 and 11):



and that the only reaction, viz acetylation with acetic anhydride, glacial acetic acid and sulphuric acid causes the striking rise in alkali-solubility which is associated with the  $N \rightarrow O$  peptide shift. They also showed the disulphide bonds and carboxylic and phenolic side-chains of wool play little part in heat-yellowing in dry air or nitrogen at 150 °C, but the hydroxylic side chains of serine or threonine, or both, are an important cause of yellowing.

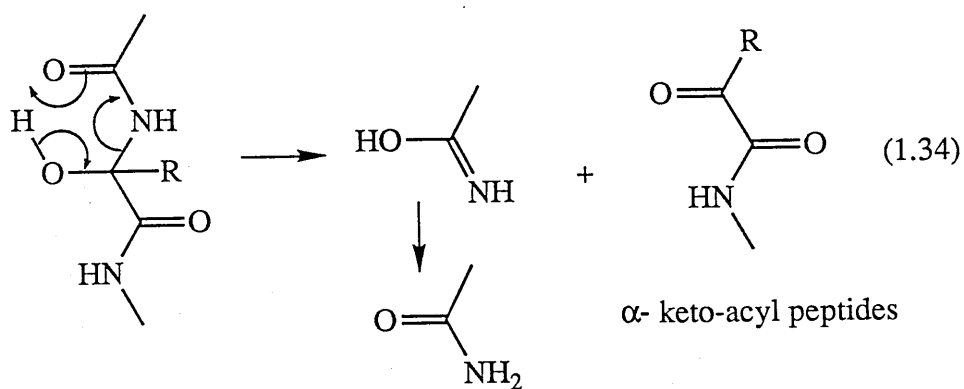
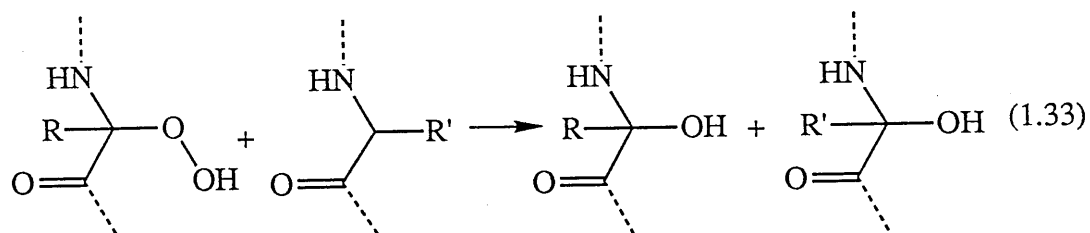
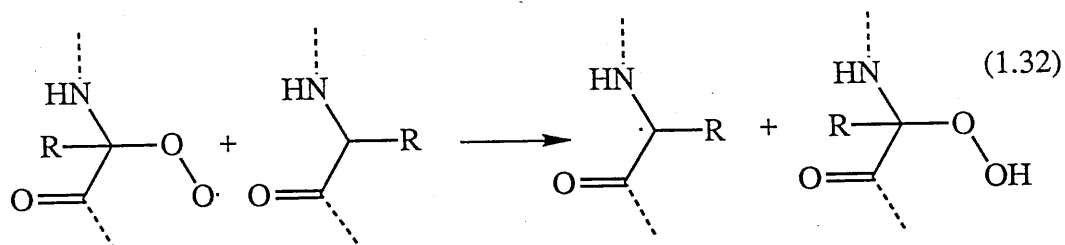
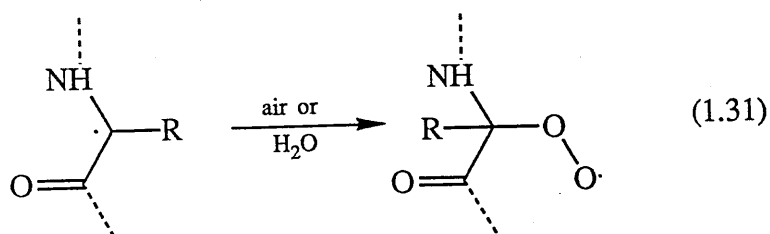
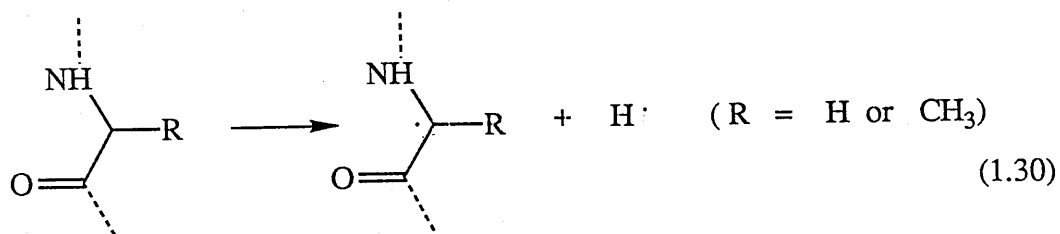
Tyrosine was also shown to be implicated in the heat yellowing of wool when it is heated above 160 °C; Earland et al. [1960] suggested that structure 12 may occur in oxidised proteins.



Postulated melanine crosslink in oxidised proteins.

They suggested that tyrosine is oxidised by a similar pathway to that for its biochemical oxidation to melanine. The role of tryptophan in the thermal degradation of wool is not clear. Norton and Nicholls [1960] observed that free amino acid tryptophan is oxidised to coloured compounds, and that tryptophan is labile in wool heated at 130 °C. Glycine and alanine have also been implicated in wool yellowing. Meybeck and Meybeck [1965] have shown that on heating glycine and alanine residues break down in a similar manner to that which occurs in photolysis, leading to the formation of hydroxyglycine or hydroxy alanine which further rearranges to give  $\alpha$ -keto acyl peptides, eqns. 1.30, 1.31, 1.32, 1.33 and 1.34. It is not clear, however, how the free radical is produced (eqn. 1.30) which may give rise to a peroxy radical in the presence of air and water (eqn. 1.31). This peroxy radical subsequently reacts to give a hydroperoxy derivative (eqn. 1.32) [Meybeck and Meybeck, 1967a]. The hydroperoxide then may react with an adjacent peptide chain to give a hydrated dehydro peptide which finally rearranges to produce an  $\alpha$ -ketoacyl peptide (eqns. 1.33 and 1.34) [Meybeck and Meybeck 1967a, 1967b]. These peptides on hydrolysis produce pyruvic acids. The

breakdown of the main chain accounts for fibre weakening after heating, but it is not yet clear whether these compounds are involved in heat yellowing.





Thus while alkaline yellowing has been attributed to an initial  $\beta$ -elimination reaction involving mainly the amino acid cystine and to lesser extent cysteine, serine and threonine to form dehydroalanyl residues, which then either rearrange or react further to form coloured compounds, no satisfactory explanation has been proposed to explain the dry heat yellowing despite suggestions that the basic amino groups and the amino acids serine and threonine are involved.

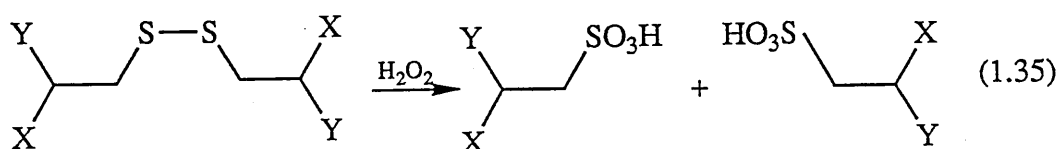
## **1.6 Photochemistry**

### **1.6.1 Photoyellowing of wool**

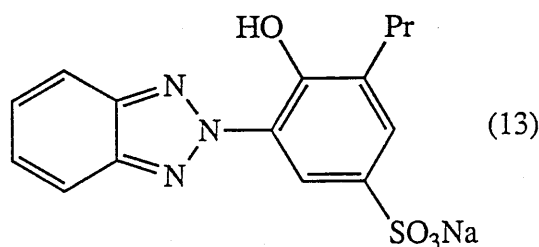
Wool undergoes degradation when exposed to sunlight. Such degradation manifests itself as yellowing and after a prolonged exposure phototendering results which includes the loss of tensile strength and abrasion resistance and altered dyeing properties. Since the enhanced yellowing by sunlight is so easily observed and has such serious commercial consequences, it has been the subject of most of the investigations into sunlight damage in wool.

Several environmental factors have been investigated in relation to their effect on the rate of photodegradation of wool by sunlight. Holt and Waters [1985] have shown that wavelength, temperature and moisture content all have profound effects on the rate of wool photodegradation. Yellowing is caused by the ultra violet component of sunlight, i.e. wavelength range from 400 nm down to 290 nm. The amino acid residues, tyrosine, tryptophan, cystine and phenylalanine have significant absorption up to 350 nm and may be implicated in the photo yellowing. Wavelengths below 290 nm are filtered out by the ozone layer and hence do not reach the Earth's surface. In contrast, irradiation with wavelengths above 400 nm (the visible region) causes bleaching to occur, the effect being maximal between 420-450 nm [Launer L.A., 1965; Holt et al., 1966]. It is often necessary to bleach wool, either oxidatively with alkaline hydrogen peroxide or reductively with bisulphites and when a brilliant white is required wool is treated with fluorescent

whitening agents (FWAs). Unfortunately wool that has been chemically bleached especially by alkaline peroxide or treated with FWAs, yellows much more rapidly and by a wider wavelength range than does natural wool [Milligan and Tucker, 1962]. One of the most important effects of hydrogen peroxide bleaching of wool is the oxidation of disulphide bonds, arising from the high content of cystine in the fibre which leads to the formation of cysteic acid (eqn. 1.35).

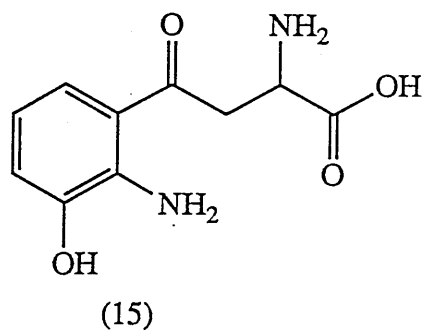
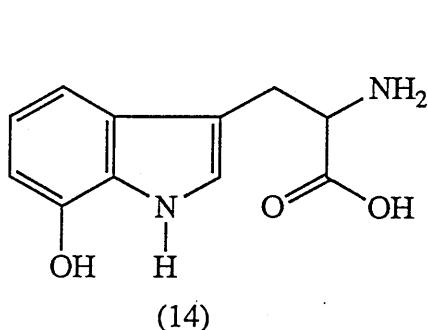


It is suggested that phototendering is essentially due to both disulphide bond breakdown and main chain peptide bond breakdown [Weatheral, 1976; Simpson, 1979]. Wilshire et al. [1985], Simpson et al. [1979] found that useful protection against phototendering and photoyellowing can be achieved by the prior application of a uv-absorber such as sulphonated 2-(2'-hydroxyaryl) benzotriazoles (13) with suitable reducing agents such as hydroxylamine to screen the fibre from the damaging ultraviolet light.



Numerous studies on the yellowing of wool and silk by u.v. light have confirmed that tryptophan is the most likely amino acid residue to be affected. These studies have been nicely summarized [Lewis et al., 1985] and will be mentioned in this section. Many authors [Wool Sc. Review, 1970; Maclaren, 1963; Asquith et al., 1971] have reported that cystine, tyrosine and tryptophan are involved in photodegradation of wool, with tryptophan being as the precursor of the yellow pigment. Holt and Lennox [1966] suggested that oxidation can take place at the benzene ring of tryptophan to give

a hydroxytryptophan (14) which on rupturing of the indole ring would yield 3-hydroxy kynurenine (15), a yellow pigment also isolated from butterfly wing.



### 1.6.2 Ultraviolet and visible spectra

The uv spectra of most aliphatic disulphides show a broad maximum at about 250 nm, which is attributed to conjugation of unshared electrons of the sulphur atom. The uv spectra of aliphatic disulphides (Fig. 1.20) show that each replacement of a hydrogen atom of methyl group results in a hypsochromic shift of about 5 nm and in an increased molecular absorption coefficient [Rosenthal A.N., 1961].

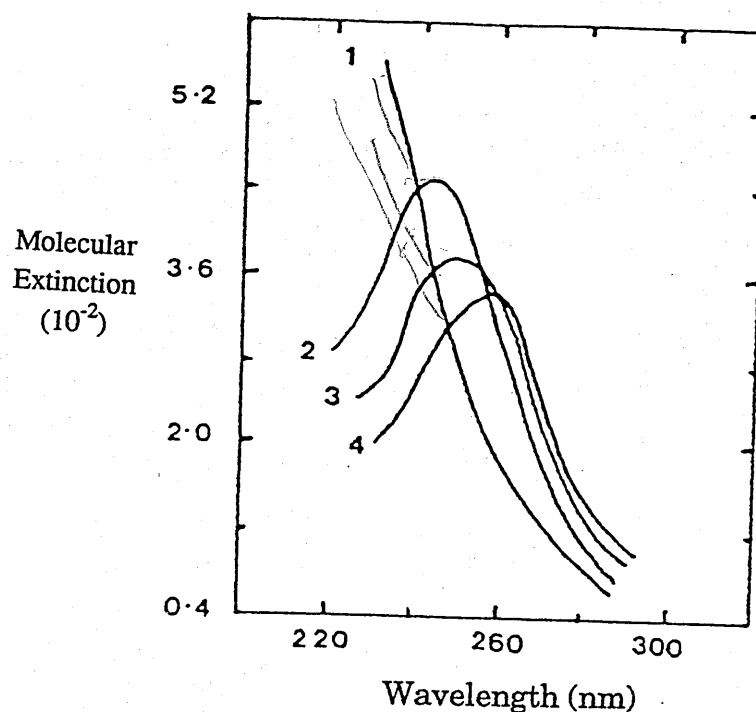


Figure 1.20 Spectra of  $\alpha$ -substituted disulphides in methanol:

- 1 Di-t-butyl disulphide;
- 2 Di-isopropyl disulphide;
- 3 Di-propyl disulphide;
- 4 Dimethyl disulphide.

A hypsochromic shift of 2.5 nm is observed with unsymmetrical alkyl disulphides. The hypsochromic shift of the spectra of the substituted disulphides is ascribed to hyperconjugative interactions of the electrons on the  $\alpha$ -carbon atom with 3d-orbital of the sulphur atom to expand the sulphur octet as expressed in the general form in eqn. 1.36.—



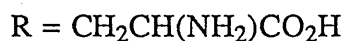
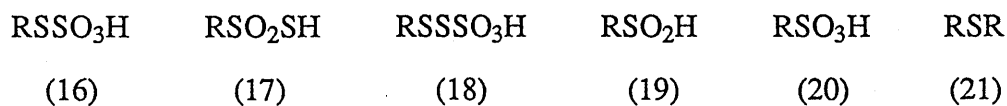
When a pair of electrons on the atom adjacent to sulphur cannot be donated, because of competitive resonance interactions such as with alkyl or dibenzyl disulphides, no characteristic 250 nm absorption maximum was seen [Rosenthal A.N., 1961]. Most disulphides absorb negligibly in the visible region and hence are colourless.

### 1.6.3 Photochemistry of cystine

Although evidence for tryptophan and oxygen causing photoyellowing has been substantiated and the role of cystine appears secondary, the high content of cystine in wool protein prompted a number of studies on photochemistry of this residue. The photolysis of cystine either in the presence or absence of air leads to a plethora of photoproducts, some of which must be presumed to arise from secondary thermal and photochemical processes. The main points of contention with respect to the primary events in direct photolysis seems to be whether S-S (eqn. 1.37) or C-S (eqn. 1.38) bond cleavage predominates. There is evidence for the occurrence of both processes with S-S cleavage probably predominant. All these aspects are well reviewed by Creed [1984].



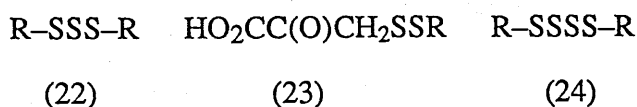
The first thorough study of cystine photochemistry using modern chromatographic and electrophoretic methods of product separation was carried out by Forbes and Savage [1962a]. These authors irradiated saturated aqueous solutions of cystine under either air or N<sub>2</sub> using sunlamp irradiation at excitation wavelengths greater than 280 nm. The products of photolysis in air in diminishing yield were: alanine thiosulphuric acid, 16, alanine thiosulphonic acid, 17, an unidentified product, possibly 18, alanine sulphinic acid, 19, cystic acid, 20, H<sub>2</sub>S and some unknowns. In the absence of air the reaction was much slower, and 19 and 20 were not observed.



Irradiation at 245 nm gave cysteic acid as a major product together with 17 and small amounts of glycine (gly), alanine (ala), serine (ser), cysteine (cys) and lanthionine (lan). A direct hydrolytic reaction of excited cystine with water was proposed [Dose and Rajewsky, 1962] for the formation of alanine sulphinic acid, 19, which is a product of cystine photolysis in air and under N<sub>2</sub>, eqns. 1.39 and 1.40.



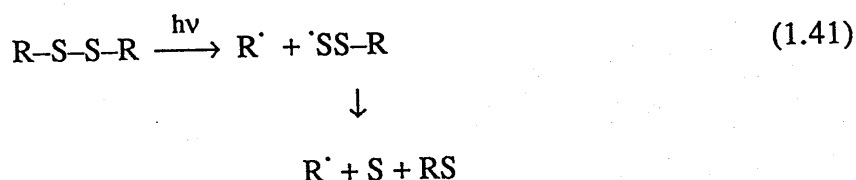
Forbes and Savage [1962b] also repeated 254 nm irradiation of cystine in dilute hydrochloric acid. Under N<sub>2</sub>, cys, 19, 20, gly, ala, ser and the trisulphide, 22, together with several other photoproducts were observed. Risi et al. [1967] measured cys and NH<sub>3</sub> production from 254 nm irradiation of cystine at pH 1 under N<sub>2</sub>. Their results showed that cysteine production accounted for 65% of cystine loss, and the presence of oxygen increased the rate of cystine destruction. Dixon and Grant [1967] isolated a new deaminated keto acid product,  $\alpha$ -amino- $\alpha'$ -oxo- $\beta,\beta'$ -dithiodipropionic acid, 23, together with ammonia with equal quantum yields when irradiated cystine at 254 nm in oxygen-saturated 0.05 N HCl.



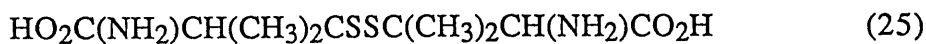
R = CH<sub>2</sub>CH(NH<sub>2</sub>)CO<sub>2</sub>H.

Asquith and Hirst (1969) irradiated air-saturated aqueous solutions of cystine through quartz at pH 1 and pH10. The most important products at pH 10 were pyruvic acid, cys, NH<sub>3</sub>, 20, 19, 16, ala, ser, gly, and sulphate ion, and at pH 1 21, the trisulphide, 22, a tetrasulphide, 24, and H<sub>2</sub>S. Hydroxylamine, NH<sub>2</sub>OH, was

observed at both pH values. The tri- and tetrasulphides and some cystine were presumed to arise from coupling and cross-coupling of thiyl ( $\text{RS}^\cdot$ ) and perthiyl ( $\text{RSS}^\cdot$ ) radicals. On the basis of the yields of the different types of products, it was concluded that S-S, C-S, and C-N cleavage had occurred in the approximate ratio of 1.0 to 0.6 to 1.0 [Asquith and Hirst, 1969]. It was assumed that cys, 19 and 20 arose from initial S-S cleavage, where as pyruvic acid, ala, ser and  $\text{NH}_3$  arose from initial C-S cleavage. Asquith and Shah [1971] continuing the above work but in the presence of  $\text{N}_2$  found far fewer products. Major products included cys, ala,  $\text{NH}_3$ , sulphur, and  $\text{H}_2\text{S}$ . Traces of ser, gly, 21, 19, and tri- and tetrasulphides were obtained. It was suggested that the significant yield of 21 and the polysulphides were due to C-S bond fission followed by sulphur loss from the perthiyl radical (eqn.141).



Alanine sulphinic acid was thought to arise *via* hydrolytic fission of cystine as in eqns. 1.39 and 1.40. The most direct method of determining the relative importance of S-S and C-S bond cleavage in disulphide was partly achieved by Morine and Kuntz [1981]. These authors studied a microsecond flash photolysis of pencillamine disulphide, 25, cystine, cystamine, 26, and general alkyl disulphides.



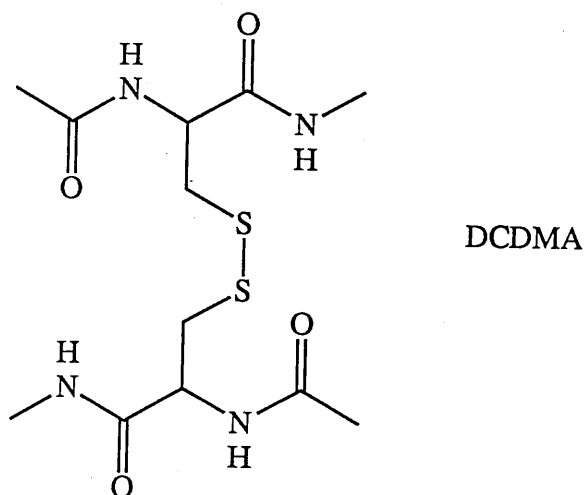
They observed the formation of perthiyl ( $\text{RSS}^\cdot$ ) radicals but failed to observe thiyl radicals most probably because of their low absorption coefficients and, probably, rapid cage recombination. They did, however, report that the relative yields of the

perthiyl radicals in aqueous solution were penicillaminyl > cysteinyl > 2-aminoethyl. It was not surprising that the penicillaminyl radical was formed in greatest yield since C-S cleavage of 25 yields a tertiary alkyl radical, rather than a primary radical. The results unequivocally demonstrated C-S bond fission for cystine but the failure to observe thiyl radicals left open the question of the extent of S-S bond fission.

In view of the chemistry of sulphur-containing radicals [Friswell and Gowenlock, 1967; Kice, 1973] and discussions of the photochemistry of disulphides discussed above, it appears that photolysis of disulphides proceed mainly via S-S bond fission (eqn. 1.30), although there is strong evidence for C-S bond fission where photolysis yields a tertiary alkyl radical. These studies show that despite evidence for dominance of tryptophan photochemistry in wool photoyellowing cystine is a photolabile component of protein structures.

### 1.7 The Objectives of the project

The objectives of the research described in the following chapters centre around the use of *N,N*-diacetyl-L-cystine-*N,N*-dimethylamide (DCDMA) as a model for cystine in wool proteins. The thermal chemistry of this compound has been





explored under a variety of conditions involving absence or presence of water, alkali and oxygen mainly by product analysis. Similar, but less exhaustive studies of other mono peptides including those of *N*-acetyl-*N*-methylamides of alanine, cysteine, glycine, histidine, methionine, phenylalanine, proline, serine, threonine, tryptophan and tyrosine have also been carried out. We have attempted to use the results to identify possible mechanisms for thermal and/or alkaline degradation on wool. The work concluded with a brief study of the photochemistry of DCDMA.

## 2 Experimental

### 2.1 Materials

#### 2.1.1 Reagents

#### 2.1.2 Preparation of buffers

#### 2.1.3 *N,N*-Diacetyl-L-cystine-*N,N*-dimethylamide (DCDMA)

#### 2.1.4 *N,N*-Diacetyl-RS-lanthionine-*N,N*-dimethylamide (DLDMA)

#### 2.1.5 *N,N*-Diacetyl-RS-cystine-*N,N*-dimethylamide (RS-DCDMA)

#### 2.1.6 *N*-Methylpyruvamide (MPA)

#### 2.1.7 *N*-Acetylglycine-*N*-methylamide (NAGMA)

#### 2.1.8 *N*-Acetylalanine-*N*-methylamide (NAAMA)

#### 2.1.9 *N*-Acetyls erine-*N*-methylamide (NASMA)

#### 2.1.10 *N*-Acetyltyrosine-*N*-methylamide (NAYMA)

#### 2.1.11 *N*-Acetyltryptophan-*N*-methylamide (NAWMA)

#### 2.1.12 *N*-Acetylphenylalanine-*N*-methylamide (NAFMA)

#### 2.1.13 *N*-Acetylmethionine-*N*-methylamide (NAMMA)

#### 2.1.14 *N*-Acetylhistidine-*N*-methylamide (NAHMA)

#### 2.1.15 *N*-Acetylthreonine-*N*-methylamide (NATMA)

#### 2.1.16 Separation of thermolysis products by high performance liquid-chromatography

### 2.2 Physical measurements

### 2.3 General procedures for thermal degradations

#### 2.3.1 Solid-state

#### 2.3.2 Alkaline solution

#### 2.3.3 Neutral aqueous solution

#### 2.3.4 Analytical methods

#### 2.3.5 Determination of product yields

## **2.4 Thermal degradation of DCDMA**

### **2.4.1 Solid-state**

**Exploratory studies (DCD1-3)**

**Thermolysis for product isolation (DCD4)**

**Formation of elemental sulphur (DCD5)**

***N*-Acetylthiocysteine-*N*-methylamide (DCD6)**

### **2.4.2 Alkaline solution**

**Exploratory investigation of the effect of heat and alkali (DCD7)**

**Comparison of buffered and non-buffered alkaline degradation (DCD8)**

**Large scale alkaline degradation to isolate *N*-acetyldehydroalanine-*N*-methylamide and *N,N*-diacetyl-RS-Lanthionine-*N,N*-dimethylamide (DCD9)**

**Isolation of acetamide, *N*-acetyldehydroalanine-*N*-methylamide, *N,N*-diacetyl-RS-Lanthionine-*N,N*-dimethylamide and test for the formation of hydropersulphide (DCD10)**

**Exploratory studies for the isolation of yellow components (DCD11)**

**Effect of pH on extractibility of yellow components in alkali-degraded DCDMA (DCD12)**

**Isolation of yellow components of alkali degraded DCDMA (DCD13)**

#### **2.4.3 Neutral solution**

**Effect of oxygen on degradation of DCDMA in aqueous solution (DCD<sub>14</sub>)**

**Effect of buffer on degradation of DCDMA in aqueous solution (DCD<sub>15</sub>)**

### **2.5 Thermal degradation of other mono peptides – comparative studies**

**2.5.1 Alkaline degradation of NABSMA**

**2.5.2 Alkaline degradation of NAGMA**

**2.5.3 Effect of air on the alkaline degradation of NAGMA**

### **2.6 DCDMA photolysis**

**Exploratory photolysis**

**Large scale photolysis and isolation of products**

## 2 Experimental Section

### 2.1 Materials

#### 2.1.1 Reagents

Solvents and reagents were of the highest quality/commercial grade available. Most precursor reagents for the synthesised mono-peptides were of analytical grades and supplied either by Sigma or Aldrich. *O*-Benzyl-*N*-(*t*-butoxy carbonyl)-L-serine and *N*-benzyloxy-carbonyl-L-threonine methylester were supplied by Vega Biochemicals and were HPLC pure. Meso cystine and methylamine in absolute ethanol were supplied by Pfaltz and Bauer and Fluka respectively. All peptides were stored below 0 °C and kept moisture free. All solvents were dried [Perrin et al., 1980] using  $\text{CaCl}_2(\text{CH}_2\text{Cl}_2)$ ,  $\text{CaH}_2(\text{EtOAc})$ , Na wire (ether) and  $\text{Mg/I}_2$  (ethanol or methanol). Methylamine gas was passed through a drying tube containing potassium hydroxide pellets.

#### 2.1.2 Preparation of buffers

For alkaline buffer solutions, boric acid (12.4 g) was dissolved in sodium hydroxide (1 M, 100 mL) and made up to 1 L. This was mixed with an equal volume of sodium hydroxide (0.1 M) to give an alkaline buffered solution (pH  $\approx$  10.8-11.0).

Neutral buffered solutions were prepared by mixing potassium dihydrogen phosphate (0.2 M, 50 mL) with sodium hydroxide (0.2 M, 29.65 mL).

#### 2.1.3 *N,N*-Diacetyl-L-cystine-*N,N*-dimethyl amide (DCDMA)

The method of T.A. Martin [1967] was used: L-cystine dimethyl ester dihydrochloride (34.02 g, 0.11 mole) was added to 600 mL 33% methylamine in methanol (w/v) and stirred for 0.5 h at room temperature (RT). After rotary evaporation of the solvent, pale yellow residue was treated with distilled water

(150 mL), anhydrous sodium acetate (15.16 g, 0.18 mole), and acetic anhydride (30.10 g, 0.201 mole). During the addition of acetic anhydride the reaction temperature rose and the product precipitated. After stirring with additional distilled water (150 mL) the solid was filtered, dried and recrystallised from warm methanol (20.57 g, 53.4%). Mp: 264-265 °C (Lit. 263.5 - 264.5 °C), UV (H<sub>2</sub>O)  $\lambda_{\text{max}} = 215 \text{ nm}$  ( $\epsilon$  8592 L mol<sup>-1</sup> cm<sup>-1</sup>). IR(KBr) $\nu_{\text{max}}/\text{cm}^{-1}$ : 3290, 1630, 1550; NMR <sup>1</sup>H (d<sub>6</sub>-DMSO)  $\delta$ : 1.9(s 3H), 2.65(d 3H), 3.0(AB 2H), 4.5(m 1H), 8.05(q 1H), 8.2 (d 1H). HRMS (CI) MH<sup>+</sup> = 351.11626 (C<sub>12</sub>H<sub>23</sub>O<sub>4</sub>N<sub>4</sub>S<sub>2</sub>,  $\pm$ 0.2 mmu)

#### 2.1.4 *N,N*-Diacetyl-RS-lanthionine-*N,N*-dimethylamide (DLDMA)

##### Meso-RS-Lanthionine dimethylester dihydrochloride

The general method of M. Bodansky [1984] was used. Meso-RS-lanthionine (0.9184 g, 4.4 mmoles) was suspended in redistilled 2,2-dimethoxypropane (105 mL) and concentrated hydrochloric acid (36% v/v, 10 mL). The endothermic reaction mixture was allowed to reach RT and stirred overnight giving a dark red solution. The volatiles were removed under vacuo at a bath temperature not exceeding 60 °C and the resulting off-white residue was dissolved in methanol (25 mL) and diluted by diethyl ether (125 mL) causing a gummy product to precipitate which solidified on standing in the fridge. The product was collected by filtration, washed with ether and dried in vacuo over sodium hydroxide pellets (0.7827 g, 64.2%). IR KBr  $\nu_{\text{max}}/\text{cm}^{-1}$ : 2900, 17500, 1540, 1480.

##### *N,N*-Diacetyl-RS-lanthionine dimethyl amide (DLDMA)

This compound was synthesised by modifying T.A. Martin's method. Meso-RS-lanthionine dimethylester dihydrochloride (0.71 g, 2.78 mmoles) was added to ice-cooled 33% methylamine in methanol (v/v, 20 mL) and stirred. After rotary evaporation of the solvent, the residue was treated with distilled water (5 mL), anhydrous sodium acetate (0.5 g, 6.0% mmoles), and acetic anhydride (1.04 g, 10

mmoles). On addition of acetic anhydride the reaction temperature changed very little and no solid product was precipitated – volatiles were removed under vacuo giving an off-white sticky residue. Recrystallisation from a mixture of methanol (~5%) and chloroform (~95%) and cooling gave a white crystalline product (0.27 g, 30.5%, overall 20%). Mp: 204-208 °C. IR (KBr)  $\nu_{\text{max}}/\text{cm}^{-1}$ : 3280, 1640, 1540; NMR  $^1\text{H}$  ( $\text{D}_2\text{O}$ )  $\delta$ : (s 3H), 2.7(s 3H), 2.85(m 2H), 4.3(t 1H). HRMS(CI)  $\text{MH}^+ = 319.1441$  ( $\text{C}_{12}\text{H}_{23}\text{O}_4\text{N}_4\text{S}$ ,  $\pm 0.1$  mmu);  $m/z = 319, 177, 145, 86$ .

### 2.1.5 *N,N*-Diacetyl-RS-cystine-*N,N*-dimethylamide (RS-DCDMA)

The ester was prepared from meso-cystine (1.29 g, 5.4 mmoles) by the method described for RS-lanthionine dimethylester dihydrochloride. After rotary evaporation a semicrystalline product was obtained (0.97 g, 58%). IR(KBr)  $\nu_{\text{max}}/\text{cm}^{-1}$ : 3500, 2800, 1740. This was used without further purification, in a procedure analogous to that for the preparation of DCDMA. Removal of solvents under vacuo gave a white residue which was crystallised from methanol to afford the product, a white solid (0.15 g, 8.0%). Mp: decomposed at temperature greater than 200 °C. NMR  $^1\text{H}$  ( $\text{d}_6$ -DMSO)  $\delta$ : 1.9(s 3H), 2.6(d 3H), 3(m 2H), 4.5(m 1H), 8.1(q 1H), 8.3(d 1H).

### 2.1.6 *N*-Methylpyruvamide (MpA)

The method of P.M. Pojer [1970] was used. Methylpyruvate (0.5 g, 5.8 mmoles) and methylamine (2 g, 64 mmoles) gave the crude amide as a colourless oil.

IR(neat)  $\nu_{\text{max}}/\text{cm}^{-1}$ : 3360, 1675, 1640. NMR  $^1\text{H}$  ( $\text{CDCl}_3$ )  $\delta$ : 2(s 3H), 2.8(d 3H), 7.3(br, 1H).

### 2.1.7 *N*-Acetylglycine-*N*-Methylamide (NAGMA)

*N*-Acetylglycine ethylester was prepared by Applewhite's method [1959]. Glycine ethylester hydrochloride (22.54 g, 16 mmol) and acetic anhydride (20.52 g, 0.20 mole) gave crude *N*-acetylglycine ethylester (7.8 g, 36%). Mp: 45–46.5 °C (Lit. 45.5–47 °C). The ester (7.5 g, 52 mmol) and methylamine (excess) gave the product as a white crystalline solid (5.15 g, 24.5%). Mp: 156.5–158.5 °C (Ref. 158 °C). UV (ethanol)  $\lambda_{\text{max}}$ : 220 nm ( $\epsilon \approx 813.6 \text{ L mol}^{-1} \text{ cm}^{-1}$ ). IR (KBr)  $\nu_{\text{max}}/\text{cm}^{-1}$ : 3360, 1680, 1600. NMR  $^1\text{H}$  ( $\text{d}_6$ -DMSO)  $\delta$ : 1.9(s 3H), 2.55(d 3H), 3.6(d 2H), 7.7(m 1H) and 8.1(m 1H).

### 2.1.8 *N*-Acetylalanine-*N*-Methylamide (NAAMA)

*N*-Acetyl alanine methylester was prepared by the method of H. Reihlen [1936]. Alanine methylester hydrochloride (3 g, 20 mmol) and acetic anhydride (18.36 g, 0.18 mole) gave crude *N*-acetylalanine methylester (0.83 g, 26%). NMR  $^1\text{H}$  ( $\text{d}_6$ -DMSO)  $\delta$ : 1.2(d 3H), 1.8(s 3H), 3.6(s 3H), 4.2(m 1H), 8.25(d 1H).

#### *N*-Acetyl alanine methylamide [H. Reihlen]

Methylamine (2.6 g, 84 mmol) was added to *N*-acetylalanine methylester (0.6 g, 3.82 mmol) in ice-cooled methanol (6 mL) and was allowed to stand overnight. Removal of volatiles under  $\text{N}_2$  gave a white solid which was recrystallised from toluene (0.04 g, 78%). Mp: 179–180 °C (Lit 181–182 °C) IR(KBr)  $\nu_{\text{max}}/\text{cm}^{-1}$ : 3280, 2950, 1650, 1580. NMR  $^1\text{H}$ ( $\text{d}_6$ -DMSO)  $\delta$ : 1.15(d 3H), 1.8(s 3H), 2.55(d 3H), 4.2(m 1H), 7.75(q 1H), 8(d 1H).

### 2.1.9 *N*-Acetylserine-*N*-methylamide (NASMA)

#### *O*-Benzyl-*N*-(*t*-butoxycarbonyl) serine methylamide.

This compound was prepared by modifying Paul F. Alewood's method [1984]. *O*-Benzyl-*N*-(*t*-butoxycarbonyl serine) (10.27 g, 38.4 mmol) was dissolved in



tetrahydrofuran (THF, 100 mL) at -10 °C. Triethylamine (3.9 g, 38.4 mmol) was added to the solutions followed by ethylchloroformate (3.8 g, 34.56 mmol) in THF (10 mL) and allowed to stir for 0.5h at -10 °C. Methyl amine (excess) in THF was then added and the reaction mixture was brought to RT and was allowed to stand for 45 minutes. Rotary evaporation of the volatiles gave a white residue which was dissolved in dichloromethane (DCM) and washed with sodium hydrogen carbonate (3 x 10 mL), hydrochloric acid (0.1 N, 3 x 10 mL) and the organic layer was dried over magnesium sulphate. Recrystallization from a mixture of hexane/methanol gave the product, a white solid (5.6 g, 47%). Mp: 97-98.5 °C (Lit. 98.5-99.5 °C). IR(KBr)  $\nu_{\max}/\text{cm}^{-1}$ : 3320, 1665, 1650. NMR  $^1\text{H}$  ( $\text{CDCl}_3$ )  $\delta$ : 1.35(s 9H), 2.8(d 3H), 3.6(m 1H), 4.2(m 1H), 4.5(s 2H), 5.3(br 1H), 6.4(br 1H), 7.2(br 5H).

***N*-Acetyl-*O*-benzylserinemethylamide (NABSMA) [Paul F. Alewood].**

*O*-Benzyl-*N*-(*t*-butoxyl carbonyl) serine methylamide (3.7 g, 12 mmol) was dissolved in a mixture of ethylacetate (16 mL) and hydrochloric acid (4 M, 16 mL), and allowed to stand at RT for 1h. Evaporation gave the hydrochloride salt which was neutralized by a cooled (-15 °C) solution of *N*-methylmorpholine (1.20 g, 11.9 mmol) in dimethyl formamide. Subsequent coupling with activated acetic acid (1.43 g, 12 mmol) was performed by the mixed anhydride procedure in a similar manner to that described for *t*Boc-Ser(Bz)-NHMe. A white solid was isolated (1.90 g, 63%). Mp: 131.5-132 °C (Lit. 136-137 °C). IR(KBr)  $\nu_{\max}/\text{cm}^{-1}$ : 3300, 1640; NMR  $^1\text{H}$ ( $\text{CDCl}_3$ )  $\delta$ : 2(s 3H), 2.8(d 3H), 3.6(m 3H), 4.5(s 2H), 6.5(br 2H), 7.3(s 5H).

*N*-Acetylserine-*N*-methylamide (NASMA) was prepared according to a method given in Greenstein and Wintz [1984]. NABSMA (1.54 g, 6.2 mmol) was dissolved in methanol (20 mL) and hydrogenated in the presence of Pd(5% on charcoal, 0.61 g), glacial acetic acid (0.2 mL), by bubbling hydrogen gas through

the reaction vessel for 2.5 h. A clear oil, which became a solid on standing, was isolated. Crystallization from methanol gave the product as a white solid (0.45 g, 45%). Mp: 118-120 °C (Lit. 117.5 °C). NMR <sup>1</sup>H (d<sub>6</sub>-DMSO) δ: 1.85(s 3H), 2.6(d 3H), 3.5(t 2H), 4.2 (m 1H), 4.8(t 1H), 7.8(m 2H).

#### **2.1.10 *N*-Acetyltyrosine-*N*-methanamide (NAYMA) [Thomas H. Applewhite, 1959]**

A solution of *N*-acetyltyrosine ethylester (2.03 g, 8.05 mmol) and 12 mL of 33% methanamine in absolute ethanol (v/v) was allowed to stand at RT for two days. Evaporation of the solvent gave a white solid which was recrystallized from a mixture of hot methanol/ethylacetate to give colourless needles (0.87 g, 46%). Mp: 182.2-183.2 °C (Lit. 185.5-186 °C). IR(KBr)ν<sub>max</sub>/cm<sup>-1</sup>: 3316, 1657, 1620, 1542. NMR <sup>1</sup>H (d<sub>6</sub> DMSO) δ: 1.8(s 3H), 2.55(d 3H), 2.8(m 2H), 4.3(m 1H), 6.8(dd 4H), 7.8(q 1H), 8(d 1H), 9.1(br 1H).

#### **2.1.11 *N*-Acetyltryptophan-*N*-methanamide (NAWMA)**

This compound was synthesised in a similar manner to that described for NAYMA using *N*-acetyltryptophan ethylester (0.99 g, 3.6 mmol), 25% aqueous methanamine solution (v/v, 12.5 mL) and methanol (12.5 mL). The product, a white solid was crystallized from hot water to give tiny dense prisms (96 mg, 10%). Mp: 184-186 °C (Lit. 181-185 °C). NMR <sup>1</sup>H(d<sub>6</sub>-DMSO) δ: 1.8(s 3H), 2.55(d 3H), 2.9(m 2H), 4.4(m 1H), 7.4(m 5H), 7.9(q 1H), 8(d 1H), 10.8(br 1H).

#### **2.1.12 *N*-Acetylphenylalanine-*N*-methanamide (NAFMA)**

Method of Thomas H. Applewhite [1959] was used. *N*-acetylphenylalanine methylester (2.0 g, 9 mmol) and 33% methanamine in absolute ethanol (v/v, 8 folds molar equivalent) gave a white solid which was recrystallized from hot water to give white prisms (1.14 g, 58%). Mp: 203-204 °C (Lit. 207.3-208.6 °C).

NMR  $^1\text{H}$  ( $\text{d}_6$ -DMSO)  $\delta$ : 1.75(s 3H), 2.6(d 3H), 2.8(m 2H), 4.4(m 1H), 7.2(br 5H), 7.9(q 1H), 8.1(d 1H).

### 2.1.13 *N*-Acetylmethionine-*N*-methylester (NAMMA)

#### *N*-Acetylmethionine methylester.

The method of T.H. Applewhite [1958] was used. *N*-Acetylmethionine (9.51 g, 54 mmol) was suspended in methanol (20 mL). Thionylchloride (7.2 g, 60 mmol) was added and the reaction mixture was heated at 40 °C for 45 minutes and allowed to stand at RT overnight. The solvent was evaporated under vacuo and the resulting oil was treated with chloroform, washed with hydrochloric acid (1M, 20 mL), sodium hydrogen carbonate (1M, 20 mL), water (20 mL) and dried over magnesium sulphate. After evaporation of the solvent, a clear oil was obtained which on turturating with pentane gave a white solid (8.23 g, 78%).  
Mp: 39-40 °C (Lit. 43.5-44.5 °C).

#### *N*-Acetylmethionine-*N*-methylester

This compound was prepared in a similar manner to that described for NAYMA using *N*-acetylmethioninemethylester (4.4 g, 23 mmol) and 90 mL of 33% methylamine in absolute ethanol (v/v). Crystallization from hot ethylacetate gave a white solid (2.1 g, 48%). mp: 184-186 °C (Lit 181-185 °C). NMR  $^1\text{H}$  ( $\text{d}_6$ -DMSO)  $\delta$ : 1.8(s 3H), 2.0(s 3H), 2.4(m 2H), 4.2(m 1H), 7.8(q 1H), 8(d 1H).

### 2.1.14 *N*-Acetylhistidine-*N*-methyl amide (NAHMA)

This compound was prepared by modifying T.A. Martin's method. L-Histidinmethylester dihydrochloride (2.41 g, 10 mmol) in 60 mL of 33% methylamine in absolute ethanol (v/v) was stirred for 25 minutes. The volatiles were removed under vacuo and the resulting white gum was treated with water (15 mL), acetic anhydride (3.0 g, 29 mmol) and sodium acetate (1.52 g,

18 mmol) to give a crude product. Crystallization from methanol gave the product as a white solid (1.40 g, 67%). Mp: 242.5 (Lit. 243-244 °C). IR(KBr)  $\nu_{\text{max}}/\text{cm}^{-1}$ ; 3280, 3160, 1660, 1640, 1570. NMR  $^1\text{H}$  ( $d_6$ -DMSO)  $\delta$ : 1.75(s 3H), 2.5(d 3H), 2.8(m 2H), 3.35(br 1H), 4.35(m 1H), 6.7(s 1H), 7.5(s 1H), 7.8(q 1H), 8(d 1H).

#### 2.1.15 *N*-Acetylthreonine-*N*-methylamide (NATMA)

##### *N*-Benzyloxycarbonyl-L-threoninemethylamide.

The method of Von Helmet Zahn [1968] was used. A solution of *N*-benzyloxycarbonyl-L-threoninemethylester (18.29 g, 70 mmol) in absolute methanol (50 mL) and methylamine (excess) was stirred at RT for 1h. The product, a white solid (5.44 g, 30%), was obtained by crystallization from absolute ethanol. Mp: 158 °C (Lit. 157 °C).

##### *N*-Acetyl-L-threonine-*N*-methylamide.

*N*-Benzyloxycarbonyl-L-threonine methylamide (1.0 g, 3.8 mmol) was hydrogenated in a similar manner to that described for NABSMA to give a clear oil which solidified on standing. This was treated with pyridine (12 mL), triethylamine (1.4 g, 14 mmol) and *p*-nitrophenylacetate (0.99 g, 5.5 mmol). The resulting oil was triturated with diethyl ether causing a green solid to precipitate which was crystallized to form a mixture of ethanol: ether to give a white solid (50 mg, 8%). Mp: 160-161 °C (Lit. 160 °C). NMR  $^1\text{H}$  ( $d_6$ -DMSO)  $\delta$ : 1(d 3H), 1.85(s 3H), 2.55(d 3H), 4(m 2H), 4.75(m 1H), 7.6(q 1H), 7.7(d 1H).

#### 2.1.16 Separation of thermolysis products by HPLC

Preparative reversed-phase high performance liquid chromatography (RPHPLC) was performed using a Gilson 303 pump 50 SC head with a Cecil 212 uv detector

and a spherisorb S<sub>10</sub>ODS<sub>2</sub> (25 cm x 20 mm I.D.) column. For semi-preparative separations a spherisorb S<sub>5</sub>ODS<sub>2</sub> column (25 cm x 8 mm I.D.) and a pye LC uv detector were used. Acetonitrile: water mixtures were used as eluting solvents. Preparative normal phase HPLC was carried out using Waters Delta Prep with Waters 484 Variable wavelength detector and a Spherisorb S<sub>10</sub>W column (25 cm x 20 mm I.D.). Column chromatography was carried out using silica gel (40-60 $\mu$ ) and eluting with dichloromethane, dichloromethane: methanol mixtures.

## 2.2 Physical measurements

Ultra-violet and visible (uv/vis) spectra were recorded in 1 mm quartz cell using Pye-Unikamp Sp8 500 or Unikon Easy-10 spectrometer. Infrared (IR) spectra were recorded either as nujol mulls using sodium chloride plates or as potassium bromide discs on a Perkin-Elmer 1310 or 1710 Fourier transform infrared spectrometers. Nuclear magnetic resonance (NMR) spectra were obtained using a Jeol FX90 Fourier-transform spectrometer with tetra-methylsilane as the internal standard. High-field 400 MHz spectra were obtained from the SERC high field NMR facility at the University of Warwick. Unless otherwise stated, NMR spectra data are quoted at 90 MHz. Mass spectra were provided either by a VG20-250 mass spectrometer or the SERC high resolution mass spectrometry facility at the University College of Swansea. Melting points (Mp) were determined in capillary tubes on a Gallenkamp apparatus and are uncorrected. The pH of the solutions was measured on an Orion gel-filled combination pH electrode and PT1-6 Universal digital pH meter calibrated with standard buffered solutions.

## **2.3 General procedures for thermal degradations**

### **2.3.1 Solid-state**

For analytical studies, approximately 5 mg of finely divided peptide was placed in each of a number of glass pyrolysis tubes (15 cm × 1 cm I.D.) with a teflon cap and septa such that they can withstand high pressure and temperature. Distilled water (0.1 mL) was added to the peptide in each tube and the sample was spread evenly over the inside surface to give a large surface area. For anaerobic experiments, the air was removed from the tubes by flushing with oxygen-free nitrogen or argon and sealing with a teflon stopper. The samples were then heated in a Varian aerograph gas chromatography oven, monitoring a sample after selected time intervals by high-performance liquid chromatography. Thermal experiments under dry nitrogen and dry air were carried out in a similar manner but with the exclusion of water.

For preparative scale thermal experiments, approximately 250 mg of the peptide was placed in a stainless steel vessel. Distilled water was added drop by drop until the sample was just wet. Care was taken to ensure that the whole of the sample was wetted uniformly throughout the pyrolysis vessel. This was then heated in the same way as described for analytical scale thermolysis.

### **2.3.2 Alkaline solution**

Approximately  $3 \times 10^{-3}$  M peptide in alkaline buffered solution (pH ≈ 10.8 borate) was heated either under reflux or in a thermostatically controlled water bath at 55 °C. Samples were taken at different time intervals and examined by HPLC. Thermolysis reaction mixtures from large scale experiments were always neutralised by concentrated hydrochloric acid, followed by separation of the suspended solids by centrifugation. For anaerobic experiments, the air was

removed from the solution by flushing with oxygen-free nitrogen overnight prior to thermolysis and maintaining the mixture under nitrogen during the experiment.

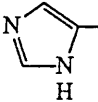
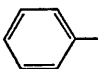
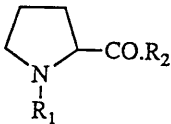
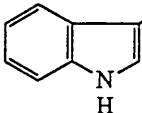
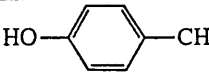
### 2.3.3 Neutral aqueous solution

Approximately  $3 \times 10^{-3}$  M peptide in buffered or non-buffered aqueous solutions (pH  $\approx$  6-7) were heated under reflux, and samples were examined by HPLC at different time intervals.

### 2.3.4 Analytical methods

Analytical reversed-phase HPLC was performed using a Varian 5000 LC with either a Spectroflow 757 detector set at 215 nm and coupled to a Shimadzu integrator, or a 9060 Polychrom diode array detector set at 215-367 nm. The latter allowed additional information such as purity parameter values and uv/vis spectra of individual compounds to be obtained. Jones matrix cartridge system S<sub>5</sub>ODS<sub>2</sub> column (25 cm x 5 mm I.D) or 5 $\mu$  Apex II ODS column (25 cm x 4.6 mm I.D). was used as stationary phase with a 40 $\mu$  pellicular ODS packed precolumn. Acetonitrile: water mixtures were used as eluting solvents for most peptide analyses at a flow rate of 1 mL/min and column temperature of 40 °C. Table 2.1 shows capacity factors ( $K'$ ) for the mono-peptides studied. Quantitative HPLC was used to determine product yields. The analyses of reaction mixtures were made in aliquots of 10-20  $\mu$ l. For quantitation, analyses were carried out in triplicate and a mean of the peak areas. Care was taken to ensure that the area or height of the standard peak area was comparable to that of the product being formed. A calibration curve (Fig. 2.1) for DCDMA shows that there is a linear relationship between the peak area and concentration of DCDMA.

Table 2.1 Capacity factors of mono-peptides (215 nm detection).

mobile phase	mono-peptide structure	$\lambda/\text{nm}$	Capacity factor/min
H <sub>2</sub> O	CH <sub>3</sub> .CH(NHR <sub>1</sub> ).COR <sub>2</sub>	215	4.1
	$  \begin{array}{c}  (\text{NHR}_1)\text{CH}.\text{CH}_2.\text{S}.\text{S}.\text{CH}_2.\text{CH}(\text{NHR}_1) \\    \qquad \qquad \qquad   \\  \text{COR}_2 \qquad \qquad \text{COR}_2  \end{array}  $	215	15.0
H <sub>2</sub> O	CH <sub>2</sub> (NHR <sub>1</sub> ).COR <sub>2</sub>	215	3.8
Ammonium acetate [0.01 M, acetonitrile: water (3:97)]	 $\text{CH}_2.\text{CH}(\text{NHR}_1).\text{COR}_2$	215	5.90
ACN:water (6:94)	CH <sub>3</sub> .S.CH <sub>2</sub> .CH(NHR <sub>1</sub> ).COR <sub>1</sub>	215	10.8
ACN:water (15:85)	 $\text{CH}_2.\text{CH}(\text{NHR}_1).\text{COR}_2$	215	8.4
ACN:water 5:95	 $\text{CO}.\text{R}_2$	215	4.2
ACN:water 1:99	HO.CH <sub>2</sub> .CH(NHR <sub>1</sub> ).COR <sub>2</sub>	215	4.2
ACN:water 1:99	CH <sub>3</sub> .CH(OH).CH(NHR <sub>1</sub> ).COR <sub>2</sub>	215	5.4
ACN:water 15:85)	 $\text{CH}_2.\text{CH}(\text{NHR}_1).\text{COR}_2$	215	11.5
ACN:water (4:96)	 $\text{CH}.\text{CH}(\text{NHR}_1).\text{COR}_2$	215	15.5

R<sub>1</sub> = CO.CH<sub>3</sub>

R<sub>2</sub> = NHCH<sub>3</sub>



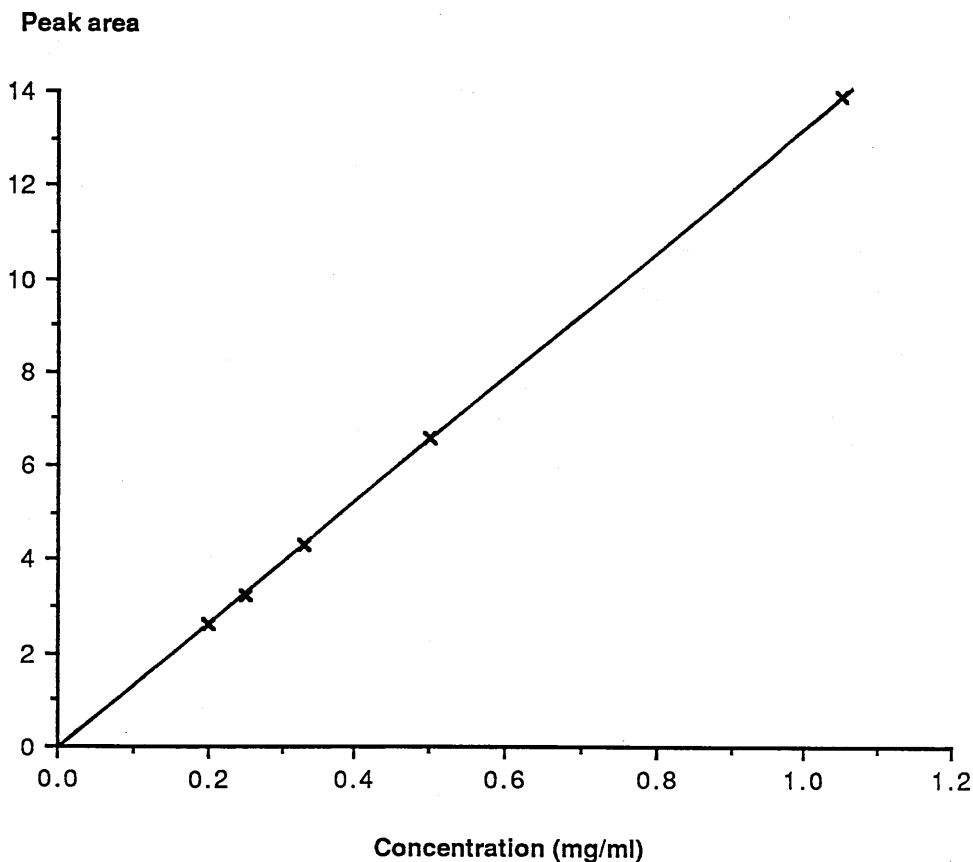


Figure 2.1 Calibration graph for DCDMA showing linear HPLC response with increasing DCDMA concentration.

Analytical normal-phase HPLC (NPHPLC) was performed using a Waters Delta Prep. with Waters 484 Variable Wavelength detector set at 245 nm. A Jones Apex II 5 $\mu$  silica column (25 cm x 4.6 mm I.D.) was used as stationary with methanol: dichloromethane mixtures as the mobile phase. Normal-phase thin layer chromatograph (TLC) was performed on silica plates with dichloromethane: methanol as the developing solvents. Starch-iodide reagents and uv lamp were used for visualization. Reversed phase TLC was carried out on KC<sub>18</sub> plates corresponding with C<sub>18</sub>-bonded HPLC columns with acetonitrile: water mixtures as developing solvents and visualization by uv illumination.

### 2.3.5 Determination of product yields

Analytical product yields were based on substrate consumed. HPLC was thus used to measure loss of substrate (reference to the sample) and, by external standard, growth of product.

## 2.4 Thermal degradations of DCDMA

	temp/°C	condition <sup>a</sup>	Proposed objectives
DCD <sub>1</sub>	150	S	exploratory effect of moisture and oxygen, and the optimum conversion for isolation of primary products
DCD <sub>2</sub>	100	S	
DCD <sub>3</sub>	125	S	
DCD <sub>4</sub>	125	S	Preparative to isolate major products and the formation of polysulphides
DCD <sub>5</sub>	125	S	To investigate the formation of elemental sulphur
DCD <sub>6</sub>	125	S	Preparative, to isolate products
DCD <sub>7</sub>	100	A,N,10.8	Exploratory investigation of the effect of heat in the optimum generation of primary components responsible for the yellowing in DCDMA degradation
DCD <sub>8</sub>	55	A,NA,10.8	To monitor pH change, loss of substrate, and formation of products
DCD <sub>9</sub>	55	A,10.8	To establish the presence of elemental sulphur. Attempts to isolate Acetamide, <i>N</i> -Acetyldehydroalanine- <i>N</i> -methylamide (NADMA), DLDMA
DCD <sub>10</sub>	55	A,10.8	Isolation of acetamide, NADMA, DLDMA and test for the formation of a hydropersulphide or a trisulphide
DCD <sub>11</sub>	100	A,10.8	To develop a method for the separation of yellow pigment(s) by TLC or column chromatography
DCD <sub>12</sub>	100	A,10.8	Isolation of yellow components of the reaction mixture
DCD <sub>13</sub>	100	A,10.80	Attempts to separate the yellow components and other products by preparative normal phase HPLC
DCD <sub>14</sub>	100	U,<7	To investigate the role of oxygen in DCDMA degradation
DCD <sub>15</sub>	100	B,<7	The effect of buffer in the degradation of DCDMA

(a) S, solid-state; A, alkaline buffered in air; N, alkaline buffered in N<sub>2</sub>; NA, alkaline non-buffered in air; NN, alkaline non-buffered in N<sub>2</sub>; U, aqueous unbuffered; B, aqueous buffered; numerical, pH of solution.

### 2.4.1 Solid-state

#### Exploratory studies (DCD1-3)

DCDMA samples (~20 x 5 mg) wet and dry in the presence or absence of oxygen were heated at 150, 100 and 125 °C (DCD<sub>1</sub>, DCD<sub>2</sub> and DCD<sub>3</sub> respectively). Each thermolysis sample was treated with distilled water (5 mL) and examined by HPLC and pH measurement.

#### Thermolysis for Product Isolation (DCD<sub>4</sub>)

DCDMA (1.25 g) was heated in the presence of water and absence of oxygen at 125 °C for 16h. The resulting yellow syrup gave a bright yellow solution with distilled water (50 mL) which became cloudy on standing. The insolubles were removed by centrifugation and the yellow matter liquor was liquid-liquid extracted with dichloromethane (100 mL) for 72h. As no useful fractionation resulted this material was returned to the aqueous fraction. Part of the mixture (~0.3 g) was separated by semi preparative HPLC into five fractions as indicated in Fig. 2.2. The solvents from the fractions were removed by freeze-drying and the resulting residues examined.

DCD<sub>4</sub>-F<sub>1</sub>, and F<sub>2</sub> were minor components and each contained more than one product.

DCD<sub>4</sub>-F<sub>3</sub>, a white solid (0.21 g). Mp: 264.2-265 °C, IR(KBr)  $\nu_{\text{max}}/\text{cm}^{-1}$ : 3290, 1650, 1540, 1410, 1380. NMR <sup>1</sup>H(D<sub>2</sub>O)  $\delta$ : 2(s 3H), 2.65(s 3H), 3(m 2H), 4.5(m 1H).

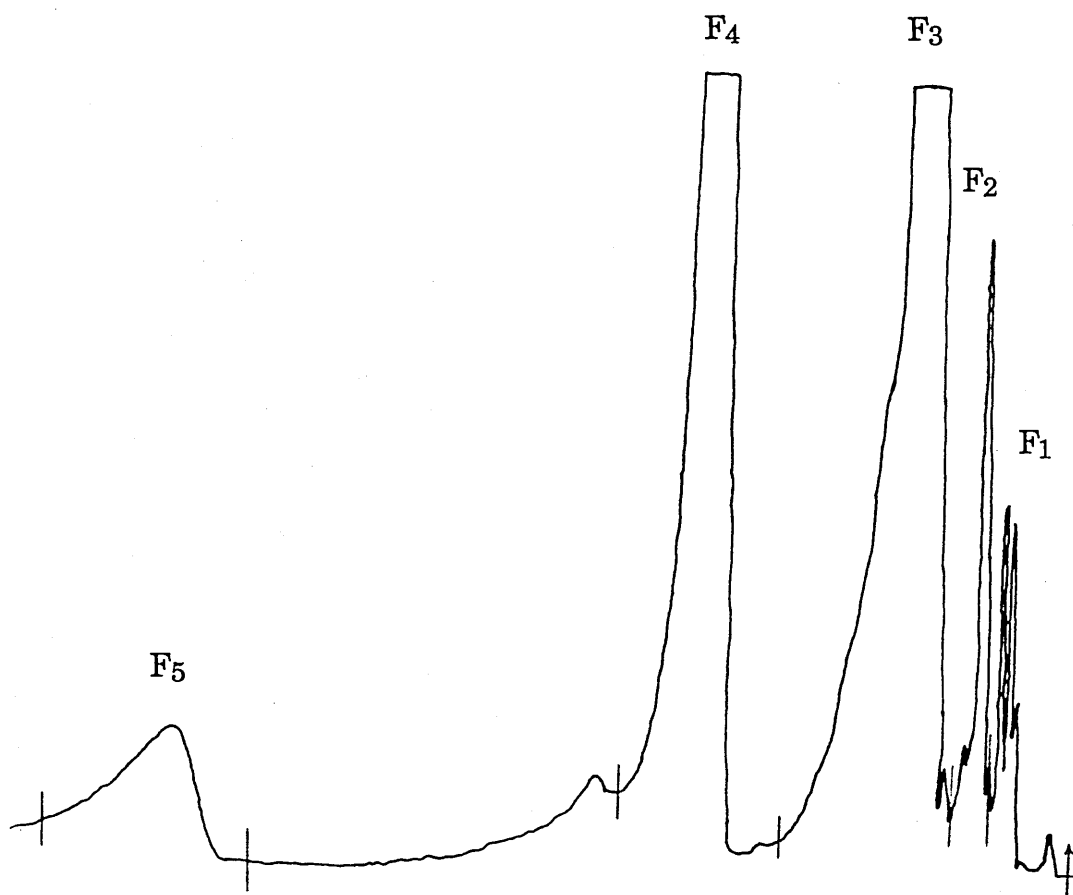


Figure 2.2 Semi-preparative HPLC elution profile of thermally degraded DCDMA reaction mixture at 125 °C.

DCD<sub>4</sub>-F<sub>5</sub>, an off-white solid. HPLC showed only one major product peak with a long retention time. Mp: 227-229 °C. IR(KBr)  $\nu_{\text{max}}/\text{cm}^{-1}$ : 3290, 1640, 1540, 1410, 1380. NMR <sup>1</sup>H (D<sub>2</sub>O)  $\delta$ : 2(s 3H), 2.65(s 3H), 3.0(m 2H), 4.5(m 1H). HRMS (FAB) MH<sup>+</sup> = C<sub>12</sub>H<sub>23</sub>N<sub>4</sub>O<sub>4</sub>S<sub>3</sub> ( $\pm 0$  mmu). HRMS (CI) MH<sup>+</sup> = C<sub>6</sub>H<sub>13</sub>N<sub>2</sub>O<sub>2</sub>S<sub>1</sub> ( $\pm 0.3$  mmu); m/z = 177, 143, 86 and 60. MS(FAB) MH<sup>+</sup> = 383, m/z = 383, 351, 320, 208, 177, 146 (base peak). DCD<sub>4</sub>-F<sub>4</sub> (13.4 mg) was heated in the presence of water and N<sub>2</sub> for 16h at 125 °C and examined by HPLC.

DCD<sub>4</sub>-F<sub>5</sub>, a pale brown solid. HPLC showed a few product peaks with short retention times and a major product with a very long retention time. IR(KBr)  $\nu_{\text{max}}/\text{cm}^{-1}$ : 3300 (br), 1710, 1445, 1380. NMR <sup>1</sup>H (D<sub>2</sub>O)  $\delta$ : 2(s 3H), 2.7(s 3H), 3.3 (m 3H).

### Formation of elemental sulphur (DCD<sub>5</sub>)

DCDMA (0.26 g) was treated in a similar way to that described in DCD<sub>4</sub>. A fine white solid (0.010 g) was precipitated and separated after centrifugation.

Microanalysis on the precipitate gave C,8.73; N,1.43 and S,82.42%. 5.11 mg of the precipitate gave an intense green colour with 2 mL oleum, identical with that obtained with elemental sulphur. DCDMA (6 mg) on treatment with oleum (2 mL) gives a brown colour under the same conditions.

### *N*-Acetylthiocysteine-*N*-methanamide (DCD<sub>6</sub>)

DCDMA (0.74 g) was heated in the presence of water and nitrogen at 125 °C for 24h. After the filtration of the suspended solids and evaporation, the thermolysis mixture was dissolved in water and separated into three fractions by preparative HPLC as illustrated in the chromatograph in Fig. 2.3. The examination of the fractions showed:

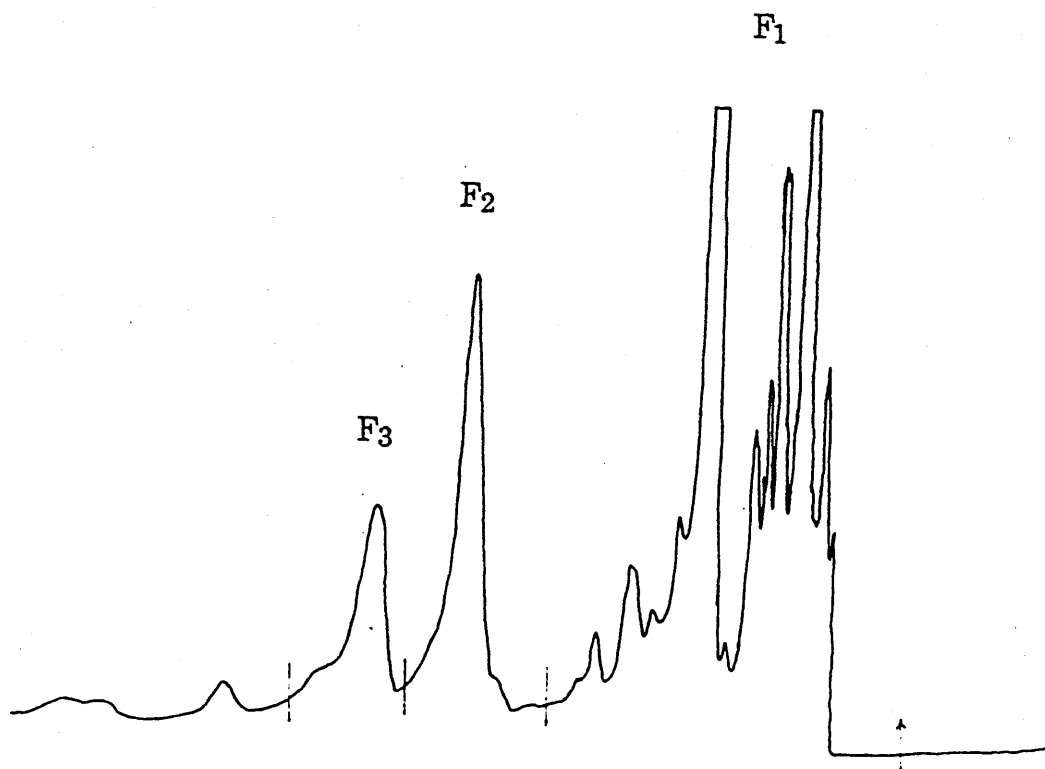


Figure 2.3 Prep-HPLC profile of thermally degraded DCDMA at 125 °C for 24 h.

Fractions 1 and 3 were minor components and each contained more than one product.

DCD<sub>6</sub>-F<sub>2</sub> (*N*-Acetylthiocysteine-*N*-methylethylamide) was an off-white solid (42.2 mg). HPLC showed a little decomposition. Mp: some melted at a temperature around 80 °C, but the bulk of the sample melted at 155 -160 °C. Microanalysis gave C, 34.5; H, 5.2; N, 9.1%. LRMS (CI) NH<sup>+</sup> = 275. m/z = 194, 177, 143, 103, 77, 52 (base peak). NMR <sup>1</sup>H (D<sub>2</sub>O) δ: 2(s 3H), 2.7(s 3H), 3.1(m 2H), 4.6(m 1H).

#### **Test for hydropersulphides [Cavallini, 1960]**

A mixture of DCD<sub>6</sub>-F<sub>2</sub> (3 mmoles, 0.3 mL), borate solution (2 mL), and sodium cyanide (1 mL) was stirred for 15 minutes, when the addition of ferric (III) nitrate reagent gave an orange-red colour. The uv/vis spectrum of the solution was recorded. Additions of ferric (III) nitrate reagent (0.8 mL) to thiocyanate (0.2 mL) gave a dark red colour. Its uv/vis spectrum was recorded.

#### **2.4.2 Alkaline solution**

##### **Exploratory investigation of the effect of heat and alkali (DCD<sub>7</sub>)**

DCDMA (8.64 x 10<sup>-5</sup> and 8.6 x 10<sup>-5</sup> M) were heated in alkaline buffered solutions under reflux in the presence and absence of nitrogen respectively. Samples were taken at 0, boiling, 0.5, 1, 2, 4, 19, 24 and 48h, and analysed by HPLC. The uv/vis spectra and pH values of the reaction mixtures were recorded.

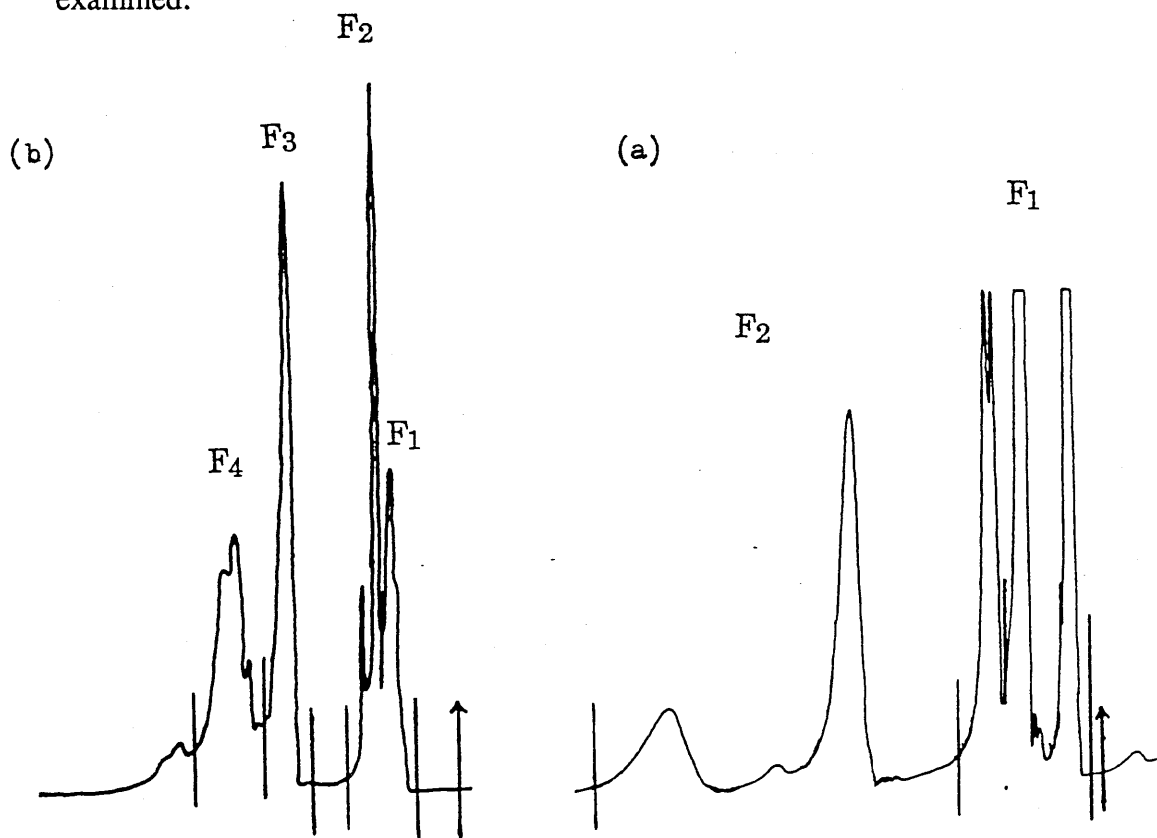
##### **Comparison of buffered and non-buffered alkaline degradation (DCD<sub>8</sub>)**

DCDMA (0.1523 and 0.1527 g) were heated in buffered (50 mL, initial pH = 10.8) and non-buffered solutions (50 mL, pH = 10.7) respectively at 55 °C. The reactions were monitored by HPLC at 0, 0.5, 1, 2, 4, 21 and 24 h. The uv/vis spectra and the pH values were recorded.

**Large scale alkaline degradation (*N*-acetyl-dehydroalanine-*N*-methylethylamide and *N,N*-diacetyl-RS-lanthionine-*N,N*-dimethylamide), DCD<sub>9</sub>.**

DCDMA (1.51 g, 0.035M) in alkaline buffered solution (initial pH = 10.8) was heated at 55 °C for 2h. After neutralization with concentrated hydrochloric acid, a fine solid (9.6 mg) was precipitated which was separated by centrifugation.

Microanalysis on the precipitate gave C, 9.42, N, 0.19; S, 81.72%. The mother liquor, a clear yellow solution was divided into two equal portions. One of which was separated into two fractions by preparative HPLC as indicated in Fig. 2.4a. Fraction two contained the starting material and was discarded. Fraction one was further separated into four fractions by preparative HPLC (Fig 2.4b). The solvents were removed by freeze-drying and the isolated products were examined:



Figures 2.4 a and b show the prep-HPLC elution profiles for the separation of products from alkali degraded DCDMA reaction mixtures.

DCD<sub>9</sub>-F<sub>1</sub>, a pale brown solid (50 mg). HPLC showed a few minor products with short retention times. IR(KBr)  $\nu_{\text{max}}/\text{cm}^{-1}$ : 3420(br), 1650, 1630, 1400, 1150(br). NMR <sup>1</sup>H (D<sub>2</sub>O) was very weak.

DCD<sub>9</sub>-F<sub>2</sub>, an off-white solid (300 mg). HPLC was similar to that of DCD<sub>9</sub>-F<sub>1</sub>. IR(KBr)  $\nu_{\text{max}}/\text{cm}^{-1}$ : 3200 (v. br), 2260, 1650, 1450(br), 1195, 800(br). NMR <sup>1</sup>H (D<sub>2</sub>O)  $\delta$ : 2(s), 2.65(s), 3.4(m).

DCD<sub>9</sub>-F<sub>3</sub> (*N*-Acetyldehydroalanine-*N*-methylamide), a white solid (22.6 mg). HPLC showed only one major product. IR(KBr)  $\nu_{\text{max}}/\text{cm}^{-1}$ : 3300, 1667, 1653, 1631, 1556, 1531, 1416, 1380. NMR <sup>1</sup>H (D<sub>2</sub>O) and <sup>13</sup>C (D<sub>2</sub>O) at 400 MHz showed considerable decomposition. HRMS (CI)  $\text{MNH}^+_4 = \text{C}_6\text{H}_{14}\text{N}_3\text{O}_2$  ( $\pm 0.1$  mmu).

DCD<sub>9</sub>-F<sub>4</sub> (*N,N*-diacetyl-RS-lanthionine-*N,N*-dimethyl amide), a white solid (110 mg). HPLC showed a major product peak with a minor one. Mp: 196-199 °C. IR(KBr) and proton NMR spectra are very similar to those of the synthesised compound.

**Isolation of acetamide, NADMA, DLDMA and test for the formation of a hydropersulphide (DCD<sub>10</sub>).**

DCDMA(0.029 M) in alkaline buffered solution (initial pH = 10.80) was heated at 55 °C for 2h. The reaction mixture was neutralised with concentrated hydrochloric acid, centrifuged, and the mother liquor was separated into five fractions by preparative HPLC (Fig 2.5). The solvents were removed by freeze-drying and the products were examined:



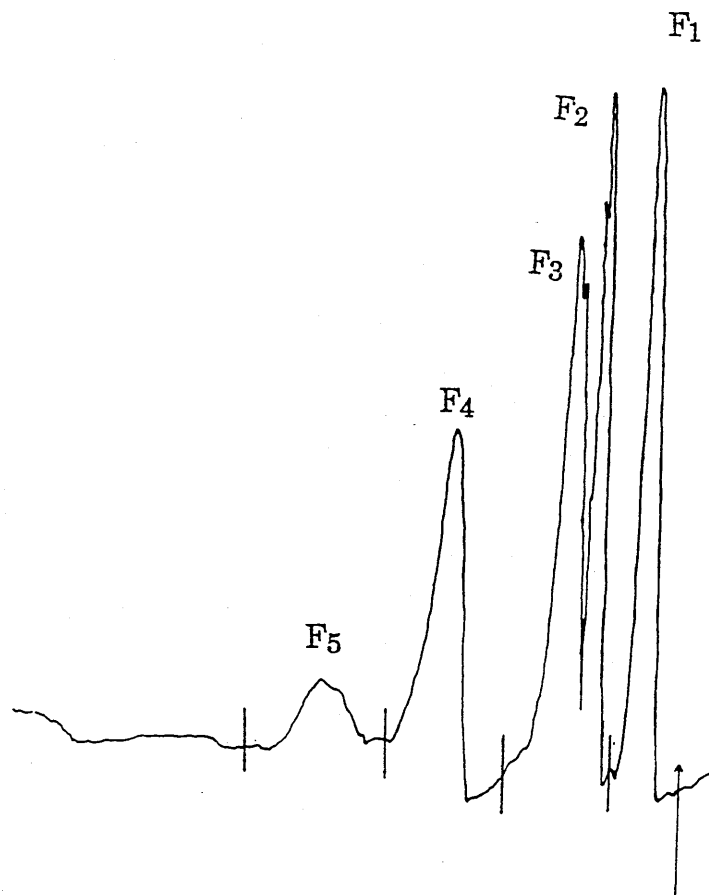


Figure 2.5 Prep-HPLC chromatogram of DCDMA reaction mixture under alkaline buffered conditions (pH = 10.8) at 55 °C for 2h.

DCD<sub>10</sub>-F<sub>1</sub> (Acetamide), a pale brown solid (530 mg) containing sodium borate and sodium chloride, was soxhlet-extracted with dichloromethane for 7h. After the rotary evaporation of dichloromethane, a white solid (250 mg) was obtained. IR(KBr)  $\nu_{\text{max}}/\text{cm}^{-1}$ : 3380, 3230, 1660, 1450, 1350, 1100, NMR <sup>1</sup>H(d<sub>6</sub>-DMSO): 1.8 (s, 3H), 8.2 (m, 1H).

DCD<sub>10</sub>-F<sub>2</sub> (NADMA), a white solid (50 mg). HPLC showed a clean product. NMR <sup>1</sup>H (d<sub>6</sub>-DMSO)  $\delta$ : 2.0 (s, 3H), 2.6 (d, 3H), 5.3 (s, 1H), 6.0 (s, 1H), 8.3 (q, 1H), 9.0 (s, 1H).

DCD<sub>10</sub>-F<sub>3</sub> (DLDMA), a pale brown solid. HPLC showed a major twin product peak. NMR <sup>1</sup>H (d<sub>6</sub>-DMSO)  $\delta$ : 1.8 (s, 3H), 2.55 (d, 3H), 2.7 (m, 2H), 4.3 (q, 1H), 8.0 (m, 1H).

DCD<sub>10</sub>-F<sub>4</sub> was unchanged DCDMA.

DCD<sub>10</sub>-F<sub>5</sub> (*N,N*-Diacetylthiocystine-*N,N*-dimethyl amide), an off-white solid (21.5 mg). HPLC showed a major product peak with long retention time and a minor one due to the starting material. IR(KBr)  $\nu_{\text{max}}/\text{cm}^{-1}$ : 3290, 1926, 1542, 1375. Test for hydropersulphide, was carried out in the same way as described for DCD<sub>6</sub>-F<sub>2</sub>, when the addition of ferric(III) nitrate reagent gave a colourless solution. It's uv/vis spectrum was recorded.

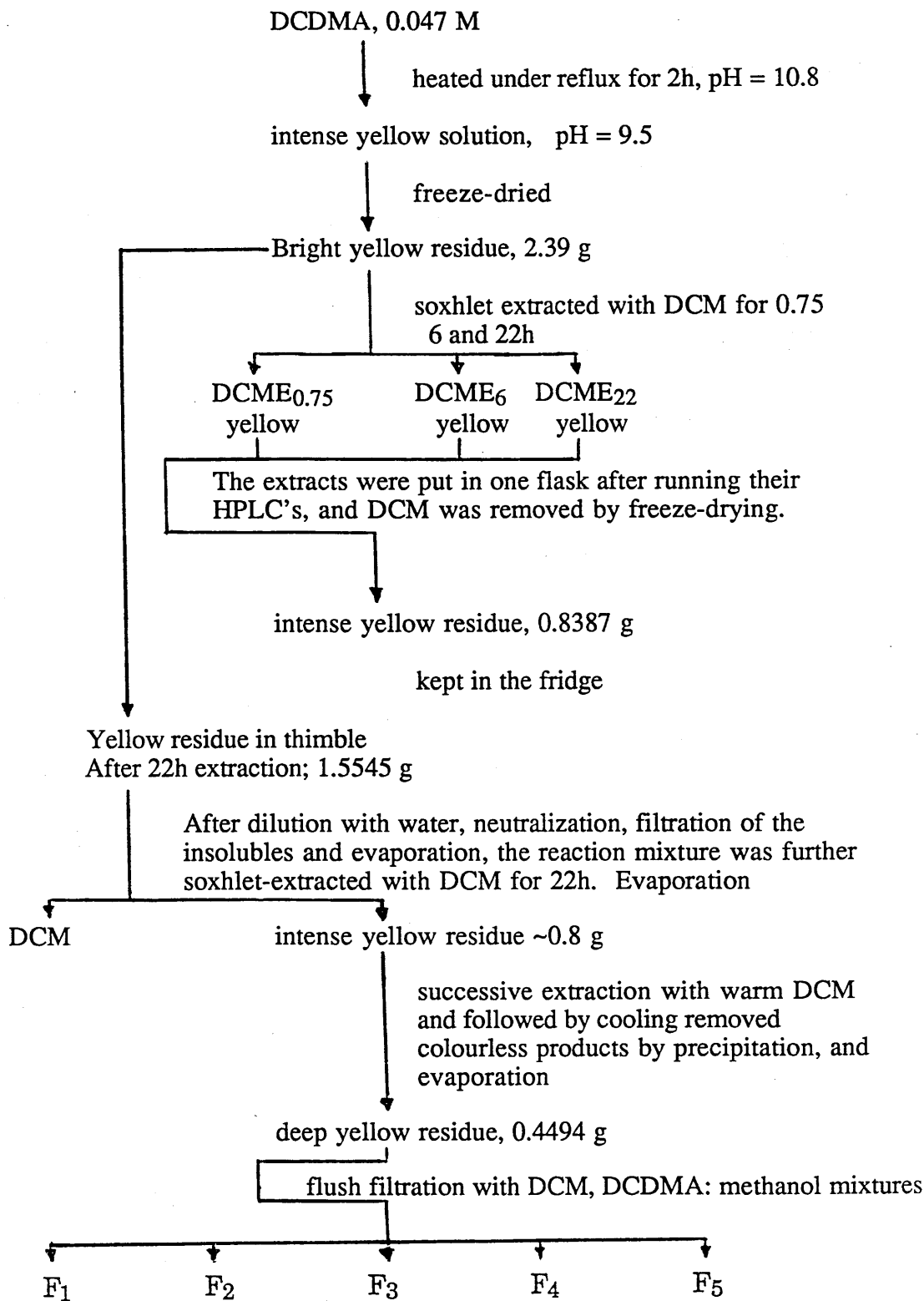
#### **Exploratory study for the isolation of yellow components (DCD<sub>11</sub>).**

DCDMA (1.03 g) was refluxed in alkaline buffered solution for 2h resulting in an intense yellow solution. After neutralization and filtration of the insolubles and evaporation, the yellow residue (0.92 g) was Soxhlet-extracted into dichloromethane. Removal of the dichloromethane and successive extraction of the residue with warm DCM followed by cooling removed colourless products by precipitation and lead to a deep yellow soluble fraction. Evaporation of DCM gave a yellow residue (0.55 g)  $\lambda_{\text{max}} = 215, 310, 385$  and  $452 \text{ nm}$ . TLC separation of the yellow component from other products (visualized by starch-iodide reagents and uv lamp) was achieved with silica and methanol/dichloromethane mixtures. The reaction mixture was fractionated by column chromatography into 23 fractions. Fractions 7, 9 and 15 were yellow and different from the rest.

F<sub>7</sub> in 3 mL DCM deposited a colourless solid on standing overnight. Evaporation of the solvent gave a yellow residue (~20 mg). Uv/vis (methanol)  $\lambda_{\text{max}} = 255, 380$  and  $455 \text{ nm}$ . IR(neat)  $\nu_{\text{max}}/\text{cm}^{-1}$ : 3290, 1667, 1614, 1556, 1395. NMR <sup>1</sup>H (d<sub>6</sub>-DMSO): 1.85(s 3H), 2.75(d 3H), 7.7(br 1H). An attempt to purify this fraction by recrystallisation from hot toluene resulted in decomposition.

The HPLC's of DCD<sub>11</sub>-F<sub>9</sub> and F<sub>15</sub> showed these fractions to be mixtures and further attempts to isolate pure compounds were abandoned.

Effect of pH on extractability of yellow components in alkali-degraded DCDMA(DCD<sub>12</sub>).



Examination of the fractions by HPLC showed no pure compound was isolated. Further fractionation was not attempted.

#### **Isolation of yellow components of alkali-degraded DCDMA (DCD<sub>13</sub>).**

An intense yellow thermolysis mixture was prepared as in DCD<sub>11</sub>. 250 mg of this was separated into seven fractions by preparative normal-phase HPLC as shown in Fig 2.6. Fractions 1, 2, 4 and 5 were either colourless or slightly yellowed and were not examined further. Fraction 3, a yellow gum (10.6 mg) remained a mixture of a few components (HPLC). NMR <sup>1</sup>H (d<sub>6</sub>-DMSO) δ: 1.2(s), 2(s), 2.85(m), 4.6(m), 6.7(m), 7.2(m). Uv/vis (CHCl<sub>3</sub> 95%: MeOH 5%) λ<sub>max</sub>: 290, 340 and 440 nm. Fraction 6, a yellow residue (29.5 mg) appeared to contain a significant amount of DCDMA (HPLC). Extraction of the yellow component(s) by chloroform gave on removal of the solvent a yellow gum (8 mg). Uv/vis (CHCl<sub>3</sub> 95%: MeOH 5%) λ<sub>max</sub>: 340 and 480 nm. Microanalysis gave C, 51.31; H, 8.14; N, 9.92; S, 12.01. Fraction 7, a yellow solid (91.2 mg) was further purified, by successive extraction with warm chloroform followed by cooling to remove the suspended colourless products by precipitation, to give an intense yellow residue (10 mg). NMR <sup>1</sup>H (d<sub>6</sub>-DMSO) δ: 2(s 3H), 2.8(d 3H), 5(m 1H), 7(m 1H), 7.7(m 1H). Microanalysis gave C, 53.55; H, 8.39; N, 8.6; S, 9.61%.

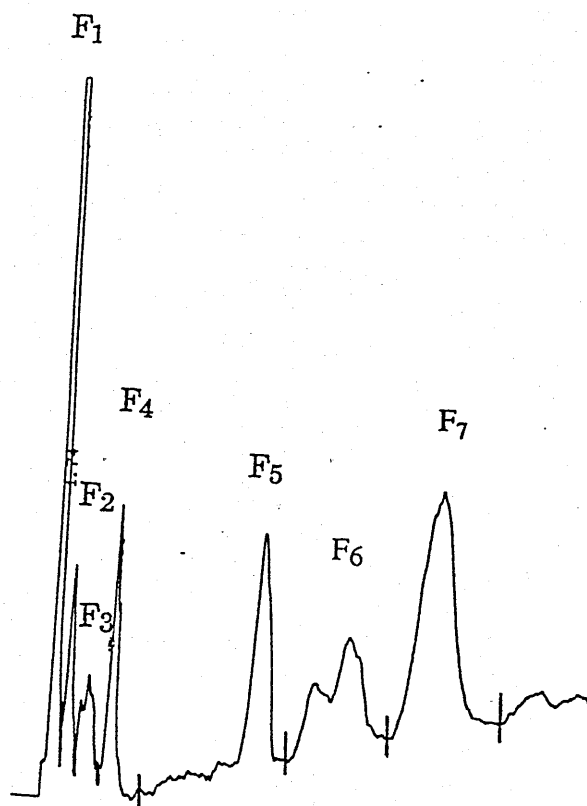


Figure 2.6 Prep-NPHPLC chromatogram of yellowed DCDMA reaction mixture.

### 2.4.3 Neutral solution

#### Effect of oxygen on degradation of DCDMA in aqueous solution (DCD14).

Aqueous solutions of DCDMA ( $8.56 \times 10^{-3}$  and  $8.6 \times 10^{-3}$  M) were refluxed under nitrogen and air respectively and degradation monitored by HPLC.

#### Effect of buffer on degradation of DCDMA in aqueous solution (DCD15).

Aqueous buffered solution of DCDMA ( $8.87 \times 10^{-3}$  M) was refluxed and thermolysis mixtures were analysed at different time intervals by HPLC.

### 2.5 Thermal degradation of other mono peptides - comparative labilities

*N*-Acetyl-*N*-methylamides of alanine, phenylalanine, glycine, histidine, methionine, serine, threonine, tryptophan, tyrosine, and diacetyl dimethylamides of cystine and lanthionine [NAM's] were heated according to the general

procedures described in section 2.3 and the resulting thermolysis mixtures were monitored by HPLC. The pH values of the reaction mixtures were also recorded.

#### 2.5.1 Alkaline degradation of NABSMA

NABSMA ( $8 \times 10^{-3}$  and  $4.03 \times 10^{-3}$  M) were heated in alkaline buffered solutions at 55 and 100 °C respectively. The reaction mixtures were monitored by HPLC and compared with standard samples of NADMA, benzylalcohol and phenol.

#### 2.5.2 Alkaline degradation of NAGMA

NAGMA (28.5 mg) in alkaline buffered solution (20 mL, pH = 10.8) was refluxed for 48h. The reaction was monitored by HPLC and compared with standard samples of acetamide, glycine, *N*-acetylglycine and *N*-acetylglycine amide. After the removal of solvent a portion of the reaction mixture (17.1 mg in 10 mL water) was mixed with *N*-fluoronylmethylchloroformate (N-FMOC, 19.4 mg in 10 mL of acetone) [Näsholm T., 1987] and stirred for 10 minutes. The resultant solution was shaken with equal volume of pentane and the aqueous portion analysed by HPLC together with that of F-MOC glycine using ammonium acetate [0.01 M (acetonitrile 30: water 70)] as the mobile phase.

#### 2.5.3 Effect of air on the alkaline degradation of NAGMA

NAGMA (47.1 mg and 255 mg) were refluxed in alkaline buffered solution (25 mL) in the presence of nitrogen and sodium hydroxide (0.01 M, 50 mL) in the presence of air respectively. The reactions were monitored by HPLC.

### 2.6 DCDMA Photolysis

#### Exploratory photolysis

DCDMA ( $5.01 \times 10^{-3}$  M) was irradiated in the absence of air at RT using a centrally placed 400 W medium pressure mercury arc and pyrex photolysis tubes

in a Carousel apparatus. Air was removed from the space at the top of the tubes by flushing with oxygen-free nitrogen or argon and sealing with a neoprene stopper. Samples were taken at 1, 2, 4, 8, 16, 32 and 64h and examined by HPLC and their pH values measured.

### Large scale photolysis and isolation of products

DCDMA (0.045 M) was irradiated in the absence of air at RT using a Pyrex photochemical reactor and 400 W medium pressure mercury arc for 24h. The resulting yellow reaction mixture was separated by full prep HPLC into four fractions (Fig. 2.7). Examination of the fractions showed: Fraction 1, a white solid (30 mg), very hygroscopic. The HPLC showed a mixture of two or three products. IR(KBr)  $\nu_{\text{max}}/\text{cm}^{-1}$ : 3350(br), 1670, 1650, 1560, 1540. NMR  $^1\text{H}$  ( $\text{d}_6$ -DMSO)  $\delta$ : 1.25(d), 1.8(m), 2.5(d), 3.6(d), 5.1(m), 6(m), 7.1(m), 7.7(m), 8(m).

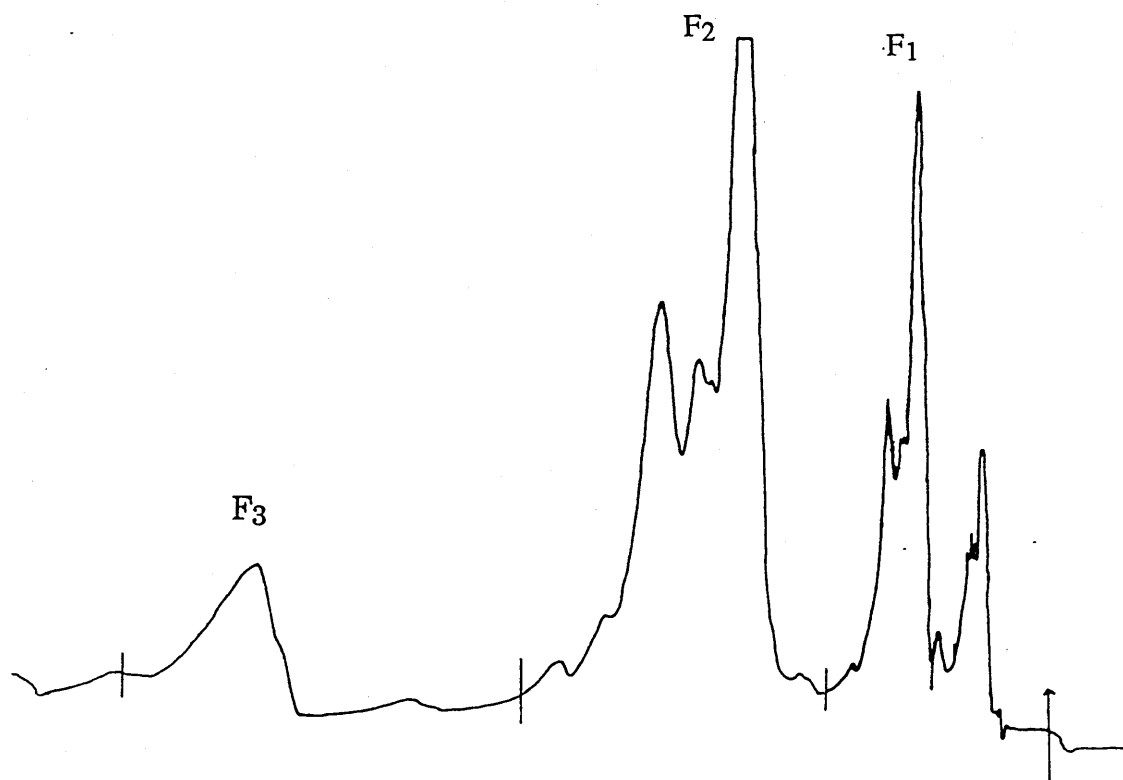


Figure 2.7 Prep-HPLC chromatogram of DCDMA photolysis mixture.

Fraction 2, a white solid (68 mg). HPLC showed one product peak in consistent with that of NACMA. IR (KBr)  $\nu_{\text{max}}/\text{cm}^{-1}$ : 3290, 2556, 1646, 1546. NMR  $^1\text{H}$  ( $\text{d}^6$ -DMSO)  $\delta$ : 1.9(s 3H), 2.6(m 3H), 4.3(m 1H), 8 (m 2H).

Fraction 3 was the unchanged starting material.  $\text{DCD}_2\text{-F}_4$ , off-white solid (150 mg). Both HPLC and NMR spectra showed it to contain a number of components. IR(KBr)  $\nu_{\text{max}}/\text{cm}^{-1}$ : 3520, 3380, 1645, 1140(br).



### **3 Results**

#### **3.1 Degradation of DCDMA in solid-state**

##### **3.1.1 Diacetylthiocystine dimethylamide**

##### **3.1.2 *N*-Acetyl-thiocysteine-*N*-methylamide**

#### **3.2 Alkaline degradation of DCDMA**

##### **3.2.1 Exploratory experiments**

##### **3.2.2 Isolation of products (a) sulphur, *N*-Acetyldehydroalanine-*N*-methylamide, and *N,N*-Diacetyllanthionine-*N,N*-dimethylamide**

##### **3.2.3 Isolation of products (b) acetamide methylpyruvamide and other products**

##### **3.2.4 Quantitative analysis**

##### **3.2.5 The yellow products**

#### **3.3 Degradation of DCDMA in neutral media**

#### **3.4 Thermal degradation of other mono peptides**

#### **3.5 Photochemistry of DCDMA in aqueous solution**

### 3 Results

#### 3.1 Degradation of DCDMA in solid-state

The results of exploratory thermal experiments are shown in Table 3.1.

Expt	condition				Temp °C	time/h	%conv	comments
	wet	dry	air	N <sub>2</sub>				
DCD <sub>1</sub>	✓			✓	100	66	8.5	Little degradation degrades completely with the formation of intense yellow colour
DCD <sub>2</sub>	✓			✓	150	16.5	>99	
DCD <sub>3</sub>	✓			✓	125	0.5	1.9	degrades slowly with the formation of bright yellow colour
	✓			✓		2.0	12.4	
	✓			✓		4.0	15.8	
	✓			✓		8.0	22.4	
	✓			✓		16.5	31.5	
	✓			✓		32.0	41.0	
	✓		✓			16.5	26.0	
		✓	✓			32.0	<1	
		✓		✓		32.0	<1	

Table 3.1 Degradation of DCDMA in wet/dry solid-state in the presence of air or nitrogen at 100, 125 and 150 °C

Thus it appears that negligible reaction occurs in dry samples under either nitrogen or in the presence of air, but significant reaction occurs in samples in the presence of water. The presence of oxygen appeared to inhibit the degradation of DCDMA. Approximately, 8.5 and 31% of DCDMA had reacted after 6 and 16.5 hours at 100 and 125 °C, respectively, giving a few minor product peaks and a major product peak with useful resolution and retention on RPLC (Fig. 3.1), but poor chromatograms are obtained on NPLC. Figures 3.2 and 3.3 show some parameters of the degradation in wet samples under N<sub>2</sub>. The drop in pH and the constant yield of what appears to be the major product with a long retention time (LRTP) is worth noting. Yellowing was observed after only 0.5h in solid-state

wet conditions. A strong sulphureous smell was noted whose intensity increased with heating time.

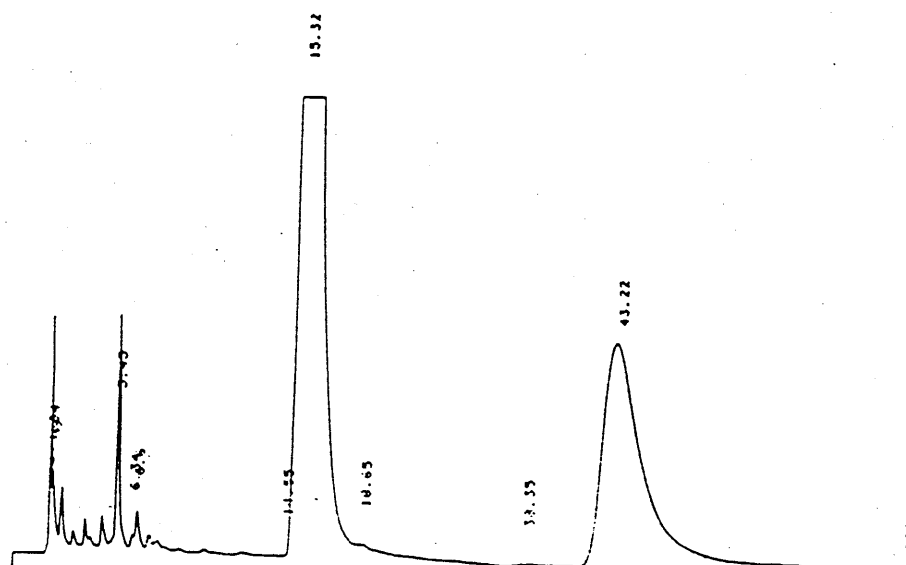


**Figure 3.1** Analytical HPLC elution profile of DCDMA reaction mixture in wet solid-state conditions at 125 °C.

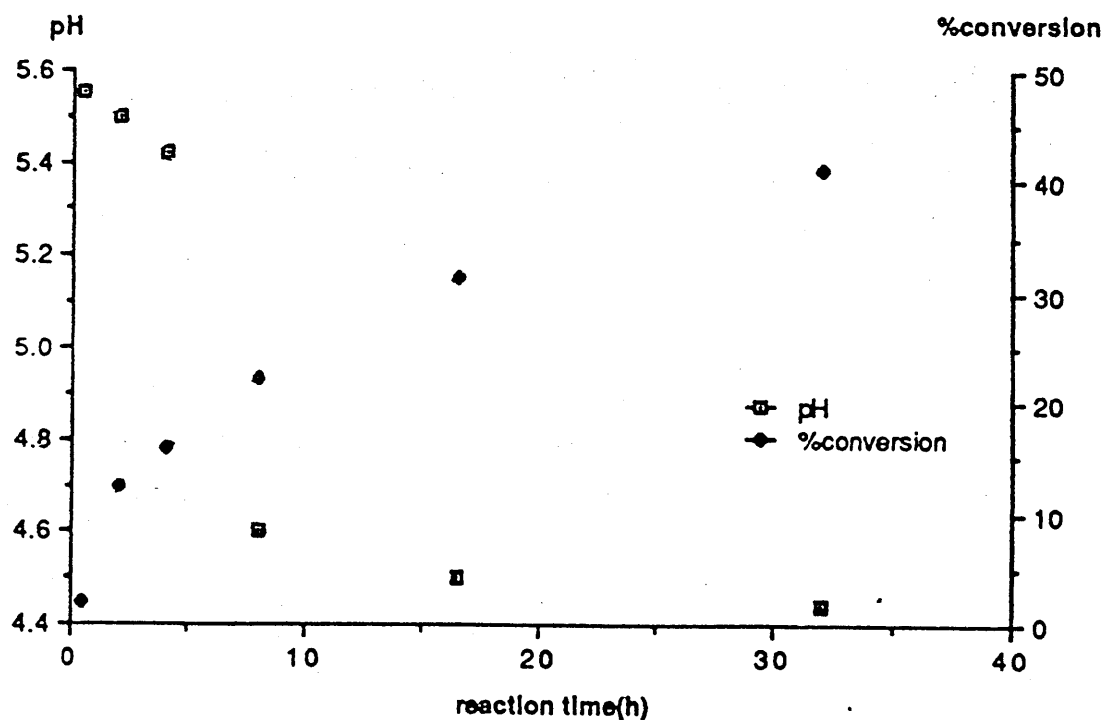


Figure 3.2 The effect of time on pH and breakdown of DCDMA in wet solid-state conditions at 125 °C.

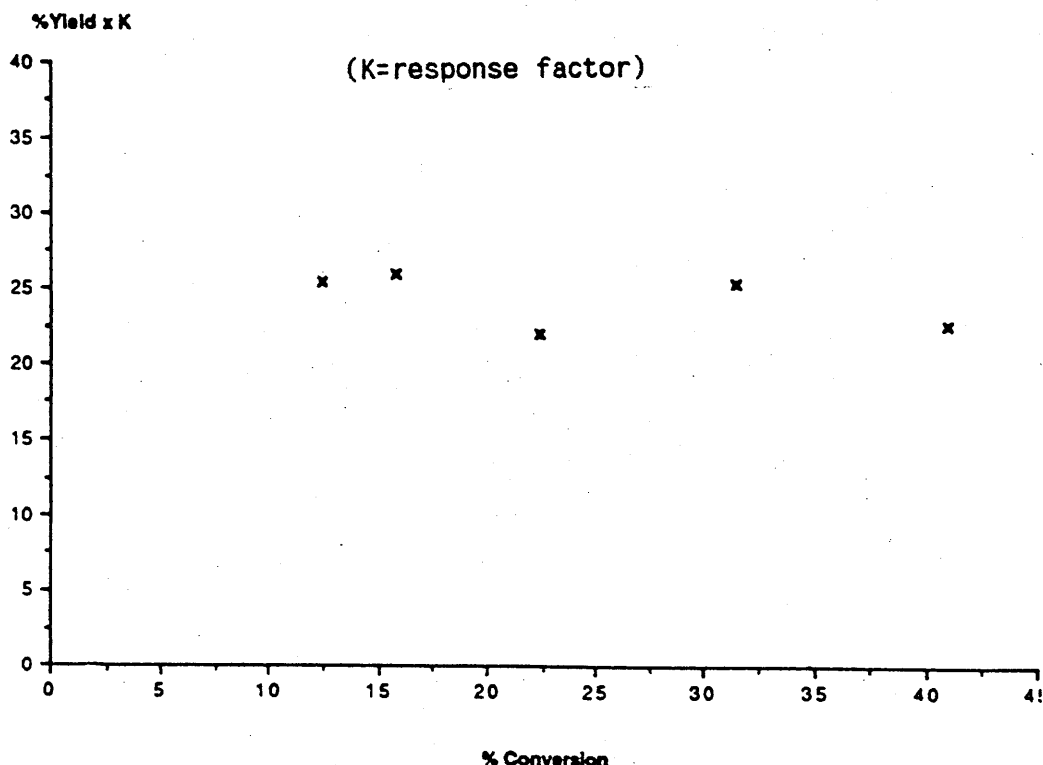


Figure 3.3 A plot of theoretical yield of the long-retention time product  $\times K$  vs. conversion of DCDMA in wet solid-state condition.

### 3.1.1 Diacetylthiocystinedimethylamide (DTCDMA)

Large scale thermal degradation experiments on wet solid samples under  $N_2$  were carried out at  $125^\circ C$  for 16h in order to isolate the primary products. Addition of water to the resulting yellow syrup gave a bright yellow aqueous solution with a fine precipitate which was separated by centrifugation. This was shown to be elemental sulphur by combustion analysis and the characteristic green colour obtained with oleum. The yield of sulphur was determined in a separate experiment (DCD<sub>5</sub>) to be 35%. Continuous liquid-liquid extraction of the aqueous reaction mixture with DCM proved unsatisfactory, but semi- prep HPLC allowed the long-retained product to be isolated in a reasonably pure state. Ir and mass spectra of the compound were almost identical to those of DCDMA. Although its  $^1H$  NMR spectrum in  $D_2O$  was very similar to that of DCDMA at 90

MHz, a 400 MHz spectrum showed a repeat pattern of signals similar to those responsible in DCDMA but at different chemical shifts (Fig. 3.4). The compound

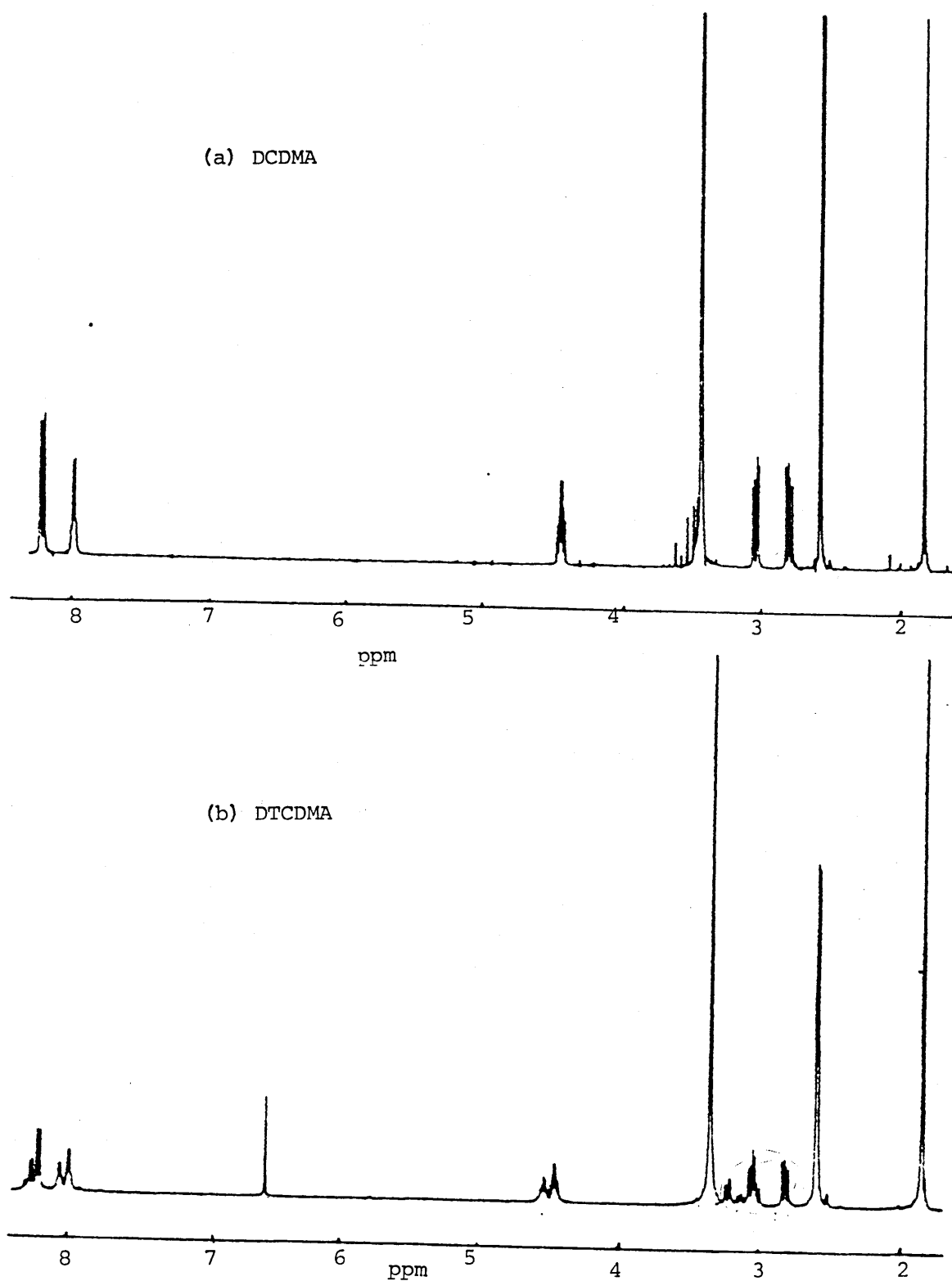
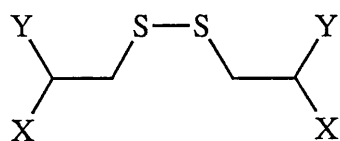
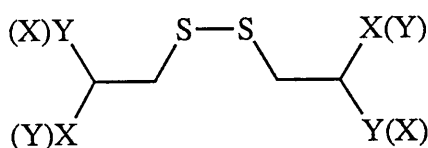


Figure 3.4 shows  $^1\text{H}$  NMR spectra (400 MHz) of DCDMA (a) and the long-retention time product (b).

is somewhat labile, however, and HPLC analysis of the NMR sample subsequently showed considerable decomposition largely to the starting material. The similarities in IR, NMR and mass spectra with DCDMA suggested this major product may be the RS-(meso)stereoisomer of DCDMA (27). The RR isomer (the starting material) is shown in structure 28. However, the widely



Meso - DCDMA (27)



RR & SS enantiomers=racemic (28)

differing chromatographic behaviour seemed inconsistent with this assignment. Accordingly, a sample of RS-(meso) DCDMA was synthesised from commercially available meso-cystine. Its HPLC showed two peaks at closely similar retention times (Fig. 3.5), one of which was identical with the RR isomer used for the thermolyses. The fact that the other peak had a much shorter retention time contrary to our expectation confirmed that the long-retention time product is not the RS-(meso)-isomer of DCDMA as originally suggested. It is important to note that in the synthesis of RS-meso-DCDMA, a racemic mixture of isomers is also inevitably produced in addition to the meso-isomer.

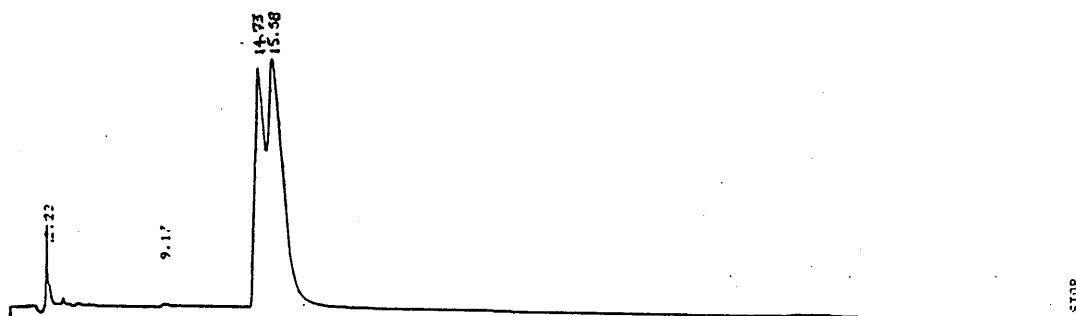
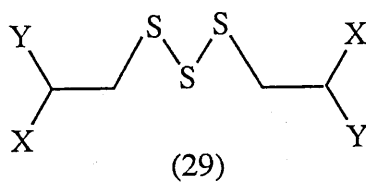


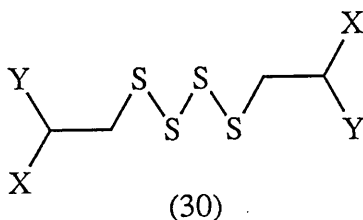
Figure 3.5 shows analytical HPLC of meso and DL-DCDMA as a twin peak.

When the major product of thermolysis is heated in the presence of  $N_2$  and water at 125 °C for 16.5h, it decomposes to the DCDMA stereoisomers and a few

products with shorter retention times on RPLC. In fact, the HPLC resembles that obtained in the original thermal degradation of DCDMA under identical experimental conditions. The sample also yellowed intensively and gave a very strong smell of hydrogen sulphide after 16.5h. The fact that this unknown long-retention time product is very labile suggests it may not have withstood the chemical ionization treatment in mass spectrometry and that the molecular ion was absent from the spectrum. So a spectrum was taken with ionization by fast atomic bombardment. This showed a heaviest ion of mass 383 with a molecular formula of  $C_{12}H_{23}N_4O_4S_3$  ( $MH^+$ ,  $\pm 0.3$  mmu). All these data indicate strongly that the unknown long-retention time product is *N,N*-diacetylthiocystine-*N,N*-dimethylamide (DTCDMA), 29. In repeat experiments, the yield of DTCDMA

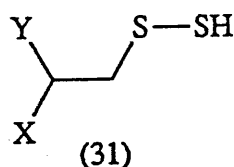


was found to be 65% by HPLC. Subsequently an even longer-retained product peak was isolated from a thermolysis mixture. Again on manipulation this substance gave a range of secondary products similar to that observed from the original DCDMA thermal degradation. The IR spectrum of this product was similar to, but not identical with those of DCDMA and DTCDMA. The  $^1H$  NMR in  $D_2O$  showed the presence of acetyl ( $\delta = 2.0$ ), methylamide ( $\delta = 2.70$ ) and a multiplet at  $\delta = 3.30$  which integrated to three hydrogens may be attributable to methylene group and hydrogen on the chiral carbon. The HPLC decomposition pattern and the data above suggested the unknown may be the tetrasulphide (30).

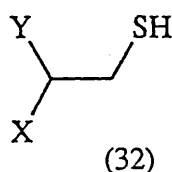


### 3.1.2 *N*-Acetyl-thiocysteine-*N*-methylethylamide

In one attempt to isolate the trisulphide the procedure was modified by increasing the sample weight and the reaction time which allowed the isolation of a further product less well retained than the trisulphide (Fig. 2.3). The compound appeared to be very labile. Again the  $^1\text{H}$  NMR spectrum in  $\text{D}_2\text{O}$  and the IR spectrum showed features closely similar to, but not identical with DCDMA. However, an additional band in the IR spectrum at  $2553\text{ cm}^{-1}$  (S-H) suggested the compound may be the thiocysteine derivatives (31). Support for this assignment was



obtained when a representative quantity of the alkali-treated compound was mixed with sodium cyanide at room temperature and then was mixed with acidic ferric nitrate. A chromophore was generated ( $\lambda_{\text{max}}$  at 460 nm) which was characteristic of ferric thiocyanate and diagnostic for R-S-S-H [Cavallini, 1960] (Fig. 3.6). Similar treatment of a sample of the trisulphide gave little coloured reaction and hence no  $\lambda_{\text{max}}$  at 460 nm. Further evidence for the formation of 31 was present in the  $^1\text{H}$  NMR in  $\text{d}^6$  DMSO of a degraded sample of the trisulphide. This included a singlet at 6.55 ppm whose integration was fully consistent with those for a set of signals with chemical shifts appropriate for the rest of the molecule. The SH signal for the cysteine derivative (32) is a triplet in DMSO. Due to the very labile nature of this compound it was not possible to determine its yield in DCDMA thermal degradation experiments.





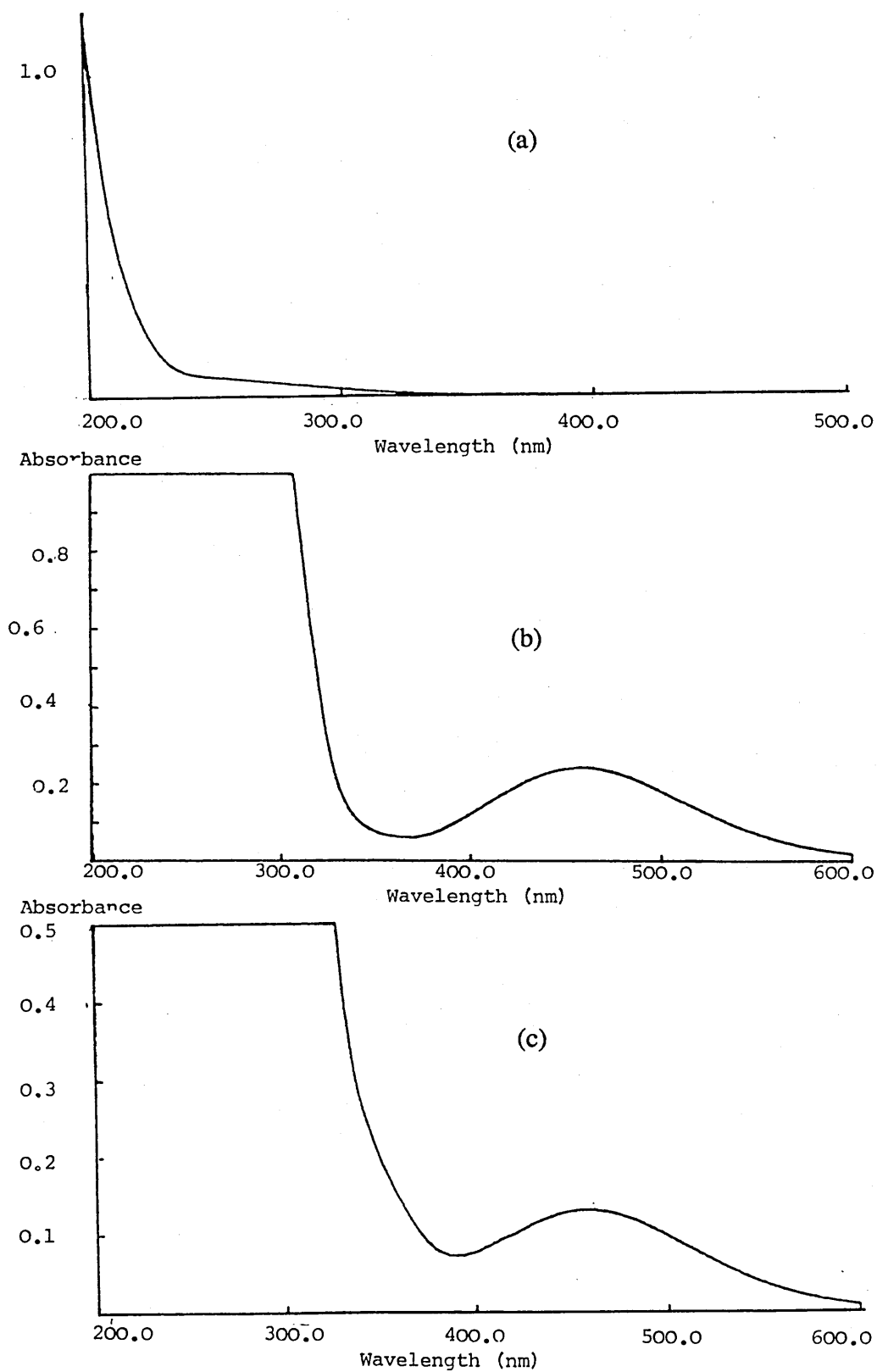


Figure 3.6 The uv/vis spectra of (a) thiocystine derivative (b) thiocyanide and (c) thiocysteine derivative upon cyanolysis.

*N*-Acetyl-L-cysteine-*N*-methanamide (32) was expected to be a product of the degradation of DCDMA, so a sample was synthesised by reduction of DCDMA and its HPLC compared with those of degradation mixtures from DCDMA found under a variety of conditions. The yield of NACMA was determined in wet solid-state samples under N<sub>2</sub> and is given in Table 3.2.

Table 3.2 Yield of NACMA in DCDMA wet solid-state degradation under N<sub>2</sub>.

% conversion	5	12	22	32
yield of NACMA %	21	32	23	20

So three products have been isolated from the wet solid-state thermal degradation of DCDMA in addition to elemental sulphur. The trisulphide was shown to be a major product formed almost immediately after heating DCDMA while NACMA and the hydropersulphide were present as minor products. All the above compounds are colourless.

### 3.2 Alkaline degradation of DCDMA

#### 3.2.1 Exploratory experiments

The results of exploratory alkaline buffered experiments under reflux (DCD<sub>7</sub>) showed that (i) the presence of oxygen has little effect on either the amount of DCDMA reacted or the uv/vis spectra of the reaction mixtures taken under reflux. (ii) DCDMA is almost completely degraded after 0.5h. Yellowing was observed on dissolving the sample in alkali, and the effect of nitrogen is negligible. The uv/vis spectra of the thermolysis mixtures at reflux shows two absorption bands at  $\lambda_{\text{max}} \approx 300$  and 385 nm. Prolonged alkaline treatment causes an increase in A<sub>385</sub> up to 2 h which declines and disappears after 19h. The A<sub>300</sub> declines slightly up to 2h and then increases to a maximum at T = 4h. This absorption maximum also disappears after 24h. A weak absorption maximum is also observed at  $\lambda_{\text{max}} = 455$  nm which disappears on prolonged alkaline treatment ( $t_h > 24\text{h}$ ) (Fig. 3.7).

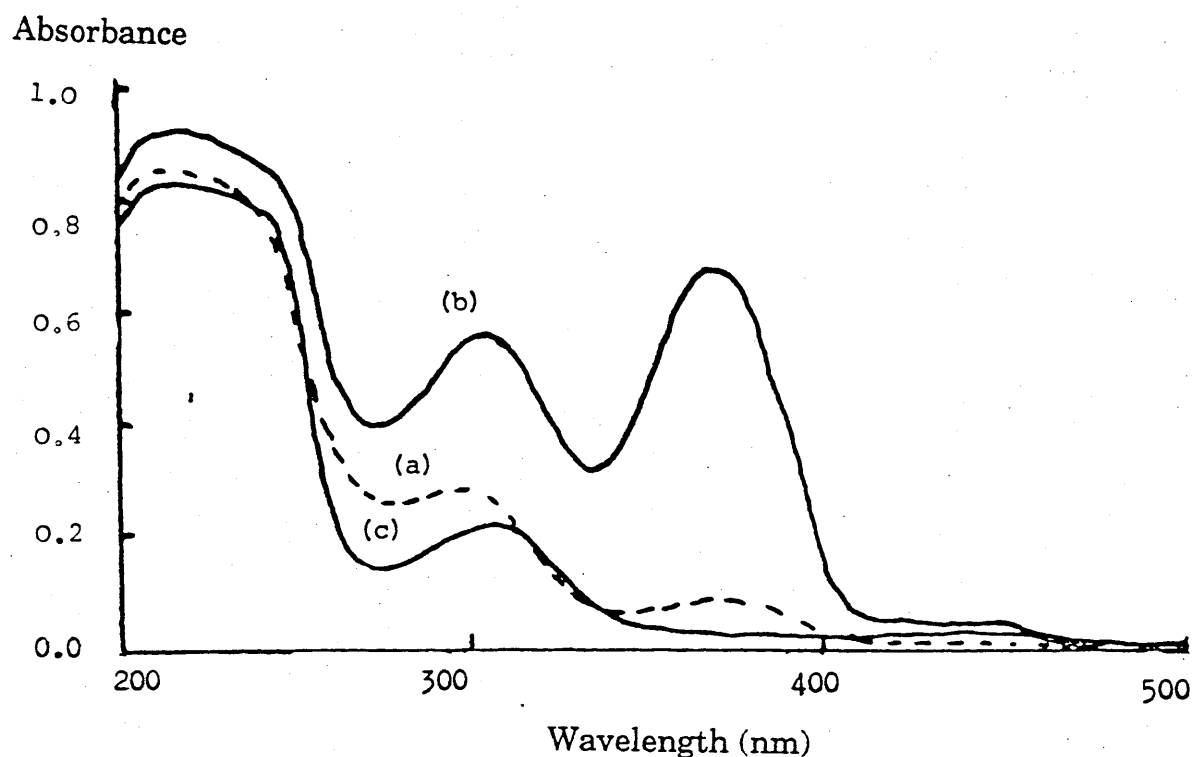


Figure 3.7 Uv/vis spectra of alkali-treated DCDMA reaction mixtures in the presence of buffer at 100°C for (a) T = boiling (refers to the point at which refluxing commences), (b) T = 4h and (c) T = 24h.

Thermal degradation experiments were repeated in alkaline buffered and non-buffered solutions at 55 °C in air (DCDg) in order to follow the break down products in DCDMA in alkali and the results are given in Table 3.3. The pH of the non-buffered samples drops from 10.8 to 8.7. Approximately 15 and 85% of DCDMA had reacted in non-buffered and buffered samples respectively after 24h. Yellowing requires more than 120h for samples in non-buffered medium, but this was observed immediately on warming for the buffered samples.

Table 3.4      Degradation of DCDMA in alkaline buffered and non-buffered media at 55 °C.

react <sup>n</sup> time(h)	pH		% conversion	
	buffered	non-buffered	buffered	non-buffered
0.0	10.8	10.8	28	13
0.5	10.7	10.4	33	12
1.0	10.7	10.3	32	12
2.0	10.6	10.0	41	11
3.0	10.5	9.8	46	13
4.0	10.5	9.0	48	13
24.0	10.2	8.7	86	16

HPLC chromatograms (Fig. 3.8) for products showed three major product peaks with short retention time and a few minor product peaks.

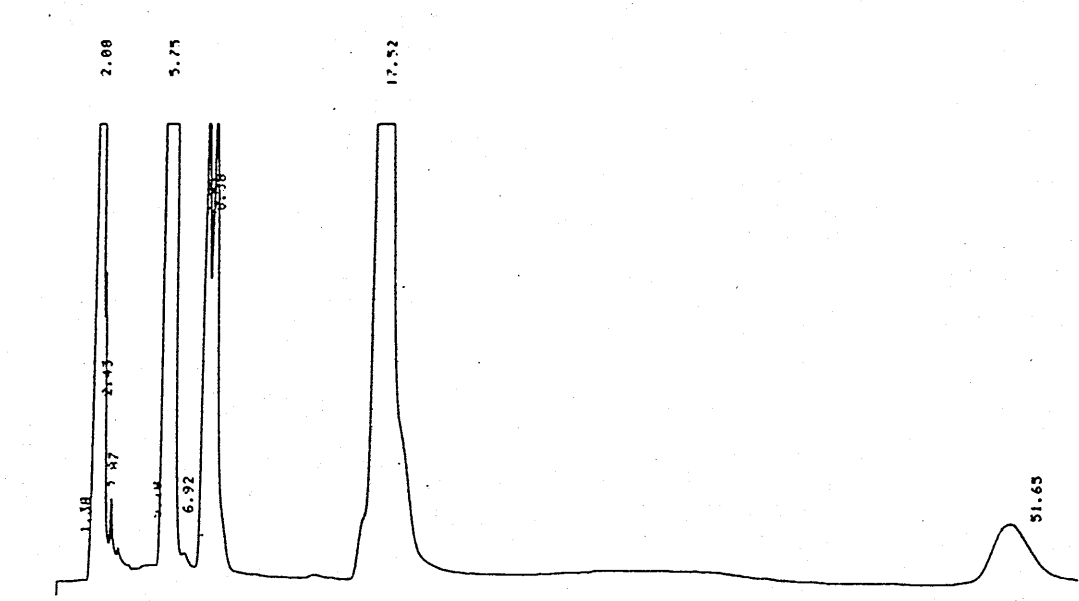
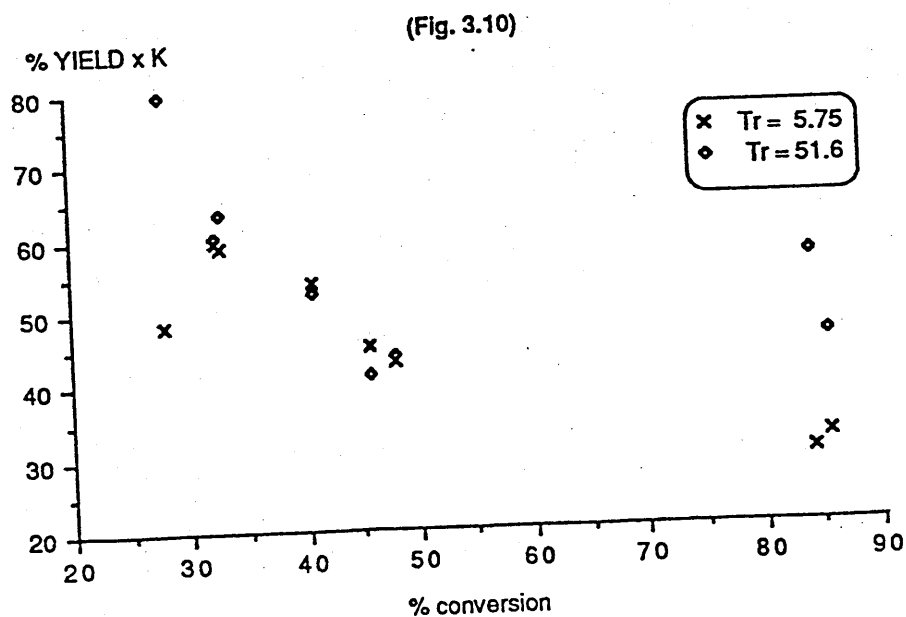
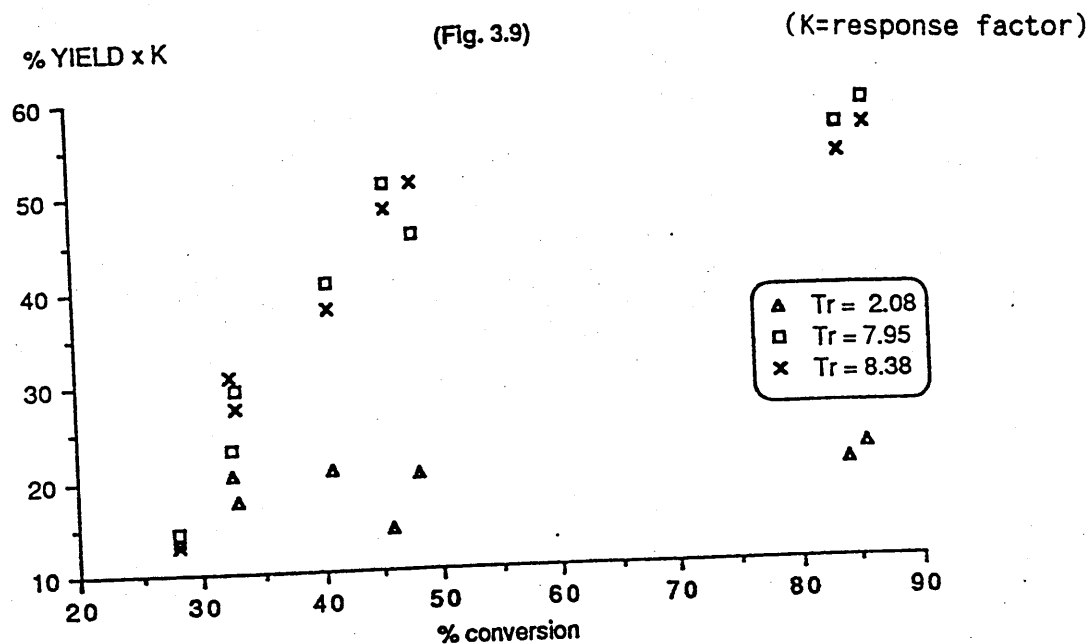


Figure 3.8      Analytical HPLC of DCDMA alkaline reaction mixture at 55 °C for 2h.

Plots of the theoretical yield x K (response factor) vs conversion for product peaks at retention times, 2.08, 7.95 and 8.38 minute indicate that they are secondary products (Fig. 3.9) and those at 5.75 and 51.65 could be primary products (Fig. 3.10).



Figures 3.9 and 3.10 represent plots of theoretical yields x K of alkaline degradation products of DCDMA vs. its conversion.

### 3.2.2 Isolation of products. (a) sulphur, *N*-Acetyldehydroalanine-*N*-methanamide, *N,N*-Diacetylthionine-*N,N*-dimethyl amide, (DCD<sub>9</sub>)

Attempts were made to isolate the major products such as those shown in Fig. 3.8. DCDMA (35mmol) was subjected to buffered alkali at 55 °C for 2 hours. After neutralization, a fine precipitate was separated. This was shown to be elemental sulphur by combustion analysis and the characteristic green colour obtained with oleum. Its yield was about 13% theoretical maximum from converted substrate. Four fractions were separated by prep-HPLC (Fig. 2.4b). Fraction 1 showed a mixture of few components with short retention times and its spectra were inadequate for structure analysis.

Fraction 2 appeared to have decomposed by HPLC and showed a few low retention-time products ( $t_R \approx 2, 2.2$  and  $2.7$  min) in addition to DCDMA and DTCDMA (39). Its IR spectrum showed a very broad band at  $3300\text{ cm}^{-1}$  (H-bonded N-H or O-H stretching), a sharp band at  $2260\text{ cm}^{-1}$ , a very broad band at  $1450\text{ cm}^{-1}$ , a strong band at  $1195\text{ cm}^{-1}$ , a band at  $650\text{ cm}^{-1}$ .  $^1\text{H}$  NMR suggested the presence of acetyl (singlet at  $\delta = 2.0$  ppm) and methanamide (singlet at 2.65 ppm). No assignment was made at this stage. (See Discussion later.). The HPLC of Fraction 3 showed a single major peak at 5.75 min. The IR spectrum of this substance was consistent with a secondary amide with characteristic absorption bands at  $3339\text{ cm}^{-1}$  (N-H stretching), 1667 and 1653 (amide carbonyl),  $1556\text{ cm}^{-1}$  (N-H bonding). It also showed a moderately intense band at  $1631\text{ cm}^{-1}$  characteristic of alkenes.  $^1\text{H}$  NMR and  $^{13}\text{C}$  NMR at 400 MHz indicated the sample had decomposed in the preparation of a solution in  $d_6$ -DMSO. The preparative separation (DCD<sub>10</sub>) was repeated. The  $^1\text{H}$  NMR of the freshly separated unknown (Fig. 3.11) showed a singlet at 2.0 ppm (acetyl), a doublet at 2.6 ppm (methanamide), two singlets at 5.3 and 6.0 ppm (methylene protons), a quartet at 8.3 ppm resulting from the coupling of amide hydrogen with hydrogens on methyl and a singlet at 9.0 ppm attributable to NHAc.

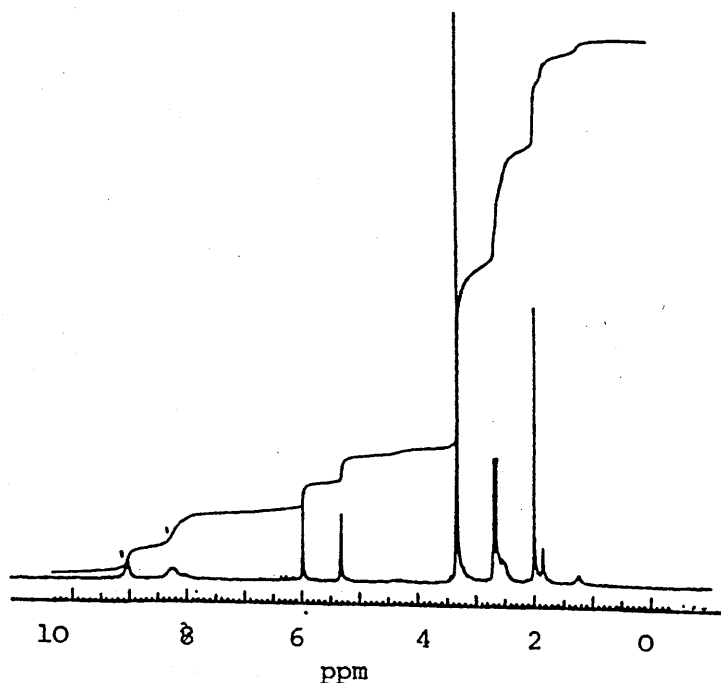
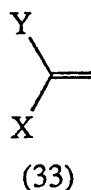


Figure 3.11  $^1\text{H}$  NMR spectrum of NADMA showing the well resolved olefinic methylene protons.

The integration, chemical shifts and coupling patterns of the signals are consistent with *N*-acetyldehydroalanine-*N*-methanamide (33).

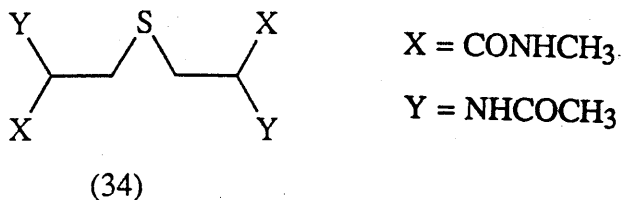


$\text{X} = \text{CONHCH}_3$

$\text{Y} = \text{NHCOCH}_3$

Further confirmation was obtained from the high resolution mass spectrum which contained the molecular formula.

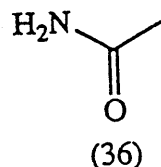
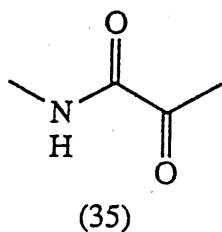
Fraction 4 comprised two peaks ( $t_R \approx 7.6$  and 8 minutes) close in retention time and area. The sample was shown to be a diastereomeric mixture of *N,N*-diacetyl lanthionine-*N,N*-dimethanamide (34) by spectroscopic analysis and independent synthesis from meso/racemic lanthionine.



### 3.2.3 Isolation of products. (b) Acetamide, methylpyruvamide and other products

In an attempt to identify the early-retained products of DCDMA alkaline degradation, a large scale experiment was repeated and four products were separated by prep-HPLC (DCD<sub>10</sub>). The analytical HPLC chromatogram of the reaction mixture was similar to that shown in Fig. 3.8 and therefore it is used as a reference. Fraction 1 contained a major product ( $t_R \sim 2$  minute). The IR spectrum indicated an amide but also showed strong bands at 1450 and 1350  $\text{cm}^{-1}$ . The  $^1\text{H}$  NMR in  $d_6$ -DMSO suggested the presence of acetyl (singlet at 1.8 ppm) and showed a singlet at 6.5 ppm and an NH resonance at 8.2 ppm. No assignment is made at this stage. (But see Discussion later.) Fractions 2 and 3 were identified as NADMA (33) and DLDMA (34) respectively as described previously. Fraction 4 was unchanged DCDMA. Fraction 5 had a long retention time on HPLC and also showed some decomposition and both of which indicated it may be either DTCDMA (29) or *N*-acetylthiocystiene-*N*-methylethylamide (31). The possible formation of (31) was investigated by uv/vis spectroscopy after cyanolysis, but no absorption band was observed at 460 nm which is diagnostic of hydropersulphides (31). The IR and  $^1\text{H}$  NMR spectra were similar to the previously identified DTCDMA, a product of solid-state DCDMA degradation, supporting its formation also in the alkaline degradation of DCDMA but in much smaller quantities. The HPLC of the reaction mixtures also indicates that NACMA is present as a minor product. Methylpyruvamide (35), together with acetamide (36) is expected to be a hydrolysis product of NADMA, so they were compared by HPLC with Fraction 1, several degradation mixtures, and that





of decomposed NADMA. Although methyl pyruvamide has a retention time very close to that of NADMA, further study of the HPLC chromatograms suggested that 35 is a major product in the decomposition of NADMA, and a minor product in the reaction mixtures. Acetamide was not found under these HPLC conditions and has a longer retention time than Fraction 1.

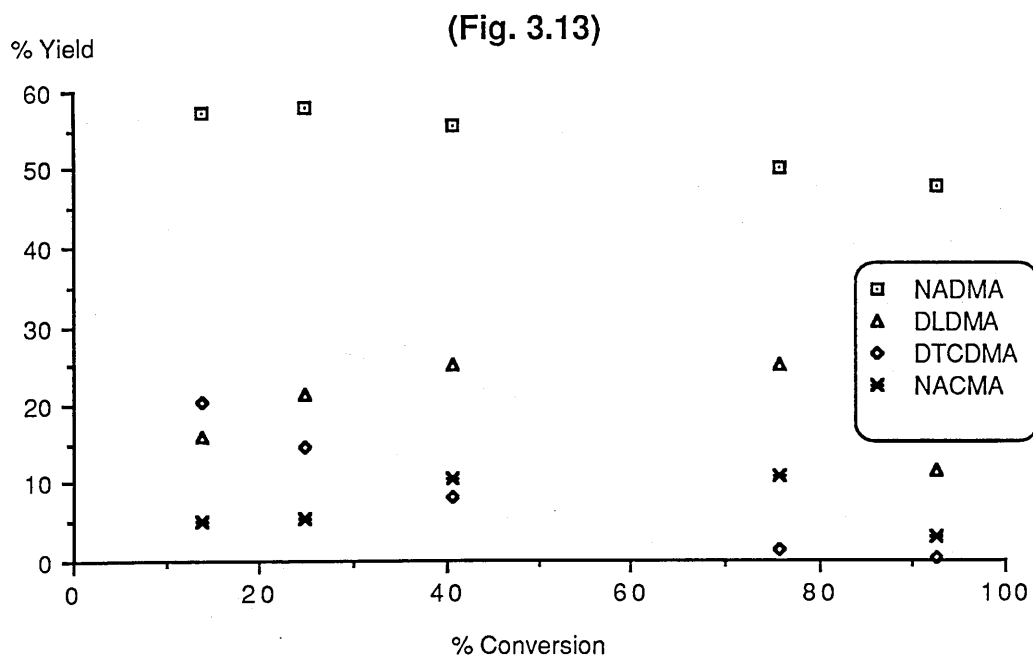
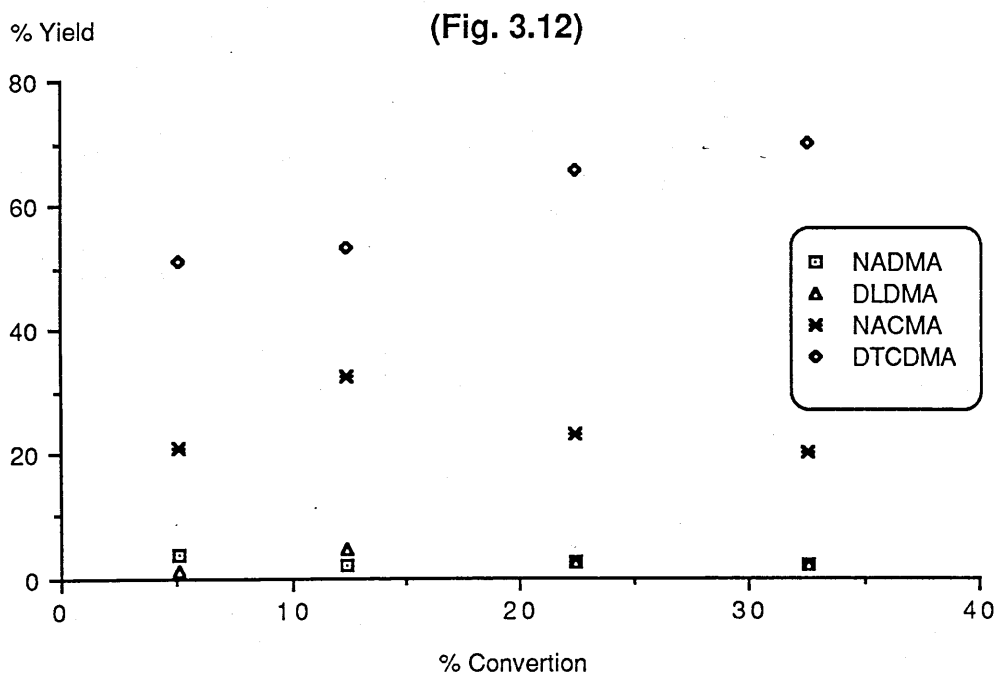
### 3.2.4 Quantitative analysis

The yield of products NACMA (32), NADMA (33), DLDMA (34) and DTCDMA (29) were determined in alkaline degradation of DCDMA at 55 °C and are given in Table 3.4.

Table 3.4 %Yield of products in alkaline thermolysis of DCDMA

react <sup>n</sup> time(h)	%conversion	NACMA	NADMA	DLDMA	DTCDMA
2	14.0	5.2	57.0	16.0	20.5
4	25.0	5.3	58.0	21.5	14.5
8	41.0	10.6	55.5	25.0	8.0
24	76.0	11.0	50.0	25.0	1.4
48	93.0	3.1	48.0	11.5	0.4

At approximately 25% conversion of DCDMA, 5.3, 58, 21.5 and 14.5% of NACMA, NADMA, DLDMA and DTCDMA were found in alkaline but the percentage yield of these products were 20, 2.7, 8.60 and 65% in solid-state conditions. Figures 3.12 and 3.13 suggest (i) DLDMA and NACMA are secondary products in the alkaline degradation of DCDMA, but may arise from a different pathway in the solid-state; (ii) NADMA is a primary product in both the alkaline and the wet solid-state degradation of DCDMA. (iii) DTCDMA appears to be a secondary product in wet solid-state, but a primary product in alkaline



Figures 3.12 and 3.13 represent the yield of products, NADMA, NACMA, DLDMA and DTCDMA vs. conversion of DCDMA in wet solid-state and under alkaline conditions.

degradation of DCDMA. Thus it appears that DTCDMA is the most significant product followed by NACMA with DLDMA and NADMA as the minor products in solid-state conditions, whereas the reverse is true for the products under alkaline conditions of DCDMA. Yields of acetamide and methylpyruvamide could not be determined due to a very close retention time to other products.

### 3.2.5 The yellow products

It was seen in Section 3.2, three regions of increased absorptions at  $\lambda_{\max} = 300$ , 385 and 455 nm are observed with degradation mixtures from DCDMA under alkaline conditions. Attempts have been made to identify the component(s) which may be responsible for the absorption at 385 and 455 nm and hence the yellowing. TLC examination on silica of a reaction mixture obtained by treating DCDMA with alkaline buffered solution (pH = 10.8) under reflux for two hours showed a diffuse yellow spot remained unmoved with eluent while colourless products including starting material eluted. Separation of the products by column chromatography (DCD<sub>11</sub>) resulted in three yellow fractions, namely, numbers 7, 9 and 15 of 27 fractions. Although fractions 9 and 15 had uv/vis spectra similar to that of yellowed reaction mixture, the HPLC and IR spectra showed considerable contamination with the starting material and other products. The uv/vis spectrum of F<sub>7</sub> is partly similar to that of the DCDMA reaction mixture showing  $\lambda_{\max} = 255$ , 380 and 455 nm (Fig. 3.14). RPLC showed a little-retained major peak and a few minor peaks. The ir spectrum indicated a secondary amide, 3290 cm<sup>-1</sup>, 1667 cm<sup>-1</sup>, 1556 cm<sup>-1</sup>. A sharp absorption band at 1165 cm<sup>-1</sup> may be attributable to thiocarbonyl C=S stretching. The <sup>1</sup>H NMR spectrum suggested the presence of acetyl (singlet at  $\delta = 1.85$  ppm), methylamide (doublet at  $\delta = 2.75$  ppm) and an amide proton (broad signal at  $\delta = 7.7$  ppm). These data (RPLC, <sup>1</sup>H NMR and IR spectra) are consistent with those of methylthiopyruvamide (37) or its

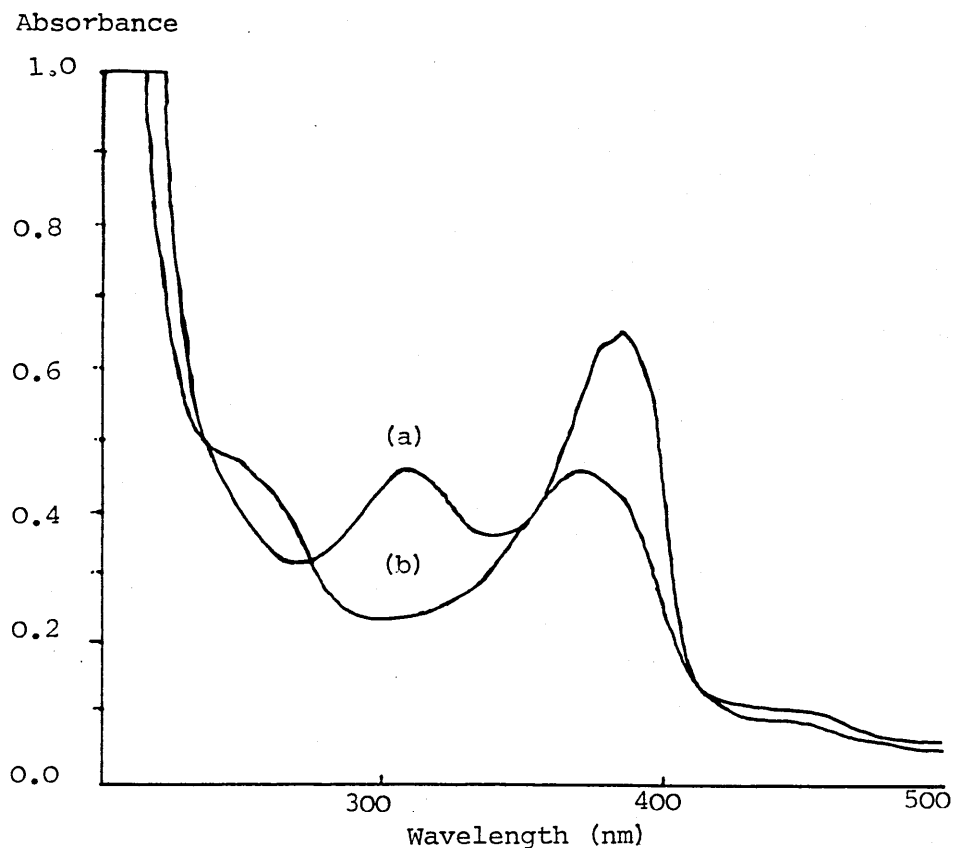
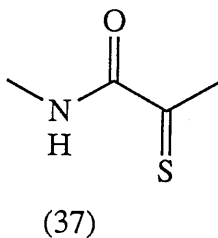


Figure 3.14 The uv/vis spectra of DCDMA reaction mixture (curve a) and F<sub>7</sub> (curve b) showing  $\lambda_{\text{max}} = 385 \text{ nm}$

decomposition product. Although methylpyruvamide is a colourless oil, *N*-methylthiopyruvamide (37) is a yellow compound. A solution of the latter was generated by bubbling hydrogen sulphide through a solution of methylpyruvamide.



The examination of the resulting labile product by <sup>1</sup>H NMR in deuterated chloroform showed a singlet at  $\delta = 2.0 \text{ ppm}$  (acetyl), a doublet at  $\delta = 2.80 \text{ ppm}$  (methylamide) and a broad signal at 7.3 ppm (amide). The IR spectrum (neat) showed absorption bands characteristic of secondary amides at 3300  $\text{cm}^{-1}$ ,

1645  $\text{cm}^{-1}$ , 1545  $\text{cm}^{-1}$ , and thiocarbonyl at 1155  $\text{cm}^{-1}$ . The uv/vis spectrum was very similar to that of Fraction 7 showing an absorption maximum at 380 nm which may be responsible for the yellow component.

In a search to identify the yellow component(s) by HPLC, the RPTLC of the yellowed reaction mixture was explored. The results showed that only at high concentrations of acetonitrile (>50%) the yellow component(s) elute which would correspond to using 25% acetonitrile in the mobile phase in RPHPLC. In addition the deuterium lamp which has a detection range of 200-367 nm was replaced with tungsten lamp so that coloured component(s) could also be monitored. The examination of the yellowed reaction mixture by the RPHPLC under modified conditions indicated that there at least three component(s) responsible for the yellowing in DCDMA degradation under alkali.

The HPLC examination of the yellow dichloromethane extract after evaporation of (Section 2.4.2 - DCD<sub>12</sub>) showed little extraction of the products including the yellow component(s) into dichloromethane. Although the extract was yellow, when dissolved in distilled water after evaporation of the dichloromethane, this gave only a pale yellow suspension. A fine solid was precipitated on standing. So the yellow residue in the thimble was dissolved in distilled water and neutralised by concentrated hydrochloric acid as in previous alkaline experiments and soxhlet extracted. This clearly illustrated that the components responsible for yellowing are more soluble in alkaline medium and are only extracted into dichloromethane once the alkaline reaction mixture is neutralised.

Since the separation of the yellow component(s) by RPLC was unsuccessful, attempts were made to isolate it by NPLC. A yellowed reaction mixture was generated by heating DCDMA in alkaline buffered solution (pH = 10.8) for two hours under reflux and separated into seven fractions by prep-NPLC (Fig. 2.6). Three products appeared to be most interesting when examined spectroscopically

in addition to being yellow. Fraction 3 was shown to contain at least five component(s) by RPHPLC which included methylthiopyruvamide or its decomposition product, NADMA, DCDMA and an unknown, so no attempt was made to purify it further. However this fraction had a uv/vis spectrum very similar to that of Fraction 7 described previously in this section. Examination by RPHPLC showed that Fraction 6 contained largely DCDMA and Fraction 7 contained DLDMA and the trisulphide. Thus although each of these Fractions were yellow, the components responsible for the colour was not identified. These fractions were also monitored on RPHPLC equipped with diode array detection system (200-367 nm), but no component was seen with an absorption maximum greater than 300 nm, nor was it possible to identify any product peak responsible for yellowing by monitoring at a wavelength greater than 360 nm. These results indicate that yellow components may be decomposing either before or during the elution. So far as the yellowing is concerned, therefore, our investigation indicates more than one product is responsible, one of which may be attributable to *N*-methylthiopyruvamide (37). Furthermore, HPLC analyses have shown that the yellow component(s) are very labile, and present in very small amounts.

### **3.3 Degradation of DCDMA in neutral media**

Small scale degradation studies of DCDMA were carried out in refluxing aqueous solution under N<sub>2</sub> and under air. Product analysis by HPLC revealed that samples under air react at less than half the rate of those under N<sub>2</sub> (Table 3.5). For example 15 and 22% of DCDMA had reacted after 24h respectively. The HPLC chromatograms for products showed two major product peaks, one early-retained and the other with long-retention time.

Table 3.5 shows the % conversion of DCDMA in refluxing aqueous buffered solutions.

React <sup>n</sup> time (h)	% conversion		
	refluxing aqueous (DCD <sub>14</sub> )		refluxing buffered DCD <sub>15</sub>
	N <sub>2</sub>	air	
0.0			
0.5			
2.0	3.0	3.0	-
4.0	7.6	3.8	9.0
8.0	14.5	10.0	19.4
24.0	22.5	15.0	46.2
48.0			54.0
95.0	37.5	28.0	
119.0	51.6	20.0	
144.0			96.2

Although the product distribution was similar to that observed in non-buffered experiments (DCD<sub>14</sub>), the rate of degradation was much higher in buffered samples. Furthermore, yellowing was observed after 24h in DCD<sub>15</sub>, where a similar yellowing on DCD<sub>14</sub> was observed only after 120h. The HPLC chromatograms of the DCDMA degradation in alkaline, neutral and solid-state at approximately 20% conversion are shown in Fig 3.15 which also show a clearly resolved major long-retention-time product in all three conditions. Samples in aqueous solutions give products which are comparable to those obtained for wet solid-state samples in N<sub>2</sub> at 125 °C, but at a much slower rate.

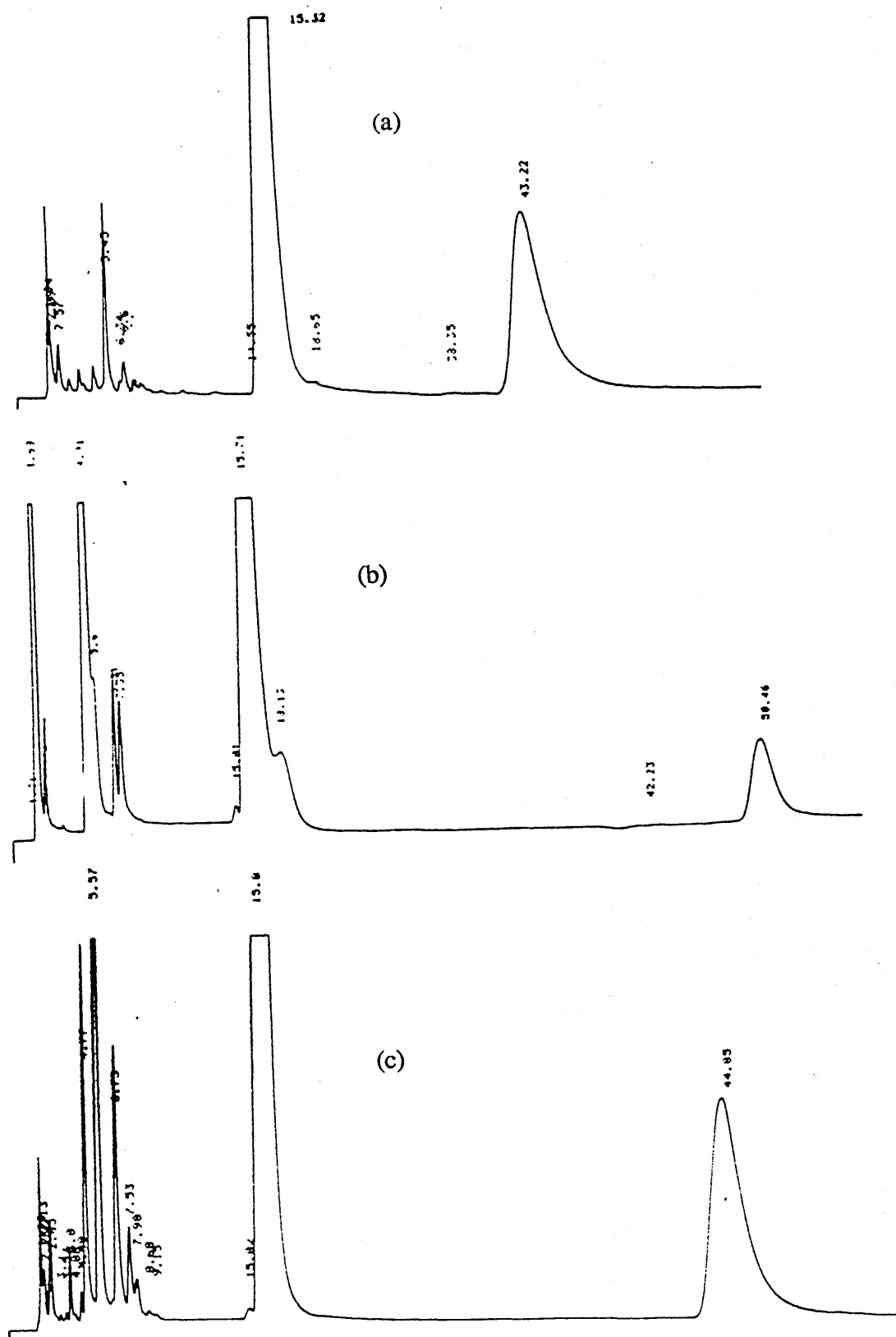
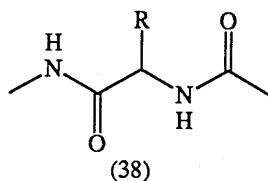


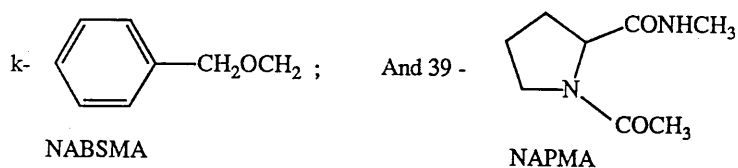
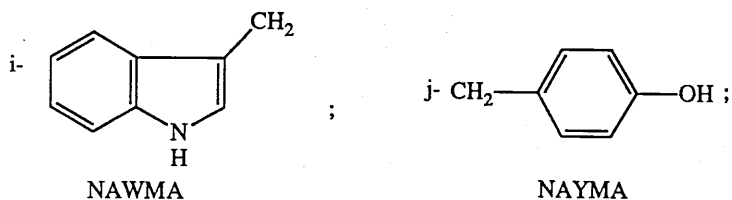
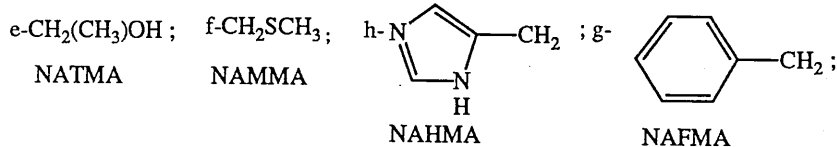
Figure 3.15 The HPLC comparison of DCDMA degradation in (a) wet solid state (T = 16h, t = 125°C), (b) buffered alkaline (pH = 10.8, T = 1h, t = 55°C) and (c) aqueous solutions (pH = 7, T = 24h, t = 100°C).



Following the detailed study of the degradation of the mono-peptide of cystine (38a) a more brief study of a series of other mono-peptides 38(b-j) and 39 were carried out.



a-  $\text{S}_2\text{CH}_2\text{CH}(\text{CONHCH}_3)\text{NHCOCH}_3$ ;    b- H;    c-  $\text{CH}_3$ ;    d-  $\text{CH}_2\text{OH}$ ;  
DCDMA                      NAGMA                      NAAMA                      NASMA



107

the order:

NAHMA>DLDMA>NAWMA>NASMA>DCDMA>NATMA>NAGMA>NAM

MA, and NAYMA, NAPMA, NAFMA and NAAMA reacted little. pH changes were approximately similar for most mono peptides and the largest pH change was observed with DCDMA in which it dropped approximately by 20%.

NAWMA and NAYMA yellowed most in wet solid state conditions and no yellowing was observed with any of the mono peptides but NASMA under dry conditions. The effect of air appears to accelerate the rate of mono peptide degradation with the exception to DCDMA in which more reaction occurs in wet solid-state under nitrogen. In alkaline media at 55 °C, DCDMA is the most reactive substrate followed by DLDMA, and the others appeared to react little. Significant yellowing was observed with DCDMA after 15h but others yellowed very little (Table 3.6).

Examination of the individual mono peptide and product analysis by HPLC revealed that:

- (i) NAGMA reacts slightly under alkaline at 55 °C and solid-state conditions (approx. 11% reaction after 32h), but degrades almost completely after 48h in alkaline buffered under reflux.

Table 3.6 Extent of reaction (%) and pH measurements in the degradation of mono-peptides in solid-state at 125 °C.

Compound	Wet				Dry	Comments
	Air		Nitrogen			
	16h	32h	16h	32h	32h	
NAGMA	*7.0 (6.4)	11.0 (5.6)	- -	10.0 -	- -	Little reaction with no yellowing
NAAMA	Little reaction with no yellowing					
NATMA	15 (5.8)	18 (5.0)	- (5.33)	3.0 (6.0)	-	Yellows slightly in N <sub>2</sub> after 32h
NASMA	6.0 (6.3)	37.0 (5.7)	-	33.0 (6.6)	2.2 (5.3)	yellows slightly, more significant in dry samples
NAMMA	(6.6)	10.0 (5.7)	- (6.9)	- (6.8)		no yellowing but sulphurous smell
NAFMA	- -	- (5.5)	- (6.7)	- (6.7)	- (6.8)	No reaction
DCDMA	28 (5.2)	29 (4.7)	35 (6.6)	44 (4.3)	- -	yellows after 32h
DLDMA	22 (6.1)	54 (5.0)		51 (4.9)	- (5.8)	no yellowing but considerable reaction
NAYMA	- -	11.2 (4.7)	- (6.7)	6.0 (6.2)	- (7.2)	bright yellow colour after 16h
NANMA	17.0 (4.8)	49 (4.8)	- (6.9)	- (6.6)	- -	bright yellow colour after 16h
NAHMA	24 (6.1)	55 (6.1)	11.0 -	- (7.0)	- (6.5)	Pale yellow after 16h becomes intense after 32h
NAPMA	Little reaction and yellowing					
NASBMA	18		<5			Little yellowing

\* % conversion of substrate with pH following addition of five mL H<sub>2</sub>O in parentheses

Table 3.7      Extent of reaction (%) in the degradation of mono peptides in buffered aqueous alkali (pH ~ 10.8) at 55 °C

compound	reaction time (h)					Yellowing
	0*	10	20	50	120	none
NAGMA	-	3	8	19	38	none
NAAMA	<1	<1	<1	<1	<1	none
NATMA	<1	7	11	15	-	none
NASMA	-	-	-	13	20	none
NAMMA	<1	<1	<1	3	23	none
NAFMA	-	-	<1	<1	-	none
NAPMA	-	-	-	-	-	none
DCDMA	29	-	96	>99	>99	after 10h
DLDMA	25	32	51	63	86	none
NAYMA	-	<1	<1	5	8	slightly after 20h
NAWMA	-	10	11	11	13	slightly after 120h
NAHMA	-	-	<1	<1	<1	none

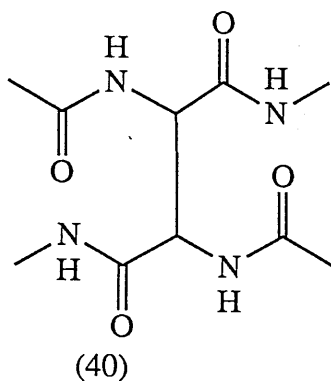
\*reaction time at t = 0 refers to the point at which the temperature of the reaction mixture reaches 55 °C.

Table 3.8      Extent of reaction (%) in the thermal degradation of mono peptides in alkaline buffered solutions (pH 10.8) under reflux

Compound	Reaction time (hrs)					
	0	4	8	24	46	49
NAGMA	-	33	53	83	96	-
NASBMA	2	75	92	99	-	-
NASMA	-	5	8	32	-	53
NAWMA	-	14	22	27	57	-
NAAMA	-	-	-	-	-	>90

(ii) NAAMA does not react under any conditions except under reflux in alkali where significant reaction had occurred.

(iii) Glycine (~18%) and alanine (~14%) were determined to be the amongst products of NAGMA and NAAMA degradation respectively by derivatizing the free amino acids in the reaction mixture with 9-fluorenylmethyl chloroformate. The HPLC's of acetamide, N-acetyl glycine, N-acetylglycine amide and glycine were compared to those from degraded NAGMA reaction mixtures. Due to the very close retention time ( $t_R$ ) of these products, acetamide ( $t_R = 2.09$  min), N-acetylglycine ( $t_R = 2.07$ ), N-acetylglycine amide ( $t_R = 2.67$ ) and glycine ( $t_R = 2.24$ ) to that of the starting material ( $t_R = 3.20$ ) and the presence of borate buffer ( $t_R = 2$ ) it was not therefore possible to confirm the formation of any of these above mentioned products apart from glycine. A product highly retained in HPLC was observed with NAGMA degradation in alkali under reflux after 48h which may be generated by autoxidation. A check by HPLC, however, showed that this was not the likely dehydrodimer of NAGMA ((40) authentic sample donated kindly by I.Stec). An attempt to isolate the product was unsuccessful.



(iv) NASMA reacts only slightly in alkaline media at 55 °C, but significant reaction occurs in the solid-state. One product was tentatively assigned by HPLC using a Spherisorb column and comparing its retention time to that of the authentic sample and spiking. This was shown to be NAGMA and its yield was determined to be 7% after 32h in wet solid-state conditions. NADMA was also found to be a product of NASMA degradation by HPLC. Due to its lability under wet solid state condition its yield was very low (<1% after 32h). An early retained peak was seen on HPLC which had a similar retention time to that of acetamide which may have come from NADMA hydrolysis.

(v) Protection of the hydroxy group in NASMA had little effect on its reaction with alkali at 55 °C or under reflux. Two products were identified from NABSMA degradation by comparing purity parameter values as shown in Table 3.9 and spiking. These were shown to be NADMA and benzyl alcohol (approx. 30% yield after 96h in alkaline under reflux).

(vi) NATMA reacted by half as much as NASMA in wet solid samples. Two major products were seen on HPLC at  $t_R$  = 4 and 6.8 min (retention time of NATMA at 5.4 min) using a Spherisorb column. The product  $t_R$  ~ 4 min was shown to be NAGMA (24%) by comparing its HPLC with the authentic sample and spiking. The peak at  $t_R$  ~ 6.8 min is not assigned at this stage but it is discussed later in the following chapter.

Table 3.9 - Comparison of purity parameter values of authentic samples (NADMA and benzyalcohol) and the products of NABSMA degradation

	standard		reaction mixture	
	NADMA	Benzyl alcohol	NADMA	Benzylalcohol
* $t_R$ (min)	4.9	7.31	4.9	7.4
$\bar{x}$	224.82	215.255	224.80	215.21
S.D.	0.01	0.1034388	0.1602	$6.97 \times 10^{-2}$

\*  $t_R$  = retention time(min)

$\bar{x}$  = mean purity parameters

S.D. = standard deviation

(vii) NAYMA reacts at a much slower rate under both alkaline (55°C) and wet solid-state conditions than does NAWMA. The degradation of latter is more significant in the wet solid-state in the presence of air (~50% reaction after 32h). Significant yellowing of NAWMA required 120h (55 °C) but similar yellowing was observed only after 20h for NAYMA. Approximately 32% and 27% of NAYMA and NAWMA had reacted after 24h in alkaline buffered media under reflux. A yellow solution was observed for NAYMA after only 4h. NAWMA appeared to be almost completely unreactive under alkaline conditions, but considerable degradation occurred in wet solid-state in the presence of air.

(viii) NAMMA, NATMA and NAPMA reacted only slightly under all conditions.

(ix) DLDMA reacted most after DCDMA in alkaline buffered media at 55 °C, but little yellowing was observed. HPLC data indicated that NACMA, NADMA and diastereoisomers of DTCDMA and DCDMA were among the products in both wet solid-state and alkali conditions.

### 3.6 Photochemistry of DCDMA in aqueous solution

Although the photochemistry of cystine and its derivatives have been studied extensively by many workers, our results from DCDMA thermal and alkaline

degradation have indicated that it is a better model of cystine residue in a protein, so its photochemistry was carried out in the absence of air and room temperature using pyrex tubes and 400 W medium pressure mercury arc.

The HPLC chromatograms (Fig. 3.16) of the irradiated samples were quite different from those obtained from the thermal degradation of DCDMA. HPLC showed five major products at 5.6, 11.6, 14.4 and a twin peak at 32 and 33 minutes, and a few minor products.

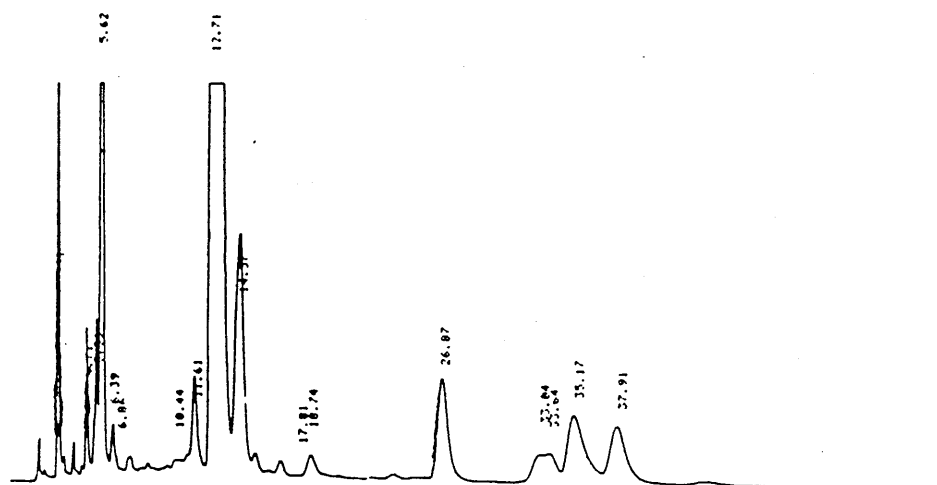


Figure 3.16 Analytical HPLC elution profile of DCDMA photolysis mixture at  $t_{ir} = 8h$ .

The pH of the photolysate dropped from 7.0 to 3.0 (Fig. 3.17) during photolysis and 40% reaction (Fig. 3.18) had occurred after 16h. The HPLC chromatograms of irradiated samples were compared with those of acetamide, DTCDMA, and the *N*-acetyl methylamides of cystine, glycine, alanine, serine and dehydroalanine. They indicate that NACMA is the major product, its yield rising approximately 40% at 40% conversion. It appears the mono peptides of glycine, alanine, dehydroalanine, together with acetamide and the thermal product are present in small quantities.



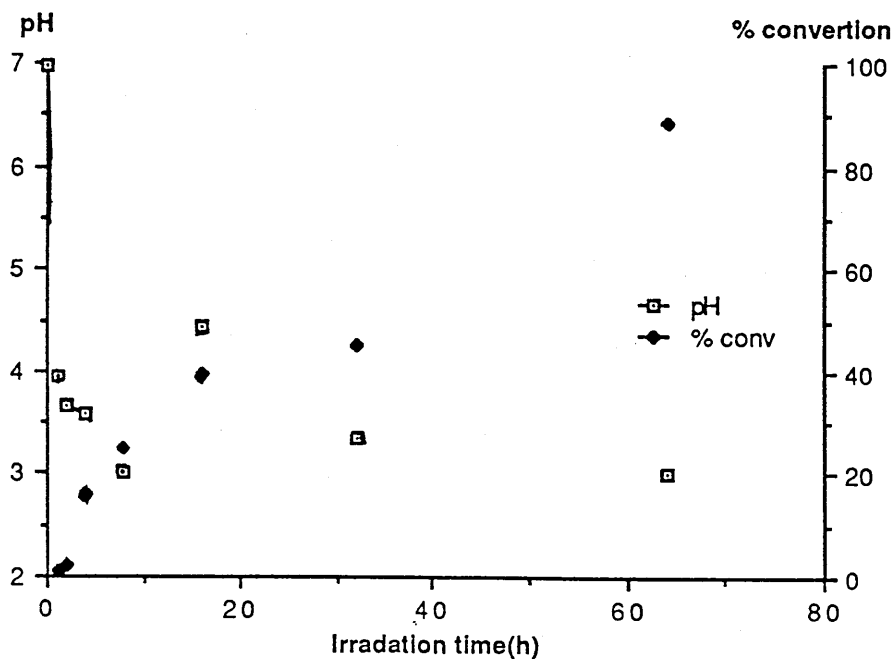


Figure 3.17 Effect of time on pH and the breakdown of DCDMA during photolysis.

In order to isolate and identify some of the major products of photodegradation, a large scale photolysis was set-up and four fractions were separated by prep-HPLC (Fig. 2.7). The HPLC of fraction 1 showed predominantly one component. It's IR spectrum suggested the presence of amide,  $3350\text{ cm}^{-1}$  (br, H-bonded (N-H) stretching),  $1670\text{ cm}^{-1}$  and  $1650$  (amide carbonyls),  $1560\text{ cm}^{-1}$  (N-H bending).  $^1\text{H}$  NMR data ( $\text{d}^6$  DMSO) from the sample is compared with those of NAGMA and NAAMA in Table 3.10.

Table 3.10:  $^1\text{H}$  NMR interpretation of fraction 1 from DCDMA photolysis, NAGMA and NAAMA

Fraction 1	NAGMA	NAAMA	Assignment
d 1.25 ppm		d 1.25 ppm	-CHCH <sub>3</sub>
m 1.80	s 1.8 ppm	s 1.80	-CH <sub>3</sub> CO
d 2.50	d 2.60	d 2.50	-CH <sub>3</sub> NH
d 3.60	d 3.60		-CHCH <sub>3</sub>
m 4.30		m 4.20	-CHCH <sub>3</sub>
m 7.30			-CONH <sub>2</sub>
m 7.80	q 7.70	q 7.70	-NHCH <sub>3</sub>
m 8.20	t 8.10		-NHCH <sub>2</sub>
		d 8.0	-NHCH

Thus it appears this fraction is predominantly a mixture of NAGMA and NAAMA. The spectrum also exhibits a distinct resonance at 7.3 ppm which may be interpreted as the primary amide resonance absorption of acetamide. The yields of NAGMA and NAAMA were approximately 1.4 and 1.3% respectively after 8h photolysis. Fraction 2 was shown to be NACMA by comparing its HPLC,  $^1\text{H}$  NMR and IR spectra to that of the synthesised compound. Fraction 3 was the unchanged starting material. Although the HPLC of fraction four showed only one major well retained peak, the complex  $^1\text{H}$  NMR spectra suggested that it consisted of at least three components (i.e. DTCDMA, and possibly product peaks at 33 and 35 minutes, (Fig. 3.16). NACMA, NADMA and DTCDMA were quantified and the results are given in Table 3.11.

Table 3.11: Yields of NACMA , NADMA and DTCDMA in DCDMA photolysis

Irr <sup>n</sup> time (h)	1	2	4	8	16	32	64
NACMA	4.5	16.0	20.0	31.6	38.7	39.5	37.0
NADMA	-	-	-	6.9	<1	<1	-
DTCDMA	3.0	9.0	10.0	7.4	11.3	12.7	3.7

Plots of yields vs. conversion in DCDMA photolysis suggest that NACMA is not a primary product (Fig. 3.18). There was little evidence for the formation of diastereoisomers of DLDMA from the HPLC of the photolysis mixtures, but RR(SS) isomer of DLDMA was present as minor product. Therefore, DTCDMA

which is a major product in wet solid-state thermolysis, NADMA and DLDMA, which are major products in alkaline degradation of DCDMA, are shown to be minor products in photolysis.

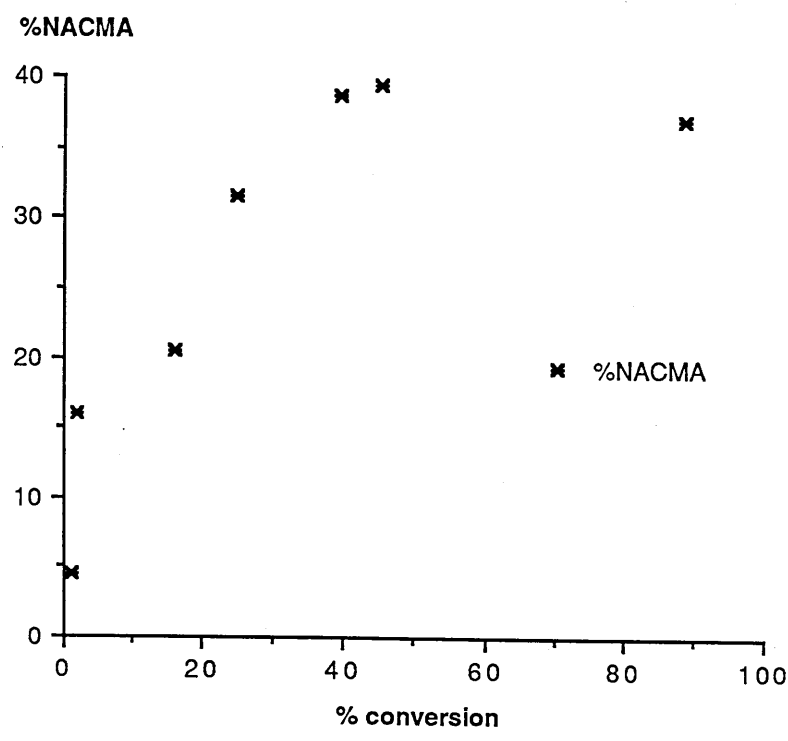


Figure 3.18 shows formation of NACMA during DCDMA photolysis.

## **4 Discussion**

### **4.1 DCDMA in solid-state**

**4.1.1 *N,N*-Diacetylthiocystine-*N,N*-dimethylamide (DTCDMA)**

**4.1.2 *N*-Acetyl-thiocystine-*N*-methylamide**

**4.1.3 Thiocystine and thiocystine**

**4.1.4 Proposed reaction mechanism for the degradation of DCDMA in wet solid-state conditions.**

### **4.2 Alkaline degradation of DCDMA**

**4.2.1 Elemental sulphur**

**4.2.2 *N*-Acetyldehydroalanine-*N*-methylamide, *N,N*-diacetyl lanthionine-*N,N*-dimethylamide and other products.**

**4.2.3 Possible reaction mechanisms for the formation of products from the alkaline degradation of DCDMA**

### **4.3 Yellow products**

### **4.4 Degradation of DCDMA in neutral media**

### **4.5 Thermal degradation of other mono-peptides**

***N*-Acetylhistidine methylamide**

***N*-Acetylmethylamides of glycine and alanine**

***N*-Acetylmethylamides of serine and benzylserine**

***N*-Acetyl threonine methylamide**

***N*-Acetylmethylamides of tyrosine and tryptophan**

***N,N*-Diacetyl lanthionine dimethylamide**

### **4.6 DCDMA Photolysis**

## 4 Discussion

### 4.1 DCDMA in solid-state

DCDMA is degraded and yellowed by heat above 100 °C. Heating DCDMA in the presence of oxygen caused comparatively less degradation than heating in presence of nitrogen under similar conditions. NACMA which is a product of degradation of DCDMA is probably oxidized to the starting material and may account for the low conversion of DCDMA in air conditions. In general, increasing the temperature accompanied with moisture caused more degradation of DCDMA, while the effect of increasing temperature was negligible in dry samples.

The drop in pH of an aqueous solution of the reaction mixture with time (Fig. 3.2) indicated the formation of acidic components. Indeed a strong sulphurous smell such as hydrogen sulphide was noted. Woodmansey [1918], Raynes [1927] and many others found that hydrogen sulphide was evolved by wool at temperatures in excess of 100 °C, the amount increasing if the wool was moist and/or at higher temperature. Most of these authors concluded that hydrogen sulphide comes from the cystine degradation and some from unidentified amino acid residue break down. Besides hydrogen sulphide other gaseous products such as ammonia, sulphur dioxide, methylmercaptan, ethylmercaptan, carbon dioxide, carbon monoxide and methane have been identified [Horio et al., 1965, Launer and Black, 1971]. Most of these products, however, are not expected from DCDMA break down because the experiments were carried out in nitrogen and, moreover, the amino and carboxyl groups were protected.

#### 4.1.1 *N,N*-Diacetylthiocystine-*N,N*-dimethylamide(DTCDMA)

That the most significant product of DCDMA break down under wet solid-state conditions is a compound highly retained in HPLC. Its ready formation is even

evident from its presence in freshly synthesised DCDMA. The evidence summarized below suggests it is *N,N*-diacetylthiocystine *N,N*-dimethylamide. Initial examination of the IR, NMR (90 MHz) and mass spectra (chemical ionization) showed close similarities with those of DCDMA. But the superimposed PMR spectra (Fig. 3.4) of the product and DCDMA recorded at 400 MHz exhibited six additional distinct resonances at increased chemical shift. Examination of the sample by HPLC after recording the spectrum showed the sample had partially decomposed to DCDMA. Trisulphides are known to be unstable. Sweetman et al. [1965] showed that small amounts of trisulphide occur in the combined state in weathered or irradiated wool. Massey et al. [1971], proposed the probable presence of the corresponding trisulphide of glutathione in a commercial sample. The chemical shifts ( $\delta$ ) in ppm downfield from the reference for 400 MHz spectra of DCDMA and the product (DTCDMA) in addition to that of *N*-acetyl-lanthionine *N*-methylamide (DLDMA) in 90 MHz are given in Table 4.1.

Table 4.1  $^1\text{H}$  NMR chemical shifts of DLDMA, DCDMA and DTCDMA

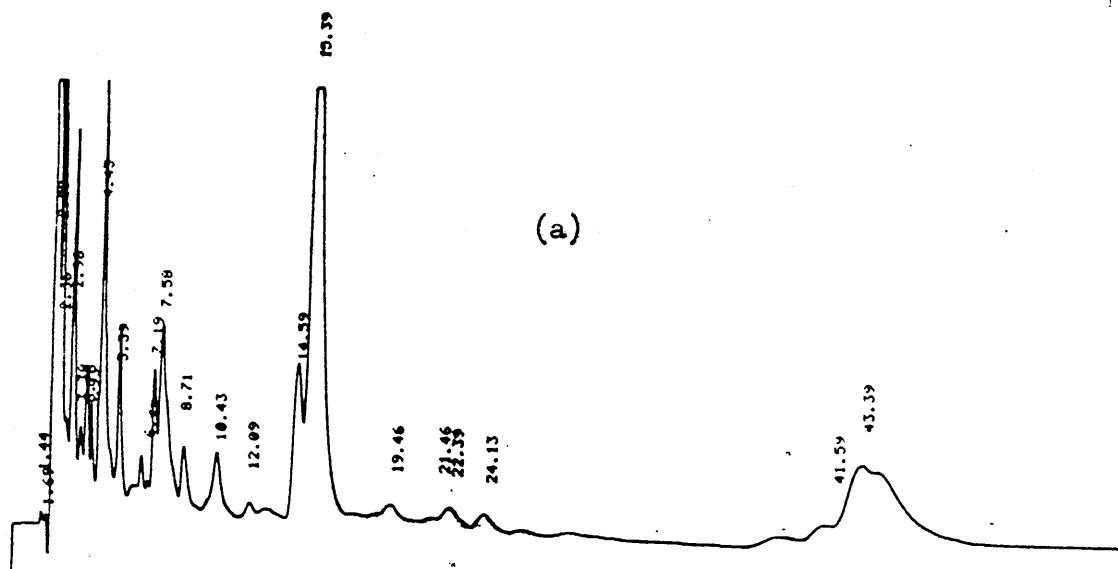
Assignment	chemical shift (ppm)		
	DLDMA	DCDMA	DTCDMA
–CH <sub>3</sub> CO–	1.80	1.84	1.85
–CH <sub>3</sub> NH–	2.55	2.57	2.58
–CH <sub>2</sub> S–	*2.60	2.8 and 3.05	3.11 and 3.20
$\alpha$ CH–	4.30	4.45	4.53
–CH <sub>3</sub> NHCO–	7.95	7.99	8.05
–CONHCH	8.10	8.18	8.23

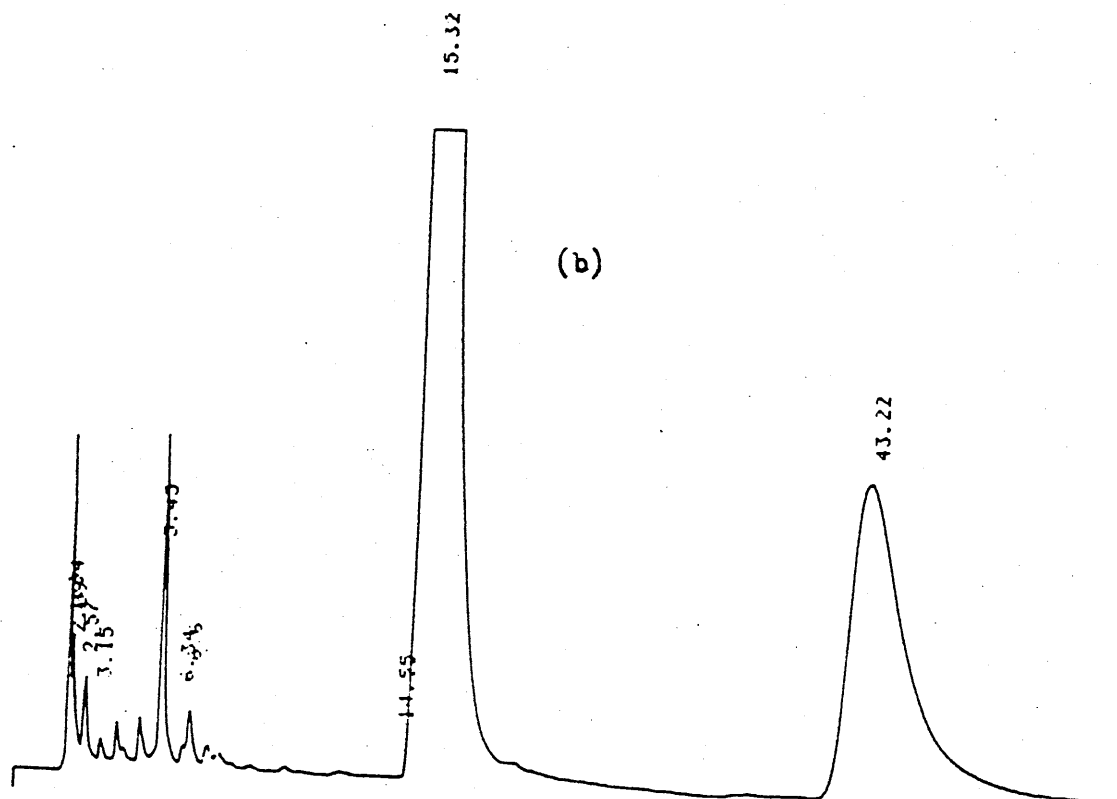
\* methylene protons are not very well resolved using 90 MHz NMR spectroscopy.

The trisulphide CH<sub>2</sub> and CH protons resonate at lower fields than their counterparts in DCDMA and DLDMA, as might be expected from the presence of

a further electronegative atom in the bridge. This finding is in good agreement with data on the amino acids reported by Bartle et al. [1968]. The shift increment for both CH<sub>2</sub> and CH is found to increase with increasing substituent group electronegativity. Fletcher et al. [1963a], however, reported that for CH<sub>2</sub>, the shift increment is greater than that between lanthionine and cystine, but for CH the trisulphide-cystine and cystine-lanthionine shifts are about the same.

Our results indicate that DTCDMA breaks down on heating in the presence of moisture to produce DCDMA, DLDMA, NADMA, NACMA and some other unidentified products. The HPLC chromatograms of DCDMA and DTCDMA thermosylates are shown in Figures 4.1 and 4.2. The interesting feature of the reactions is the similarities in the products distribution from each degradation. These suggest that similar reaction mechanisms must be responsible for the break down of DCDMA and DTCDMA. On standing for approximately a few weeks, an aqueous solution of DTCDMA becomes turbid and deposits a white solid which is almost certainly elemental sulphur.





Figures 4.1 and 4.2 show analytical HPLC elution profiles of DTCDMA (a) and DCDMA (b) in wet solid-state conditions at 125 °C for 16.5h.

The increased reactivity of DTCDMA may be attributed to the presence of a third sulphur atom present in the molecule . Fletcher et al. [1963] studied the chromatographic behaviour of bis-(2-amino-2-carboxyethyl) trisulphide and showed that it was very labile under neutral and alkaline conditions, and that cystine and meso-cystine were among the products of decomposition. As might be expected, the infrared spectra of DTCDMA and DCDMA are very similar being dominated by amide absorptions. But the uv/vis spectra differ considerably probably due to the increased polarizability of the trisulphide group. At 215 nm the absorption coefficients for DCDMA and DTCDMA were, 8592 and 15477 L mol<sup>-1</sup> cm<sup>-1</sup> respectively. Although the chemical ionization mass spectra of DCDMA and DTCDMA are almost identical, ionization by FAB showed a molecular ion of mass 383 with some useful fragmentations. Loss of 32 and 64 mass unit from the molecular ion indicates the exclusion of one and two sulphur



atoms respectively. The presence of  $m/z$  209 and 177 among fragments, could be due to *N*-acetylthiocysteine-*N*-methylamide (31) and *N*-acetylcysteine-*N*-methyl amide (32) respectively.

Thus evidence for the assignment of DTCDMA, for the major product in the thermal degradation of DCDMA in the solid-state may be summarized:

- (i) HPLC shows a well resolved long retention time product.
- (ii) IR and CI mass spectra show close similarities to those of DCDMA. The easy exclusion of sulphur to give DCDMA during the CI is highly probable due to the labile nature of DTCDMA
- (iii) FAB mass spectroscopy gives a molecular ion of mass 383.
- (iv) Thermal decomposition in solution takes place to produce DCDMA as well as its thermal degradation products.
- (v) NMR of partially degraded sample in solution shows  $\text{CH}_2$  and CH protons at lower fields than their counterparts in DCDMA.
- (vi) Enhanced uv absorption over DCDMA.

Furthermore, as we shall see, treatment with alkali produces the same compound as a pair of peaks suggestive of diastereoisomerism, a feature that would be expected from the trisulphide structure and observed with DCDMA.

#### 4.1.2 *N*-Acetyl-thiocysteine-*N*-methylamide

This compound is assigned to a fairly labile minor product in the thermal degradation of DCDMA in the solid state and DTCDMA in solution. It was separated by prep-HPLC during the isolation of DTCDMA as was explained fully in the previous chapter. The IR spectrum shows characteristic amide absorption bands but also one at  $2553\text{ cm}^{-1}$  typical of  $-\text{SH}$  stretching. The  $^1\text{H}$  NMR

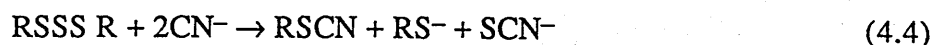
spectrum in D<sub>2</sub>O exhibited four distinct resonances at 2.0, 2.7, 3.15 and 4.16 ppm to the –CH<sub>3</sub>CO, –CH<sub>3</sub>NH, –CH<sub>2</sub>S and C(α)H protons respectively. Further confirmation for the formation of hydropersulphide was observed in the <sup>1</sup>H NMR in d<sup>6</sup>-DMSO of a degraded sample of DTCDMA which showed the presence of a third minor product with its own set of CH resonances integrating consistently with a singlet S-H resonance at 6.55 ppm. The fact that this is a singlet is important evidence for the formation of thiocysteine residue. NACMA –SH is a triplet in DMSO which implies that the thiol proton couples with the methylene protons. Thus the singlet in DMSO must mean that there is no coupling between the perthiol proton and the methylene protons (i.e. –CH<sub>2</sub>–S–S–H). Further evidence for this assignment is provided by the cyanolysis reactions with λ<sub>max</sub> at 460 nm which is due to the formation of ferric thiocyanate (4.1 and 4.2) and diagnostic for hydropersulphides, RSSH [Cavallini, 1960].



Similar treatment of a fresh sample of DTCDMA and DCDMA does not give λ<sub>max</sub> at 460 nm. However, the cyanolysis of a trisulphide can be obtained by allowing it to react with potassium cyanide under the condition of Sörbo [1957], as reported by Fletcher et al. [1963]. The reaction for cyanolysis of trisulphide is represented in equation 4.3.



Many authors [Fletcher et al., 1963; Abdolrasulnia, 1980; John L Wood, 1980] have reported that the cyanolysis of trisulphide involves production of sulphhydryl groups by initial attack of cyanide ion on S–S bond [A. Schöberl, 1937]. The sulphhydryl groups function in a catalytic role and cause extensive decomposition of thiocystine (4.4-4.7).



Further reports of the reaction of hydropersulphides with cyanide is found in the chemistry of S-transferring enzyme systems [Hyllin and Wood, 1959; Cavallini, Demarco, Mondovi and Mori, 1960]. Sulphur reacts with cysteine in alkaline solution to form a substance which gives thiocyanate when reacted with cyanide at room temperature, and which might be involved in the enzyme reactions. Cavallini et al. [1960] suggest this substance is CySSH.

Clearly, the cyanolysis of a trisulphide under the conditions described by Cavallini et al. [1960] does not take place. Cyanide ion reacts much faster with the hydropersulphide (eqn. 4.8) than with disulphide or trisulphide groups. The slower rate is presumably due to the steric hindrance by the two methylene groups attached to the  $\alpha$ -carbon atom.



Rao and Gorin [1959] showed the hydropersulphide group absorbs weakly at 330-350 nm. Figure 4.3 shows the development of the characteristic absorption of persulphide when thiocystine is incubated with cysteine. The low absorption is due in part to the reversal of the reaction by the cystine formed as a product [reaction (4.5), where R is Cy]. The decrease in the absorption peak with time (curve B) reflects the instability of the hydropersulphide species. When cyanide was added to the alkaline medium, there was an immediate loss of the characteristic absorbance of the persulphide group due to thiocyanate formation and the absorption spectrum was that of thiocystine (curve C). The above data is

consistent with our findings regarding the uv/vis spectrum of the minor product under discussion.

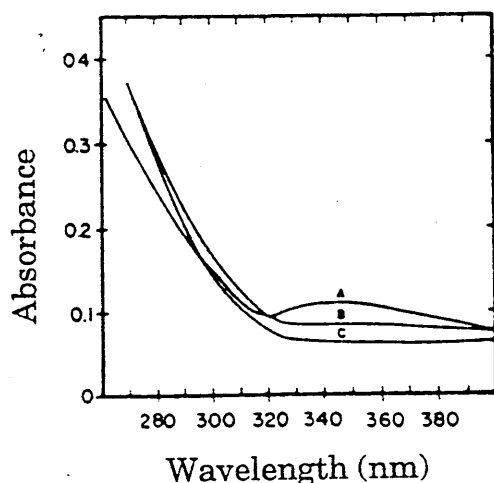


Figure 4.3 Formation of persulphide by the reaction of thiocystine and cysteine. (A) 0.5 mM cysteine and 0.28 mM thiocystine 15 min. after preparation. (B) curve (A) after 2.5h. (C) 0.28 mM thiocystine without cyanide.

Although no molecular ion was seen in the CI (NH<sub>3</sub>) high resolution mass spectrum of NATCMA, significant fragment ions were observed. Loss of 32 mass unit from (41) involves exclusion of one sulphur atom giving a molecular ion of m/z 177 (42) which corresponds well to NACMA. Presence of m/z 145 involves loss of two sulphur atoms. The proposed fragmentation of the molecular ion is given in Figure 4.4 and accounts for the most important peaks. The observed fragment ions are indicated by \*.

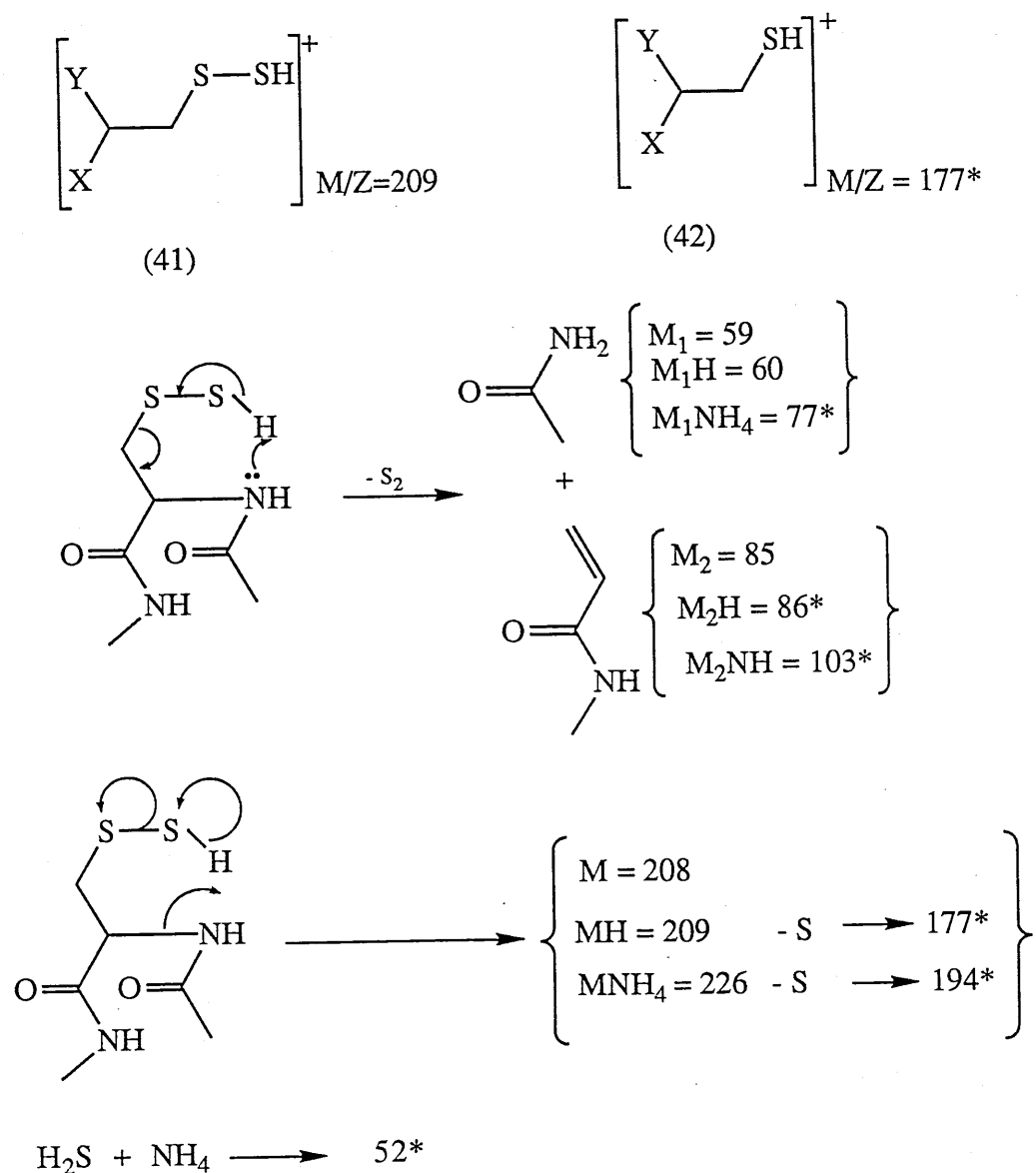


Figure 4.4 Possible fragmentation pathways of NATCMA in mass spectroscopy by chemical ionization.

Thus, in summary, the presence of NATCMA among the products of the thermal degradation of DCDMA is strongly supported by the isolation of a compound by HPLC, that:

- (i) the IR spectrum shows an absorption band at  $2553\text{ cm}^{-1}$  typical of  $\text{--SH}$  stretching.

(ii) gives positive cyanolysis reaction, furthermore it has a uv/vis spectrum similar to those of persulphide groups.

(iii) although the heaviest molecular ion is not obtained by HRCI mass spectroscopy, the fragmentation pattern is consistent with the assignment.

Moreover, an aged sample of DTCDMA in d<sup>6</sup>-DMSO has a pmr spectrum that includes signals fully consistent with this compound.

#### 4.1.3 Thiocystine and thiocysteine

The formation of trisulphide and hydropersulphide derivatives in the thermal degradation of DCDMA prompts consideration of earlier reports of analogous compounds.

Thiocystine [bis-(2-amino-2-carboxyethyl)trisulphide] was first isolated by Fletcher and Robson [1963] from the hydrochloric acid hydrolysates of proteins that are rich in cystine. The trisulphide and a small amount of accompanying tetrasulphide were considered to be artifacts produced by acid-catalysed exchange reactions between cystine and its decomposition products. Sandy et al. [1975] isolated thiocystine and the corresponding mixed trisulphide of glutathione from *Rhodopseudomonas Spheroides* by a mild extraction procedure involving ion exchange chromatography. The products were evidently naturally occurring in this organism.

Szczepkowski and Wood [1967] showed thiocystine was produced by the action of the enzyme cystathionase on cystine and, further, it served as a substrate for the enzyme rhodanese. When it was incubated in the rhodanese assay system, thiocystine was observed by Abdolrasulnia and Wood [1980] to be more unstable than had been previously reported. The compound readily transferred its persulphide sulphur to the enzyme but also decomposed rapidly to free sulphur and cystine [Volini and Wang, 1973]. This is a property characteristic of

persulphides. Abdulrasulnia and Wood [1980] studied the cause of the instability. Their report suggests thiocystine is relatively stable between pH 2 and 9 . However, rapid decomposition to free sulphur and cystine occurs in the presence of sulphhydryl compounds, sulphite, or cyanide. This effect is due to the intermediary formation of the unstable persulphide, thiocystine (CySSH). Similar effects were noted in trisulphides related to thiocystine. The proposed reactions of rhodanese-thiocystine are given in equations 4.9 to 4.12.



Reaction 4.9 is reversible. Therefore, addition of disulphide reduces thiocystine formation and hence the amount of turbidity observed. This was demonstrated by adding oxidized glutathione or lipoic acid to buffered solutions of thiocystine catalysed by mercaptasuccinate.

Studies on the reaction of rhodanese indicate that a persulphide form is the most stable form of the enzyme [Abdalrasulnia, 1979], but decomposes slowly to yield free sulphur [Volini and Wang, 1973], eqn. 4.12. It has been shown that the initial step in utilization of thiocystine is conversion to a persulphide (eqn. 4.9) by catalytic action of rhodanese. The formation of a rhodanese persulphide compound by transfer from thiocystine was confirmed by fluorescence measurements in which persulphide groups on the enzyme were removed by cyanide followed by restoration of the persulphide structure by addition of thiocystine.

Szczepkowski and Wood [1967] reported that cysteine catalysed the decomposition of thiocystine. In the absence of the thiol, virtually no turbidity

occurred during a period of 24 minutes. The mechanism of the decomposition was similar to that described for rhodanese – thiocystine reaction which involved production of unstable thiocystine by S-S bond scission catalysed by an SH group. Cyanide ion produces sulphydryl groups initially by attack on S-S bond [Schöberl et al., 1934]. The sulphydryl groups function in a catalytic role and cause extensive decomposition of thiocystine. Due to the intrinsic instability of thiocystine, Abdolrasulnia et al. [1980] were unsuccessful in isolating this compound.

It is known among microbiologists that cystine-rich nutrient media become antibacterial after autoclaving and that thiol containing compounds usually abolish this inhibition. Concentrations of thiol above a certain limit has been suggested [Fletcher and Robson, 1963] to inhibit the formation of thiocystine. Many authors [Schuhardt et al., 1952; Rose et al., 1952; Konowalchuk et al., 1954 and b; Woiwod, 1954] suggested that elementary sulphur may be the antibacterial agent formed by the degradation of heated cystine, or of cysteine plus iron. However, Jonsson et al. [1980] showed that bis-(2-amino-2-carboxyethyl) trisulphide (Bactin) indeed had a bacterio static action on *lactobacillus plantum*, and was formed by heating of cystine. Ferric chloride catalyzes the oxidation of cysteine to cystine, which otherwise abolished the inhibition due to bactin. Moreover, nitrite and ferric chloride facilitate the conversion of cysteine to this compound. Bactin has been shown to prolong the lag-phase of growth of *L. plantanum* without affecting its maximum growth rate.

Thiocystine has been shown [Wood, 1980] to support the growth of young rats *in lieu* of cystine. These authors also reported that thiocystine protected rats against two to three times the LD<sub>50</sub> dosage of sodium cyanide. Although thiocystine results from the action of cystathionase on cystine, its properties suggested that it does not accumulate in the body. It was seen that thiocystine breaks down to cystine and elemental sulphur *in vitro* and the process is



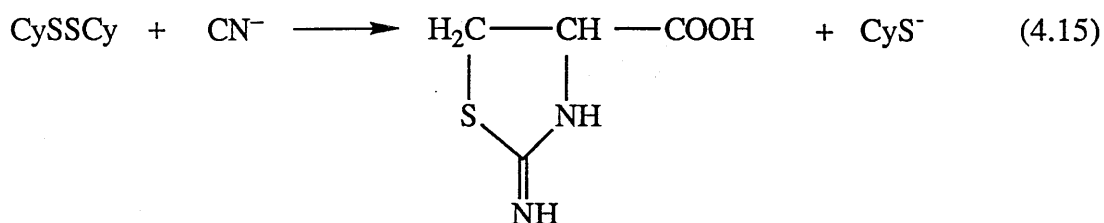
accelerated by sulphhydryl compounds. This probably never occurs in the body because it appears as persulphide sulphur from the reaction with an equivalent amount of sulphhydryl compound according to eqn. 4.13 [Abdolrasulnia, 1980]



In the mitochondrion the persulphide sulphur of thiocystine is transferred to rhodanese, a persulphide enzyme that is more stable than most persulphides [Westley, 1962]. Thiocystine was expected to be effective for protection against cyanide by reacting with it to form thiocyanate and cystine [Szczepkowski, 1967] according to equation 4.14.



The cystine byproduct of reaction (4.14) was shown by Wood and Cooley [1956], to react further with cyanide to form 2-iminothiozolidine-4-carboxylic acid (eqn. 4.15). This reaction is uncatalysed and is too slow to provide effective protection against cyanide poisoning.



Szczepkowski et al. [1967] showed that thiocystine provided marginal protection against lethal amounts of x-ray irradiation. Since cystine is without any protection effect against radiation [Doherty, 1957] the small effect observed with thiocystine may be ascribed to the trisulphide group.

Thiocystine has also been implicated in mammalian cystine metabolism *in vitro* and *in vivo* [Fellman et al., 1982] It is also an important precursor for the formation of 2-amino 3-(thio-thiosulphonate) propionic acid (cysteine

thiosulphonate). Fellman and Avedovech, 1982 suggest its biosynthetic pathway begins with the cleavage of cystine by cystathionase  $\alpha$ -lase to form thiocystine, which undergoes sulphinolysis to form cysteine thiosulphinatate as shown in Figure 4.5.

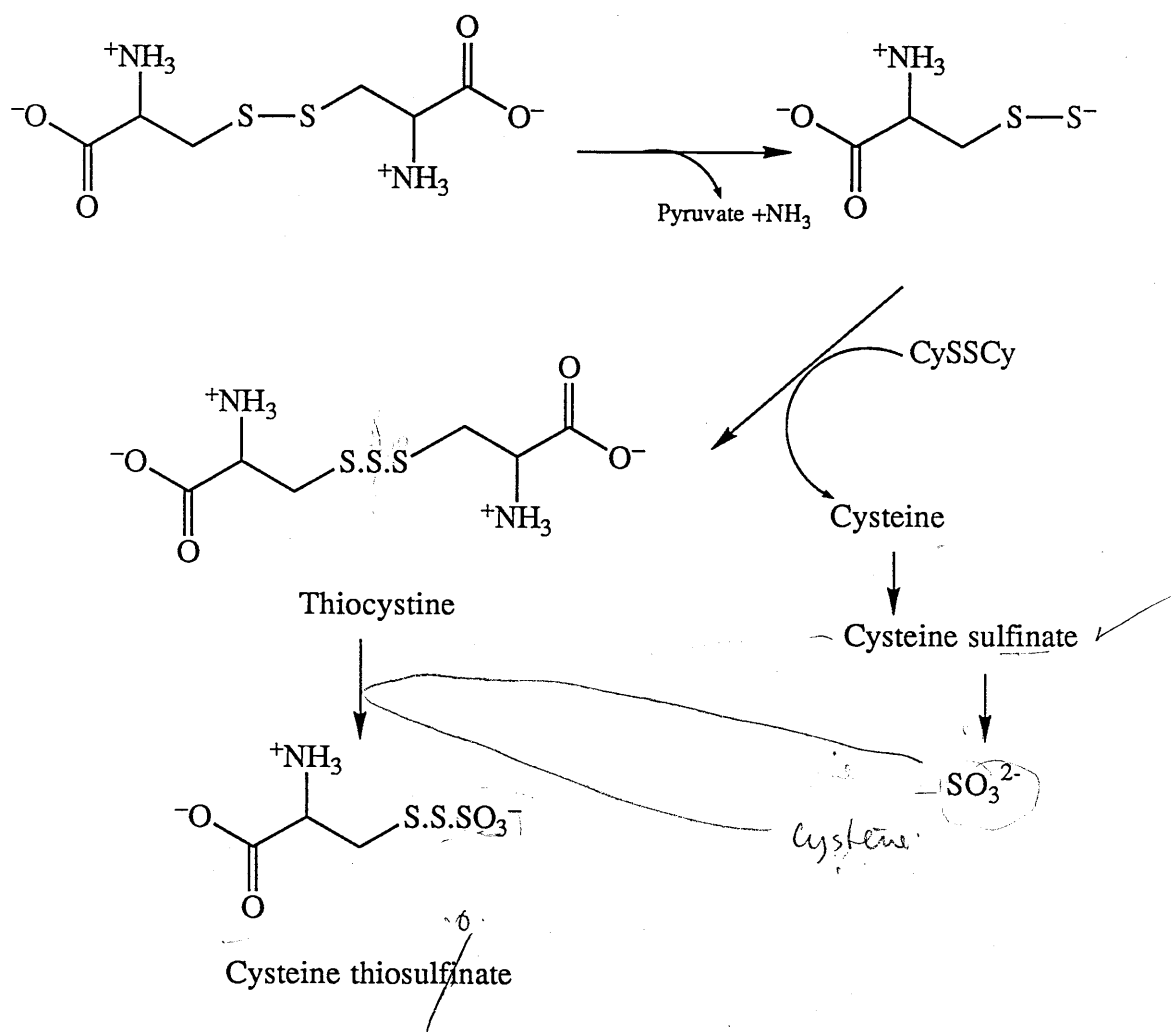
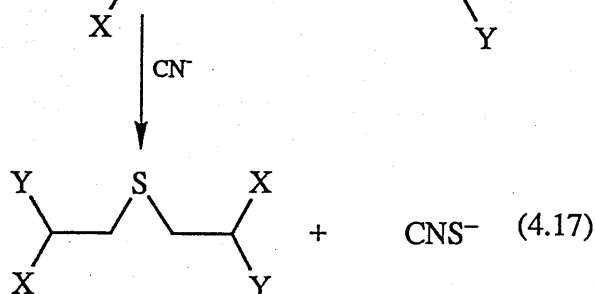
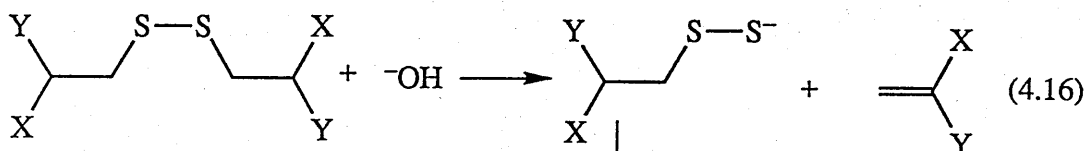


Figure 4.5 Proposed pathway for the formation of cysteine thiosulphinatate.

The hypothesis propose a nonenzymetic nucleophilic attack on cystine by thiocysteine produced by cystathionine  $\alpha$ -lase action on cystine to form thiocystine and cysteine. Cysteine generated in this sequence is converted into cysteine sulphinate by the  $\text{O}_2$ -dependent enzyme which can be disulphinated to  $\text{SO}_2$  and alanine.

The formation of persulphides in proteins by action of alkali and their detection by cyanolysis was formulated by Tarbell and Hornish as represented in eqns. 4.16 and 4.17.



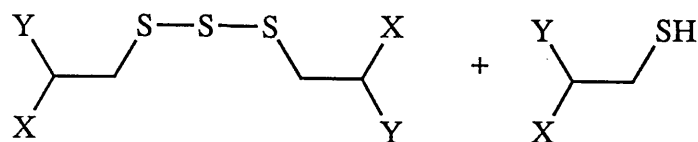
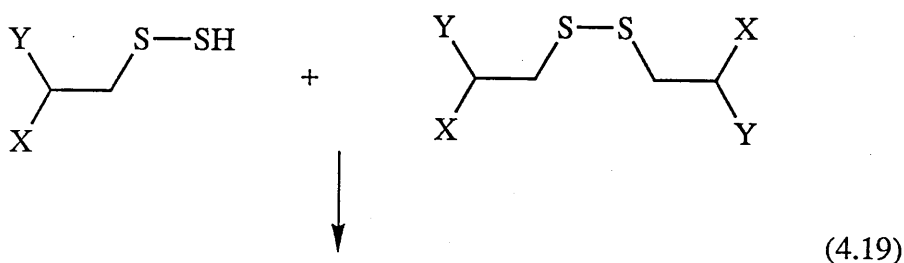
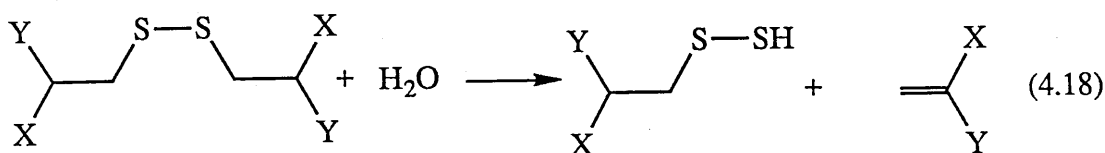
Catsimpoolas and Wood [1980] incubated bovine serum albumin at pH 10 for a day and the resulting product was cyanolysed giving thiocyanate similar to those given in reactions 4.16 and 4.17. Cavallini et al. [1970] obtained spectroscopic evidence for the formation of thiocysteine persulphide groups on insulin which had been treated with 0.025 N sodium hydroxide.

Thus participation of trisulphide and hydropersulphide is already implicated in reactions of cystine and its derivative, and, significantly, in proteins. The vulnerability of trisulphide to nucleophilic attack on sulphur, particularly by  $\text{RS}^-$ , may go some way to explaining why our samples of DTCDMA are so labile.

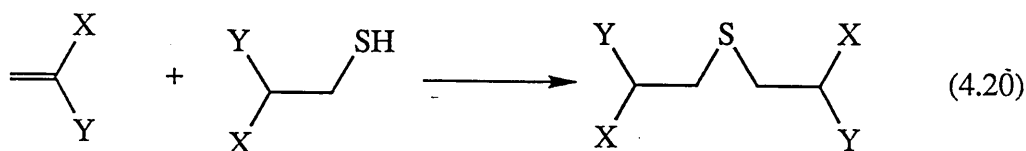
#### 4.1.4 A possible mechanism for the degradation of DCDMA under wet solid-state conditions

DTCDMA is the major product in the thermal degradation of DCDMA under wet solid conditions. It appears immediately on heating; indeed, it can be detected by HPLC as a contaminant in freshly prepared DCDMA. The yield of NACMA is less than half of that of DTCDMA which rises slightly initially and then declines

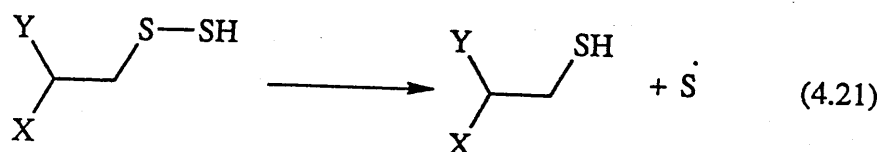
and remains constant. Both NADMA and DLDMA grow little with the conversion of DCDMA and remain constant. The plots of the yields vs conversion for DTCDMA and NACMA suggest that they are secondary products. Our hypothesis proposes  $\beta$ -elimination catalysed by water to form thiocysteine and dehydroalanyl derivatives. Nucleophilic attack of DCDMA by thiocysteine produces the thiocystine and cysteinyl derivatives as presented in eqns. 4.18 and 4.19.



The cysteinyl derivative produced among the reaction may then add to the double bond of the dehydroalanyl residue to give the lanthionyl derivative (eqn. 4.20).



The thiocysteinyl residues are generally unstable and may also decompose to cysteinyl residue and free sulphur if thiophilic acceptors are not present (eqn. 4.21).



The thiocystine derivative has the potential to build up polysulphides, and such reactions must be occurring in the thermolysis of DCDMA. Suggestive evidence includes, for example, the presence of a long retention-time product in the Prep-HPLC chromatogram of a thermally degraded DCDMA (Section 2.4, F<sub>5</sub> in Fig. 2.4). Although this product was isolated, the spectroscopic data as well as the analytical HPLC showed significant decomposition during processing, but it could be the tetrasulphide derivative.

The low yields of NADMA and DLDMA are not surprising because localized acid conditions on the surface of the solid decomposes NADMA. The observation of elemental sulphur further supports the proposed reaction mechanism. Hydrogen sulphide and yellow products produced in solid-state may arise via some of the reactions suggested under alkali, replacing RS<sup>-</sup> by RSH, but these are minor processes. The main differences between alkali and solid state decomposition arise because (a) water on surface of solid creates more scope for reactions between molecules because concentration is very much greater than in homogeneous solution and for alkali experiments; (b) the drop in pH gives RSH instead of RS<sup>-</sup> which causes some reactions to be more favoured under the two different conditions; (c) reactivity of NADMA towards decomposition differs, ie NADMA is more labile at the lower pH.

## 4.2 Alkaline degradation of DCDMA

Exploratory experiments (Section 3.2.1) illustrated quite clearly the effect of temperature and the influence of pH on the decomposition of DCDMA. The extent of both yellowing and degradation increases with an increase in temperature and application of a buffer. George et al. [1977] showed that when oxidized glutathione is treated with dilute alkali little reaction occurs, but treatment with concentrated alkali causes extensive decomposition. We have found that (Table 3.3) heating alkaline aqueous DCDMA in the absence of buffer causes the pH to drop from 10.7 to 8.7 which results in considerably less degradation. This underlines the important role of pH in the decomposition of DCDMA.

The low conversion of DCDMA in non-buffered samples may be explained by the formation of products with acidic groups which counteract the influence of alkali. These results clearly indicate that DCDMA is relatively more stable in acidic conditions such as those that develop on heating in the solid-state.

We recall from section 3.2 that elemental sulphur, NADMA, NACMA, DLDMA, DTCDMA were identified among the products of alkaline-buffered degradation of DCDMA. Acetamide and N-methylpyruvamide appear to be present in minor amounts. The following section discusses the significance of these products and in particular for the mechanism of degradation.

### 4.2.1 Elemental sulphur

We have shown that elemental sulphur is formed during both the alkaline and wet solid-state treatment of DCDMA. Elemental sulphur is suggested to form from the breakdown of the unstable thiocysteine derivative which is an intermediate product in DCDMA degradation in both cases. The formation of  $S^{\circ}$  from polysulphides (eg tri or tetrasulphides) is also possible. This was noted when a

solution of DTCDMA became turbid after a few months precipitating sulphur. Therefore, the turbidity which was observed during the neutralization stage of the alkaline medium and dilution of the resultant yellowed syrup from DCDMA wet solid-state degradation is attributed to the formation of free sulphur.

Elemental sulphur has also been shown to form from other amino acid derivatives. Friedrich Krauss [1984] showed that during growth on L-cysteine ethyl ester, *Chlorella Fusca* accumulated a substance which contained bound sulphide, which could be liberated by reduction with dithioerythritol as inorganic sulphide. The bound sulphide and the authentic free elemental sulphur were studied chromatographically by TLC and RPHPLC. The results showed identical  $R_f$  values and retention times for both bound sulphide and  $S^0$  by TLC and HPLC respectively. They obtained further evidence for  $S^0$  from reactions with thiols forming free sulphide and the formation of thiocyanate after incubation at 80 °C. But this test is not specific for  $S^0$  because thiocystine [Fletcher et al., 1963], polythiosulphides, polysulphides, disulphides and tetrasulphides react in the same manner with cyanide forming thiocyanate [Foss, O., 1950]. The absorption spectrum of bound sulphide in comparison with authentic  $S^0$  is shown in Figure 4.6 both fractions showed a relative absorption maximum at 263 nm. The extinction coefficient in methanol was determined to be  $\epsilon_{263} = 3.29 \times 10^6 \text{ cm}^2 \text{ mol}^{-1}$ . The identity of bound sulphide with  $S^0$  was demonstrated using mass spectroscopy showing a molecular ion 256 m/e typical for  $S_8$  [Foss, O., 1950].

Thus it appears that free sulphur may contribute to the enhanced uv/vis spectra of the alkali/thermal treated DCDMA. It may also react with sulphur containing products such as hydrogen sulphide, cystine and thiocystine derivatives to give polysulphides.

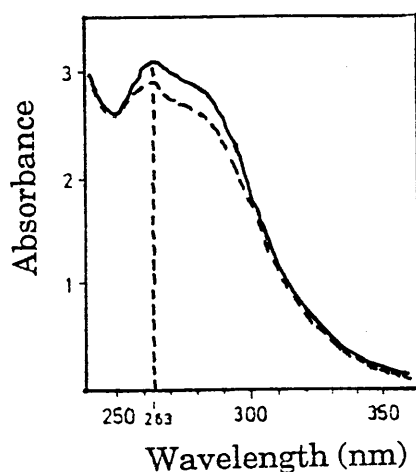


Figure 4.6 Uv-visible spectra of bound sulphide and sulphur ( $S^{\circ}$ ). (—) Methanol extract containing bound sulphide; (---), sulphur-flower dissolved in methanol.

#### 4.2.2 *N*-Acetyldehydroalanine-*N*-Methylamide, *N,N*-diacetyl lanthionine *N,N*-dimethylamide and other products.

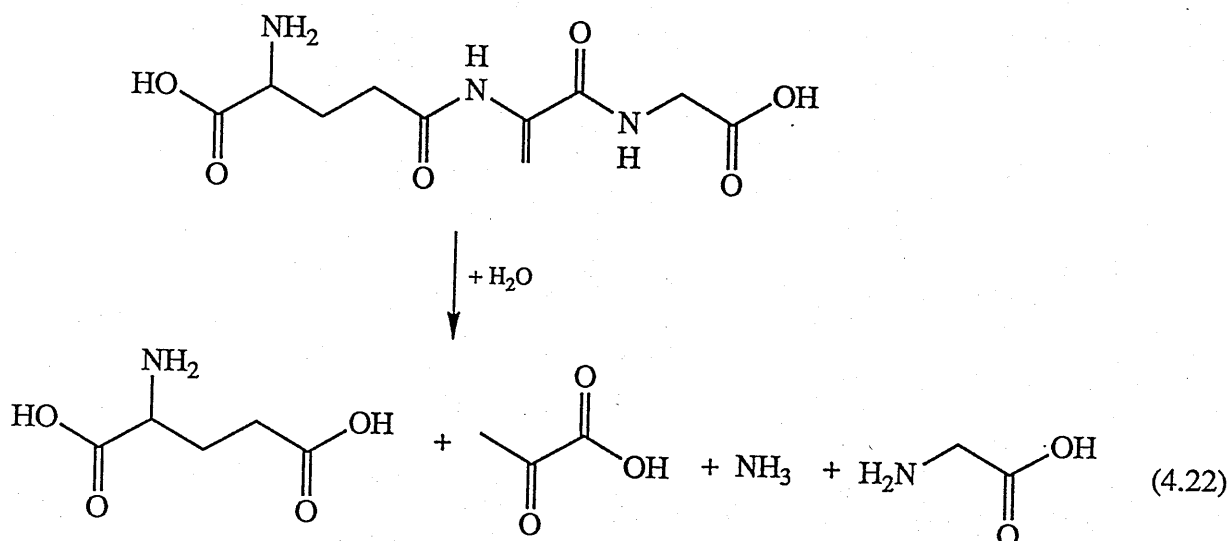
Dehydroalanine has long been postulated as an intermediate in the degradation of cystine residues in proteins, after treatment with alkaline solutions.  $\beta$ -elimination mechanism is commonly invoked to explain the lysis of the disulphide bonds of proteins in alkali. The formation of pyruvate is presumed to arise from the decomposition of DHA during acid hydrolysis [Gawron and Odstrohel, 1967]. To our knowledge, no compounds retaining the dehydroalanyl group have been isolated and characterised following the alkaline cleavage of disulphide bonds in peptides and proteins. But Asquith and Carthew [1972b] reported the formation of dehydroglutathione from alkaline decomposition of oxidized glutathione.

Jones et al. [1983] studied the rate of formation of DHA residues resulting from the lysis of the disulphide bonds in insulin and oxidized glutathione in base at  $pD_3$

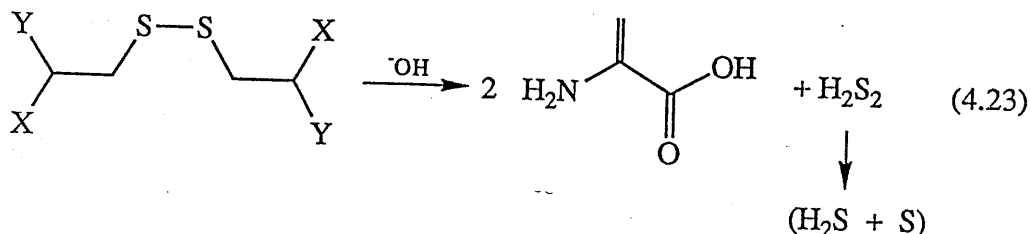


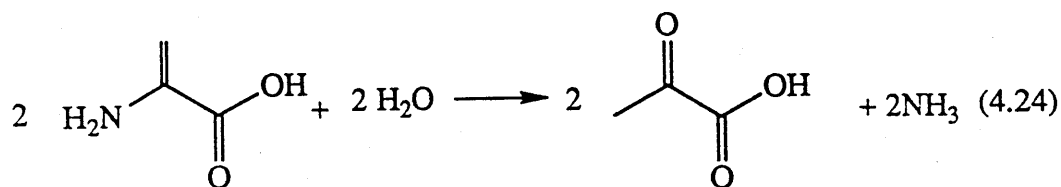
by direct  $^1\text{H}$  and  $^{13}\text{C}$ -NMR measurements. We have isolated NADMA and shown it to be the major product in the alkaline degradation of DCDMA.

NADMA has been observed to be fairly stable for several months in the absence of acid and reagents that could promote addition reactions to the reactive double bonds. The extra stability is contributed by the protection of the amino and carboxylate groups since dehydroalanine on its own is very unstable and has never been isolated. However, Gawron and Odstrohel [1967] reported the decomposition of DHA to pyruvate during the acid hydrolysis of oxidized glutathione. Patchornick [1964] showed dehydroglutathione breaks down on acid hydrolysis to give glutamic acid, glycine and pyruvic acid (eqn. 4.22).

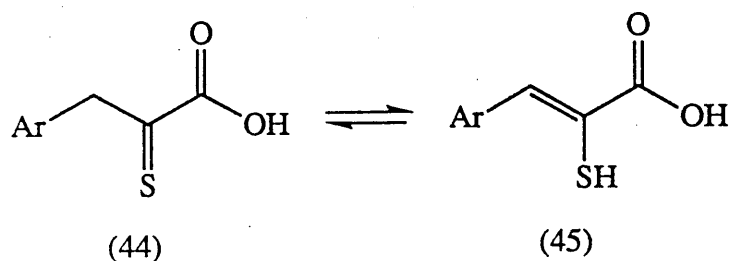
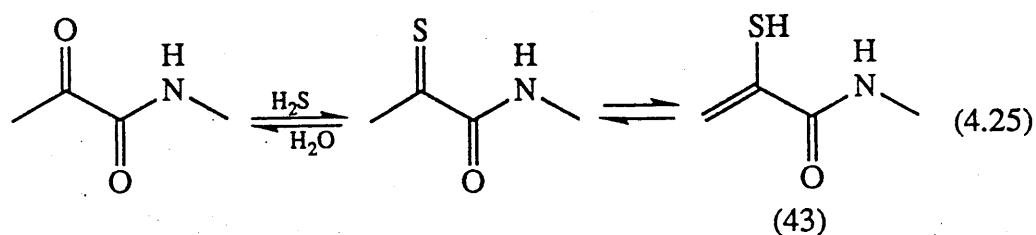


There have also been reports [Bergman, 1926; Clarke, 1930; Nicolet, 1931] claiming that pyruvic acid is formed from the alkaline decomposition of cystine by a bimolecular elimination reaction (Eqns. 4.23 and 4.24).





The above observations prompted a search for acetamide and *N*-methylpyruvamide (MPA) among the products of DCDMA thermolysis. A close examination of the  $^1\text{H}$  NMR spectra of selected fractions in the work-up of the reactions showed they were indeed present among the products (Section 3.2.2 and 3.2.3). Moreover, the IR spectrum of one of the fractions (fraction 2) indicates the presence of sulphoneous groups. This is supported by the absorption bands at 2260 and 600  $\text{cm}^{-1}$  which are ascribed to thiol ( $-\text{SH}$ , stretching), and carbon-sulphur bonds respectively. MPA may react with hydrogen sulphide to give *N*-methyl thiopyruvamide which may tautomerize to *N*-methylthiolpyruvamide 43, (eqn. 4.25). E. Campaigne [1956] reported that the products of the alkaline hydrolysis of 5-(aryl-methylene) rhodanines include thiopyruvic acids (44), although they are usually regarded as in equilibrium with their ene-thiol forms (45) in solution [Campaigne, 1946]. There is little evidence for the existence of aliphatic thione forms such as 44.



Crowe et al. [1950] showed that arylthione products exist preferentially in the thiol form. Thus the interpretation of our results indicate that both acetamide and MPA are formed during the thermolysis of DCDMA, but in very small quantities.

The structure of DLDMA was assigned by both isolation of a HPLC-pure fraction and by an independent synthesis. It is the second major product after NADMA; and is formed from the reaction between NADMA and NACMA. DTCDMA which is a major product in wet solid-state thermal degradation, is a minor product under alkaline conditions. A double peak in HPLC indicates that both meso- and racemic diastereoisomers of DTCDMA are formed under alkali whilst the HPLC of the thermally degraded DCDMA shows the formation of only one isomer. In the investigation of yellow components (section 4.3), a separation of an alkali-degraded reaction mixture by normal phase HPLC showed the resolution of diastereoisomers of DTCDMA are possible by this technique. Similar results are obtained for the diastereoisomers of DLDMA and DCDMA by NPHPLC. These results show that the formation of DTCDMA may follow a different pathway in alkali to that under solid-state conditions. It appears that *N*-acetyl-thiocysteine-*N*-methylanide would not survive alkaline conditions. Furthermore, the absence of absorption maxima at 330-350 nm in the uv/vis spectrum of the alkali-treated DCDMA reaction mixture is a further evidence for its ready decomposition.

#### **4.2.3 A possible mechanism for the degradation of DCDMA on treatment with alkali**

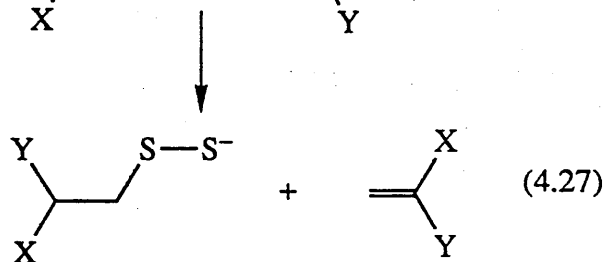
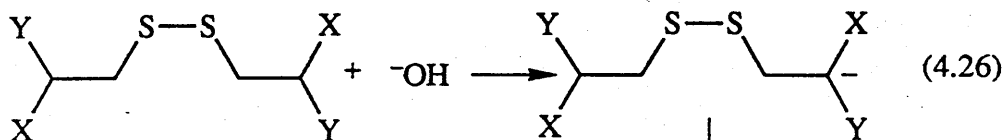
Yield profiles (Fig. 3.13) indicate NADMA is a primary product of alkali thermolysis of DCDMA and that DLDMA and NACMA are secondary products. The yield of diastereoisomers of DTCDMA declines almost to zero after an initial rise supporting the suggestion that trisulphides are unstable in base.

The percentage yields of NACMA, NADMA, DLDMA and DTCDMA at 25% conversion of DCDMA in solid-state and under alkaline conditions are compared in Table 4.2.

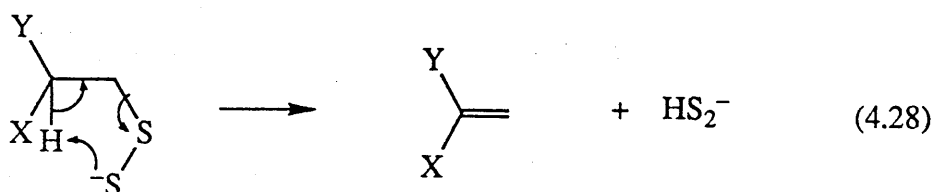
Table 4.2 Yield% of products at 25% conversion of DCDMA.

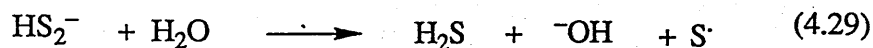
type of product	wet solid-state (125 °C)	buffered alkali pH = 10.8 at 55 °C
DTCDMA	64	14.5
NADMA	3	58
DLDMA	9	22
NACMA	23	5

We suggest that a  $\beta$ -elimination mechanism also operates under alkaline conditions. A hydroxide ion abstracts a proton  $\beta$  to the disulphide bond to form a carbanion, which then fragments to NADMA and unstable thiocysteine derivative (eqns. 4.26 and 4.27.)

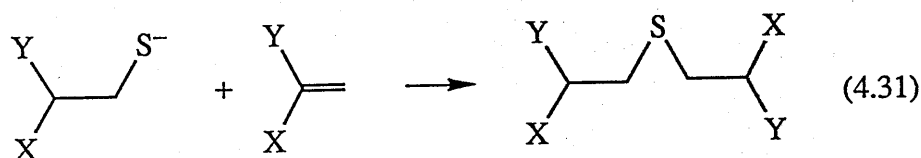
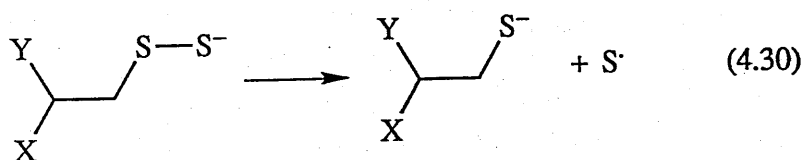


At high pH an internal  $\beta$ -elimination may occur giving a second molecule of NADMA and sulphide according to reactions 4.28 and 4.29.



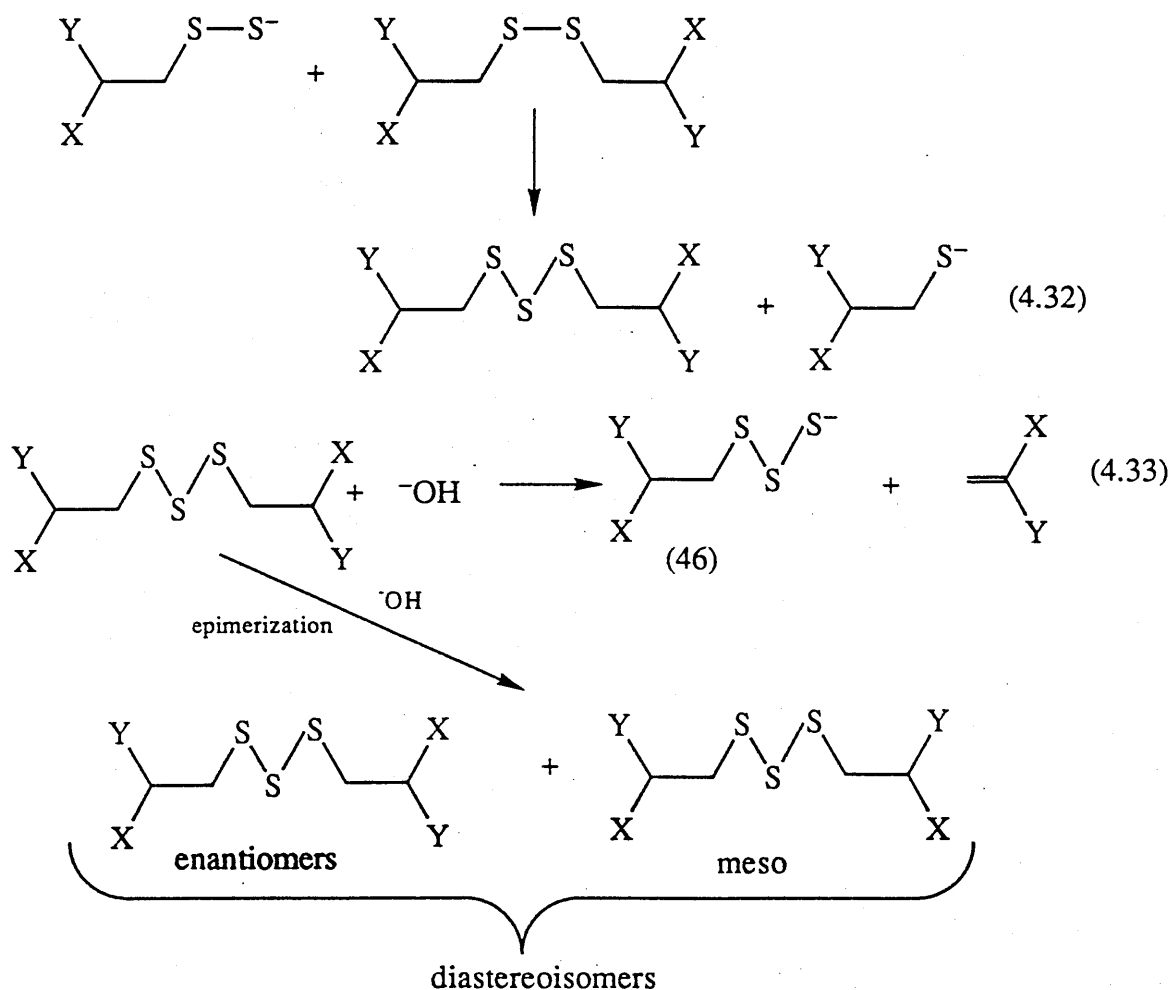


It is also possible for the thiocysteine derivative to break down to form NACMA and elemental sulphur (4.30). The formation of DLDMA is attributed to the addition of the sulphide group of NACMA across the  $\alpha, \beta$ -unsaturation of N-acetyl-dehydroalanine-N-methylamide (eqn. 4.31).

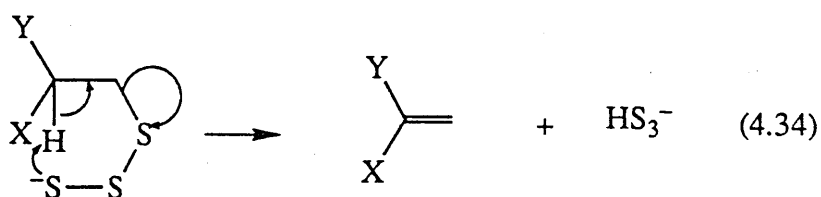


Support for the proposed reaction mechanism is provided by HPLC evidence of epimerization of the substrate demonstrating the formation of carbanion intermediate. The high yields of NADMA and hence DLDMA is in accord with the scheme. We have seen that analogous  $\beta$ -elimination mechanisms have been proposed for alkali-promoted disulphide cleavage [Bergman and Stather, 1926; Nicolet, 1931; Tarbell and Hornish, 1951; ANS S. Nashef et al., 1977; Helmerhorst and Stokes, 1983, and many others]. Direct measurements of product yields, however, have not been reported. Rather, mechanistic studies have been based on  $^1\text{H}$  NMR studies on the formation of DHA, measurements of hydrogen sulphides and kinetic studies.

The minor products observed may be rationalized with the following reactions (Eqns. 4.32 and 4.33).

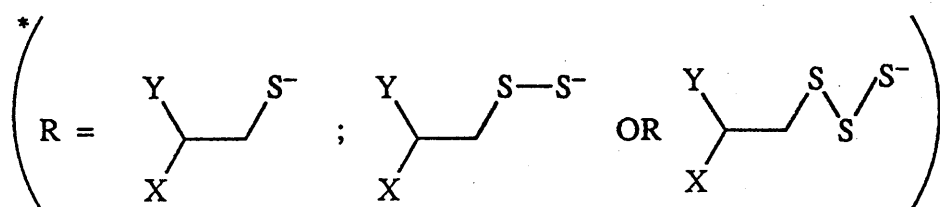


where structure (46) has the potential to build up polysulphides or fragment further (eqn. 4.34)



One interesting outcome of the separation of DCDMA alkaline reaction mixture by NPHPL was its ability to separate the diastereoisomers of DCDMA, DLDMA and DTCDMA (eqn. 4.33). These compounds are all seen as twin peaks on RPHPLC.

Although thiocystine appears to be relatively stable in the pH range 2-9 [Fletcher and Robson, 1963; Abdulrasulnia and Wood, 1980], rapid decomposition to free sulphur and cystine occurs in the presence of sulphhydryl compounds, sulphites, or cyanides. This may explain the low yield of DTCDMA under alkaline conditions. As indicated earlier, the distribution of degradation products in alkaline solution differs from that in the solid-state for two reasons other than that of the different physical states involved; first, NADMA is unstable at the low pH and second the deprotonation of  $\text{RSH}^*$  makes available additional pathways of degradation that compete effectively with those operating in the solid-state.



### 4.3 Yellow Products

Most of the reports on wool degradation, whether they have been concerned principally with the loss in regaining strength, or with yellowing, invariably cite the importance of cystine, but as yet to our knowledge the nature of yellow chromophore(s) produced in wool or the detailed structural changes that give rise to them in heat and alkali treated wools remain unknown. Furthermore, no satisfactory evidence has appeared to explain the involvement of amino acid cystine in the yellowing of wool. Our results showing the ready formation of deep yellow pigments in the alkaline degradation of DCDMA further implicates cystine in wool yellowing. Attempts have also been made to identify and characterise some of the pigments responsible for the yellowing or furnish some clues to the structural changes occurring during the yellowing of DCDMA.

All the principal products (ie acetamide, MPA, NACMA, NADMA, DLDMA and DTCDMA) which have been identified so far are colourless. We recall that the uv/vis spectra of alkali-treated DCDMA reaction mixtures show three regions of increased absorption at  $\lambda_{\text{max}} = 300, 385$  and  $455$  nm and the last two are clearly associated with components responsible for yellowing. In a qualitative search for these component(s) several yellowed reaction mixtures were examined by RPHPLC equipped with a diode array detection system cable of monitoring between 190-367 nm. The uv/vis spectrum of each individual product peak eluting through the column was recorded. Unfortunately, no product peak could be detected which would have similar uv/vis absorption spectrum to that of the yellowed reaction mixture. This clearly demonstrated that either the yellow component(s) never eluted through the column or they decomposed in the column before reaching the detector under the HPLC conditions adapted. The fact, the yellow components only eluted in RPTLC at high concentrations of acetonitrile (>50%) is consistent with the first explanation. Such behaviour may be expected from the presence of inorganic hydro or polysulphide species in the reaction mixture as will be seen later. The yellowed reaction mixture showed only a few peaks with short retention time under the modified RPHPLC conditions (ACN = 25%). Due to the very close retention times of these peaks and the uncertainty of the nature of those products their isolation was not attempted using RPHPLC.

On the other hand the separation of three yellow components was achieved by column chromatography, one of which was consistent with methylthiopyruvamide, a yellow compound. The formation of MTPA during DCDMA alkaline yellowing could occur via the following reaction scheme. (Fig. 4.7)



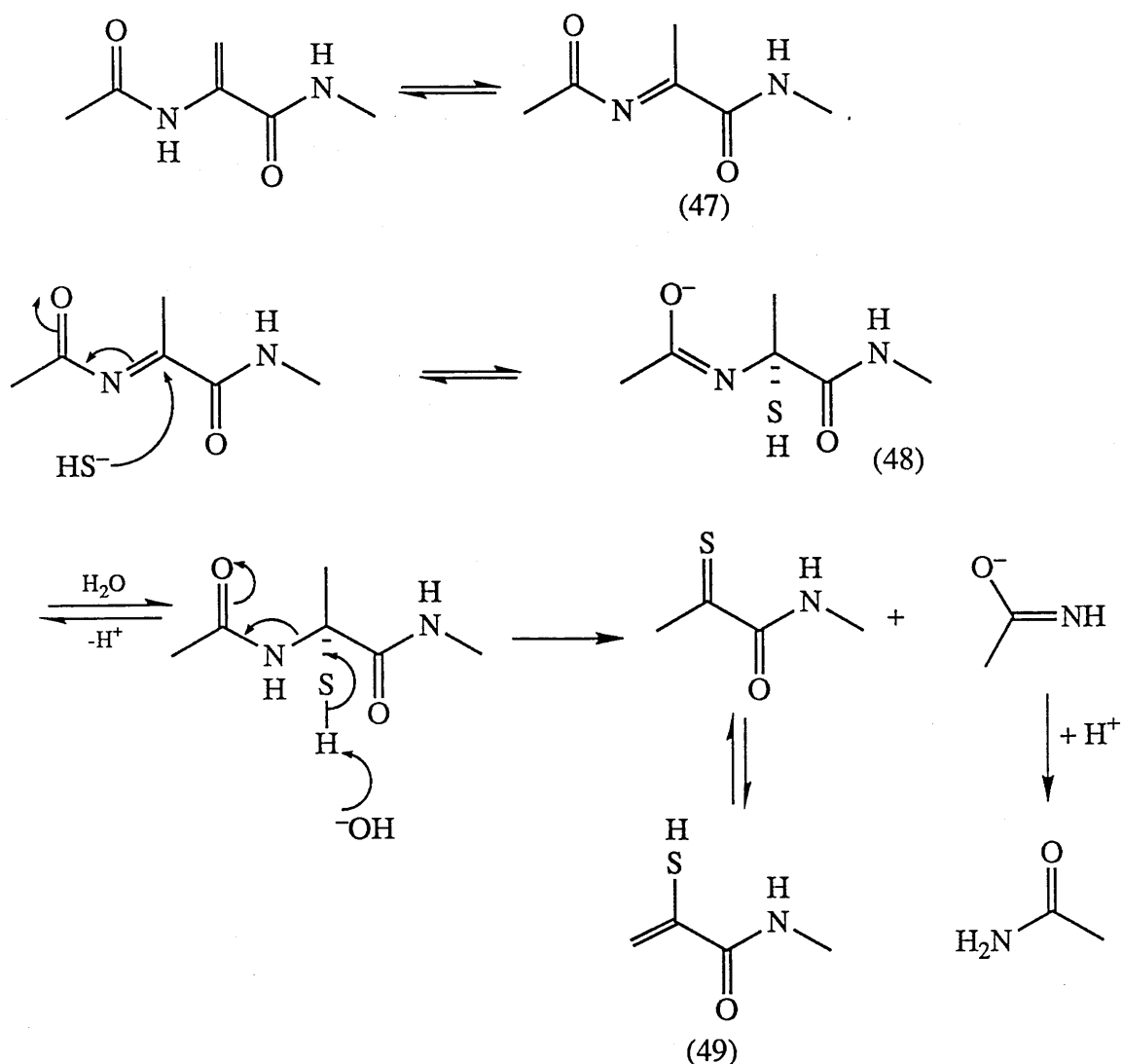


Figure 4.7 Proposed reaction scheme for the formation of *N*-methylthiopyruvamide

NADMA is produced by  $\beta$ -elimination reaction which may tautomerize to give (47) which is attacked by a nucleophile such as  $\text{RS}^-$ ,  $\text{RSS}^-$  or  $\text{HS}^-$  to give structure (48) which decomposes to MTPA and acetamide. A similar reaction mechanism could account for the yellowing of DCDMA in wet solid-state conditions except that NADMA first decomposes to MPA and acetamide. MPA may then react with hydrogen sulphide which is also produced during DCDMA degradation to give MTPA. MTPA may tautomerize to give *N*-methylthiopyruvamide (49). This is supported by the presence of an absorption

band at  $2260\text{ cm}^{-1}$  in the IR spectrum of the synthesised MTPA. This band is absent in the IR spectrum of MPA. Many workers [Kirkpatrick and McClaren, 1964; Asquith et al. 1969] have shown that DHA residues are formed during the alkaline treatment of wool which can be hydrolyzed to produce  $\alpha$ -keto-acyl peptide, but the relevance to yellowing has not been apparent.

The two other yellow fractions (F<sub>9</sub> and F<sub>15</sub>) isolated in column chromatography had uv/vis spectra similar to those of the original reaction mixtures suggesting that these components may also contribute towards the yellowing of DCDMA but result from different chemical pathways to that of first fraction. In spite of the colour, most of the material in these fractions was DCDMA or other colourless decomposition products. Furthermore, no component(s) could be detected on the diode array detection system in HPLC analysis that had appropriate absorption spectrum. Possibly hydro or polysulphides may be involved in yellowing of DCDMA as mentioned before. Takeshige et al. [1964] synthesised Bis(triphenylmethyl) mono to octa sulphides and studied some of their properties. The uv absorption spectra (Fig. 4.8) in chloroform solution show strong absorption bands with a maxima between 240 and 250 nm that may be ascribed to triphenylmethyl group. However, a broad absorption band in the range of 290-330 nm is probably due to linear S-S linkage in the polysulphides. A similar broad band in the same region (290-330) was reported by Bohme et al. [1954] in the uv/vis spectra of dibenzyl and dibenzyl hydryl polysulphides. Figure 4.8 shows that, as the number of sulphur atom in these polysulphides increases, the absorbance becomes more intense, and the displacement toward the longer wavelength occurs.

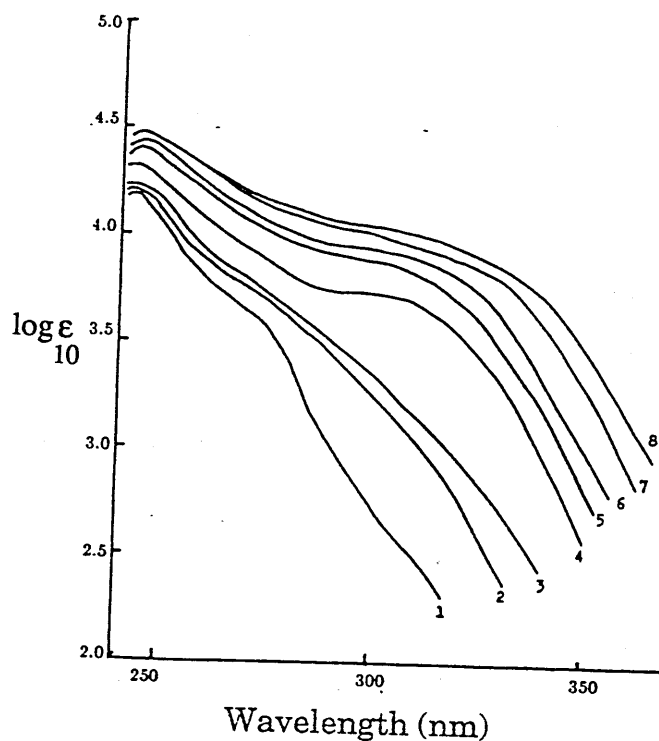


Figure 4.8 Ultraviolet absorption spectra of bis(triphenylmethyl) polysulphides in chloroform solution: 1, mono-; 2, di; 3, tri-; 4, tetra-; 5, penta-; 6, hexa-; 7, hepta-; and 8, octasulphide

Table 4.3 indicates colour and melting points of bis(triphenylmethyl) polysulphides.

Table 4.3 Melting points and colour of bis(triphenylmethyl) polysulphides

compound	colour	m.p. °C
mono-sulphide	white	182
di	white	155
tri	p. yellow	147-148.5
tetra	"	146-148
penta	"	146-147
hex	"	146-147
hepta	"	136-137
octa	yellow	43-47

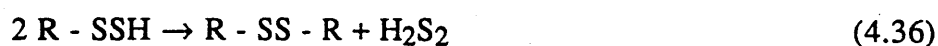
We have found that the melting points drop with increasing the number of sulphur atoms (ie from DLDMA → DCDMA to DTCDMA) while there is an enhanced uv absorption with increasing the number of sulphur atoms. These data are consistent with those (Table 4.3 and Fig. 4.8) reported by Takeshige et al. [1964].

It is known inorganic polysulphides [Cotton and Wilkinson, Cavallini et al. 1960] are yellow at room temperature and turn dark red on being heated. A similar observation was made during the prolonged alkaline treatment of DCDMA. Further evidence for the involvement of polysulphides in yellowing was noted during the extraction of yellowed reaction mixture into DCM. Little extraction of the products including most of the yellowed components, would take place unless the reaction mixture was neutralized after alkali-treatment. The alkaline yellowed residue appeared to be more soluble in aqueous media than in organic solvents. Although an intense bright yellow colour was transferred to DCM from the un-neutralized thermolysate, after only a few hours of extraction, the treatment of the yellow residue after removal of DCM with water gave a turbid pale yellow solution which on standing precipitated elemental sulphur. The yellow component which is extracted into DCM prior to neutralization of the alkaline reaction mixture is suggested to be attributed to MTPA which decomposes to MPA and elemental sulphur in aqueous medium and absence of sulphide. Alkali metal sulphides dissolve sulphur in aqueous solutions giving polysulphide ions and this type of reaction may be occurring during the alkaline treatment of DCDMA. During the neutralization of alkaline reaction mixtures by HCl, hydrogen polysulphides are formed which are oily liquids [Cotton and Wilkinson, 1988; Greenwood et al., 1984] and soluble in non-polar solvents. This further supports their formation in DCDMA alkaline degradation as they were not extracted into DCM as sodium salts when the reaction mixture remained alkaline.

Cavalini et al. [1960] showed a yellow product was formed in an attempt to prepare thiocysteine from cysteine and elemental sulphur according to eqn. 4.35.

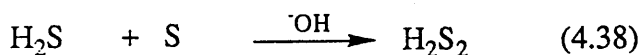
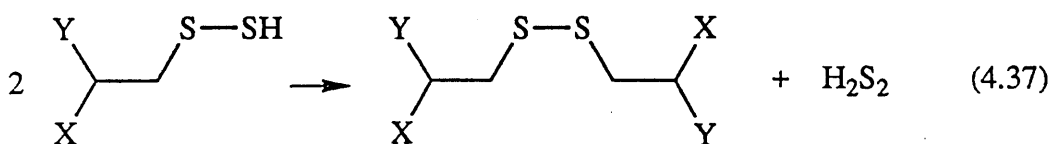


These authors showed that the yellow colour was produced because of the conversion of thiocysteine to cystine and inorganic disulphide by the further reaction (4.36).



This may be analogous to one of the reactions occurring in DCDMA alkaline thermal degradation and hence contributing to the yellowing. As indicated in Chapter 3, neither reverse phase nor normal phase HPLC was effective in isolating polysulphide derivatives.. Moreover, combustion analyses of samples in which these yellow components were concentrated did not confirm a high sulphur content. It should be noted, however, only small amounts of polysulphides may be required to give substantial yellowing.

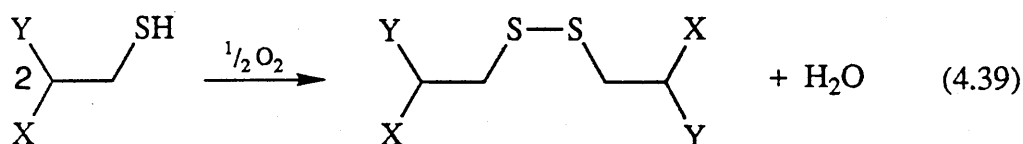
Thus in summary, several components appear to be responsible in yellowing in the degradation of DCDMA. The formation of MTPA is suggested by both isolation and the independent synthesis. This yellow product is known to be fairly unstable. Our results suggest that polysulphides may be heavily implicated in DCDMA yellowing. Finally sulphides such as hydrogen disulphides may be produced according to reactions (4.37 and 4.38) which may contribute towards yellowing.



In all cases, the yellow products are very minor components of the reaction mixture .

#### 4.4 Degradation of DCDMA in neutral aqueous solution

The neutral aqueous thermal degradation of DCDMA appears to follow the pathway of wet solid-state degradation but at much lower rates. The observed inhibition by oxygen might be expected, as some of the NACMA produced could be reoxidized to the starting material (eqn. 4.39).



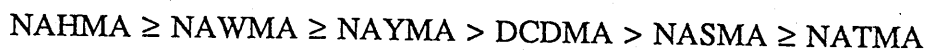
The rate of DCDMA break down (Table 3.5) is much higher in the presence of a buffer (pH  $\approx$  7) underlining the combination effects of heat and pH. NACMA, NADMA, DTCDMA and acetamide are identified as some of the products from the refluxing aqueous degradation of DCDMA. NACMA is found to be the major product followed by DTCDMA. NADMA which is a major product in alkaline, is also shown to be present in significant amounts but less than NACMA and DTCDMA in aqueous neutral degradation of DCDMA. However, the formation of DLDMA is hardly detected. The formation of products almost certainly occurs by  $\beta$ -elimination reaction similar to those seen in DCDMA wet solid-state decomposition.

#### 4.5 Thermal degradation of other mono-peptides

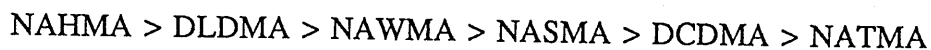
From the literature reviewed in Chapter 1 it appears that some or all of the residues cystine, tryptophan, serine, threonine, tyrosine, alanine, glycine and lysine may be involved in the heat/alkali degradation of wool proteins. Three principal effects of alkali upon wool have been noted. These include fibre weakening which is attributed to amino chain alkaline hydrolysis, cross-linking

which results in the formation of lysinoalanine and lanthionine from DHA residues, and yellowing which is believed to be connected with the production of DHA from cystine, serine and perhaps tryptophan, but this is no way directly proven. As yellowness increases the amounts of certain amino acids namely cystine, serine, tryptophan and tyrosine decrease, but no direct evidence connecting specific chromophores responsible for yellowness or specific structural changes involving these amino acid residues has been obtained. Since DCDMA appears to be a good model for cystine amino acid residues, it was considered appropriate to examine some selective amino acid derivatives known to be most prone to heat/alkali degradation. The results of the thermal and alkaline degradation of these monopeptides are given in Tables 3.6, 3.7 and 3.8 and the ensuing discussion makes frequent reference to this data.

When monopeptides are heated in wet solid-state conditions (Table 3.6) intense yellow coloured solutions are formed from the degradation of some of the amino acid derivatives. The intensity of yellowness in the decreasing order is as follows:



However, the conversion rate of these monopeptides are somewhat different and are given in the decreasing order.



Other monopeptides yellow or degrade marginally. Little reaction is apparent with any of the monopeptides under dry solid-state conditions apart from NASMA which yellows considerably at relatively low conversion. In contrast to the above, DCDMA is the most reactive monopeptide under the alkali which produces an intense yellow reaction mixture. DLDMA is the second most reactive monopeptide under alkali but it doesn't yellow! Some yellowing is

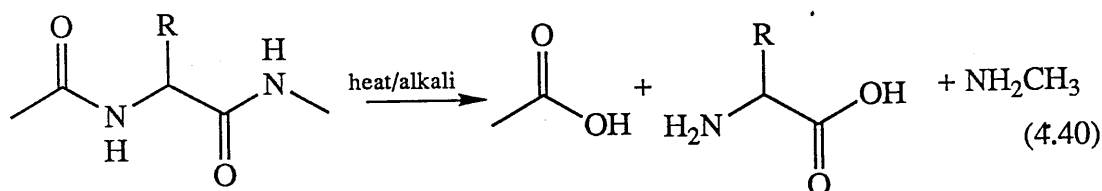
observed with NAWMA and NAYMA. Generally, apart from DCDMA and DLDMA, all the other mono-peptides degrade and yellow a lot more in wet solid-state conditions than under alkali. The following section gives a short discussion on each of the mono-peptides studied.

### ***N*-Acetyl histidine-*N*-methylamide**

Although NAHMA degraded and yellowed more than all the other mono-peptides in wet solid-state conditions no major product peak was seen on HPLC with the exception to a few peaks with short retention times. NAHMA appeared to be completely unreactive when treated with alkali at 55 °C and no yellowing was observed after 120 h. No work has been reported regarding the heat/alkali decomposition of histidine either in isolation or in a protein chain apart from the work reported by Asquith, Hirst and Rivett [1971] in which they noted that histidine is implicated in photoyellowing of wool.

### ***N*-Acetylglycine-*N*-methylamide and *N*-Acetyl alanine-*N*-methylamide**

Our investigations have shown that NAGMA and NAAMA break down on alkaline treatment to give glycine and alanine respectively, the expected products of amide hydrolyses (eqn. 4.40, R = H, CH<sub>3</sub>).

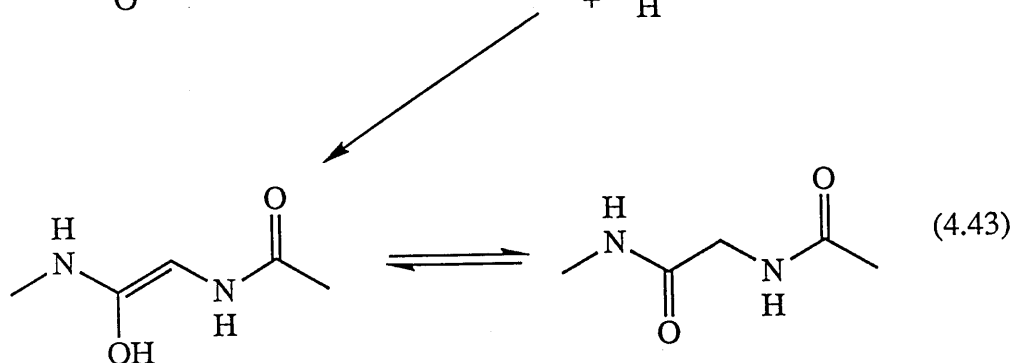
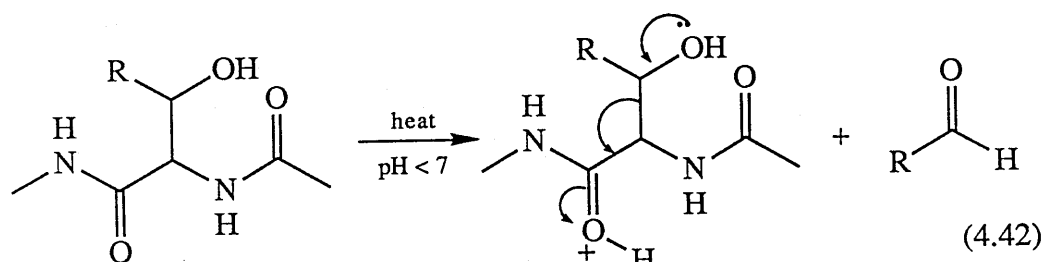
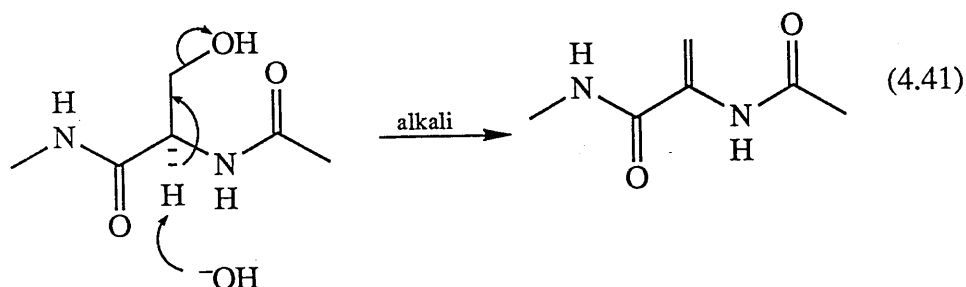


This reaction, however, accounted for only 20% of the degraded substrate but no other products were identified. It is proposed that the intermediate hydrolysis products *N*-acetylglycine and glycine methylamide were also present.



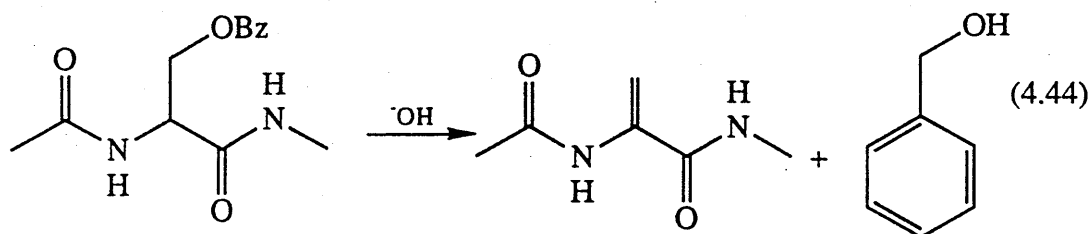
### *N*-Acetyl serine-*N*-methanamide and *N*-Acetylbenzyl serine-*N*-methyl amide

NASMA and NASBMA degrade under all the conditions used. The effect of alkali was considerably less on NASMA decomposition than heat on either wet or dry solid samples. The protection of the hydroxyl groups by benzyl in serine residues were found to be ineffective against heat or alkali. Contrary to our expectation the decomposition of the protected serine residues on treatment with alkali under reflux was far greater than on unprotected serine residues. NAGMA, NADMA and acetamide were identified among the products of NASMA degradation. NASMA probably undergoes  $\beta$ -elimination reaction to produce NADMA which decomposes to acetamide and MPA as seen before. These reactions are presented in eqns. 4.41 - 4.43.



(R = H)

NABsMA may also undergo  $\beta$ -elimination reaction similar to NASMA to give benzylalcohol and NADMA (eq. 4.44). No NAGMA was detected from NABsMA thermal or alkaline degradation.



NASMA was the only monopeptide residue which yellowed on dry heating. In contrast to this, slight yellowing was observed with the benzyl protected NASMA. NASMA also yellowed in hot alkaline solutions whereas NASBMA showed less tendency towards yellowing. The intensity of yellowing from NASMA degradation was more prominent under thermal than under alkaline conditions and these results clearly indicated that hydroxyl groups in NASMA play an important role. The above finding is consistent with the fact that with acetylated wools, in which the  $-OH$  groups were protected, yellowing is not observed [Speakman and Janowski, 1965]. The origin of the chromophore in these cases remains obscure.

NATMA does not yellow on dry heating as might have been expected on the basis of the observations with serine residue. Two major products were seen on HPLC. One was shown to be NAGMA by comparing its HPLC to that of authentic sample and purity parameter values. The second product, although it was not proven, was thought to be crotonaldehyde which had similar uv absorption to that of the unknown. However, neither the purity parameter values nor the HPLC retention times for the unknown and crotonaldehyde support the assignment. No evidence was apparent to support  $\beta$ -elimination mechanism in NATMA thermal or alkaline degradation. The proposed reactions for the

formation of NAGMA are similar to those given in equations 4.42 and 4.43 where  $R = CH_3$ .

#### *N*-Acetyl tyrosine-*N*-methylester and *N*-Acetyl tryptophan-*N*-methylester

When these monoesters were heated in wet solid-state conditions, they both degraded but the rate of degradation of NAWMA was considerably more than that of NAYMA. However, the intensity of yellowness appeared to be similar in both reaction mixtures. A long retention time product and a few minor product peaks were seen by HPLC from the degradation of each monoester. Attempts to isolate the long retention time products by scaling up the experiments and increasing the reaction time were unsuccessful because the retained products broke down on prolonged heating. Although little reaction was noted in alkali at 55 °C, a gradual decomposition of NAYMA and NAWMA occurred with time at 100 °C. The only major products had short retention times. It is suggested that both NAYMA and NAWMA undergo hydrolysis in hot alkaline solutions to give tyrosine and tryptophan.

Our results indicate clearly that both NAYMA and NAWMA break down during heat/alkaline treatment. This is in disagreement with a report by Norton and Nicholls [1964], in which the effect of heat and alkali on NAYMA is reported to be insignificant with no yellowing. In fact we have observed that NAYMA yellowed much faster than NAWMA under alkali at 55 °C and 100 °C. No evidence was gathered for the component(s) responsible for yellowing in these mono esters because of the complex nature of the reaction mixtures.

#### DLDMA

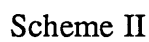
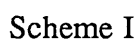
DLDMA behaved very similarly to DCDMA when treated either with heat or alkali except that it yellowed only slightly. The formation of products (NACMA, NADMA, diastereoisomers of DTCDMA and DCDMA) indicated that DLDMA

may also undergo a  $\beta$ -elimination reaction. The fact that DLDMA did not yellow and NADMA was formed from its decomposition casts doubt upon the degree of involvement of NADMA in heat/alkali yellowing of wools.

Thus it appears that heating under wet solid-state conditions causes extensive damage to *N*-acetyl methylamides of histidine, tryptophan, tyrosine, cystine and serine with the formation of brilliant yellow solutions. The derivative of cystine is by far the most reactive mono-peptide on treatment with alkali (55 °C) which both degrades and yellows. Other mono-peptides are much more resistant to attack by alkali with the exception of DLDMA. The reactions for NASMA, NABSMA, DCDMA and DLDMA appear to proceed by an initial  $\beta$ -elimination except in hot alkaline media (100 °C) where the hydrolysis of amide groups are predominant.

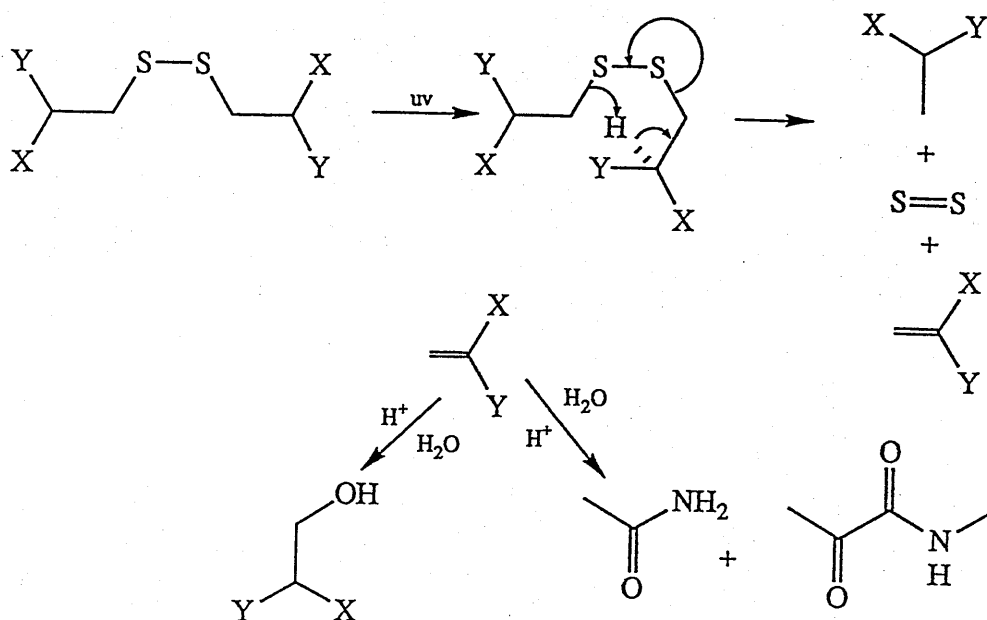
#### 4.5 Photochemistry of DCDMA

*N*-Acetylmethylamides of glycine, alanine, dehydroalanine and thiocystine were shown (section 3.6) to be minor products in the photolysis of aqueous DCDMA and serine, thiocystine, and acetamide may also be present but the evidence was not conclusive. There is little evidence for the formation of diastereoisomers of DLDMA from the HPLC of the photolysis mixtures, but one isomer is present as a minor product. NACMA appears to be the dominant product in DCDMA photolysis. Its yield rises sharply and levels off after 10 h irradiation. Possible reaction schemes for the formation of NACMA are presented in Figure 4.9.



159

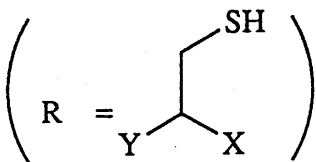
Scheme II may be favoured if the evidence for the formation of acetamide was conclusive. Thioformaldehyde is unstable and may hydrolyse, polymerize or attack other components. *N*-methyl pyruvamide is expected to be photochemically active and is unlikely to be detected. The formation of other minor products may arise by the initial cleavage of the C-S bonds (Figure 4.10, Scheme III).



Scheme III

Figure 4.10 Proposed reaction scheme for the formation of NADMA, NAAMA and other minor products.

Scheme III is supported by the identification of NAAMA, NADMA and NASMA and acetamide amongst the products of DCDMA photolysis. All these products are shown to be in small amounts. NAGMA may arise from the break down of thiyl radical. (eqn. 4.45)



161

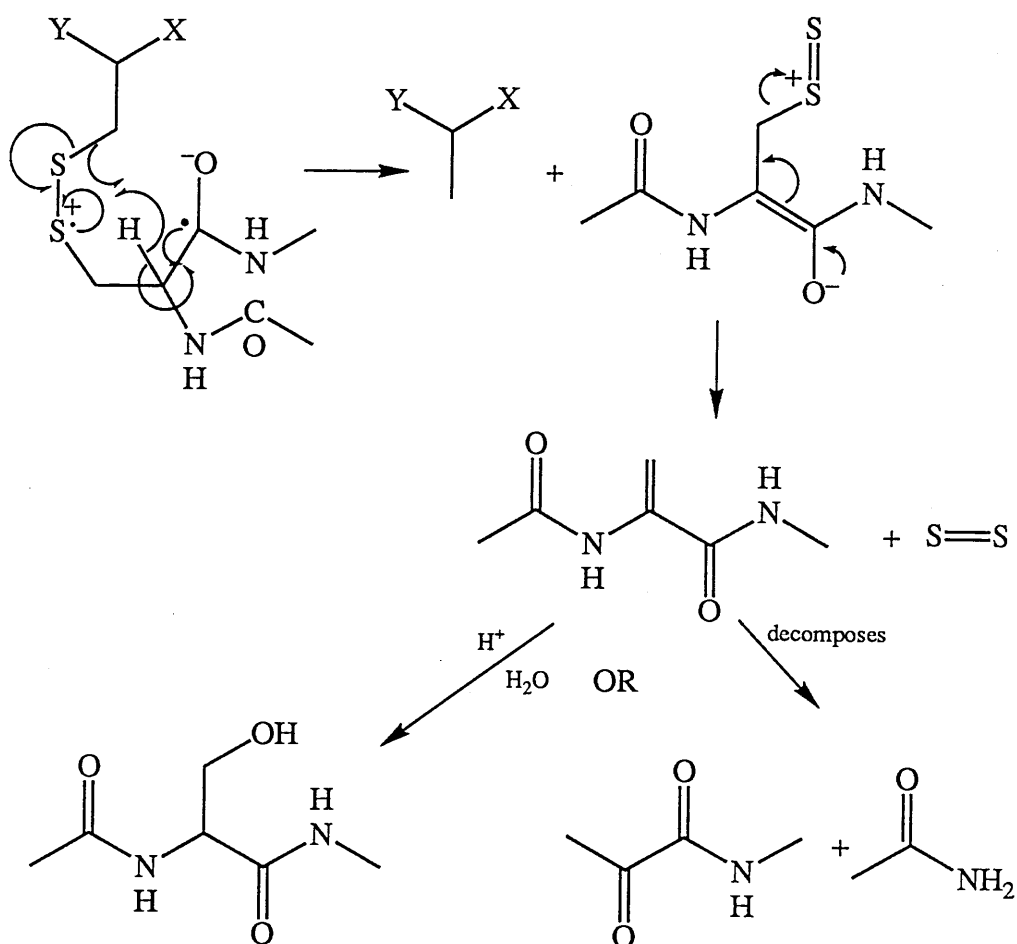


Figure 4.11 Proposed reaction schemes via electron transfer mechanism.



Support for the reaction schemes IV and V is provided by a plot of  $\log \epsilon$  for the

sum of NAGMA and dimethyldisulphide, and DCDMA vs. wavelength (Fig. 4.12). The increased absorption coefficient values of DCDMA is attributed to the extra absorption caused by the electron transfer, i.e. charge-transfer transition from sulphur to the carbonyl amide.

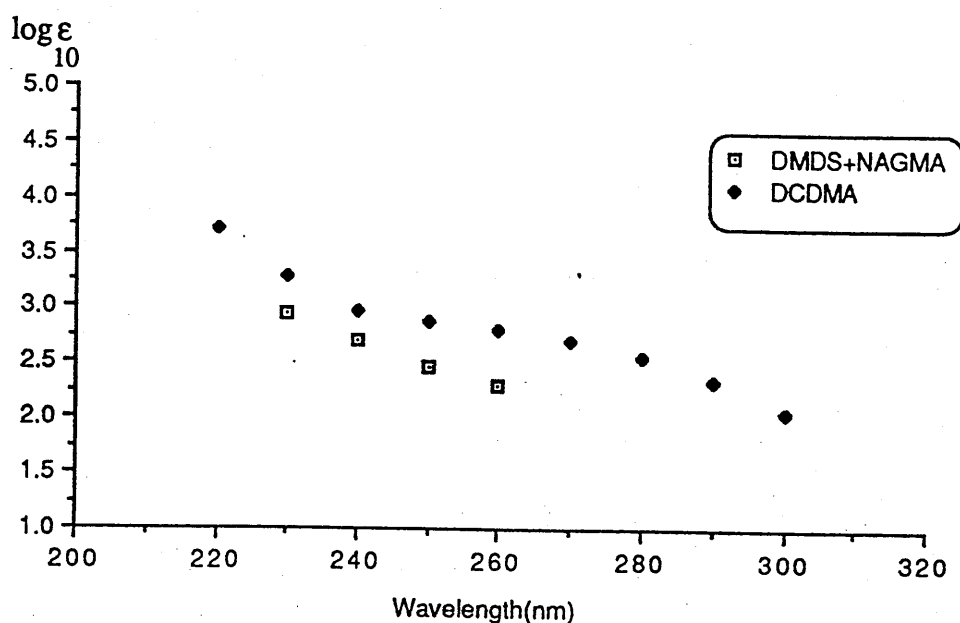


Figure 4.12 Uv spectra of DCDMA (♦) and computed sum of DMDS and NAGMA (□).

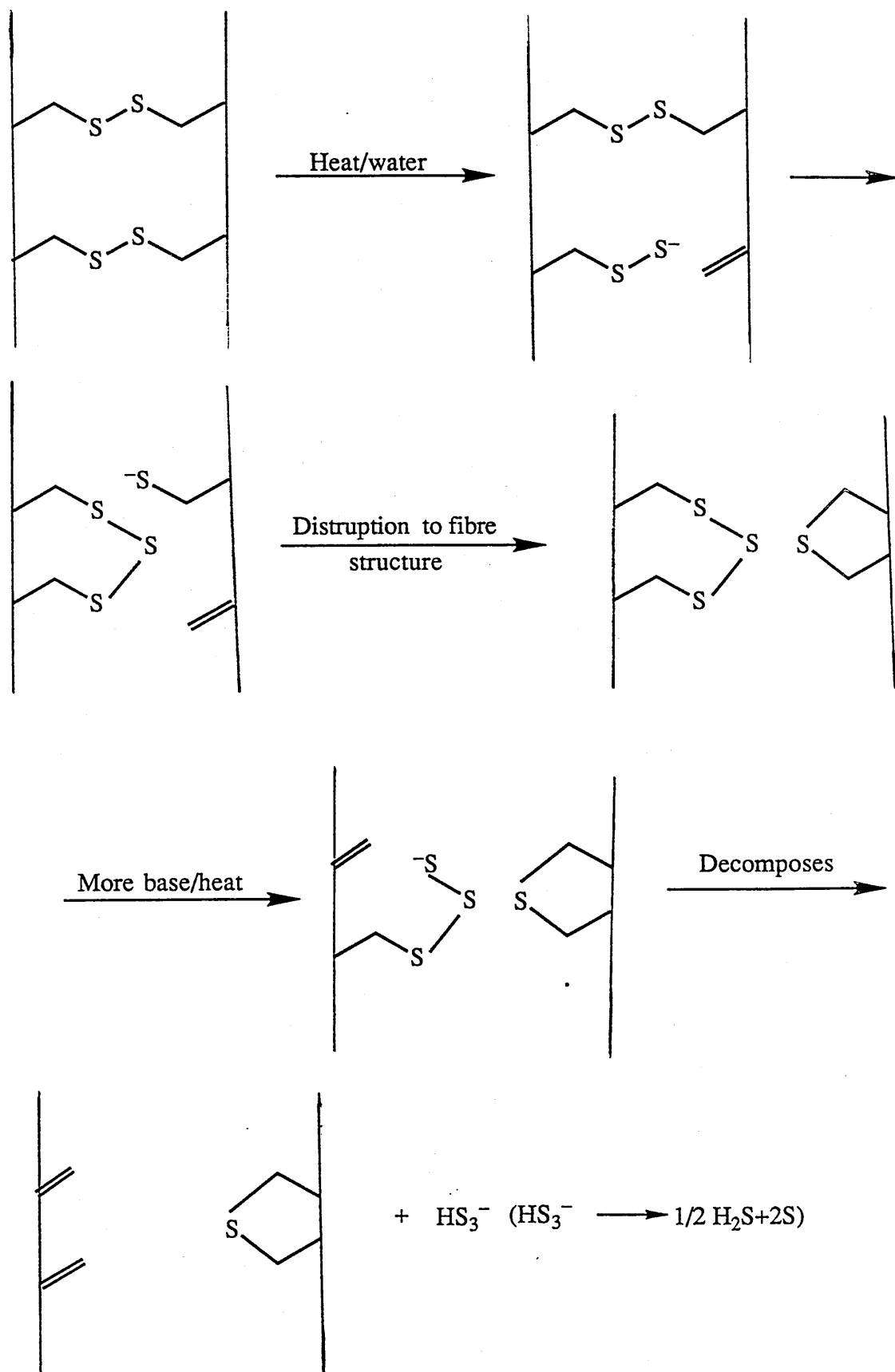
Thus, it appears that DCDMA degrades rapidly and yellows when irradiated, but the product distribution is widely different from that in thermal degradations. The formation of high yield of NACMA as the principal product suggests that photolysis of DCDMA proceeds mainly via S-S bond fission, although there is also strong evidence provided by the occurrence of NAGMA, NAAMA and perthiyl radicals for the cleavage of C-S bonds. The results from DCDMA photolysis supports most of the findings on the photochemistry of cystine reported by many authors as described in Chapter 1. Although we were unable to detect any oxides of sulphur compounds from DCDMA photolysis, many such products are reported [Fobers and Savige, 1962a; Dose and Rajewsky, 1962] from cystine

photolysis, the sharp drop in pH is indeed suggestive of their formation during the photolysis. These may account for some of the unidentified major product peaks on HPLC of the DCDMA photolysis mixture.

## Conclusion

The results from studies on heat/alkaline degradation of DCDMA have clearly demonstrated that it is an excellent model of cystine in a protein. It reproduces faithfully the lability of cystine relative to other amino acid residues and the formation of dehydroalanine and lanthionine derivatives previously observed in wool degradation studies. This enhances the relevance of the present work to both the yellowing of wool and the possible role of trisulphide formation in fibre weakening. Similar studies with *N*-acetyl-*N*-methyl amides of alanine, glycine, serine, threonine, tryptophan, tyrosine and proline have indicated that they are probably also good models.

Although DCDMA reacts principally by a  $\beta$ -elimination mechanism under both wet solid-state and buffered alkali conditions, the distribution and yield of products differ significantly. The ready formation of DTCDMA and the fact that it is the major product in DCDMA solid-state degradation suggest that analogous reactions may play a significant part in wool chemistry that has hitherto been overlooked. During the processing of wool, bond fission and bond rebuilding occurs which may either involve hydrogen bonds and/or disulphide bonds. The latter leads to the formation of new covalent bonds such as reformed  $-S-S-$  linkings, lanthionine ( $-C-S-C-$ ) linkages, lysinoalanine linkings, etc. However, the present work suggests the chemistry of trisulphides may form an integral part of these and perhaps, other as yet uncharacterized transformations, possibly along the lines depicted in Scheme 5.1. The disulphide bonds in the fibre break by nucleophilic attack of water on the hydrogen  $\beta$  to the sulphur atom to produce thiocyst<sup>e</sup>inyl and dehydroalanyl residues. The former may then attack another disulphide bond in the fibre to form thiocystinyl and cysteinyl residues. The cysteinyl residues add across the reactive double bond of dehydroalanyl residues to give a new cross-link (i.e. lanthionine). Thiocyst<sup>e</sup>inyl residues are unstable and therefore may either break down or react further to build-up (yellow)



Scheme 5.1

polysulphides. When disulphides rupture and new cross-links are formed, irreversible destruction of the  $\alpha$ -form results (Fig. 1.6, Section 1.3) to give a disoriented  $\beta$ -form leading to an opening of the structure. Although in the helical structure of wool, hydrogen bonds are largely responsible for holding the peptide chains in position within the matrixes, these bonds may be broken more easily in the absence of disulphide cross-links which stabilizes the miscelles possibly by holding them embedded in a disulphide  $\alpha$ -linked cement. Therefore thiocystinyl residues could play an important role in the weakening of wool fibre.

Interestingly, although their occurrence and reactions in other biological systems have been extensively studied, little attention has been given to their possible role in wool chemistry.

In contrast to the wet solid-state conditions, DTCDMA is a minor product under buffered alkaline conditions. The intermediate thiocysteinyl residue which is the precursor to the formation of DTCDMA is unstable and undergoes rapid decomposition in buffered alkaline media. In addition, trisulphide is also vulnerable to attack by alkali. The separation and identification of NATCMA, though not in pure form, in wet solid-state suggest that this compound is more stable in acid than under alkali. Although DHA is reported to be very unstable and has thus far not been isolated, NADMA was obtained in pure form from the alkali-degraded DCDMA reaction mixtures and has fully been characterized. Clearly, extra stability is conferred by protected amino and carboxylate groups since DHA with free amino group would readily decompose in the presence of water to give ammonia and pyruvic acid. NADMA is the major product under alkali and reacts with cysteinyl residue present in the alkaline reaction mixture to give DLDMA. The low yield of NADMA in wet solid-state reflects its tendency to decompose under acidic conditions ( $\text{pH} < 7$ ); acetamide and MPA are observed in its decomposition. While DTCDMA is the most prominent product followed by NACMA with DLDMA and NADMA as the minor products in solid-state

conditions, the reverse is true for the products under alkaline conditions of DCDMA. Acetamide and MPA appear to be present in small amounts under both conditions. The plots of yields vs. conversion of substrate suggest that NADMA is a primary product under both conditions, and DLDMA, NACMA and DTCDMA are secondary products. This accords with the operation of a  $\beta$ -elimination mechanism via dehydroalanyl residue as an intermediate product in a similar manner to those from proteins treated in alkali.

In spite of considerable research in an attempt to explain the chemical reactions leading to the thermal/alkali yellowing of wool, as yet neither the nature of the yellow component(s) nor the specific amino acid(s) involved, has been identified. The intense yellowing of DCDMA both in wet solid-state and under alkaline conditions arises from three regions of increased absorption at 300, 385 and 455 nm. Our results suggest MTPA may be one of the pigments and that polysulphides (organic and inorganic) are also heavily implicated. These possibilities are worthy of future investigations as candidates for the yellow pigments generated in wool.

Results from the comparative studies of mono peptides are consistent with the known prominence of cystine in alkaline degradation of wool. While *N*-acetylmethylamides of histidine, tryptophan, tyrosine, serine and cystine both degrade and yellow in wet solid-state conditions, DCDMA is the most reactive mono peptide under the alkaline conditions which produces an intense yellow reaction mixture. DLDMA is the second most reactive but it does not yellow! All the other mono peptides degrade and yellow marginally. No reaction is apparent with any of the mono peptides in dry solid-state conditions apart from NASMA which yellows significantly. This implies that the hydroxyl group is involved in the formation of yellow pigment since the protection of the hydroxyl groups by benzyl in serine residues are found to reduce heat-yellowing, but are ineffective against degradation. Considering these results, it is conceivable that more

yellowing occurs during the setting processes (pressure settings or full decating) of wool than scouring processes. Setting processes may be compared to the experiments in wet solid-state conditions in which more of the mono-peptides degrade and yellow due to the combined effect of heat and pressure while scouring may be compared to heating mono-peptides under alkali in which the degradation of DCDMA is the main cause of yellowing.

Photolysis of DCDMA leads to degradation and formation of a bright yellow reaction mixture with large drop in pH. The products of DCDMA photolysis are similar to those identified from the photodegradation of cystine and its derivative. NACMA is the major product which implies that photolysis of DCDMA proceeds mainly via S-S bond cleavage, although there is also evidence provided by the occurrence of NAGMA, NAAMA and perthi- $\alpha$ yl radicals for the cleavage of C-S bonds. Although tryptophan is widely considered to be the principal target in wool, these studies show that the cystine residue would be both photolabile and likely to give yellow products in the presence of uv radiation.

The results from this project demonstrate that our models are well chosen. They also draw attention to trisulphides as reactive intermediates in wool chemistry, and to new lines of enquiry that may be followed up in seeking source of yellowing in degraded wool fibres.

## References

- Abdolrasulnia, R. and Wood, J.L. (1979). *Biochim. Biophys. Acta*, **567**, 135.
- Abdolrasulnia, R. and Wood, J.L. (1980). *Bioorgn. Chem.*, **9**, 253.
- Alewood, P.F., Palma, S. and Johns, R.B. (1984). *Aust. J. Chem.*, **37**, 425-428.
- Alexander, P. and Hudson, F.R. (1963). *Wool, its Chemistry and Physics*. London: Chapman and Hall Ltd.
- Applewhite, T.H. and Niemann, C. (1959). *J.A.C.S.*, **81**, 2213.
- Applewhite, T.H., Waite, H. and Nieman, C. (1958). *J.A.C.S.*, **80**, 1465.
- Asquith, R.S. and Booth, A.K. (1969). *Biochem. Biophys. Acta.*, **181**, 164.
- Asquith, R.S. and Carthew, P. (1971a). *Biochem. Biophys. Acta*, **278**, 346-351.
- Asquith, R.S. and Carthew, P. (1972b). *Tetrahedron*, **28**, 4769-4773.
- Asquith, R.S. and Carthew, P. (1973). *J. Textile Inst.*, **64**, 10.
- Asquith, R.S. and Garcia-Dominguez, J.J. (1968). *J. Soc. Dyers and Colourists*, **85**, 155.
- Asquith, R.S. and Hirst, L. (1969). *Biochem. Biophys. Acta*, **184**, 346-347.
- Asquith, R.S. and Leon, N.H. (1977). Chemical Reactions of Keratin fibres. In: Asquith, R.S., (Ed). *Chemistry of Natural Protein Fibres*. London: John Wiley and Sons, 193-259.
- Asquith, R.S., Otterburn, M.S. and Gardener, K.L. (1971). *Experientia*, **27**, 13.
- Asquith, R.S. and Otterburn, M.S. (1977). *Advances in Experimental Medicine and Biology*, **86B**, 93-121.
- Asquith, R.S. and Shah, A.V. (1971). *Biochem. Biophys. Acta*, **224**, 547-556.
- Asquith, R.S., Hirst, L. and Rivett, D.E. (1971). *Appl. Polym. Symp.*, **18**, 333.
- Astbury and Sisson (1935). *Proc. Roy. Soc.*, **150A**, 533.
- Astbury and Street (1931). *Phil. Trans. Roy. Soc.*, **203A**, 75.



Astbury and Woods (1933). *Phil. Trans. Roy. Soc.*, **232A**, 333.

Astbury, W.T. and Bell, F.O. (1941). *Nature*, **696**.

Bartle, K.D., Fletcher, J.C., Jones, D.W. and Amic, R.L. (1968). *Bioch. M. Biophys. Acta*, **160**(1). 106-111.

Bell, J.W., Clegg, D. and Whewell, C.S. (1960). *J. Textile Inst.*, **51**, T1173.

Bergmann, M. and Stather, F. (1926). *Z. Physiol. Chem.*, **152**, 189.

Bodansky, M. (1984). *The Practice of Peptide Synthesis*, **33**.

Bohme, H. and Zimmer, G. (1954). *Ann. Chem. Liebigs*, **585**, 142.

Brown, T.D. and Onions, W.J. (1961). *J. Textile Inst.* **52**, T107.

Campaigne, E. (1946). *Chem. Revs.*, **39**, 20-22.

Campaigne, E. and Cline, R.E. (1956). *J. Org. Chem.*, **21**, 32.

Catsimpoolas, N. and Wood, J.L. (1964). *J. Biol. Chem.*, **239**, 4132-4137.

Cavallini, D., DeMarco, C., Mondovi, B. and Mori, B.G. (1960). *Enzymologia*, **22**, 161-173.

Cavallini, P., Federici, G., Barboni, E. and Marcucci, M. (1970). *F.E.B.S. Lett.*, **10**, 125.

Clarke, H.T. and Inovye, J.M. (1928). *J. Biol. Chem.*, **80**, 191.

Cotton, F.A. and Wilkinson, G. (1988) *Advanced Inorganic Chemistry*. 5th Ed. John Wiley & Sons, Inc: USA. 501-502.

Creed, D. (1984). *Photochemistry and Photobiology*, **39**(4), 557-583.

Crewther, W.G., Fraswer, R.D.B., Lennox, G.L. and Lindley, H. (1965). *Advan. Protein Chem.*, **20**, 19.

Crowe, and North (1950). *J. Org. Chem.*, **15** 18.

- Davis, R.E. and Perrin, C. (1960). *J.A.C.S.*, **82**, 1590.
- Dixon, C.J. and Grant, D.W. (1967). *Biochem. J.*, **105**, 8C-9C.
- Dobb, M.G. (1963). *PhD Thesis, University of Leeds*.
- Dobozy, O.K. (1968). *Industrie Textil*, **967**, 267.
- Doherty, D.G. Burnett, W.T. and Chapira, R. (1957). *Radiation Res.*, **7**, 13.
- Donovan, J.W. and White, T.M. (1971). *Biochemistry*, **10**, 32-38.
- Dose, K. and Rajewsky, B. (1962). *Photochemistry and Photobiology*, **2**, 181-189.
- Earland, C., Stell, J.G.P. and Wiseman, A. (1960). *J. Textile Inst.*, **51**, 817.
- Elliot, R., Asquith, R.S. and Hobson, M.A. (1960). *J. Textile Inst.*, **51**, T692.
- Fellman, J.H. and Avedovech, N.A. (1982). *Arch. Biochem. Biophys.*, **V218(1)**, 303-308.
- Fletcher, J.C. and Buchanan, J.H. (1977). The Basis of Protein Chemistry. In: Asquith, R.S. (ed). *Chemistry of Natural Protein Fibres*. London: John Wiley and Sons, 1-52.
- Fletcher, J.C. and Robson, A. (1963). *Biochem. J.*, **87**, 553.
- Fletcher, J.C. and Robson, A. (1963a). *Biochem. J.*, **68**, 553.
- Forbes, W.F. and Savige, W.E. (1962a). *Photochemistry and Photobiology*, **1**, 1-13.
- Forbes, W.F. and Savige W.E. (1962b). *Photochemistry and Photobiology*, **1**, 77-89.
- Font, M. (1916a). *J. Soc. Dyers and Colourists*, **32**, 109.
- idem (1916b) *ibid* . **32**, 184
- Foss, O. (1950). *Ada Chem. Scand.*, **4**, 404-415.

Fraser, R.D.B., MacRae, T.P. and Rogers, G.C. (1972). *Keratins – Their Composition, Structure and Biosynthesis*. Springfield, USA: C.C. Thomas.

Friswell, N.J. and Gowenlock, B.G. (1967). *Adv. Free Rad. Chem.*, **2**, 1-46.

Gawron, O. and Odstrohel, G. (1967). *J.A.C.S.*, **89**, 3263-3267.

Gillespie, J.M. (1983). *Biochemistry and Physiology of the Skin*, **2**. Oxford: Oxford University Press, 475-510.

Gillespie, J.M. and Darskins, R.L. (1971). *Aust. J. Biol. Science*, **24**, 1189-1197.

Gillespie, J.M. and Reis, P.J. (1966). *Biochem. J.*, **98**, 667-669.

Giorgio (George) Federicia, Silvestro Dupre, Rosa Marina Matarese, Sandro P. Solinas and Dorian Cavallini (1977). *Int. J. Pept. and Prot. Res.*, **10**, 185-189.

Greenstein, J.P. and Milen, W. (1984). *Chemistry of Amino acids*, **2**. Malabor, Florida: Robert E. Krieger Publishing Co., 1231.

Greenwood, N.N. and Earnshaw, A. (1984) *Chemistry of the Elements*. Pergamon Press: Oxford. (805-808)

Hearle, J.W.S. and Miles, L.W.C. (1971). *Setting of Fibres and Fibrils*. Merrow Publishing Co. Ltd.

Holt, L.A., Inglis, A.S. and Lennox, F.G. (1966). *Textile Res. J.*, **36**, 837.

Holt, L.A. and Waters, P.J. (1985). *7th Intl. Wool Textile Res. Conference, Tokyo*, **IV**, 1.

Hordvick, A. (1966). *Acta Chem. Scand.* **20**, 1885.

Horio M. and Kondo J. (1953). *Textile Res. J.*, **23**, 373.

Horio, M., Kondo, J., Selarob, K. and Faratsui, M. (1965). *Proceedings of the 3rd Int. Wool Textile Res. Conference, Paris*, **2**, 189.

Howitt, F.O. (1963) *J. Textile Inst.*, **54**, T136.

Hylin, J.W. and Wood, J.L. (1959). *J. Biol. Chem.*, **239**, 2141.

Ismail, M.G. (1987). *PhD thesis, The City University*.

Jones, A.J. Helmerhorst, E. and Stokes, G.B. (1983). *Biochem. J.*, **211**, 499-502.

Jónsson, S. and Raa, J. (1980). *J. Food Science*, **45**, 1641-1644.

Kice, J.L. (1973). In: Kochi, J.K. (Ed.). *Free Radicals*, New York: Wiley, 711-740.

Kice, J.L. and Cleveland, J.P. (1970). *J.A.C.S.*, **92**, 4757.

Kirkpatric, A. and McClaren, J.A. (1964). *Textile Res. J.*, **34**, 1082.

Konowalchuk, J. Hinton, N.A. and Reed, G.B. (1954a). *Can. J. Microbiol.*, **1**, 175.

Konowalchuk, J., Clunie, J.C., Hinton, N.A. and Reed, G.B. (1954b). *Can. J. Microbiol.*, **1**, 182.

Krauss, F., Schäfer, W. and Schmidt, A. (1984) *Plant Physiol.*, **74**, 176-182.

Launer, H.F. (1965). *Textile Res. J.*, **35**, 395.

Launer, H.F. and Black D. (1971). *Proceedings of 4th Int. Wool Textile Res. Conf., Berkeley*, **18**, 347.

Lewis, D.M. and Duffield, P.A.(1985). *Rev. Prog. Coloration*, **15**, 38.

Maclaren, J.A. (1963). *Text. Res. J.*, **33**, 773.

Martin, T.A. (1967). *J. Med. Chem.*, **10**, 1172.

Massey, V., Williams, C.H. and Palmer, G. (1971). *Biochem. Biophys. Res Commun.*, **42**, 730.

- Mazingue, G. and Van Overbeke, M. (1956). *Bull. F.T.E.*, **59**, 23.
- Meisswinkel, H.J., Blankenbury, G. and Zahn, H. (1982). *Melliand Textiber*, **63**, 160.
- Mercer, E.H. (1953). *Naturwissewshaften*, **52**, 495.
- Meybeck, J. and Meybeck, A. (1965). *Proceedings of 3rd Int. Wool Textile Res. Conference, Paris*, **2**, 525.
- Meybeck, J. and Meybeck, A. (1967a). *Photochemistry and Photobiology*, **6**, 365.
- idem (1967b). *ibid* **6**, 355.
- Milligan, B. and Tucker, D.J. (1962). *Text. Res. J.*, **32**, 634.
- Morine, G.H. and Knutz, R.R. (1981). *Photochemistry and Photobiology*, **33**, 1-5.
- Nashef, A.W.S., Osuga, D.T., Honson, S.L., Ahmed, I., Whitaker, J.R. and Feeney, R.E. (1977). *J. Agric. Food Chem.*, **25**(2), 245.
- Näsholm, T., Sanderberg, G. and Ericsson, A. (1987). *J. Chromatography*, **396**, 225-236.
- Nicolet, B.H. (1931). *J.A.C.S.*, **53**, 3066.
- Norton, G.P. and Nicholls, C.H. (1960). *J. Textile Inst.*, **51**, T1183.
- Norton, G.P. and Nicholls, C.H. (1964). *J. Textile Inst.*, **55**, T462.
- Norton, G.P. and Nicholls, C.H. (1967). *Textile Res. J.*, **37**, 1031.
- Open University (1977). *The Nature of Chemistry* (S304), Section 31.2, 31.4, 32.1.
- Patchornick, A. and Sokolovski, M. (1964). *J.A.C.S.*, **86**, 120..
- Peckett, N. (1977). *PhD Thesis, University of Leeds*.
- Perrin, D.D., Armarego, W.L. and Perrin, D.R. (1980). *Purification of Laboratory Chemicals*, 2nd ed. Pergamon Press.

- Phillips, D.C. and North, A.C.T. (1973). In: Head, J.J. (Ed.). *Protein Structure*. Oxford: Oxford University Press.
- Pojer, P.M. and Rae, I.D. (1970). *Aust. J. Chem.*, **23**, 413-418.
- Powell, B.C., Sleight, M.J., Ward, K.A. and Rogers, G.E. (1983). *Nucleic Acids Res.*, **11**, 5327-5346.
- Pryor, W.A. (1962). *Mechanisms of sulphur reactions*. New York: McGraw Hill.
- Rao, G.S. and Gorin, G. (1959). *J. Biol. Chem.*, **24**, 749.
- Raynes, J.L. (1927). *J. Textile Inst.*, **18**, T46.
- Reihlen, H. and Knöphte, L. (1936). *ANN*, **523**, 199.
- Risi, S., Dose, D., Rathinasamy, T.K. and Augerstein, L. (1967). *Photochemistry and Photobiology*, **6**, 423-436.
- Rivett, D.E., Rexburgh, C.M. and Savage, W.E. (1965). *Proceedings of 3rd Int. Wool Textile Res. Conference, Paris*, **2**, 419.
- Rogers, G.E., Reis, P.J., Ward, K.A. and Marshall, R.C. (1989). *The Biology of Wool and Hair*. London: Chapman and Hall.
- Rose, C.S., Feldbaum, E.P., Norris, R.F. and György, P. (1952). *Proceedings. Soc. Exptl. Biol. Med.*, **81**, 709.
- Rosenthal, N.A. and Oster, G. (1954). *J. Soc. Cosmet. Chem*, **5**, 286.
- Rosenthal, A.N. and Oster, G. (1961). *J.A.C.S.* **83**, 4445.
- Sandy, J.D., Davies, R.C. and Neuberger, A. (1975). *Biochem. J.*, **150**, 245.
- Schöberl, A. (1937). *Ber. Dtsch. Chem. Ges.*, **B70**, 1180.
- Schöberl, A., Berninger, E. and Harne, F. (1934). *Ber. Dtsch. Chem. GeS.*, **B67**, 1545.
- Schöberl, A. and Ludwig, E. (1937). *Ber.*, **70B**, 1422.

Schuhardt, V.T., Rode, Oglesby, G. and Lankford, C.E. (1952). *J. Bacteriol.*, **63**, 123.

Silents, cf. C. (1960). *Chem. Rev.*, **60**, 147.

Simpson, W.S. and Page, C.T. (1979). *Wool Res. Org. of N.Z.*, Report N060.

Sörbo, B. (1957). *Biochem. Biophys. Acta*, **23**, 412.

Speakman, J.B. and Janowski, Z. (1965). *Proceedings of 3rd Int. Wool Textile Res. Conference, Paris*, **2**, 157.

Steenken, F. and Zahn, H. (1986). *J.S.D.C.*, **102**, 269.

Swan, S.M. (1957). *Nature*, **179**, 965.

Sweetman, B.J., Eager, J., Maclaren, J.A. and Savage, W.E. (1965). *Zeme. Congr. Int. Res. Textile – Lainiere, Paris*, **2**, 85.

Szczepkowski, T.W. and Wood, J.L. (1967). *Biochim. Biophys. Acta*, **139**, 469.

Tarbell, D.S. and Hornish, D.P. (1951). *Chem. Rev.*, **49**, 1.

Takeshige Nakabayshi, Jitsuo Tsurugi, and Takuzo Vabuta (1964). *J. Org. Chem.*, **29**, 1236-1238.

Vladimirov, YO.A., Roschchupkin, P.I. and Fesenko, E.E. (1970). *Photochemistry and Photobiology*, **11**, 227-246.

Volini, M. and Wang, S.F. (1973). *J. Biol. Chem.*, **248**, 7392.

Von Helmet Zahn und Gerhad Reinerad (1968). *Hopper-Seyler's Z. Physio. Chem.*, **349**, 608.

Weatherall, I.L. (1976). *Proceedings Int. Wool Textile Res. Conference (Aachen)*, **11**, 580.

Westley J. and Nakomato, T.J. (1962). *J. Biol. Chem.*, **237**, 547.

Wilshire, J.F.K., Waters, P.J., Rosevear, J. and Evans, N.A. (1985). *7th International Wool Textile Res. Conference, Tokyo.*

Woiwod, A.J. (1954). *J. Gen. Microbiol.*, **10**, 509.

Wood, J.L. (1980). *Proceedings of the Society for Experimental Biology and Medicine*, **165**, 469-472.

Wood, J.L. and Cooley, S.L. (1956). *J. Biol. Chem.*, **218**, 449.

Woodmansey, A. (1918). *J. Soc. Dyers and Colourists*, **34**, 227.

*Wool Science Review* (1962). **12**.

*Wool Science Review* (1970). **39**, 27.

Yanube, H., Kato, H. and Yonezawa, T. (1971). *Bull. Chem. Soc.*, **44**, 604.

Zahn, H. (1950). *Melliand Textiber*, **31**, 481.

Zahn, H. and Golsch, E. (1962). *Z. Physiol. Chem.*, **330**, 38.

Ziegler, K., Melchert, I. and Lurkin, C. (1967). *Nature*, **214**, 404-405.